

# Sheffield Hallam University

*Study of nickel-plated iron powder for powder metallurgical applications.*

JAISWAL, Shreekant.

Available from the Sheffield Hallam University Research Archive (SHURA) at:

<http://shura.shu.ac.uk/19867/>

## A Sheffield Hallam University thesis

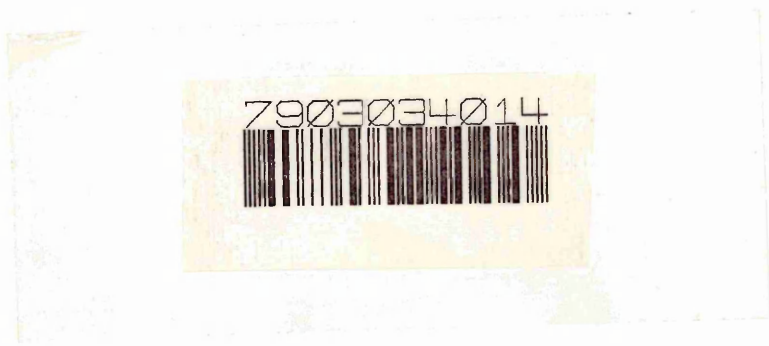
This thesis is protected by copyright which belongs to the author.

The content must not be changed in any way or sold commercially in any format or medium without the formal permission of the author.

When referring to this work, full bibliographic details including the author, title, awarding institution and date of the thesis must be given.

Please visit <http://shura.shu.ac.uk/19867/> and <http://shura.shu.ac.uk/information.html> for further details about copyright and re-use permissions.

10011  
POND STREET  
SHEFFIELD S1 1WB 6847



**Sheffield City Polytechnic  
Eric Mensforth Library**

# **REFERENCE ONLY**

This book must not be taken from the Library

PL/26

R5193

ProQuest Number: 10697173

All rights reserved

INFORMATION TO ALL USERS

The quality of this reproduction is dependent upon the quality of the copy submitted.

In the unlikely event that the author did not send a complete manuscript and there are missing pages, these will be noted. Also, if material had to be removed, a note will indicate the deletion.



ProQuest 10697173

Published by ProQuest LLC (2017). Copyright of the Dissertation is held by the Author.

All rights reserved.

This work is protected against unauthorized copying under Title 17, United States Code  
Microform Edition © ProQuest LLC.

ProQuest LLC.  
789 East Eisenhower Parkway  
P.O. Box 1346  
Ann Arbor, MI 48106 – 1346

SHEFFIELD CITY POLYTECHNIC  
ERIC MENSFORTH LIBRARY

LOAN OF THESIS

Author ...JAI SWAL S.....  
Title Study of Nickel - plated iron  
powder for powder metal applications

I undertake that neither the whole nor any part of the above-mentioned thesis shall be copied, quoted or published without the consent of the Author and of the Sheffield City Polytechnic

Signature .....  
Address Dept. of Metallurgy,  
Brunel University,  
Uxbridge, Middx.

Date 6-9-1982 .....

This undertaking is to be signed by the reader consulting the thesis and returned to:-

The Librarian  
Eric Mensforth Library  
Sheffield City Polytechnic  
Pond Street  
Sheffield  
S1 1WB



**The British Library** LENDING DIVISION  
Boston Spa, Wetherby, West Yorks LS23 7BQ UK.

### THESIS DECLARATION FORM

This form should be completed and sent with the normal request form when a British university thesis is required.

THESIS  
NO. : D *PhD*

Title of thesis ... *A STUDY OF NICKEL PLATING OF IRON POWDERS*  
Name of Author ... *S. JAISWAL*  
University ... *SHEPHERD CITY POLYTECHNIC*

I recognise that the copyright of the above-described thesis rests with the author or the university to which it was submitted, and that no quotation from it or information derived from it may be published without the prior written consent of the author or university (as may be appropriate).

Signed *C. J. Talbot*  
(to be signed by person wishing to consult thesis)

Organisation *DEPT. OF METALLURGY, BRUNEL UNIVERSITY*  
(in block capitals)

Date ... *26-8-1982*

For official use

Code No.

Req. No.

A STUDY OF NICKEL-PLATED IRON POWDER  
FOR POWDER METALLURGICAL APPLICATIONS

BY

SHREEKANT JAISWAL

A THESIS SUBMITTED TO THE COUNCIL FOR NATIONAL  
ACADEMIC AWARDS IN PARTIAL FULFILLMENT FOR THE  
DEGREE OF

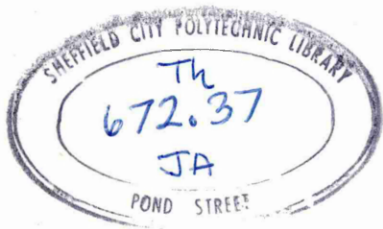
DOCTOR OF PHILOSOPHY  
IN INDUSTRIAL METALLURGY

COLLABORATING ESTABLISHMENT:-

Sheffield Laboratories,  
Hoyle Street,  
British Steel Corporation.

SPONSORING ESTABLISHMENT:-

Department of Metallurgy,  
Sheffield City Polytechnic.  
December 1979.



7903034-01

SYNOPSIS	1
1. PURPOSE OF INVESTIGATION	2
2. REVIEW OF LITERATURE	4
2.1 Polarisation	4
2.2 Anodic Passivity	6
2.3 Nickel Plating Solutions	9
2.4 Coating of Powder Particles by Electrolytic Methods	15
2.5 Alternative Methods of Coating Powders	18
2.6 Applications of Composite Powders	25
2.7 The Production of Low Alloy Steels from Metal Powders	26
2.7.1 Characteristics of Iron Powder	26
2.7.2 Mixing of Powders	29
2.7.3 Compaction of Powders	31
2.7.4 Sintering	35
2.7.5 Heat Treatment of Sintered Steels	43
2.8 Effect of Alloying Elements on the Properties of Low Alloy Steels	44
2.9 Effect of the Degree of Homogeneity on Physical and Mechanical Properties of Low Alloy Steels.	49
2.10 Effect of Porosity on Mechanical Properties of Low Alloy Steels	55
3. EXPERIMENTAL PROCEDURE	63
3.1 Raw Materials	63
3.1.1 Powders	63
3.1.2 Nickel Plating Solutions	63
3.1.3 Nickel Anodes	64
3.1.4 Cathodes	64
3.2 Development of a Plating Cell that may be used to Plate Nickel onto Iron Powder	64
3.2.1 Stage I - Cell Utilising a Porous Membrane	65
3.2.2 Stage II - Cell Utilising an Anode Bag	65
3.3 The Electrodeposition of Nickel on Iron Powder	67
3.4 Nickel Coating of Iron Powder Without a Current Source	68

	Page No.
3.5 Production of Sintered Compacts	68
3.5.1 Mixing	69
3.5.2 Compaction	69
3.5.3 Sintering	69
3.5.4 Heat Treatment	70
3.6 Determination of Properties	70
3.6.1 Density	70
3.6.2 Determination of Modulus of Rupture	70
3.7 Examination of the Microstructure of Sintered and Heat Treated Materials	71
3.8 Determination of the Homogeneity of Sintered Material	71
4. EXPERIMENTAL RESULTS	73
4.1 Stage I - Plating Cell with Refractory Membrane	74
4.1.1 Experiments with the Refractory Membrane Cell	75
4.2 Stage II - Cell Utilising an Anode Bag	76
4.2.1 Experiments Using 100X Triacetate Fabric Anode Bags	76
4.2.2 Effect of Anode Bag Fabrics on Plating Characteristics	78
4.2.3 Effect of Anode Material on Plating Characteristics	80
4.2.4 Influence of Iron Powder Particles on the Average Cell Resistance	81
4.2.5 Influence of the Total Electric Charge Passed and Average Current Density on the Quantity of Nickel Deposited.	82
4.3 "Electroless Plating"	83
4.4 Oxygen Content of Plated Powder	85
4.5 Sieve Analysis of Powders	85
4.6 Properties of Powders Used	86
4.7 Compaction of Plated and Blended Powders	87
4.8 Properties and Microstructure of Fe-Ni-C Alloys	87
4.8.1 Influence of Porosity on the Modulus of Rupture	88
4.8.2 Microstructure of Iron-Nickel-Carbon Alloy Compacts made from both Blended and Plated Powders	95
4.8.3 The Homogeneity of Blended and Plated Powder Compacts Sintered at 1150 °C	104

	Page No.
5. DISCUSSION OF RESULTS	108
5.1 Mechanism of Charge Conduction in a Fluidised Bed Electrode	108
5.2 Influence of Membrane Material on the Plating Process	113
5.3 Relationships Between Period of Plating, Total Electric Charge Passed, Average Density and Mass of Nickel Deposited	117
5.4 Electroless Nickel Coating	119
5.5 Influence of S-Nickel on the Electrodeposition of Nickel onto Iron Powder	123
5.6 Relationships between Porosity, Modulus of Rupture and Homogenisation Parameter of Sintered Compacts	126
5.6.1 Iron - 1.75% Nickel Compacts	127
5.6.2 Iron - 3.25% Nickel Compacts	130
5.6.3 Iron - 4.25% Nickel Compacts	133
5.7 Relationship between Microstructure, Homogeneity and Modulus of Rupture of Sintered Compacts	136
5.7.1 Iron - 1.75% Nickel Compacts	136
5.7.2 Iron - 3.25% Nickel Compacts	138
5.7.3 Iron - 4.25% Nickel Compacts	140
5.8 Influence of Nickel Content on the Modulus of Rupture of Sintered Compacts from both Plated and Blended Powders	143
6. CONCLUSIONS	146
REFERENCES	149
APPENDIX 1, INDUSTRIAL CASE STUDY	160
TABLES 1-24	177
FIGURES 1-84	200

## PREFACE

All the work reported in this thesis was carried out during the period for which the candidate was registered for a higher degree.

In accordance with the regulations for PhD in Industrial Metallurgy, a full course in Metallurgical Process and Management was successfully completed. The details of the course are given below:-

### MODULE - 1

Process Metallurgy

Mechanical Metallurgy

Advanced Thermodynamics

### MODULE - 2

Accountancy

Micro Economics and Financial Control

Computational Methods and Operational Research

### MODULE - 3

Powder Metallurgy

Metals and Competitive Materials

High Strength Steels

Heat Treatment and Transformations

Quality Control

Solidification of Metals

### MODULE - 4

Industrial Case Studies

One of the case studies, which is related to the current research work, is attached with the thesis, as an appendix.

The Candidate's performance during the above mentioned courses was assessed by means of written examinations and continuous assessment of specific assignments.

## ACKNOWLEDGEMENTS

Sincere thanks are especially due to Dr. A.J. Fletcher and to Dr. R.T. Cundill for their constant support and helpful advice throughout the duration of the work.

Grateful appreciation must also be expressed to the Technical Staff of the Department of Metallurgy and particularly to Mr. D. Latimer, Mr. G. Gregory, Mr. N. Rhodes, Mr. K. Woodhouse and Mrs J. Kingswood for their invaluable services. Thanks are also due to Mr. G. Stanger for his help in the preparation of the figures and diagrams.

The author would also like to express his sincere thanks and gratitude to Dr. A.W.D. Hills, Head of Department of Metallurgy, for providing the opportunity for the research work. Grateful thanks must also be expressed to Sheffield Education Authority for the financial assistance received during the course of the work.

Finally thanks and appreciation to my parents and Miss B.M. Scothern for their inspiring support without which this research work would have been extremely difficult.

## SYNOPSIS

### A STUDY OF NICKEL-PLATED IRON POWDER FOR POWDER METALLURGICAL APPLICATIONS

BY

SHREEKANT JAISWAL

The use of coated iron-nickel powders in the production of sintered components of low-alloy steels has certain advantages over blended mixtures of the elemental powders. In particular, the former produce a more homogeneous material after a specific sintering treatment. There is a limited amount of evidence that the improvement in the degree of homogeneity produces an improvement in the tensile strength of quenched and tempered sintered compacts.

The present investigation has aimed to develop a technique by which nickel coated iron powder may be produced and to determine the modulus of rupture of various sintered iron-nickel alloys produced from such powders. The coated powder was produced in a three phase fluidised bed, which contained iron powder, nickel plating solution and a fluidising gas. Coating of nickel on the iron powder particle was achieved by electro-deposition, using cathode rods suspended in a fluidised bed. The central anode consisted of nickel shot contained inside an anode bag. The apparent deposition efficiencies frequently exceeded 100%, which indicated that a process other than electro-deposition was also involved. The second process was shown to be due to a cementation reaction, in which the iron was replaced by nickel. An examination was made of the effect of temperature, anode bag fabric and type of anode material on both types of deposition process. It appears that a nickel coating may be readily prepared by the use of the electroless process alone.

The modulus of rupture of compacts prepared from both plated and blended materials was strongly dependent on porosity while the degree of homogeneity had a significant effect at the higher nickel contents only. An increase in nickel content improved the modulus of rupture after a specified sintering and hardening treatment, although the magnitude of this effect became smaller as the porosity of the compacts was increased. A comparison of the results obtained from plated and blended powder compacts showed that the former possessed higher values of modulus of rupture, although once again the magnitude of this effect was diminished as the porosity of the compacts increased.

CHAPTER ONE  
PURPOSE OF INVESTIGATION

## 1. PURPOSE OF INVESTIGATION

The majority of conventionally produced powder metallurgical components possess inferior mechanical properties to those made from wrought fully-dense material. Although it is well known that this effect is associated with the presence of porosity in the former, there is also some evidence that the heterogeneity of compacts prepared from blended mixtures of elemental powders is also a significant factor. The use of coated powders enhances the degree of homogeneity of steels, subject to a specific sintering treatment and there is some evidence that 3% nickel steels prepared from such material have superior tensile strength than similar material prepared from blended mixtures of elemental powders.

The purpose of the present investigation is to:-

- (i) Develop an electroplating technique which will enable a coating of nickel to be deposited on iron powders using a three-phase fluidised bed.
- (ii) To examine the mechanism by which this deposit is produced.
- (iii) To investigate the relationship between modulus of rupture, degree of homogeneity, microstructure and porosity in a series of steels containing up to 4.25% nickel.

(iv) To assess the suitability of nickel-coated iron powders for use in the production of sintered low-alloy steels.

CHAPTER TWO  
REVIEW OF LITERATURE

## 2. REVIEW OF LITERATURE

The present investigation has been divided in the following two sections:-

- (i) Development of a plating cell to electrodeposit nickel onto iron powders
- (ii) Assessment of the mechanical properties of sintered compacts produced from such powders.

Since, the fundamental principles of electrodeposition of nickel have been adequately covered in standard text books<sup>(1-6)</sup> and review papers<sup>(7-8)</sup>, the present review of literature is restricted to those aspects most pertinent to this investigation.

### 2.1 POLARISATION

A passage of current disturbs the electrode from its equilibrium condition; this disturbance of equilibrium associated with the flow of current is called electrolytic polarisation<sup>(4)</sup>. Polarisation results from the slowness of one or more of the processes occurring at the electrodes and the type of polarisation depends on the nature of the slow process. In general, polarisation can be of the following three types<sup>(1,4,7,9)</sup>

- (i) Activation polarisation
- (ii) Concentration polarisation
- (iii) Resistance polarisation

(i) Activation polarisation:- This can be described in terms of the activation energy required for any reaction to occur<sup>(5,7,10)</sup>. Cathodic activation polarisation tends to shift the energy level of ions in the double layer towards the potential barrier and thus allows more ions to cross the double layer per unit time in order to form a deposit. On the other

hand, at the anode, the energy level of the lattice ions is shifted away from the barrier level, thus decreasing the rate of dissolution of the metal. Activation polarisation is a logarithmic function of the current density as given by Tafel's equation

$$\text{act.} = a - b \log i \quad (\text{EQ 2.1})$$

(ii) Concentration polarisation:- This accounts for the major part of the polarising potential and occurs as a result of concentration changes in the vicinity of the electrode. At the anode, the dissolution reaction results in an increase in the concentration of metal ions and consequently numerically increases the potential of the electrode. The extent of this increase is governed by the current density. Similarly, at the cathode, deposition of the metal decreases the concentration of metal ions in the double layer and thus lowers the equilibrium potential. Agitation of the electrolyte serves to decrease the concentration gradient and therefore should also decrease concentration polarisation. However, it is widely accepted<sup>(2,7)</sup> that forced convection only indirectly helps to reduce concentration polarisation by decreasing the thickness of the diffusion layer and that only diffusion transport can supply the metal ions in the electric field.

(iii) Resistance polarisation:- This is the overvoltage required to cause a flow of current through the ohmic resistance of the electrolytic solution - the product of the current flowing and the resistance of the solution. This overvoltage is further increased in the presence of oxide films that cause passivation of anodes<sup>(4,9,11-13)</sup>.

The sum of the above mentioned forms of polarisation constitutes the total overvoltage required to maintain the

flow of a steady current through the tank.

## 2.2 ANODIC PASSIVITY

If the equilibrium potential of a metal in contact with its oxide is less than that of the metal in an electrolytic cell, an oxide film is formed on the surface of the metal, rendering it passive.

Figure 1 shows the relationship between anodic current and potential for metals which exhibit the passivity phenomenon. Passivation occurs at the flade potential with the formation of an absorbed oxygen layer and an exchange of electrons with freshly formed metal cation leads to the gradual build up of the oxide layer<sup>(11)</sup>. As this film grows in thickness, the potential drop across the film increases to the value at which oxygen evolution or the dissolution of metal in higher valency forms takes place.

Passivity is usually considered to involve two basic mechanisms - mechanical passivity and chemical passivity. The dissolution of the metal and the migration of hydrogen away from the anode results in saturation of the solution in the vicinity of the electrode. Consequently precipitation of a metal salt occurs on the anode. This reduces the effective surface area of the anode and leads to increased current density, which favours reactions other than metal dissolution (e.g. discharge of hydroxyl ions). Studies of the anodic behaviour of iron in 40% NaOH at 70°C have shown that iron dissolves as  $Fe^{++}$  ions at a potential of -0.85 volt. However, a slight increase in current density (0.0083 ampere/cm<sup>2</sup>) covers the anodic surface with a black oxide layer and the potential increases abruptly to 0.63 volt. This film then becomes brown (formation of  $Fe_3O_4$ ) and oxygen evolution occurs<sup>(12)</sup>.

However, in the case of chemical passivity, the passive film is generally not visible. Chemical passivity produces a permanent change in the anode surface and makes it behave as a more noble metal. Certain oxides, such as  $\text{Fe}_3\text{O}_4$ , although normally soluble in acidic solutions, are also known to be insoluble in certain forms - e.g. after heating<sup>(11)</sup>.

Anodic dissolution of nickel has received considerable attention in electroplating literature and has been well reviewed by Hoar<sup>(14)</sup>. Although it has been established that non-activated nickel anodes show a strong tendency to become passive, the mechanism of anodic passivation is not totally clear and there is disagreement regarding the number of steps involved in the process. Gabe<sup>(9)</sup>, in a discussion of nickel anode materials suggested that the tendency of nickel in the unactivated condition to become passive was effectively inhibited by the presence of chloride ions. However, Hart<sup>(13)</sup> reported that non-activated nickel anodes became passive readily even in the presence of chloride ions. He was of the opinion that passivation had occurred in two to three steps depending upon the solution. In the presence of chloride ions, non-activated nickel dissolved when a sufficiently noble potential was reached and the dissolution occurred through pit initiation and growth<sup>(15,16)</sup>, which ultimately led to uneven dissolution and a spongy residue.

The increasing use of chloride free baths based on sulphamate or fluoborate compounds has led to the use of depolarised or sulphur-activated nickel. The value of the additions of chloride ions is not clear but most nickel plating solutions usually contain small quantities of nickel chloride; for example, the Ni-speed sulphamate bath contains 5 g/l of nickel chloride. Saubestre<sup>(17)</sup> suggested that nickel chloride

may exist in solution in an intermediate form, such as  $\text{NiCl}_2 (\text{H}_2\text{O})_3^+$  which assisted anodic corrosion. However, the presence of chloride ions in high concentrations is associated with an increase in the stress level in the deposits; therefore this constituent should be avoided if a low stress level is necessary. Di Bari and Petrocelli<sup>(18)</sup> studied the effect of various elements on the anodic dissolution of nickel and concluded that sulphur produced the greatest improvement in the anodic dissolution of nickel. The results of various other workers<sup>(18-21)</sup> have confirmed this view point. Fischer and Morris<sup>(19)</sup> were of the opinion that the sulphur contained in the anode in the form of nickel sulphide dissolved in the plating solution with the simultaneous formation of sulphur containing compounds, which prevented passivation of nickel anodes.

In a recent review, Parkinson<sup>(22)</sup> has compared the performances of the two most commonly used nickel anode materials - electrolytic nickel and sulphur depolarised nickel (S-Nickel)\*. Electrolytic nickel in titanium baskets offers the advantage of high purity, minimum amount of residue and efficient dissolution in almost all commonly used nickel plating solutions. The presence of chloride ions is a necessity when using electrolytic nickel anodes but this does not impose any serious handicaps, since most commonly used nickel plating baths contain a sufficient level of chloride ions. Although sulphur-depolarised anodes have the advantage of lower anode potentials and tank voltages, this is obtained at the cost of higher impurity levels in the anode and residue. These are detrimental to the quality of the coating. The residue formed from S-nickel anodes is 0.18% of the weight of nickel dissolved as compared to 0.01-0.05%

---

\* S-Nickel - Nickel shot containing 0.05% sulphur.

in the case of electrolytic anodes. The fineness of the residue in the former case causes additional problems for the electroplater and demands more careful anode maintenance<sup>(22)</sup>.

### 2.3 NICKEL PLATING SOLUTIONS

Over the years a large number of nickel plating baths have been suggested, the more important of which are given below:

- (i) Watts type baths
- (ii) Chloride or chloride-sulphate baths
- (iii) Fluoborate baths
- (iv) Sulphamate baths

There are three basic ingredients in all such solutions; a nickel salt to provide the required nickel ions, a buffering agent to maintain the optimum pH level, and addition agents to control pitting, to provide a bright deposit and to assist anode dissolution. Table 1 lists the most widely used nickel plating baths and gives a range of concentrations for each constituent. In most cases the range is not very critical although optimum conditions are only obtained within the stated limits. Table 2 presents a comparison of the conditions under which the important nickel plating baths are operated. The data has been compiled from the data published by various workers.<sup>(23-29)</sup>

(i) Watts type baths:- Saubestre<sup>(17)</sup> has discussed the chemistry of the Watts type baths in terms of its individual constituents. Nickel sulphate, which is the major source of nickel ions in a Watts bath, is preferred because of its cheapness, high solubility (570 g/l at 50°C), and its stable anion. In spite of the high solubility of nickel sulphate, commercial Watts type baths do not contain more than 400 g/l.

A high metal ion concentration is desirable since this ensures a high limiting current density (l.c.d.)\*. However, very high concentrations lead to crystallisation and excessive losses resulting while the plated object is removed from the tank. The chloride ions present in the Watts solution have the effect of increasing the conductivity and throwing power\*\* of the solution that results from the increased cathode efficiency<sup>(17,30)</sup>. The chloride ions also improve anode dissolution through the formation of chloro and aquo-complexes<sup>(17)</sup>. Boric acid, the third important constituent of the Watts bath, acts as a weak buffering agent which controls the pH of the bath. In its absence the deposits tend to be hard, cracked and pitted. However, some authors have obtained good deposits from boiling electrolytes that were unbuffered<sup>(31)</sup>.

Current densities greater than  $10 \text{ A/dm}^2$  are generally uncommon but can be obtained with an increase in agitation, temperature, and the ratio of chloride to sulphate ions. Cathode current efficiency of the Watts bath is comparable to any other nickel plating solution and is of the order of 97 to 99%<sup>(28)</sup>. Nevertheless, pitting occurs from slowly forming hydrogen bubbles, and anionic wetting agents have to be employed to control pitting in these baths. Anode current efficiency is dependent on the chloride content and is generally high in the case of the commonly used Watts-type

---

\* l.c.d. - The maximum current density beyond which a burnt deposit is obtained.

\*\* Throwing power of a bath is defined as the ability of a bath to produce deposits of more or less uniform thickness on cathodes having irregular surfaces.

solutions. The throwing power of these solutions is relatively poor when compared to the chloride and sulphamate baths<sup>(26,27,32,33)</sup> and approximately the same as that of the fluoborate bath<sup>(24,34)</sup>. This has been attributed to the relatively high specific resistance of the Watts bath in comparison to the other commonly used solutions<sup>(28)</sup>.

The hardness of the deposits can be varied over a considerable range by variation in the pH of the solution. The deposits are also very highly stressed and the stress level increases with an increase in both current density<sup>(27)</sup> and the chloride content of the bath. However the low cost and simplicity of these baths make them very attractive to the commercial electroplater.

(ii) Chloride baths:- Nickel plating solutions that possess a high chloride to sulphate ratio are used for certain purposes such as high speed bright nickel plating and heavy nickel plating. All the solutions in this category possess low resistivity, good throwing power and permit the use of high current densities<sup>(28,30)</sup>. The deposits from these baths possess higher tensile strength and lower ductility than those obtained from the Watts type solutions. The deposits are generally highly stressed and hard<sup>(35)</sup>, although Kendrick<sup>(36)</sup> has shown that the use of an a.c. power source, at high frequencies, can provide deposits that are soft and ductile with low internal stresses. Anode and cathode efficiencies are approximately 100% and the deposits have less tendency to form pits or trees. The maintenance of these baths is fairly simple since there are basically only two constituents - nickel chloride and boric acid.

(iii) Fluoborate baths:- The high solubility of nickel fluoborate makes this system very versatile and bath composition

can be chosen to meet a variety of requirements. Roehl and Wesley<sup>(23)</sup> suggested that an optimum bath composition of 300 grams per litre of nickel fluoborate and 30 grams per litre of boric acid may be operated at pH values between 2.7 and 3.5 (calorimetric) and at a temperature of 54°C. However, baths with higher nickel fluoborate concentration are also used whenever heavy nickel plating using high current densities is desired<sup>(24)</sup>. The resistivity of the fluoborbate baths, at equal metal concentration, is approximately half that of the Watts bath and equal to that of the chloride bath. Struyk and Carlson<sup>(24)</sup> have demonstrated the superiority of the buffering characteristics of fluoborate baths. Anode corrosion is very good without the addition of chloride ions, the presence of which tends to cause pitting of deposits and increases the internal stress. In the absence of chloride ions, the deposits from the fluoborate bath are ductile, smooth and with low internal stress. The throwing power of the fluoborate barrel plating solution has been shown to be as good as the sulphate-chloride bath<sup>(34)</sup>. The addition of ammonium fluoborate reduces the resistivity of the baths and also improves its throwing power.

However, nickel fluoborate baths have found very limited application on account of the high cost of the salt, although easy control and maintenance of this bath is of interest for special applications; where the high initial cost can be justified. Another disadvantage in the use of fluoborate baths is their incompatibility with titanium anode baskets which are so commonly used with other nickel plating solutions.

(iv) Sulphamate baths:- Although the use of sulphamate solutions for nickel plating was first suggested about 35 years ago<sup>(37)</sup>, their commercial application did not begin until 1949.

Numerous papers<sup>(25-27, 39-41)</sup> have been published since then on the operating characteristics of baths containing this material. Hammond<sup>(26)</sup> has comprehensively reviewed the various nickel sulphamate solutions that have been suggested and the properties of the deposits obtained from their use. However, the high initial cost of this solution has restricted its applications to areas which can justify the extra cost.

Nickel sulphamate  $\text{Ni}(\text{NH}_2\text{SO}_3)_2$ , the basic constituent of this bath, has a very high solubility<sup>(41)</sup> which enables the use of very high current densities with a consequent increase in the rate of deposition. The concentration of boric acid is not very critical but Ericson<sup>(42)</sup> recommended a high concentration of boric acid (40 g/l) in order to reduce hydrogen pitting which is frequently encountered with the use of sulphamate solutions. The addition of nickel chloride to the sulphamate solution is still subject to controversy<sup>(25-27,43)</sup>. Barrett's<sup>(25)</sup> sulphamate bath, although it contains no chloride ions, has been reported to give approximately 100% anode efficiency. However, several other workers<sup>(26,27)</sup> report anode passivation in the absence of nickel chloride. Fanner and Hammond<sup>(43)</sup> recommend an addition of 3.3 g/l of nickel chloride to ensure efficient anode corrosion. However, in general, the concentration of nickel chloride in sulphamate baths varies within the range of 5 to 30 g/l.

Kendrick<sup>(27)</sup> investigated the effect of nickel sulphamate concentration on the limiting current density (l.c.d.) and the stress level in the deposits. He concluded that 600 g/l of nickel sulphamate was the optimum concentration since this composition gave deposits with the lowest value of internal stress and the highest limiting current density (43 A/dm<sup>2</sup>). The cathode efficiency of the conventional sulphamate bath

(300 g/l of nickel sulphamate) was found to be similar to that of both the Watts bath and the 'Ni-speed' concentrated sulphamate bath (600 g/l of nickel sulphamate). Opinions regarding the throwing power of the sulphamate bath vary, although it is generally agreed that it is superior to the Watts bath<sup>(26,27)</sup>. Watson<sup>(32)</sup> reported that sulphamate solutions had inferior throwing power to the chloride and fluoborate baths but were superior in this respect to the Watts bath.

The effect of current density on the hardness of the deposit has been investigated by several authors but the results are not in complete agreement. Kendrick<sup>(27)</sup>, and Marti and Lanza<sup>(44)</sup> found that the hardness was reduced by an increase in current density but Diggin<sup>(45)</sup> found the reverse effect. This disagreement may have been due to the difference in the technique of hardness measurement of the two workers. The effect of the pH of the solution on the hardness of the deposit was also investigated by Fanner and Hammond<sup>(43)</sup> and Marti and Lanza<sup>(44)</sup>, who found that there was a sharp increase in hardness when the pH of the solution rose above 5.0. The above authors were also in agreement about the effect of temperature on hardness of the deposit. They found that an increase in temperature of the solution above 38°C resulted in a slow increase in hardness but below this temperature the hardness increased sharply as the temperature was reduced. This effect was not observed by Diggin<sup>(45)</sup>

The internal stress of the deposit from the sulphamate solution can be varied over a wide range depending on the chloride content and other operating variables such as current density, pH and temperature. Thus an increase in current density raises the tensile stress in the deposit<sup>(26,27,43,45,46)</sup>.

Although, the rate of increase in stress produced by an increase in current density was found to be the highest in the case of the concentrated sulphamate bath, the values were always lower than those obtained from the Watts bath<sup>(27)</sup>. The minimum internal stress of the deposits was obtained by the use of a pH between 4.0 and 5.0, although it increased sharply when the pH of the solution lay above or below this range<sup>(43,47)</sup>. The effect of temperature on the internal stress is not quite clear. Marti<sup>(47)</sup>, who used a chloride free sulphamate bath, found that the stress was reduced when temperature was increased and became compressive at about 49°C whereas both Fanner and Hammond<sup>(43)</sup>, who used a low chloride bath and Diggin<sup>(45)</sup>, who used a high chloride solution, obtained the minimum stress at 50°C and 43°C respectively. Kendrick<sup>(27)</sup>, who worked with a concentrated sulphamate bath that contained 5 g/l of nickel chloride, observed a similar effect to that observed by Marti<sup>(47)</sup>.

#### 2.4 COATING OF POWDER PARTICLES BY ELECTROLYTIC METHODS

In order to obtain an even coating on each individual powder particle, it is necessary to maintain the powder particles freely suspended in the coating solution, so as to ensure complete exposure of the total surface area of the powder particles to the coating process. This condition can be achieved using a fluidised bed electrode.

Extensive studies of the performance of fluidised bed electrodes have been carried out in the recent years and the clear advantages of using such electrodes for processes such as electrowinning have been established<sup>(48-59)</sup>

The possible mechanisms for charge conduction within a fluidised bed electrode are:-<sup>(49)</sup>

(i) Electrolyte phase conduction.

(a) ionic conduction within the electrolyte as a result of migration of ions under the influence of an electric field.

(b) ionic conduction together with short circuiting of the conduction paths through the particles (Fig. 2a)

(ii) Electronic phase conduction.

(a) electronic conduction through particles in contact (Fig. 2b)

(b) a 'conductive mechanism' - the electric double layer of the particle becomes charged by contact with the current feeder or another particle and then moves to a different part of the bed and discharges either by charge sharing with another particle or by electrochemical reaction (Fig. 2c)

Backhurst et al<sup>(48,50)</sup> also suggested that charge conduction within fluidised bed electrodes is largely through electronic phase conduction. They also pointed out that although fluidisation is normally brought about by the electrolyte, gas flow through the powder electrolyte slurry could also be successfully used. Foster and Kariapper<sup>(60)</sup>, working on the production of composite nickel plating, found strong absorption of nickel ions onto the alumina particles, thus giving them a charge which attracted them towards the cathode where they were co-deposited with nickel. However, in the case of copper plating, the alumina particles were not charged unless thallium or rhodium ions were added to improve surface absorption.

Sabacky and Evans<sup>(49)</sup>, who investigated the electrical

conductivity of fluidised bed electrodes, were of the opinion that it was the effective electrical conductivity of the particulate phase which was of major importance. They found that beds that contained particles of low conductivity produced poor power and current efficiencies. Furthermore, they also observed excessive reactions at the current feeder and cell divider when the bed contained particles possessing much greater conductivity than the electrolyte itself. However, under the conditions of their investigation, the resistivity of the bed was always less than that of the parent electrolyte. The results also showed that, although the resistivity was relatively independent of particle size, it was strongly dependent on the expanded bed height. Sabacky and Evans found that their experimental results on bed resistivities did not agree with results predicted by the models of earlier workers<sup>(61)</sup> this misfit was attributed to the omission of electronic phase conduction in the earlier models.

Flett<sup>(51)</sup> found that as the expanded bed height increased, the cell current increased to a maximum point beyond which any increase in the bed height resulted in a decrease in cell current. Under their experimental conditions, a 33% bed expansion was found to be the optimum. Similar findings have been reported by Backhurst et al<sup>(50)</sup> and Kreysa and Heitz<sup>(54)</sup> They suggested that the relationship between cell current and bed expansion was due to the greater surface area available on fluidisation as compared to a static bed. However, as fluidisation was increased further a loss of electronic contact occurred which eventually outweighed any advantage gained by an increase in surface area.

The advantages obtained by the use of a denser bed initiated investigations into the field of pseudo-fluidised bed electrodes

that were stimulated ultrasonically<sup>(53)</sup>. In continuously operated processes, such electrodes offered the advantages of high residence times and better extraction efficiencies by the use of velocities insufficient to produce fluidisation. These electrodes also overcome the problem of 'bridging' caused by plating in the high density conventional fluidised bed electrodes.

The limiting current density can be increased by an improvement in the mass transport process which in turn can be improved by using fluidised bed electrodes<sup>(56)</sup>. Mass transport within a fluidised bed electrode, has also been shown to be strongly dependent on bed expansion and a maximum has been reported for bed voidage within the range of 0.52 to 0.65<sup>(56)</sup>. This again emphasises the advantages of using a denser bed.

Stainless steel powder has been coated with iron or nickel using a fluidised bed plating cell<sup>(62)</sup>. Although, the mechanism of electrodeposition of a metal onto powders was not clearly explained, it was suggested that the deposition occurred either by direct contact with the current feeder or through a chain of particles. The apparatus used for coating stainless steel powder by electrolytic means is shown in Fig. 3 and the operating conditions of the laboratory scale plant are given in Table 3.

## 2.5 ALTERNATIVE METHODS OF COATING POWDERS

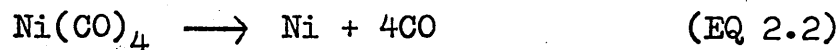
The various methods of coating powders may be classified in three basic sections, depending on the phase from which the deposition has taken place -

1. Vapour phase deposition
2. Liquid phase deposition
3. Solid phase deposition

Vapour phase deposition may be further divided into three major sections:- (63)

- (a) Thermal decomposition
- (b) Displacement from vapour phase
- (c) Hydrogen reduction of vapours.

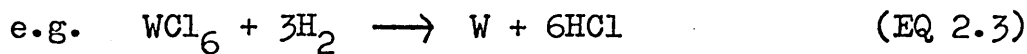
Thermal decomposition of carbonyl vapours of metals such as iron, nickel, chromium and some platinum group metals have received considerable attention<sup>(64,65)</sup>. The Mond process for nickel production utilises this principle.



The carbonyl vapour is led into a chamber where the powder to be coated is held in suspension by the passage of an inert gas. This chamber is maintained at the temperature ( $\sim 166^\circ\text{C}$ ) at which the vapours decompose and deposit the metal onto the suspended powder particles.

The contact of a metal-bearing vapour with a base metal can result in a displacement reaction which induces the coating of the base metal with the metal in the vapour. However, such a reaction requires a sufficiently high temperature, so as to ensure rapid diffusion of the base material through the deposited layer to the surface at which the reaction takes place. This method can be used to coat iron and steel with metals such as chromium, zinc and manganese. However, powders coated in this manner exhibit a steep concentration gradient in the radial direction, as compared with a sharp discontinuity in powders coated by the other methods.

Hydrogen reduction of many volatile halide vapours has been shown to be a useful method by which powders may be coated with metals such as nickel, iron, cobalt and tungsten<sup>(63)</sup>

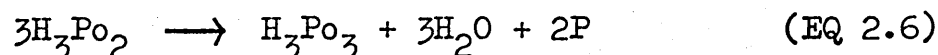
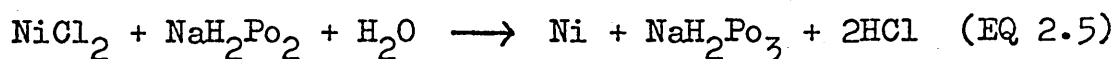
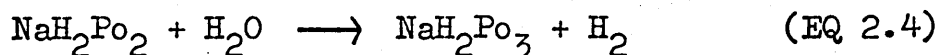


This method can also be used to deposit metal alloys by the use of the required mixture of halide vapours. All vapour phase deposition processes require that the powder to be coated be in continuous motion so as to expose their entire surface area to the vapour. This is normally achieved by the fluidisation of the powder using the reacting vapour as the fluidising gas. However, in the hydrogen reduction process, the sintering of the powder particles and undesirable reactions between powder substrate and the reacting vapour have been considered to be major drawbacks<sup>(66)</sup>

The three main types of liquid phase deposition process, apart from electro-coating, are:-

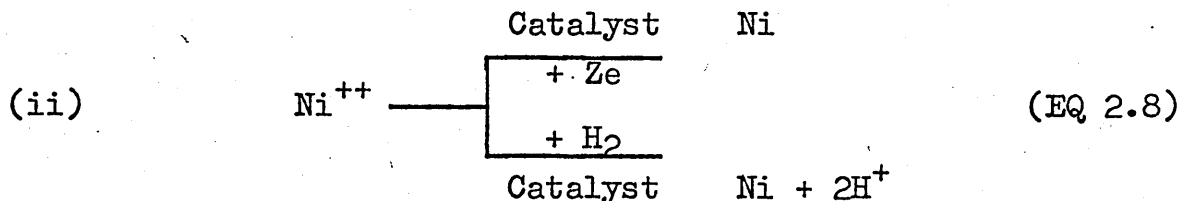
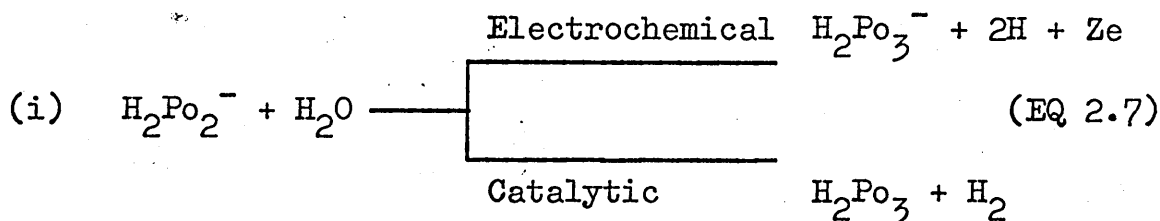
- (a) Electroless deposition
- (b) Hydrogen reduction
- (c) Chemical displacement (cementation)

(a) Electroless deposition:- This is a process of chemical reduction and has been used for plating many metals including nickel. Although, the mechanism involved in electroless plating has received considerable attention, there is a great deal of controversy regarding the intermediate steps involved in the mechanism<sup>(67-70)</sup>. The basic reactions may be represented as follows:-



Gouda et al<sup>(71)</sup> have reviewed the various mechanisms proposed and on the basis of their own investigations have put

forward a mechanism involving both electrochemical and catalytic decomposition of the hypophosphite viz:-



The rate of deposition of electroless nickel is relatively low in comparison with electrolytic deposition. However, it has an advantage of the form that it produces a more uniform coating, even on intricate shapes. The rate has been found to vary between 10 and 25  $\mu\text{m/hr}$ <sup>(72)</sup> depending on the freshness of the solution. Murksi<sup>(73)</sup> observed a fall in the rate of deposition when the size of the load was increased. It was therefore suggested that large loads can only be plated for short periods and in such cases only thin coatings were possible. The problems associated with the coating of large objects were also pointed out. Greenwood<sup>(74)</sup> recommended a load of 1  $\text{dm}^2/\text{l}$  for optimum results. However, Gouda et al<sup>(71)</sup>, who studied the effect of surface area on the rate of deposition of nickel onto iron powder, found that both the rate of deposition and hydrogen evolution increased with increase in the total surface area of the iron powder within the solution. A similar effect was observed when an increase in surface area was effected by an increase in the total mass of powder (107  $\mu$  size) within the solution. However, Gouda et al<sup>(71)</sup> used very small quantities of powder (0.1-0.5 g) in approximately 400 ml of

solution and it would be of considerable interest to determine whether large quantities of powders could be coated using a denser bed than that used in their experiments. Rao et al <sup>(75)</sup>, who used 5 to 15 g of iron powder in 200 ml of solution, observed that:-

- (i) An increase in the amount of reducing agent from 2.0 to 2.8 g resulted in an increase in the nickel content of the coated powder from 7.14% to 10.57%.
- (ii) An increase in the mass of powder input from 5 to 15 g resulted in an increase of the process efficiency from 28.2 to 53.7% as compared to the maximum efficiency for solid objects of 36%. The increase in process efficiency was probably associated with an increase in the amount of surface area available for plating.

Rao et al <sup>(75)</sup> also studied the effect of time on the amount of nickel deposited on tungsten powder but observed no increase in nickel content after the first thirty minutes of plating. However the additions of fresh solution increased the plating rate.

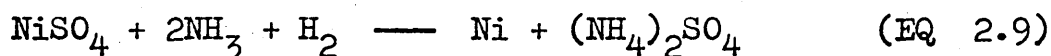
Electroless nickel deposits are generally hard <sup>(76-78)</sup> but, in the case of composite powders which need to be compacted to high density values, hard coatings can be detrimental. Lunyatskas <sup>(78)</sup> found that hardness values of electroless nickel deposits, in the un-heat treated condition, range between 300-600 kg/mm<sup>2</sup> depending upon the operating conditions, as compared to 190 kg/mm<sup>2</sup> for nickel electrodeposited using the nickel sulphamate solution.

Feldstein and Amodio <sup>(79)</sup>, who examined the effect of agitation on electroless deposition on activated surfaces, showed that agitation could result in a reduced plating rate, particularly at lower operating temperatures and in mechanically

stirred tanks. This decrease was primarily associated with a reduction in the deposition rate during the early stages of deposition but once a continuous layer was formed the effect of agitation was far less pronounced. However, when iron powder was used as substrate for electroless nickel deposition, a thin coating of nickel was rapidly deposited, as a result of chemical displacement reactions.

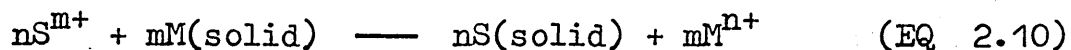
The control of electroless plating baths is more complex than is the case with electroplating baths. Furthermore, the former also possesses higher operating costs and poor efficiency (33-37%)<sup>(74,80)</sup>. It is for these reasons that application of electroless nickel plating is restricted to special applications only.

(b) Hydrogen reduction:- The hydrogen reduction of an ammonical solution of nickel ammonium sulphate is one of the most widely accepted processes for the preparation of composite powders containing nickel<sup>(81,82)</sup>. A typical solution for this process contains 40 to 50 g of nickel, 200 to 400 g of ammonium sulphate and 20 to 30 g of free ammonia per litre of solution. The reduction is carried out in autoclaves at 180 to 210°C and under a positive hydrogen pressure of 0.21 to 0.35 kg/mm<sup>2</sup>. The basic reaction taking place may be represented as follows:-



A detailed examination of the mechanisms and kinetics of the above mentioned process has been presented by Burkin<sup>(83)</sup> who suggested that the powders to be coated should be kept in suspension by mechanical agitation and should therefore receive a uniform covering of the metal in solution. Powder particles as small as 1 µm could be coated uniformly by this process.

(c) Chemical displacement:- Another possible method that may be used for coating powders involves the cementation reaction. Such a reaction occurs when the electrode (reduction) potential of the metal M in the solution of  $M^{n+}$  ions is more negative than that of the metal S in a solution of its ions. The reaction may be chemically represented as follows<sup>(84)</sup>:-



In a review of composite metal powders Prema and Rao<sup>(85)</sup> discussed the commercial application of the cementation process for the production of copper coated lead powders (60%Cu - 40%Pb). The preparation of copper coated iron powder was also mentioned. In a recent report (1978) Schaleh et al<sup>(86)</sup> studied the influence of cupric ion concentration, total mass of copper deposited, temperature and the addition of thiourea on the rate of cementation of copper on an iron substrate. The rate was found to be independent of cupric ion concentration when the total mass of copper deposited was limited to  $0.584 \text{ mg/cm}^2$ . However, for greater quantities of copper deposited ( $3.63 \text{ mg/cm}^2$ ) the rate was found to be strongly dependent on cupric ion concentration. They also found that the rate of cementation was retarded by the addition of thiourea, which is known to produce a denser deposit in the electrodeposition of copper. The authors were of the opinion that the rate of dissolution of the iron substrate was the rate controlling step and consequently denser deposits led to slower rates of deposition. Although the cementation of nickel onto an iron substrate is also theoretically possible, the kinetics of the reaction is such that it is considered impracticable. Wesley and Copson<sup>(87)</sup> observed that when a well cleaned steel was immersed in a solution of nickel chloride at  $70^\circ\text{C}$  (pH 3.5 - 4.5). a thin

coating of nickel was obtained. The thickness increased with time, although the rate of deposition decreased as the reaction continued and it was impractical to deposit coatings much thicker than 0.75  $\mu\text{m}$  commercially. The authors suggested that the iron dissolved in the solution as a result of the replacement reaction should be regularly removed and the ferrous ion content of the bath should be kept below 5 g/l. In an unpublished report, Rigg<sup>(88)</sup> has shown that it is possible to coat iron powder with nickel by making use of the cementation reaction (EQ 2.10). Rigg used a solution of nickel chloride and emphasised that the temperature and pH of the solution should be carefully controlled if optimum results were desired. Nickel deposits of up to 50% were claimed but the continuity of the coating was not discussed.

## 2.6 APPLICATIONS OF COMPOSITE POWDERS

Although a number of methods have been developed for the coating of powder particles, the applications of such powders have been very restricted and specialised. One of the most striking applications is the use of pyrolytic graphite coated fuel element spheres in a pebble bed reactor. Other well established applications lie in the fields of flame spraying and degassing of steel by nickel coated teflon.

The use of composite powders significantly increases the rate of homogenisation and the strength of sintered compacts when compared to compacts prepared from mixtures of elemental powders<sup>(89,90)</sup>. These powders do not show any tendencies of segregation during processing. These advantages clearly show the potentials of composite powders in the field of alloying.

Many possible applications of composite powders, including production of dispersion strengthened materials and porous strips, have been discussed by several workers<sup>(82,83)</sup>.

## 2.7 THE PRODUCTION OF LOW ALLOY STEELS FROM METAL POWDERS

### 2.7.1 Characteristics of Iron Powder

The physical and chemical properties of powders have a strong influence on the characteristics of the material during pressing and sintering. Zapf<sup>(91)</sup> has shown that even small percentages of alloying constituents and non-metallic admixtures present in commercial iron powders have a deleterious influence on compressibility. Thus reduced iron and atomised powders were found to be less compressible than high purity electrolytic iron powder and consequently possessed lower strength after identical sintering treatments. However, when the above three powders were compared at identical densities, the strengths of the compacts made from electrolytic iron powder were lower than those made from the other two powders.

Zapf<sup>(91)</sup> has also discussed the effects of hydrogen loss, screen analysis and particle shape and size on the pressing and sintering behaviour of commercial iron powders. He pointed out that oxidation of green compacts increased sinterability in contrast to the decreased sinterability of pre-oxidised powders. This was ascribed to the fact that oxidation of green compacts did not alter the existing metallic bridges and only tended to activate the remainder of the powder surface. Zapf<sup>(92)</sup>, in a separate paper, also evaluated the influence of powder type on the mechanical properties of hot recompact iron-0-10% nickel alloys. He found that the best mechanical properties were achieved using electrolytic iron powders. Reduced iron powder (MH300) had comparable strength but slightly lower ductilities. Although water atomised iron powder was not included in this investigation, the author believed that it would give properties similar to electrolytic iron powder.

Krishnamoorthy<sup>(93)</sup> studied the influence of the type of iron powder on the properties of sintered iron within the density range of 6.8 - 7.87 kg/dm<sup>2</sup>. He concluded that the use of carbonyl iron powder generally gave the best mechanical properties. The strength values of fully dense compacts were similar for all types of powder except the carbonyl iron. Although, the latter had the highest strength at lower densities, it had the poorest tensile strength in the fully dense condition. It was suggested that this was due to the porous compacts ability to pick up carbon from the admixed lubricant and thus have greater strength. The fully dense compacts were unable to absorb carbon from admixed lubricant and therefore gave relatively poor tensile strengths. Amongst the other powders, electrolytic and high purity atomised powders gave the best compressibilities, tensile ductilities and impact strengths. However, the high purity of these powders produced relatively poor tensile strengths at any given density. The highest strengths were obtained with normal purity atomised powder, although this was coupled with poor ductility. However, Krishnamoorthy<sup>(93)</sup> also pointed out that the behaviour of the powders investigated could alter when alloyed with carbon or other alloying elements.

Squire<sup>(94,95)</sup> reported that both reduced and electrolytic iron powder of similar mesh sizes exhibited similar strengths and ductilities and that there was an improvement in strength levels when finer powder was used. Cundill et al<sup>(96)</sup> confirmed that the tensile strength of samples made from various types of powders, including atomised powder, were essentially similar but that the ductility and impact strength were to a certain extent dependent on powder type.

Electrolytic powder gave the best ductility and water atomised iron powder the best impact resistance. Hulthen<sup>(97)</sup> has pointed out that the evaluation of different iron powders on the basis of compressibility can be very misleading. He examined four types of iron powder that possessed different specific surface areas and found that the powder with the lowest specific surface area had the highest compressibility although the green strengths of compacts made from this powder were very low. The strength of sintered low alloy steel compacts were shown to increase as the specific surface area of the base iron powder increased. However, very high specific surface area was also found to be detrimental on account of large dimensional changes and low apparent density. Hulthen then went on to evaluate the different types of iron powder on the basis of relative material requirements and raw material costs and concluded that reduced sponge iron powder was the most economical choice for sintered density levels of up to  $7.2 \text{ kg/dm}^2$ .

Esper et al<sup>(98)</sup> studied three different types of plain iron powders e.g. sponge iron, atomised and electrolytic iron powder, in relation to their pressing and sintering behaviour. Their results showed that, in spite of some pronounced differences in the sintering behaviour of the three types of iron powders investigated, the associated variation in the mechanical properties was of little significance for all practical purposes.

The sintering behaviour of three types of iron powder (carbonyl electrolytic and sponge iron powder) was examined by Poster and Hausner<sup>(99)</sup>, who reported that carbonyl iron powder compacts produced the highest density when sintered

at 870°C. Furthermore the density decreased as the sintering temperature was raised. The strength values of the compacts made from carbonyl iron powder were higher than those made from the other two powders, after sintering at any temperature, although a maximum was again observed after sintering at 870°C. A major reason for the very high strengths of the compacts made from this material was the small particle size (-325 mesh) which led to small individual closed pores even at relatively low densities. This fine powder also contributed to the small grain size, which also increased the strength of the sintered compact.

A similar study, that involved a comparison of sintering behaviour of atomised and carbonyl powder was carried out by Lenel et al<sup>(100)</sup>. They also reported that the rate of sintering was much faster in the case of compacts made from carbonyl iron powder. The relatively poor sinterability of atomised powder was the result of the particle size and the contaminated surface of the atomised powders used. However, the cost of carbonyl and electrolytic iron powders is prohibitive for most applications despite their superior properties. Thus, for economic reasons, sponge iron and atomised iron powders are the most widely used material in the powder metallurgy industry.

### 2.7.2. Mixing of Powders

Several authors<sup>(101-103)</sup> have expressed the view that improper mixing can offset the benefits of deliberate use of fine alloy powders for the purpose of rapid homogenisation during sintering. Dixon and Clayton<sup>(102)</sup> pointed out that consistent results from pressing and sintering operations could only be expected when consistent uniform mixtures of

powders were used. Although a great deal of importance has been attached to the mixing process, Marshall<sup>(104)</sup> (1968) and Hausner<sup>(105)</sup> (1970) pointed out that the mixing process was not fully understood and that the present state of knowledge was insufficient to allow the prediction of the optimum mixing conditions for any given powder.

Goetzl<sup>(106)</sup> pointed out that mixing of metallic powders was influenced by several factors, viz., specific gravity, particle shape and size, structure and surface condition of the particles and the type of mixing equipment. Hausner<sup>(105)</sup> in a review of the mixing process, expressed the view that mixing was predominantly governed by friction within the powder mass which in turn was dependent on powder characteristics such as particle shape, size and surface condition. His preliminary investigations confirmed this view point and showed that the degree of mixing of a powder mass increased as the friction within the mass was reduced, although a reduction in the amount of friction also facilitated segregation. These conflicting processes allowed a low-friction powder mixture to reach a state of maximum mixing very rapidly, after which the process of segregation became dominant. This led to poorer homogeneity of mixing after the use of prolonged mixing times.

Marshall<sup>(107)</sup>, in a review of the production of powder metallurgy parts, referred to the various types of industrial mixers designed to give optimum mixing in as short a time as possible. He pointed out that long mixing times were not only uneconomical but that they could alter the powder characteristics. Dixon and Clayton<sup>(102)</sup> recommended the use of air mixers which reduce the mixing time to less than ten minutes.

### 2.7.3. Compaction of Powders

Kunin and Yurchenko<sup>(108.109)</sup> were of the opinion that the applied pressure in compaction of metal powders was the sum of two pressures, viz:-

- (i) pressure needed to overcome external friction
- (ii) deformation and compacting pressure

The effectiveness of the applied pressure was reduced on account of the external friction; here the major loss came from the friction between powder particles and the die-wall. In normal commercial practice lubricants are used, either in admixed form or applied to the die-wall, in order to reduce losses in applied pressures resulting from the effect of frictional forces. However, Donachie and Burr<sup>(110)</sup> have reported that the effects of lubricants on pressure-density relationship were negligible except at very low pressures. A similar view was expressed by Hausner and Sheinhartz<sup>(111)</sup>, who reported that lubricants only contributed to a reduction in ejection pressures and had little effect on pressure-density relationships. The Hoganas iron powder handbook<sup>(112)</sup> also confirmed this viewpoint and pointed out that there was an initial increase in the density followed by a sharp decrease as the lubricant content was increased. The maximum density was associated with a lubricant content of between 1-2%. Yarnton and Davies<sup>(113)</sup> reported that the application of a lubricant in the form of monomolecular layer over each particle brought about a 20% increase in packing density relative to unlubricated mixes. However, any lubricant in excess of the monomolecular layer reduced the packing density. The decrease in the packing density

in the case of high lubricant contents, was attributed to an increase in particle size. Afanas'ev et al<sup>(114)</sup> observed that additions of zinc stearate decreased the compaction pressure required to produce any given density level, although additions of more than 0.25 weight percent of zinc stearate did not provide any further reduction in the compaction pressure. Reid<sup>(115)</sup> studied the influence of various commercially used lubricants on pressure density relationships and concluded that the metal stearates were the most effective. A compaction pressure of  $462 \text{ N/mm}^2$  was required to achieve a density of  $6.6 \text{ gm/cm}^3$  for sponge iron compacts using any of the metal stearates, whereas the use of stearic acid as lubricant required a pressure in excess of  $617 \text{ N/mm}^2$ , if the same density was to be achieved. Ejection pressures were very similar irrespective of the type of lubricant employed with the exception of stearic acid, which gave marginally lower ejection pressures. Geiger and Jamison<sup>(116)</sup> reported that additions of zinc stearate and stearic acid reduced the sintered strength slightly but increased the compressibility relative to unlubricated compacts.

Several workers have reported that die-wall lubrication is more effective than admixed lubrication and does not produce harmful reactions during sintering nor does it require the use of a 'dewaxing' step. Leopold and Nelson<sup>(117)</sup> take the view that admixed lubricants have little effect on the true density of small compacts, but have a marked effect on larger components. Marshall<sup>(104)</sup> pointed out that, since small amounts of admixed lubricants gave higher values of bulk density, it may be beneficial to include  $\sim 0.02\%$  admixed lubricant together with die-wall lubrication.

In a comprehensive review, James<sup>(118)</sup> discussed the three main stages in the process of consolidation of powders. The three stages suggested were:-

- (i) transitional restacking and particle sliding
- (ii) local flow and fragmentation
- (iii) bulk compression

These stages were considered to overlap to a certain degree and to be influenced by particle shape and size distribution, lubrication, tooling and method of compaction and residual stresses in the particles. James was of the opinion that the residual stresses could promote densification in two basic ways:-

- (i) high tensile stresses on the surface could enhance particle fragmentation and re-arrangement, thus leading to greater packing efficiency.
- (ii) residual tensile or compressive stresses could promote plastic deformation.

However, it was also pointed out that since the stress patterns set up during compaction were very complex, the exact nature of the contribution of residual stresses to particle fragmentation and deformation was not clear.

In the die compaction of electrolytic iron powder, Goetzel<sup>(106)</sup> found that compaction pressures of the order of  $700 \text{ N/mm}^2$  were needed if 90% of the theoretical density was to be obtained. However, several other workers have reported lower values of compaction pressure at the same density level, which indicates that green densities are very much influenced by specific pressing conditions.

A comparative study of die and isostatic compaction must involve a discussion of the uniformity of density in the compacts made by the two methods. Unckel<sup>(119)</sup> reported that the lack of uniformity in die-pressed compacts of iron could give rise to density differences of up to  $\sim 30\%$ . In contrast, Morgan and Sands<sup>(120)</sup> reported the attainment of uniform density distribution in isostatically compacted components. They attributed the uniformity to the absence of die-wall friction and the application of a more uniform pressure from all sides. VanBuren and Hirsch<sup>(121)</sup> observed a substantial improvement in ductility of isostatically compacted components as compared to those that were die-pressed. They believed that this improvement was due to uniform density distribution and uniform shrinkage during the sintering of these compacts. Although, it would appear that there is some controversy over the effect of de-airing of powder in the mould<sup>(121,122)</sup>, Jackson<sup>(123)</sup> was of the opinion that vibration or de-airing lead to higher green densities. Several examples of the pressure-density relationships obtained from iron powders are available and it can be concluded from these data that whereas a compaction pressure of  $\sim 300 \text{ N/mm}^2$  is required to achieve 80% of theoretical density, the attainment of 90% of theoretical density would require pressures well above  $600 \text{ N/mm}^2$ . In general, densities obtained by isostatic compaction, at any given pressure, are higher than those die-pressed at the same pressure.

Zapf<sup>(92)</sup>, working with iron-nickel alloys, obtained densities close to the theoretical maximum coupled with mechanical properties equivalent to wrought materials of the same composition. The following production route was employed:-

- (i) preparation of the powder mix
- (ii) production of compacts under a pressure of  $8 \text{ MP/cm}^2$
- (iii) heating the compact to  $1000^\circ\text{C}$
- (iv) repressing the hot compacts in a die heated to  $300^\circ\text{C}$
- (v) cooling in air
- (vi) sintering under optimum conditions.

He concluded that the influence of the pre-sintering process before hot-recompaction was relatively unimportant compared to the effect of the tool temperature. Furthermore, the compacts that had not been sintered before hot recompaction, showed a greater capacity for recompaction. Cull<sup>(124)</sup>, who used a similar production route, stressed the importance of time at forging temperature which allowed inter diffusion of alloying elements. Cundill et al<sup>(96)</sup> used a pre-sintering step before hot-recompaction and have reported tensile and fatigue properties equivalent to those of the corresponding wrought material. The ductility values, at a given tensile strength, were also within the general specification of the relevant low-alloy steel. Although there appears to be some disagreement between several workers<sup>(125-129)</sup> regarding the optimum sintering and forging temperature and sintering time, sintering temperature usually varies between  $1050^\circ\text{C}$  and  $1150^\circ\text{C}$  and sintering times vary between 15 and 30 minutes for low-alloy steel components.

#### 2.7.4 Sintering

Thummler and Thomma<sup>(130)</sup>, in a comprehensive review of the sintering process, defined sintering as "The heat treatment of a system of individual particles or of a porous body, with or without the application of external pressure, in which some or all of the properties of the system are

changed with the reduction of the free enthalpy in the direction of those of the porosity free system". In spite of extensive research on the subject, the mechanisms governing the process are not yet clearly understood. However, it is agreed that the process consists of three basic stages:-

- (i) the early stage of neck growth
- (ii) the stage of densification and grain growth
- (iii) the stage of pore spheroidisation and slow densification.

Kuczynski<sup>(131-134)</sup> described the phenomenon of sintering as one of coalescence of particles and shrinkage of pores on account of the presence of capillary forces which were responsible for mass flows and enlarged contact areas between adjacent particles. Kuczynski<sup>(134)</sup> utilised the criterion of rate of neck growth to differentiate between various mass transfer mechanisms. However Rhines<sup>(135)</sup> was of the opinion that such an approach was invalid since the only geometric change necessary to bring about densification was the approach of particle centres and that neck growth could occur without any changes in the positions of particle centres. The model proposed by Rhines et al<sup>(136)</sup> was based on the genus of the powder compact which was defined as

$$G = C - P + 1 \quad (\text{EQ 2.11})$$

where, G = genus of the aggregate  
C = number of particle contacts  
P = number of particles

According to the above model, the genus of compact remains unchanged in the first stage of sintering, while the pore surface are smoothed out and the pore surface area

and its mean curvature reduced. During the second stage, when closure of interconnected porosity occurs, the genus approaches to a minimum value accompanied with a reduction in the pore surface area. Finally, the stage of pore spheroidisation is accompanied by a non-linear reduction in the pore surface area together with a decrease in the mean curvature of the pores<sup>(136)</sup>.

It is widely accepted<sup>(131,137)</sup> that the major driving force responsible for densification is high surface energy of the powder particles and that it is surface tension which tends to reduce the surface area and the porosity of the compact. DeHoff et al<sup>(138)</sup> and Rockland<sup>(139)</sup> were of the opinion that since the required geometrical changes could not be brought about by any single mechanism; the sintering process was invariably brought about by the combination of several mechanisms - namely surface and grain boundary diffusion, lattice or volume diffusion, evaporation and condensation, and plastic or viscous flow<sup>(139-141)</sup>. However, the possibilities of several mechanisms has lead to much debate about the relative importance of the proposed mechanisms at each stage of sintering. Several authors have attempted to distinguish between the various mass transport processes using wire models<sup>(134)</sup>. However, Stone<sup>(142)</sup> criticised such an approach on the basis of the simple geometry of the model which bore little resemblance to that of actual powders. Lenel<sup>(143)</sup> emphasised the similarity between sintering and low stress creep and stated that during the early stages of sintering the predominant mechanism was that of plastic flow by dislocation movement. A similar view was also expressed by Tikkanen and Ylasaari<sup>(144)</sup>. Coble<sup>(140)</sup>

pointed out that although all the above mentioned mechanisms contributed to neck growth, shrinkage and densification is only brought about by lattice and grain boundary diffusion and plastic flow.

Kuczynski<sup>(134)</sup> considered that the most important mechanism involved in the process of densification was volume diffusion while surface diffusion only contributed to shape changes. He believed that the gradient of vacancies under the curved surface of a cavity led to a flow of vacancies directed towards the interior of the system; a counter flow of atoms took place in the opposite direction until the cavity was eventually filled. However, Ichinose and Kuczynski<sup>(145)</sup> experimentally demonstrated that for any appreciable shrinkage to occur, the vacancies must be annihilated in the grain boundaries or diffused through them to the outside. The importance of grain boundaries as vacancy sinks has been investigated by several authors<sup>(145,147)</sup> - Alexander and Balluffi<sup>(146)</sup> showed that pores continued to shrink as long as they were connected to a network of grain boundaries but this process ceased as soon as the grain boundaries were detached from the pores. Gifkins<sup>(148)</sup> reported that the capability of grain boundaries as vacancy sinks was very limited unless they were linked to the free surface by a continuous path through other grain boundaries or else there was a small applied compressive stress to facilitate the fit between grains.

A statistical review of the sintering process was carried out by Mikiyelj et al<sup>(149)</sup>, who concluded that volume diffusion was by far the most widely accepted mechanism of densification during sintering. Stablin and Kuczynski<sup>(150)</sup>

who worked with wire models, reported that in iron-nickel synthetic compacts diffusion of nickel occurred around the iron surfaces and was followed by grain boundary diffusion during the early stages of neck formation. They concluded that the volume changes produced during sintering were predominantly diffusion controlled and that interdiffusion between different elements hindered sintering by the creation of porosity. Furthermore, they believed that surface diffusion was probably predominant at low temperatures.

Thummler and Thomma<sup>(130)</sup>, in a discussion of the sintering of multi component systems, differentiated between the following conditions;

- (i) Sintering with homogeneous solid solution
- (ii) Sintering with simultaneous homogenisation
- (iii) Sintering with the decomposition of solid solutions

In the sintering of homogeneous solid solutions (e.g. pre-alloyed iron-nickel powders) changes in homogeneity take place as a result of different rates of diffusion of the two elements to the interparticle neck regions.

Kuczynski et al<sup>(151)</sup> reported a similar behaviour in the sintering of copper-indium solid solution where an indium rich intermetallic compound was found at the neck surfaces.

The second category i.e. sintering with simultaneous homogenisation appears to be the most important phenomena in the sintering of low-alloy steels (e.g. blended iron-nickel powders). In such cases the creation of lattice vacancies by diffusion would assist sintering by an increase in the atom mobility. However, the coagulation of vacancies to form Kirkendall porosity would inhibit sintering.

Margerand and Eudier<sup>(152)</sup>, who examined the effect of metallic additions on the elimination of porosity during sintering; emphasised the following points:-

(i) The metal added must be almost insoluble in the basis metal, otherwise it will be dissolved in the basis metal and its effect very short lived.

(ii) The basis metal must possess limited solubility in the metal added so as to permit its atoms to pass through.

It was suggested that the critical factor was the difference in partial diffusion coefficients of the elements added, which allowed the formation of new vacancies and increased atom mobility.

Fisher and Rudman<sup>(153)</sup> observed shrinkage in copper nickel compacts during the early stages of sintering. However under certain conditions expansion was produced instead of contraction. According to the authors, these effects were directly related to the degree of homogenisation. They reported that once the degree of inter-diffusion exceeded 55% further homogenisation was accompanied by expansion. On the basis of activation energy measurements, Thummler and Thomma<sup>(130)</sup> concluded that homogenisation was effected by grain boundary and surface diffusion rather than by lattice diffusion.

Goetzel<sup>(106)</sup> stated that since densification and its associated advantages were the main objectives of sintering, the lowest practicable sintering temperature should be used in order to avoid any grain growth. However, industrial sintering practices vary widely. Jones<sup>(154)</sup>, on the basis of mechanical properties, cost and dimensional change, proposed an optimum sintering temperature range of 1000-1150°C

for iron powders. This view was also shared by Dixon and Clayton<sup>(102)</sup> although these authors also pointed out that higher temperatures (1300-1350°C) should be used for parts that require greater ductility. However, Huseby<sup>(155)</sup> was of the opinion that temperatures higher than 1150°C should be avoided on account of their adverse effect on furnace equipment, which resulted in higher maintenance costs.

It has been shown that non-reducible oxide layers, inhibit sintering of powders and therefore it is necessary to use reducing atmospheres during sintering which prevent the formation of such barriers<sup>(130)</sup>. Hulthen et al<sup>(156)</sup> classified ferrous base materials in categories based upon the ease with which sintering could be achieved; they recommended the optimum atmosphere composition for each category. For low alloy steel samples containing 0.3C, they suggested an atmosphere of rich endothermic gas and dissociated ammonia or hydrogen with additions of carbonaceous gases. Huseby<sup>(155)</sup> recommended the use of an endothermic atmosphere with low carburising activity. Furthermore, rapid cooling in the recarburising temperature range was also suggested.

Although chlorinated gases have given some promising results, they suffer from the disadvantage of corrosive attack on furnace equipment.

#### 2.7.5 Heat Treatment of Sintered Steels

Although several workers<sup>(104, 157-159)</sup> have reported that sintered steel<sup>a</sup> may be heat treated in similar manner to wrought steel, the potential benefits of the operation have not been fully explored. The common heat treatment processes<sup>es</sup> used for ferrous sintered parts are:-

- (i) hardening and tempering
- (ii) carburising
- (iii) carbonitriding
- (iv) slowly cooled from sintering temperature

Eggleston and Spangler<sup>(160)</sup> stated that the effects of the above mentioned processes on sintered parts depended on factors such as powder composition, method of mixing, hardenability characteristics, time, temperature and density. Of these density had the most pronounced influence and thus the time-temperature transformation diagrams normally associated with wrought steels could not be applied to sintered parts that possessed interconnected porosity. Steam treatment of ferrous compacts was shown to result in increased hardness, compressive strength, wear and corrosion resistance. However, hardening and tempering, carburising and carbonitriding, although more expensive than steam treatment, gave better mechanical properties. They also emphasised that although the heat treatment of high density sintered parts was similar to wrought steels, extra precautions had to be taken for parts that possessed greater porosity contents (Density  $< 7.0 \text{ g/cm}^3$ )

Bobo<sup>(161)</sup> pointed out that, in spite of the greater severity of quench obtained with water, it was not suitable for powder metallurgical parts, on account of the water being entrapped within the pores and consequently enhancing the corrosion of the parts<sup>(162)</sup>. Chadwick and Broadfield<sup>(163)</sup>, who investigated the quenching of iron-graphite alloys, were of the opinion that oil, which produced a less severe quench, was more suitable for porous specimens. However, Bobo<sup>(161)</sup> emphasised that since oil quenching was less severe than water

quenching, it was necessary to use a greater quantity of alloying elements in order to achieve the required hardenability. Lindskog<sup>(162)</sup> stated that the three major factors that determined the hardenability of steels were carbon content, the quantity of alloying elements and the grain size of material. He suggested a carbon content of 0.5-0.7% for low alloy steels intended for through hardening. He also stated that provided oxidation could be minimised, manganese and molybdenum should be used in preference to copper and silicon. Munro<sup>(164)</sup> reported that the hardenability of steels containing <3% nickel and 0.4% carbon was not sufficient to produce martensite, except in small sections. His results also showed that additions of molybdenum to nickel steels resulted in higher tensile strengths. This was attributed to the increased martensite formation at a particular cooling rate and also increased resistance to tempering at a specific temperature.

Table 4 compares the properties of some sintered low alloy steels in the as sintered and heat treated conditions. The results quoted have been <sup>c</sup>accumulated from the works of various researchers in the field. Fischer<sup>(165)</sup> pointed out the drawbacks of the heat treatment operation; viz: increased cost, problems concerned with atmosphere control, formation of surface cracks, surface distortion and the requirement of additional steps that involved degreasing and surface cleaning. He also observed that in the case of sintered alloys cooled at rates between 10 and 38°C per minute from the sintering temperature, an increase in tensile strength and hardness could be obtained by increasing the nickel content of the alloy. Fedorov et al<sup>(166)</sup>, who made similar studies with

iron-copper-carbon alloys, reported that an increase in tensile strength was produced by an increased cooling rate.

Kravic and Gloor<sup>(157)</sup>, who worked with sintered nickel steels, found that optimum properties were obtained when specimens quenched in oil were tempered at 650°C. A similar view was expressed by Burr and Krishnamoorthy<sup>(158)</sup> who emphasised the necessity of high tempering temperatures (650-675°C), if optimum properties were to be obtained in nickel-molybdenum steels. Dixon<sup>(90)</sup> suggested that, for reasons of economy, quenching could be carried out from sintering temperature. His specimens were quenched in water from sintering temperature (1150; 1300°C) and then tempered at 600°C. Although slight distortion was observed, no quench cracks were found in his specimens. However, it should be noted that his specimens were relatively small in size.

## 2.8 EFFECT OF ALLOYING ELEMENTS ON THE PROPERTIES OF LOW ALLOY STEELS

Arbstedt<sup>(167)</sup> has summarised the various processing routes used in the production of sintered ferrous components under the following four headings:-

- (i) mixture of elemental and master alloy powders
- (ii) mixtures of partially pre-alloyed powders
- (iii) coated iron powders
- (iv) fully pre-alloyed powders

Although the use of mixtures of constituent elements in powder form was shown to be the most popular method of alloying, the inherent disadvantages were also pointed out: these included segregation, variation in properties and

relatively poor hardenability. Although use of partially pre-alloyed or coated powders minimised segregation, coated powders were not used on account of their high production costs. It was also suggested that compacts prepared from pre-alloyed powders should be sinter forged in preference to conventional pressing and sintering methods. Napara-Volgina et al<sup>(168)</sup> reported that the use of pre-alloyed powders rather than mixtures of elemental powders resulted in an increase in the mechanical properties. They found that compacts made from Kh6 (Fe-6%Cr) alloy powder and sintered at 1250°C for three hours possessed about 2.5 times the transverse rupture strength of compacts made from elemental mixes and then sintered under identical conditions. The ductilities of compacts made from alloy powders were also shown to be much higher than those of compacts made from elemental mixes. Although quantitative homogenisation studies were not made the authors attributed the superior ductilities, observed in compacts made from pre-alloyed powders, to their superior homogeneity and finer grain size. However, it was also pointed out that, since alloy powder compacts exhibited greater porosity than those of elemental mixes, use must be made of techniques such as hot forging in order to attain improved properties. Cundill et al<sup>(96)</sup> were also of the opinion that the use of blended powders in the production of sinter forged low alloy steels resulted in inferior mechanical properties in comparison to those obtained by the use of pre-alloyed powders. This was attributed to lower hardenability, which resulted in non-martensitic structures in quenched blended alloy samples. They reported a tensile strength of 695 N/mm<sup>2</sup> from a 2%Ni, ½%Mo blended alloy compact compared to 803 N/mm<sup>2</sup> from a pre-alloyed compact of similar composition.

Harrison and Dixon<sup>(169)</sup> investigated the influence of various alloying elements (Mn, Si and Mo) on 2%Cu and 2%Ni steels using elemental mixtures of powders. They concluded that alloying additions did not have a marked influence on mechanical properties at low sintering temperatures (1100°C), on account of incomplete diffusion of the alloying elements. They found that a tensile strength of 958 N/mm<sup>2</sup> could be obtained from a 3% nickel steel containing 1.5%Mo, 0.25%Mn and 0.8%C. This was in contrast to 479 N/mm<sup>2</sup> obtained from a slightly different steel (2%Ni, 1.0%Mo, 0.5%Mn, 0.8%C) sintered at 1150°C.

Arbstedt<sup>(167)</sup> pointed out that in commercial production of powder metallurgical parts, the choice of alloying elements depended on:-

(i) their affinity for oxygen  
(ii) the dimensional change brought about by their addition.

However, in the opinion of the author, the latter condition did not impose any great restriction since an optimum combination of alloying elements minimised either growth or shrinkage. Arbstedt also pointed out that it was <sup>because of</sup> the high affinity for oxygen, of elements such as chromium, manganese and silicon, that they were not commonly used in the production of sintered steels. However, it has been shown that chromium and manganese steels could be successfully sintered in vacuum furnaces<sup>(170)</sup>. Unfortunately, the high costs of vacuum sintering prohibits its usage for mass production of sintered parts.

Zapf and Dalal<sup>(171)</sup>(1976) stated that the most commonly used alloying elements in the production of sintered parts

are carbon, phosphorus, copper and nickel, either alone or in combination. Although carbon produces the highest strength increment in fully dense wrought material, in sintered alloys its efficiency is less evident on account of the poor ductilities associated with large additions of this element. Durdaller<sup>(172)</sup> obtained a maximum in the transverse rupture strength of iron alloys that contained 1% graphite. However, the impact strength of iron-graphite alloys decreased with increasing graphite content. Crooks<sup>(173)</sup> also recommended the use of these alloys on account of the wide range of tensile strengths (275 - 412 N/mm<sup>2</sup>) that can be obtained. Furthermore, these alloys do not possess the brittleness generally exhibited by iron-copper alloys. Several workers<sup>(169, 171)</sup> have reported that the tensile strength of sintered steels was influenced more markedly by copper than by nickel and that a combination of these two elements resulted in greatly improved properties relative to similar amounts of the single element. Adler<sup>(174)</sup> found that in heat treated iron-copper-nickel alloys the highest strengths were obtained when the copper/nickel ratio was maintained at 1:4. However, additions of copper reduced the impact strength of the sintered alloys<sup>(157, 171, 172)</sup>. It has been shown that in the case of carbon-free iron-nickel alloys, a maximum strength of 730 N/mm<sup>2</sup> and 4.3% elongation can be obtained in an iron-20% nickel alloy that has been pressed and sintered twice<sup>(175)</sup>. However, Zapf<sup>(92)</sup> expressed the opinion that only iron alloys containing up to 6% nickel were of special interest since any increase in nickel content beyond this level resulted in less favourable ratios of strength to elongation at fracture.

In a study of the ternary alloy of iron-nickel - 0.4% carbon, Benesovsky<sup>(176)</sup> obtained maximum strength at 8% nickel; any further additions of nickel resulted in inferior properties due to an increase in the amount of retained austenite. However, Delisle and Knopp<sup>(177)</sup> found that tensile strength increased with increasing nickel content in the range studied (0-10% nickel with 0.4% carbon). Durdaller<sup>(172)</sup> obtained transverse rupture strengths of 653 N/mm<sup>2</sup> from an alloy containing 0.4% carbon and 3% nickel, which increased to 703 N/mm<sup>2</sup> when the nickel content was raised to 4%.

Nickel steels containing 0.5%Mo have been shown to possess sufficient hardenability for heat treatment to high strength levels with acceptable ductilities<sup>(164,178,179)</sup>. Holcomb<sup>(178-179)</sup>, working with a 1.7%Ni, 0.47%Mo, pre-alloyed powder reported as-sintered transverse rupture strengths of 910 N/mm<sup>2</sup> at a density level of 7.0 g/cm<sup>3</sup>. A further improvement was achieved on subsequent heat treatment. Williams and Burr<sup>(180)</sup> found that with IN505 alloy (5%Ni, 0.5%Mo, 0.5%C) sintered strengths of the order 700 MN/m<sup>2</sup> could be achieved using a single pressing and sintering operation and that any subsequent pressing and sintering did not bring about any marked improvement in the strength levels.

In a recent review, Zapf and Dalal<sup>(171)</sup> pointed out that strengths of 730 MN/m<sup>2</sup> with 6% ductility and 750 MN/m<sup>2</sup> with 3.5% ductility could be obtained using an Fe-4.5Cu-5Ni alloy and 'Dista Alloy AE'\* respectively. However, 9.5% and 6% of

---

\* Trade name for partially pre-alloyed powder (4%Ni, 1.5%Cu, 0.5%Mo)

expensive alloying elements were required to attain these properties as compared to 1.8% that would be necessary to achieve similar properties in a fully dense rolled steel. Zapf et al<sup>(181)</sup>, in a later paper, showed that the economics of sintered parts production could be improved by the use of 'master alloys'. They showed that the use of 'master alloys' containing (Mn, Cr, Mo, C) or (Mn, V, Mo, C) produced very high strengths and acceptable ductilities. It was emphasised that only 0.2 - 0.6% of each alloying element was required to obtain strengths in the range of 500 - 700 MN/m<sup>2</sup> with 3-6% elongation.

## 2.9 EFFECT OF THE DEGREE OF HOMOGENEITY ON PHYSICAL AND MECHANICAL PROPERTIES OF LOW ALLOY STEELS

The effect of the degree of homogeneity on the mechanical properties of sintered steels is not clear. Delisle and Knopp<sup>(177)</sup>, who worked with 3.5% nickel steels, found that the diffusion of nickel was not complete even after 6 hours at 1280°C. The microstructure produced on quenching was found to contain nickel-rich martensitic areas in a mainly pearlitic structure. An increase in nickel content led to the formation of networks of martensitic regions, which were considered to be responsible for the observed decline in ductility. The authors suggested that uniform structures would lead to improved mechanical properties. However, Rhines et al<sup>(182,183)</sup> found that the hardness and strength of 70% copper, 30% nickel alloy reached a maximum value before homogenisation was complete on account of the formation of a network of a constituent that contained 50% copper and 50% nickel. The authors, therefore, suggested that it was possible

to obtain better properties from slightly heterogeneous material through controlled heat treatment.

Lindskog and Skoglund<sup>(184)</sup> investigated the influence of homogeneity on the properties of 2.0% nickel, 0.5% molybdenum, 0.5% carbon steel at two density levels. (7.5 g/cm<sup>3</sup> and fully dense). They reported that the rate of homogenisation was more rapid in the porous compact during the initial sintering period but that the fully dense material was more homogeneous after longer periods of sintering. They also found that the rate of increase in hardenability was slow initially, which indicated that a certain degree of diffusion of nickel was necessary before the properties of the bulk material were affected. This slow increase in hardenability was then followed by a sharp rise, which tapered off at longer sintering times, on account of the reduction in the rate of homogenisation. Eloff and Kaufman<sup>(185)</sup> were also of the opinion that hardenability of low-alloy steel preforms made from blended powders was low, on account of the retention of areas depleted in nickel. Lindskog<sup>(162)</sup> reported that the CR50 (critical cooling rate for 50% martensite formation) for blended 2%Ni, 0.5%Mo, 0.8%C steel compact was 19°C/second as compared with 2.25°C/second for pre-alloyed powder compact of similar composition.

Heck<sup>(186)</sup> found that pre-alloyed compacts (2%Ni, 0.25%Mo, 0.4%C) in the as sintered condition possessed greater tensile strength than blended powder compacts of the same composition. However, the reverse was true in the case of materials that were quenched and tempered, although this difference in strength properties decreased as the specimen density increased. The ductility of these alloys were ~1% irrespective of the

type of powder used. The suggestion that increased homogeneity may lead to higher ductility was refuted on the basis of the uniform structures obtained from pre-alloyed powders. In a more extensive study, which involved electron probe micro-analysis, Fischer et al<sup>(187,188)</sup> observed mixtures of pearlite and ferrite in some parts of the microstructures of both pre-alloyed and blended compacts in the as sintered condition. Nevertheless, a more uniform distribution of these phases was found in the compacts made from pre-alloyed powders. In the oil quenched microstructures of blended compacts three different phases were observed:-

- (i) A pure white area (ferrite) with nickel concentration in the range 0 to 1.5% and a hardness of Rb74.
- (ii) Dark etching areas (bainite) with nickel concentrations between 1 and 3% and hardnesses of Rb90 or Rc10.
- (iii) Light etching areas (martensite near centre and bainite near the periphery) containing 3 to 11% nickel and hardnesses in the range Rc30 to Rc60.

X-ray diffraction studies were also carried out which revealed that there was less than 2% retained austenite. The molybdenum concentration was not found to vary to any appreciable extent and thus it was believed that the nickel content of the area was basically responsible for the types of transformation products formed on quenching. These views were found to be in agreement with continuous cooling transformation and isothermal transformation diagrams.

Lindskog and Skoglund<sup>(184)</sup> also expressed the opinion that heterogeneity may offer advantages of improved strength in certain alloys and under certain conditions e.g. heat

treated 2%Ni, 0.5%Mo, 0.5%C alloys. These authors found that the microstructure of sintered compacts (15 minutes at 1120°C) made from partially pre-alloyed powders contained a mixture of phases viz: ferrite, coarse and fine pearlite, upper bainite and martensite; all these phases exhibited a wide range of nickel concentration (0.1-31.0%). The microstructures of the compacts made from pre-alloyed powders were basically composed of upper bainite, after all sintering treatments. The strengths of fully dense pre-alloyed compacts were not affected by an increase in sintering time, whereas the strengths of partially pre-alloyed compacts were steadily improved by increasing the sintering time up to one hour, after which they attained the strength levels of the pre-alloyed compacts. It was considered significant that the partially pre-alloyed compacts were still very heterogeneous after this treatment. In compacts that contained about 4% porosity, the tensile strength steadily increased with increasing sintering time but was always lower than those obtained by the use of partially pre-alloyed powders. The authors believed that such a parity in the strength levels of the two materials could only be explained in terms of differences in pore structure and that the rate of sintering was adversely affected by pre-alloying. (184)

Fischer (165) found that the controlled cooling (10-38°C/minute) of Ni-Mo-Mn steels from the sintering temperature (1120°C) resulted in a microstructure that contained ferrite, pearlite, bainite and martensite. The degree of martensitic transformation increased with increasing nickel content - 25 volume % of martensite was observed in a 4% Ni steel as compared with 9 volume % in a 3% Ni steel. The increase in nickel content was also accompanied by an increase in

the amount of retained austenite (2-4% in the 4% nickel steel). The presence of austenite accounts for the fact that there was no difference in hardness between specimens containing 3 and 4% nickel, even though the martensite content was far greater in the 4% nickel steel. Svensson<sup>(189)</sup> also pointed out the detrimental influence of retained austenite and suggested that its occurrence could be minimised by:-

- (i) addition of ferrite stabilisers e.g. molybdenum
- (ii) addition of nickel in the form of partially pre-alloyed powder
- (iii) reduction in carbon content as nickel content increased
- (iv) increase in the degree of homogeneity

Dixon et al<sup>(190)</sup> carried out an extensive investigation on the influence of homogeneity on mechanical properties of Fe-3%Ni-0.3%C alloys. They arrived at a homogeneity parameter by the statistical analysis of electron-probe micro-analysis results. The nickel content of forty randomly selected areas of each specimen was determined using a probe magnification of 4800X. The variance of the distribution was then taken to represent homogeneity. On the basis of these results, Dixon et al concluded that the presence of retained austenite in the structure was detrimental to mechanical properties. Furthermore, they recommended that the homogeneity parameter should be maintained below 0.45 if high strengths are desired. However, they found that tensile ductility was not affected by the degree of homogeneity<sup>(190)</sup>.

Burr and Krishnamoorthy<sup>(158)</sup> studied the relationship between microstructure and mechanical properties of 5%Ni - 0.5%Mo - 0.5%C alloys. Their compacts were sintered at

1300°C for 1 hour, cooled to room temperature, re-austenitised at 870°C followed by quenching in oil and tempering at 650°C or 675°C. They observed that compacts made from insufficiently mixed powders possessed inferior mechanical properties to those that possessed a greater degree of homogeneity by virtue of a more efficient mixing procedure. However, it should be noted that no quantitative measurement of homogeneity was made by these authors. Nevertheless, some very interesting differences were observed in the microstructures of the two materials. The microstructure of the more homogeneous alloy consisted of light and dark etching regions, the latter being more continuous. Micro-hardness measurements showed that both these regions were martensitic. Micro-analysis revealed that the two regions were different in composition, the lighter etching areas being high in nickel and low in carbon. The microstructure of the heterogeneous alloy also contained light and dark etching areas. However, micro-hardness within the light etching region revealed the presence of retained austenite surrounded by high nickel martensite. The darker etching areas were found to contain some intermediate transformation products. The authors attributed the inferior properties of the heterogeneous alloy to the presence of retained austenite and intermediate transformation products<sup>(158)</sup>.

From the data available in the literature, it may be concluded that the presence of heterogeneity is particularly detrimental in the case of compositions where austenite remains in the structure after heat treatment but that the position is unclear in other cases.

## 2.10 EFFECT OF POROSITY ON MECHANICAL PROPERTIES OF LOW ALLOY STEELS

Squire<sup>(95)</sup> found that the density of iron powder compacts increased steadily with compaction pressure up to  $1103 \text{ N/mm}^2$  but that no further increase was observed when the pressure was increased to  $1378 \text{ N/mm}^2$ . Similar behaviour was also found in the relationship between tensile strength and compaction pressure. However, when tensile strength, hardness and modulus of elasticity were plotted against density, a linear relationship was observed. An exponential relationship was observed between tensile ductility and density and also between impact resistance and density. Krishnamoorthy<sup>(93)</sup> examined the effect of sintered density on mechanical properties of iron compacts within a range of 86-100% of theoretical density. He reported that the presence of porosity had a much more adverse effect on elongation and impact resistance than on tensile strength. Young<sup>(191)</sup> also reported that tensile strength was roughly proportional to the porosity but elongation, reduction in area and impact resistance exhibited an abrupt improvement when porosity levels were less than approximately 3%. Kravic<sup>(192)</sup>, who investigated the effect of porosity on the mechanical properties of 2, 4 and 7% nickel steels concluded that tensile and yield strengths, hardness and elongation were proportional to density but impact strength was an exponential function of density (Fig. 4). However, it should be noted that the maximum density obtained was  $7.4 \text{ g/cm}^3$  (95% of theoretical density). Consequently, Kravic did not observe the abrupt improvement in elongation that was reported by Young.

McAdam<sup>(193)</sup> examined the relationship between elastic modulus and fractional porosity using the results of various earlier investigations together with his own: despite the variation in alloy composition and sintering conditions within the results under consideration, all the data fell within a very narrow band. Thus McAdam concluded that the modulus of elasticity was a function of fractional porosity and was governed by the equation:-

$$E_n = 29(1 - \epsilon)^{3.4} \times 10^6 \text{ p.s.i.} \quad (\text{EQ 2.12})$$

where  $E_n$  = nominal elasticity  
and  $\epsilon$  = fractional porosity

Eudier<sup>(194)</sup> proposed that the strength of sintered material was related to that of the pore-free material by an equation of the type:-

$$\sigma = \sigma_0 (1 - KP)^{2/3} \quad (\text{EQ 2.13})$$

where  $\sigma$  = strength of sintered compact  
 $\sigma_0$  = strength of pore-free material  
 $K$  = constant  
 $P$  = fractional porosity

The above relationship was based on the assumption that, at fracture, the effect of stress concentration by the presence of pores was negligible. Eudier<sup>(194)</sup> considered sintered compacts to be composed of small cubic elements, each of which contained a spherical hole, which were arranged in a simple cubic array: the strength of such materials was governed by the load bearing capacity of the solid material

at the minimum cross-section. Haynes<sup>(195)</sup>, who was very critical of these assumptions, believed that the good fit between experimental data and Eudier's relationship was purely fortuitous. He pointed out that it was necessary to take into account the theoretical stress concentration effects of the pores but premature failure due to the presence of other flaws should be ignored. According to Haynes, the upper and lower strength limits of sintered materials could be predicted by the use of the following equation:-

$$\sigma_{\text{Rel}} = \frac{\sigma_{\text{TS}}}{\sigma_{\text{OTS}}} = \frac{1-P}{1 + a(F-1)P} = \frac{1-P}{1 + bP} \quad (\text{EQ 2.14})$$

where  $\sigma_{\text{Rel}}$  = strength of porous material relative to pore-free material

$\sigma_{\text{TS}}$  = tensile strength of porous material

$\sigma_{\text{OTS}}$  = tensile strength of pore-free material

P = fractional porosity

a = arbitrary constant

b = a(F-1)

F = stress concentration factor

The value of 'b' was shown to be 2.0 for many ductile materials. The crucial influence of a ductile matrix on the value of 'b' was supported with experimental data from a 0.8% carbon steel. The strengths of such materials, which possessed very little ductilities, was shown to lie close to the curve with a value of 'b' equal to five. Haynes<sup>(196)</sup>, in a further development of this theory, showed that a minimum acceptable ductility was obtained when

$$\frac{\text{yield strength}}{\text{tensile strength}} = \frac{1}{1 + bP} \quad (\text{EQ 2.15})$$

For pure iron this ratio was found to be 0.5 which indicated that pure iron compacts should possess acceptable ductility even at 50% porosity.

Although the importance of the stress concentration factor has been pointed out, no experimentally derived values of this factor are readily available in the literature. They are generally arrived at by theoretical consideration based on elasticity theory. The elastic modulus has been shown to vary linearly with changes in porosity up to  $\sim 30\%$  (193, 195, 197-199) and calculations of stress concentration factors have been based on this linear relationship. Nazare and Ondracek<sup>(197)</sup> who worked with cermet materials, reported that the stress concentration factor for oblate shaped dispersed phase particles was 3.8 as compared with 2.0 for spherical particles. These authors expressed the relationship between Young's modulus and porosity as

$$E_p = E_s (1 - FP) \quad (\text{EQ 2.16})$$

where  $E_p$  = modulus of porous material

$E_s$  = modulus of solid material

Experimental data for a wide range of materials was shown to be in agreement with the proposed relationship, except at very high porosity levels. These values of stress concentration factors were in agreement with those suggested by Pohl<sup>(200)</sup>

Napara-Volgina et al<sup>(168)</sup> and several other Russian workers have shown that tensile strength of sintered materials

are exponentially related to porosity - viz:

$$\sigma_s = \sigma_o \exp(-BP) \quad (\text{EQ 2.17})$$

where  $\sigma_s$  = tensile strength of sintered material  
 $\sigma_o$  = tensile strength of pore-free material  
P = fractional porosity  
B = an experimentally determined coefficient

Using the above equation, the authors predicted strength values that were in very good agreement with experimental data. The importance of a ductile matrix, as emphasised by Haynes, became evident, since the close agreement between predicted and experimental values in Napara Volgina's investigation could be attributed to the ductile matrix in the austenitic stainless steel powder compacts used in the investigation.

Jenkins<sup>(201)</sup> pointed out that although most proposed relationships at the time (1964) did not take into account pore shape, size and distribution, they appeared to be in good agreement with experimental data. However, he also pointed out that the results obtained by Zapf<sup>(91)</sup> indicated that the relationships between strength and ductility were different for different types of iron powder. This suggested that certain other factors such as pore shape were also related to the tensile strength of the material. Jenkins was of the opinion that further investigation was needed to establish the exact nature of the relationship. Kaufman and Mocarski<sup>(202)</sup> observed that the residual porosity that resulted from powder forging operations was irregular in shape and could generate notch effects leading to poorer properties. These authors also believed that further investigation was

needed in this area. Dudrova and Kubelik<sup>(203)</sup> investigated the relationship between the strength and porosity of sintered iron compacts during isothermal sintering. Their specimens were compressed at 299, 598 and 797 N/mm<sup>2</sup> followed by sintering at 1100°C for periods ranging between 5 minutes and 16 hours. They compared samples having the same total porosity (9.5 - 10.5%) but compressed at different pressures (598 and 797 N/mm<sup>2</sup>). They concluded that the same value of total porosity did not guarantee the same level of strength. The authors presented two empirical relationships of the type

at 299 N/mm<sup>2</sup> compaction pressure 
$$\sigma_{PT} = \frac{1}{0.00297P_c + 0.019}$$
 (EQ 2.18)

at 797 N/mm<sup>2</sup> 
$$\sigma_{PT} = \frac{1}{0.00359P_c + 0.016}$$
 (EQ 2.19)

where  $\sigma_{PT}$  = strength at a total porosity PT  
 $P_c$  = fractional closed porosity

The above two equations were used to describe the functional dependence of tensile strength and porosity. However, the authors considered these equations valid only for the experimental range used. Fig. 5 is a plot of tensile strength against total porosity as obtained by these authors.

Salak et al<sup>(204)</sup> stated that the strength of sintered iron was best expressed by the following equation:

$$\sigma_s = \sigma_0 \exp(-0.043P) \text{ MN/m}^2 \quad (\text{EQ 2.20})$$

where  $\sigma_s$  = tensile strength of sintered iron  
 $\sigma_0$  = tensile strength of solid iron (MN/m<sup>2</sup>)

P = fractional porosity

0.043 = empirical constant

When the curve corresponding to the above equation was plotted together with results obtained by several other workers, a considerable scatter was obtained. This was attributed to different shape, size and distribution of the pores in the various compacts. Esper et al<sup>(98)</sup> examined the effect of pore structure on radial crushing strengths of sintered compacts and presented a relationship which included a factor related to the mean linear pore size.

$$K = AL \exp(-BP)^{2/3} \quad (\text{EQ } 2.21)$$

where K = radial crushing strength

L = mean linear pore size

P = fractional porosity

A and B = constants that were dependent on the type of iron powder used.

Dixon, Fletcher and Cundill<sup>(190)</sup> investigated the porosity strength relationship of 3% nickel 0.3% carbon steel compacts made from blended, plated and atomised powders. In their opinion, the relationship was complex and could not be governed by single equations such as those proposed by Haynes<sup>(195,196)</sup> and Eudier<sup>(194)</sup>. In order to obtain a satisfactory correlation with Haynes's equation it was necessary to use values of 'b' that varied between 3.5 and 11.0. Moreover, the values of 'b' were also found to decrease as the sintering temperature was increased. A similar range of 'b' values were required for plated powder compacts sintered at 1150°C but the range was considerably reduced

(2.8 - 3.9) for compacts sintered at 1300°C. However, in the case of atomised powder compacts, the 'b' values were fairly constant and fell within the same range as those of plated material sintered at 1300°C. Dixon et al<sup>(190)</sup> suggested that the compacts requiring very high values of 'b' possessed a high degree of heterogeneity. In the case of alloys of high homogeneity, best correlation was obtained using the following equation, due to Pohl<sup>(200)</sup>.

$$\sigma_B = \sigma_o (1-FP) \quad (\text{EQ 2.22})$$

The stress concentration factor 'F' was found to vary with sintering time and temperature, as would be expected. The values of 'F' were found to be in agreement with those given in literature for iron and steels.

Despite the ease of measuring the modulus of rupture, there is very little published data that relates to low alloy steels. This may be partly due to the variations in the results, obtained with specimens that possess reasonable ductilities. Landgraf<sup>(205)</sup>, who worked with low alloy nickel steels, reported a linear increase in the transverse rupture strength with increasing density within the range investigated (6.9 - 7.6 g/cm<sup>3</sup>). In the case of certain categories of alloys this relationship departed slightly from linearity.

CHAPTER THREE  
EXPERIMENTAL PROCEDURE

### 3. EXPERIMENTAL PROCEDURE

#### 3.1 RAW MATERIALS

The following raw materials were used in the present investigation:-

- (i) Iron, nickel, and graphite powders
- (ii) Nickel plating solutions
- (iii) Nickel anodes
- (iv) Stainless steel cathode rods

##### 3.1.1 Powders

Sponge iron powder (Makins Grade JJM 100 P1; - 100 B.S. mesh) was used for the production of the nickel coated iron powder as well as the main constituent in the compacts prepared from blended mixtures of the constituent elements. A standard sieve analysis, using a 1000g sample, was carried out on this powder. A similar sieve analysis was carried out on the composite powders obtained by the electrodeposition of nickel onto iron powder. Carbonyl nickel powder (supplied by the International Nickel Company) was used for the preparation of compacts made from blended powders. Carbon was added in the form of analytical grade natural graphite.

##### 3.1.2 Nickel Plating Solutions

Two commercial plating solutions were used in the present investigation - (a) conventional sulphamate bath (b) concentrated sulphamate bath. However, the major part of the investigation utilised the latter. The composition and operating conditions of the two plating solutions are given in Table 5.

### 3.1.3 Nickel Anodes

The following materials were used as anodes at different stages of the investigation:-

- (i) Rolled electrolytic nickel sheet
- (ii) Pure nickel shot
- (iii) S-nickel shot

The nickel sheet (i) was used in the case of the plating cells in which the anode and cathode compartments were separated by a refractory membrane. The nickel shot (ii) and (iii) were used in those cells which made use of fabric anode bags. This type of anode is discussed in detail in Section 3.2.2.

### 3.1.4 Cathodes

18-8 niobium stabilized stainless rods, 0.32 cm in diameter, were used to form the cathode. The construction of the cathode varied with the design of the cell.

## 3.2 DEVELOPMENT OF A PLATING CELL THAT MAY BE USED TO PLATE NICKEL ONTO IRON POWDER

The development of a plating cell for the purpose of plating nickel onto iron powder was carried out in two distinct stages. Detailed descriptions of the two plating cells, used in the present investigation are given in Sections 3.2.1 and 3.2.2. The cathode chamber was separated from the anode by the use of a membrane through which an inert fluidising gas entered the chamber under pressure. The cathode, which consisted of a set of rods hanging vertically in the cathode chamber, facilitated the uniformity of current distribution.

### 3.2.1 Stage I - Cell Utilising a Porous Membrane

In order to avoid contact between the powder particles and the anode it was necessary to separate the anode from the cathode compartment. This was achieved with the use of a porous refractory membrane. The suitability of a high density sintered polythene material (Vyon\* Grade F) was also investigated for this purpose. Figs (6a) and (6b) show the details of the cells utilising a refractory membrane.

(i) The Cathode Compartment:- A porous refractory tube (6.35 cm O.D.) formed the inner wall of the cathode chamber and rested on a high density sintered polythene fluidising membrane (Vyon\* Grade D). The cathode consisted of stainless steel rods soldered onto a copper plate in two concentric circles.

(ii) The Anode Compartment:- This consisted of a perspex tube (15.25 cm O.D.) which surrounded the refractory membrane tube. A perspex flange formed the base of this compartment. The anode consisted of a rolled electrolytic nickel sheet shaped into a tubular form.

(iii) The Gas Compartment:- This formed the base of the plating cell and consisted of a copper tube (6.35 cm O.D.) closed at the bottom and welded to a flange at the top end. The fluidising gas entered through a tube attached horizontally to the wall of the chamber. The gas compartment was attached to the plating compartments with the help of flanges.

### 3.2.2 Stage II - Cell Utilising an Anode Bag

The second stage in the development of the cell involved a change in the arrangement of the anode and cathode. The

---

\* Vyon - Trade name of high density sintered polythene material

porous refractory membrane of the Stage I cell was replaced by twin anode bags. Fig. 7(a) is a diagrammatic illustration of the plating cell, which consisted of two basic sections:-

- (i) the plating section
- (ii) the gas compartment

The two sections were made from perspex tube (15.25 cm O.D.) and were joined together with perspex flanges with a fluidising membrane (Vyon Grade-D) placed in between the two flanges. The apparatus was made gas tight with the help of an O-ring and a silicone rubber sheet placed in between the two flanges. Fig. 7(b) shows the assembled cell.

At a later stage in the investigation, when higher temperature operation was found necessary, the perspex tubes were replaced by QVF glass columns. However, the basic design of the cell was not altered. Fig. 8 shows a photograph of the plating cell utilising QVF glass columns.

The anode, used in this cell, consisted of a fabric bag filled with nickel shot. A second fabric bag was then used to cover the filled bag and provide additional insulation. The anode assembly was then positioned in the centre of the plating cell. Two different types of nickel shot were used in the present investigation:-

- (i) pure nickel shot.
- (ii) S-nickel shot.

Four different types of fabrics were used to make the anode bags. Table 6 lists the type of bags and the combination in which they were used. Fig. 9 shows an assembled anode.

The cathode assembly initially comprised of twenty four niobium stabilized 18-8 stainless steel rods (0.32 cm  $\emptyset$ ) attached to a copper plate. At a later stage, the number of rods was reduced to twenty. These rods were arranged in two concentric circles round the anode assembly. Fig. 10 shows the cathode assembly.

### 3.3 THE ELECTRODEPOSITION OF NICKEL ON IRON POWDER

Although two different plating cells were employed, the basic procedures adopted were the same in all cases; viz:-

1. A known volume of standard nickel plating solution, of known composition and hydrogen ion concentration was heated to 10°C above the operating temperature and then poured into the plating cell.
2. Nitrogen gas, at a low flow rate (5l/min), was passed through the fluidising membrane.
3. A known weight of iron powder was then introduced into the cathode chamber of the plating cell.
4. The flow rate of nitrogen gas was adjusted to achieve complete suspension and random movement of the iron powder particles in the plating solution.
5. The anode and cathode assemblies were then placed in position and connected to the power source.
6. Voltage and current readings were recorded at the start of the experiment and then at 15 minute intervals.
7. Samples of plated powder and the plating solution were taken out after fixed intervals of time (15 minutes). The pH of the plating solution sample was measured after which the nickel content of this solution was determined.

8. If necessary appropriate adjustments were made to the pH of the solution.
9. The plated powder samples were washed thoroughly in water followed by a final rinse in alcohol. The powder was then dried in air at 120°C. The nickel content of the powder was then determined.
10. The plating process was continued for a period that varied between 45 and 70 minutes.
11. The powder remaining in the cell was washed several times in water and then finally rinsed in alcohol. It was then dried in air at 120°C.

#### 3.4 NICKEL COATING OF IRON POWDER WITHOUT A CURRENT SOURCE

These experiments were carried out in the stage II plating cell described in Section 3.2.2. However, the anode and cathode assemblies were now not included. The plating chamber was contained within a water bath held at temperatures between 60 and 90°C. Nickel sulphamate solution of similar composition to that used in the electroplating experiment was heated to 70°C and poured into the cell. One kilogram of iron powder was then added to the cathode chamber and the fluidising gas flow was adjusted to achieve complete suspension of the powder particles in the plating solution. The process described in Section 3.3, but without the application of an electric potential, was continued for times of up to 120 minutes, after which the powder was washed and dried in the way previously described.

#### 3.5 PRODUCTION OF SINTERED COMPACTS

In order to assess the mechanical properties sintered compacts were prepared to MPIF standard specifications

(MPIF - 13-62). The preparation of the test pieces incorporated the following steps:-

- (i) mixing
- (ii) compaction
- (iii) sintering
- (iv) heat treatment

### 3.5.1 Mixing

Compacts of blended material were made from mixtures of iron powder, carbonyl nickel powder and natural graphite. These powders were mixed in a turbolator mixer for a period of 25 minutes prior to compaction. In the case of composite and pre-alloyed powders, carbon was added in the form of natural graphite prior to mixing in the turbolator mixer.

### 3.5.2 Compaction

The compacts from which rupture test specimens were to be prepared were produced by die-compaction in a single acting hydraulic press of 500 KN capacity. Fig. 11 shows a diagrammatic illustration of the die used for this purpose. The compaction pressure was varied between 600 and 900 MN/m<sup>2</sup>. Zinc stearate suspension in acetone was used as a lubricant on the die-walls and punches so as to minimise the effect of friction.

### 3.5.3 Sintering

Specimens were sintered in a pure hydrogen atmosphere at 1150°C  $\pm$ 5°C for various times in the range of 30 and 240 minutes. In order to remove moisture and oxygen, hydrogen was first passed through both an U-tube containing magnesium perchlorate and a De-ox tube containing palladinised asbestos. After

the requisite sintering treatment was complete, the specimens were directly quenched in water.

#### 3.5.4 Heat Treatment

The heat treatment of the quenched samples consisted of a tempering operation carried out at 600°C. This treatment was carried out in an air circulatory furnace for a period of 1 hour after which the specimens were allowed to cool in air. In order to avoid decarburisation of specimens, the test pieces were coated in a proprietary compound (Berkotekt) prior to tempering.

### 3.6 DETERMINATION OF PROPERTIES

#### 3.6.1 Density

The uniformity of shape of the die-pressed compacts facilitated the determination of their densities from direct measurements of mass and dimensions. Both green and sintered densities were determined, the latter being determined after the samples had been ground for rupture testing.

#### 3.6.2 Determination of Modulus of Rupture

Rupture test specimens were ground to an even surface finish and the dimensions of the ground specimen were recorded. After measuring, the test pieces were broken in the testing fixture shown in Fig. 12. The specimen rested on two steel rods (0.32 cm in diameter), placed one inch (2.54 cm) apart. A third steel rod pressed on the upper face of the specimen and was positioned mid-way between the supporting rods. The testing assembly was then mounted on an Instron Universal testing machine and the load at fracture was recorded. The modulus of rupture was then calculated

using the following relationship:-

$$S = \frac{3 \times P \times L}{2 \times t^2 \times W}$$

where S = modulus of rupture in pounds per square inch

P = fracture load in pounds

L = the distance between supporting rods = 1 inch

t = thickness of test piece in inches and

W = width of test piece in inches.

### 3.7 EXAMINATION OF THE MICROSTRUCTURE OF SINTERED AND HEAT TREATED MATERIALS

Microstructural examination was carried out on specimens in the as quenched and in the quenched and tempered conditions. Specimens were mounted in cold setting resin and polished to  $1/4 \mu\text{m}$  finish. The specimens were then etched in 2% Nital solution and examined under an optical microscope. Photomicrographs of the most representative areas were taken. In certain cases, the specimens were slightly overetched so as to reveal any sub structure present.

### 3.8 DETERMINATION OF THE HOMOGENEITY OF SINTERED MATERIAL

A Cambridge Microscan Mk IIA microprobe analyser was used for the determination of the homogeneity of sintered specimens. The procedure adopted was similar to that used by Dixon<sup>(90)</sup>. The probe voltage and beam current were kept constant at 25KV and 0.15  $\mu\text{A}$  respectively. Specimens were sawn out from fractured rupture test pieces and polished to  $1/4 \mu\text{m}$  finish and examined under the electron-probe with the lithium fluoride crystal spectrometer set to receive nickel

$K_{\alpha}$  radiation. The spectrometer setting was checked by establishing the position at which the maximum count rate was obtained for a pure nickel standard specimen. The sintered specimen was so aligned that the electron beam struck the specimen just off centre; consequently the specimen could be rotated such that the beam traversed the specimen in an ever-increasing spiral. Nickel concentration was determined for each of 40 areas (20  $\mu\text{m}$  square magnified X4800) and the variance of the distribution was taken as the measure of the homogeneity of the compact.

CHAPTER FOUR  
EXPERIMENTAL RESULTS

#### 4. EXPERIMENTAL RESULTS

Although the Stage II cell was used during the greater part of the investigation (Fig. 7(b)) the results of the work of the refractory membrane cell (Fig. 6(b)) have also been reported in detail, since these results constitute the base for the later developments.

In order to assess the performance of the plating cells, the influence of the following parameters on the overall performance of the cell was studied:-

- (a) Total quantity of electric charge passed
- (b) Average cell resistance\* (A.C.R.)
- (c) Apparent average current density\*\* (A.C.D.)
- (d) Apparent anodic dissolution efficiency
- (e) Apparent cathodic deposition efficiency

A determination was made of the effect of plating time on both the cell current and the potential difference across the cell. It was found that the cell current obtained at a constant potential difference did not remain constant throughout the experiment but showed, in most cases, a decline after approximately 35 minutes of plating. It was, therefore, considered necessary to quote average cell resistance figures. Since the surface area of powder particles that was in contact with the cathode at any moment during the plating process could not be determined,

---

$$* \text{ A.C.R. } = \frac{\text{Area under cell-potential-plating time curve}}{\text{Area under cell-current-plating time curve}}$$

$$** \text{ A.C.D. } = \frac{\text{Total quantity of electric charge passed}}{\text{Plating time x Surface Area of Cathode Rods}}$$

the calculation of the apparent average current density was made using the surface area of the rods that formed the cathode.

The maximum possible mass of nickel that could be deposited was determined by Faraday's Law; viz:- a gram equivalent of metal will be deposited by the passage of one faraday of electricity. In the case of the electrodeposition of nickel, the passage of one ampere hour of electric charge, under ideal conditions, results in the deposition of 1.095 grams of nickel. The experimentally determined value of the total quantity of nickel deposited was based on the total mass of iron powder used for the experiment and the chemical analysis of the plated powder. Although some powder was lost during the washing operation, it was assumed that this was of similar composition to the bulk of the plated powder. Some nickel plating was also obtained on the current distributor rods; however this was not taken into account for the calculation of deposition efficiency.

#### 4.1 STAGE I: PLATING CELL WITH REFRACTORY MEMBRANE

The plating cell used for this section of the investigation is shown in Fig. 6(b). The choice of the membrane was restricted to (a) 'Vyon' (Grade F ) sintered polythene filter material and (b) refractory membrances of different porosities. Preliminary investigations carried out to determine the suitability of the membrane material showed that high porosity (30%) fireclay refractory was best suited for the purpose on account of its relatively low resistance to the passage of ions.

#### 4.1.1 Experiments With the Refractory Membrane Cell

Figs 13-15 show the relationships between both cell current and plating time, and cell potential and plating time during experiments carried out in the refractory membrane plating cell. The cell current in all three cases showed an initial increase which required the regulation of the cell potential, in order to maintain the current at the desired level. However, apart from this initial period of instability, the cell current remained almost constant throughout the experiments. Table 7 shows that in the first two experiments, (M1 and M2), the nickel ion concentration in the solution showed a small increase but in the third (M3) a substantial increase in nickel ion concentration occurred in the anolyte while the nickel content of the catholyte remained almost constant.

The apparent density of the "fluidised bed" was varied in the second experiment (M2) in which the ratio of the mass (g) of iron powder to the total volume (ml) of plating solution in the cell was increased to 0.727 g/ml, whereas the ratio used in the case of the other two experiments was 0.625 g/ml. The denser bed did not fluidise well, although an increase in the flow rate of gas prevented any powder from settling down on the membrane. The resistance of the cell had now increased to  $0.64 \Omega$  compared to  $0.58 \Omega$  in the other two experiments. The deposition efficiency was also adversely affected and dropped to approximately 72%, as compared to 82% during the previous experiments. However, the dissolution efficiency at the anode remained practically the same for all three experiments, viz:- 94.4%. The combination of high resistance and high density of the bed, as in the case of experiment (M2) produced a very marked reduction in the quantity of nickel deposited.

## 4.2 STAGE II - CELL UTILISING AN ANODE BAG

The high cell resistance and the relatively poor deposition efficiency of the refractory membrane plating cell led to a search for other more suitable membrane materials. Some preliminary experiments, using anodes contained in fabric bags, showed that cell resistance could be markedly reduced and high current densities consequently achieved by the use of such materials. The anode arrangement consisted of nickel shot contained inside a 100% triacetate fabric bag, which in turn was covered with a second bag made from the same material. A nickel rod, in contact with the nickel shot, acted as the current feeder. Although both pure nickel and S-nickel shot were used as anode material, the results obtained using the former are reported first (in Sections 4.2.1 and 4.2.2).

### 4.2.1 Experiments Using 100% Triacetate Fabric Anode Bags

The relationship between plating time and cell current, and plating time and cell potential, for the first experiment using the new anode bags, is shown in Fig. 16. The operating conditions and the quantity of nickel deposited with the new anode arrangement are given in Table 8 (Ex NI). The cell resistance was found to be 0.26 ohms, while the corresponding figure in the case of the refractory membrane cell had been 0.58 ohms (Table 7). The higher current densities that were possible in this anode bag cell resulted in a four fold increase in the plating rate. The apparent deposition efficiency, calculated on the basis of Faraday's laws, was in excess of 100%. The plating solution was greatly depleted of nickel ions since only 30.8 g of the 82.0 g of nickel deposited was restored by anodic dissolution.

It should also be noted that the nickel deposited on the cathode rods was not taken into account in the calculation of deposition efficiency.

Fig. 16 shows that the cell current, for the above mentioned experiment, increased during the first ten minutes of plating, after which it remained steady. However, at such high currents the lead wires overheated, so the potential difference across the cell was reduced and the cell current maintained at a lower level. The cell current showed a marked decline between the 45th and 60th minute of plating. Consequently the potential difference across the cell was increased in an attempt to maintain a constant current. However, this increase in the potential difference across the cell did not check the decline in the cell current and the cell resistance at the end of the plating period was 0.32 ohms as compared to 0.24 ohms after the first ten minutes of plating.

Table 8 (NII - NV) and Fig. 17-20 give the results of certain of the other experiments that used triacetate anode bags and pure nickel shot. The relationship between cell current and the plating time was similar to that observed for Ex NI, Fig. 16; although the sharp decline in the cell current occurred between the 30th and 45th minute of plating. In the case of Ex NII Fig. 17, a slight increase in cell current was observed after 30 minutes of plating followed by a sharp decline. As is evident from Table 8 (Ex NII - NV), the cell resistance varied between 0.23 and 0.37 ohms and the current density varied between 16.8 and 20.2 A/dm<sup>2</sup>. However, it should be noted that despite the slightly greater resistances the apparent deposition efficiency was much greater than 100%

in all the experiments. The dissolution efficiencies show a wide scatter (27-67%) and were always much lower than in conventional nickel plating.

#### 4.2.2 Effect of Anode Bag Fabrics on Plating Characteristics

Fig. 21 shows a photograph of a section of a 100% triacetate fabric anode bag. The dark rings are the rust stains left by the iron powder particles that had entered the anode bag and covered the nickel shot. There was also some evidence of attack on the fabric by the acidic reagents in the solution. In order to avoid such attack, bags made from other fabrics were also examined. Fig. 22 and Table 8 (Ex NVI) give the results of an experiment carried out using a single anode bag made of a canvas type material. A decline in cell current was observed after the first fifteen minutes of plating and the overall resistance of the cell was 0.73 ohms, which was three times the best value obtained by the use of 100% triacetate fabric bags and even higher than the refractory membrane cell. Although the maximum cell potential (15 volts) was applied across the cell, the average current density achieved was only  $8 \text{ A/dm}^2$  which is less than half the value obtained when triacetate bags were used. At the end of the experiment a layer of oxide covered the iron powder particles which agglomerated on drying. An analysis of the final solution showed that a substantial amount of iron had dissolved (28 g/l) while the nickel concentration of the plating solution remained virtually unchanged. An examination of the anode assembly gave some evidence of iron powder particles entering the bag, although only a small quantity of powder was retained within the bag.

In order to prevent the entry of iron powder, the canvas bag was replaced by an outer anode bag made of a 65% polyester 35% cotton fabric which possessed a much closer weave. The inner anode bag was made of 100% triacetate fabric. Fig. 23 and Table 8 (Ex NVII) shows the result of the plating experiment using this new material. The cell current showed a slight decline after the first 15 minutes of plating which was temporarily checked by increasing the potential difference across the cell. However, the overall cell resistance was only slightly higher than that obtained with triacetate anode bags and much lower than that obtained when the canvas bag was employed. The anode efficiency had increased to approximately 90% as compared to 54% and 46% respectively when triacetate and canvas bags were used. However, the deposition efficiency was not as high as those achieved with the use of 100% triacetate bags. Although, the polyester cotton material allowed the entry of less powder the particles trapped inside contained up to 55 mass% nickel as compared to 6% in the case of powder entrapped in the triacetate bags. Fig. 24 shows a sample of the outer polyester-cotton material after use: the shiny globules, which were rigidly attached to the weave of the fabric, contained approximately 60 mass % nickel.

A further experiment was carried out in which both anode bags were made from 65% polyester, 35% cotton fabric (see Fig. 25 and Table 8 Ex NVIII). Although the maximum cell potential was applied across the cell, the cell current achieved was only 25 amperes and the cell current declined between the 15th and 30th minutes of plating. This new arrangement of the anode bags resulted in a high average cell

resistance (0.72 ohms). The close weave of the fabric had allowed very little powder to enter the outer anode bag and a chemical analysis of the powder trapped inside showed that it contained only 11.0 mass % nickel. An examination of the bag surface showed little or no attachment of nickel plated globules. Moreover, the apparent deposition efficiency was well above 100%. However, the high resistance of the cell restricted the maximum average current density attainable to  $\sim 8 \text{ A/dm}^2$ . Consequently the plating rate was restricted to only 0.66 gms of nickel per minute. It should also be noted that the use of these bags resulted in a very high dissolution efficiency (94%).

#### 4.2.3 Effect of Anode Material on Plating Characteristics

The results of the experiments that used S-nickel shot in the anode in combination with 100% triacetate bags are reported in Table 8 (Ex NIX - XI). The deposition efficiencies obtained were of the order of 80%, which was significantly lower than those obtained with the use of pure nickel anodes (cf ExNXI and NIV). Thus under conditions where the same total charge had been passed the quantity of nickel deposited was much greater in the case where pure nickel anode was used. The anode dissolution efficiencies obtained by the use of S-nickel shot were not consistent, as was the case with the pure nickel anodes. Hence it has not been possible to make a comparison of the dissolution efficiencies obtained from the different types of nickel. Fig. 26 shows a typical example of the relationship between cell current and plating time when S-nickel shot were employed. The cell current showed an initial increase but then remained constant between the 15th and 60th minute of plating. This is in contrast to

the experiments carried out using 100% triacetate bags and pure nickel shot which showed a sharp fall in cell current after approximately 35 minutes.

Experiment NXII (Table 8) used S-nickel shot with an outer anode bag made of polyester - cotton fabric. This resulted in an anode efficiency of 85.0% and an apparent deposition efficiency of 91.0%. In contrast the use of pure nickel shot with the same bag arrangement produced an apparent deposition efficiency of 104%. The anode efficiency was also of the order of 89.0%. Thus, although the S-nickel anode in conjunction with polyester-cotton fabric produced less nickel deposition than was the case when pure nickel anodes were used, the magnitude of this effect was much less than that obtained when the anode bag was made of triacetate. Irrespective of the type of anode shot used, nickel was always deposited on the polyester fabric and the powder trapped within the bag was always rich in nickel.

Table 8 shows that generally the resistances of the cells that used pure nickel shot were lower than those that used S-nickel, (0.23 - 0.37 ohms and 0.33 - 0.35 ohms respectively) in the case of cells that also used triacetate bags. Similarly, the resistances of the cells that used polyester-cotton bags with S-nickel anodes were significantly higher than those using pure nickel shot and the same anode fabric.

#### 4.2.4 Influence of Iron Powder Particles on the Average Cell Resistance

The resistance of the plating cell was determined in the absence of iron powder particles in the plating solution, although agitation of the solution was still provided by the passage of the fluidising gas through the membrane at the base of the plating chamber. Fig. 27 shows that the cell

current, for a fixed potential across the cell, remained almost constant throughout this experiment. Table 9 compares the average cell resistance obtained under these conditions with the results obtained when iron powder was present in the cell. Comparison of the average cell resistances obtained during experiments NI and NXIII indicates that the presence of powder in the cell reduced the resistance to 65% of the value obtained in the absence of iron powder. Both these experiments employed triacetate fabric bags, but the use of other fabrics in the presence of iron powder raised the resistance of the cell (cf Ex NVII and NVIII). This effect was associated with the use of polyester cotton material with a finer weave. The replacement of pure nickel anode by S-nickel produced a significant increase in resistance of the cell (cf Ex NI and NIX and also NVII and NXII). In some instances the cell resistance rose to a value in excess of that obtained from the cell when no powder was present in the solution.

#### 4.2.5 Influence of the Total Electric Charge Passed and Average Current Density on the Quantity of Nickel Deposited

Fig. 28 shows the relationship between the total mass of nickel deposited on the powder particles and the total amount of electric charge passed. The theoretical relationship calculated from Faraday's law is shown as a straight line through the origin. However, the experimentally determined values all lie significantly above the corresponding theoretical values. The values within the brackets indicate the current density at which the plating was carried out. Fig. 28 clearly shows that all values except those corresponding to current densities greater than  $17.0 \text{ A/dm}^2$  fall on a straight

line which meets the ordinate at a positive value of approximately 9.0 g. This clearly suggests that simultaneous non-electrolytic deposition of nickel on iron powder occurred during the electroplating process.

Fig. 29 shows the relationship obtained between the mass percent nickel deposited and plating time during experiments carried out at different current densities. It is evident from this figure that as the current density increased, the quantity of nickel deposited in a fixed time also increased but the magnitude of this increase was much greater at current densities in excess of  $17 \text{ A/dm}^2$ . Fig. 30 shows this effect even more clearly. The slope of the line that shows the relationship between rate of deposition and current density shows a sharp increase at a current density of  $\sim 17.0 \text{ A/dm}^2$ .

#### 4.3 "ELECTROLESS PLATING"

These experiments were carried out in the Stage II cell (Fig. 7(b) and 8) in the absence of any applied potential at the electrodes. The composition of the plating solution was similar to the concentrated sulphamate bath used during the electroplating experiments (see Table 5). An attempt was made to maintain the temperature of the bath at the level previously used, but some reduction in temperature occurred in all cases where an electric potential was not employed.

Fig. 31 shows the relationship between the mass percent of nickel deposited and the plating time, together with the variation in temperature during the experiments. It is evident that:-

- (i) the initial rate of deposition of nickel was high, but after approximately 15 minutes this rate had fallen substantially to a level that was maintained until the end of the experiment (60 minutes).
- (ii) the amount of nickel deposited in a given time increased as the temperature of the solution increased.

However, when the plating process was extended for a further hour it became evident that the rate of deposition of nickel after the first 15 minutes was not quite linear with time (Fig. 32) since a small reduction in slope now occurred as plating time was increased. The addition of 250 ml of fresh solution after 105 minutes of plating produced an abrupt increase in the rate of deposition of nickel. This indicates that the gradual reduction in the deposition rate that had previously occurred was at least partially associated with the reduction in the concentration of nickel ions in the solution.

Fig. 33 shows the relationship between time and the amount of nickel deposited in two electroless plating experiments carried out under similar conditions of temperature and solution strength. However, frothing of the bed was observed in one of the experiments (curve 2) and a silicon anti-foam agent was required, in order to restore correct fluidisation. The results clearly show the detrimental effect of the anti-foam agent since only 2.25 mass % of nickel was deposited, as compared to 3.46 mass % in the absence of frothing.

Table 10 gives the results of two experiments, one with the anode bag assembly in position (Ex NXXIII) and the other without (Ex NXXVIII). As can be seen from Table 10, only

0.7 gms of nickel dissolved from the anode when it was placed in the cell. The amount of nickel deposited was slightly higher in the case of the experiment carried out with anode bags in position; however this could have been the result of a slightly higher solution temperature.

Table 11 gives the results of an experiment that attempted to deposit 'electroless' nickel onto solid objects rather than powder particles. Three solid objects (two of mild steel and one of electrolytic iron) were suspended in the plating solution under similar conditions to those used during the coating of powder particles. No significant increase in mass was observed in any of the three samples after plating times of 60 minutes. Chemical analysis (Table 11) also confirmed that no nickel deposition had occurred.

#### 4.4 OXYGEN CONTENT OF PLATED POWDER

Table 12 gives the oxygen content of powder coated for various lengths of time. Plated powder samples were taken at various stages of the plating process, washed and then dried in air. The results do not indicate any definite relationship between the period of plating and oxygen content. It would appear probable that the oxygen content of the powder was dependant on variations in the drying process rather than the duration of plating.

#### 4.5 SIEVE ANALYSIS OF POWDERS

Table 13 gives the results of sieve analyses carried out on the parent sponge iron powder and on plated powders of varying nickel compositions. The results indicate that growth of the powder particles had occurred. The percentage of finer powder particles present had decreased whereas that of the larger particles had increased. However, it should be

pointed out that some of the finer powder particles were lost during washing. Nevertheless, an increase in the coarser fractions confirms the growth of particles as a result of coating. Nickel analyses carried out on the various sieve fractions shows substantial deviation from the nominal composition, which followed a similar pattern in every case (Fig. 34). A positive value of 'D'\* was observed in the finest and the coarsest fractions only.

Table 14 shows the results of an experiment (Ex NXIV) carried out using only -106 +90 micron size powder. The average resistance of the cell was marginally greater than those using unsieved powder. However, the apparent deposition efficiency was substantially greater than those obtained when unsieved powder was used. The plated powder from this experiment was sieved and the nickel content of the various sieve fractions determined. The results (Table 14) show that the finest (-106+90 micron) and the coarsest (+150 micron) fraction again had higher nickel contents than the mean nickel content of the bulk (unsieved) powder. In contrast, the middle sieve fractions (106 and 125 micron) had nickel contents very close to that of the bulk powder. The anode efficiency was of the order of 60%.

#### 4.6 PROPERTIES OF POWDERS USED

The mean particle size and chemical analyses of the powders are given in Table 15 . Sieve analysis of the

---

\* 'D' (Deviation from the nominal nickel content.) mass %  
= Mean nickel content of unsieved powder - nickel content of sieved fraction.

sponge iron powder showed that the majority of powder particles were smaller than the minimum sieve size. However, plating of nickel onto iron powders was associated with growth of the particles (Table 13). The process of plating was also found to increase the oxygen content of the powders although this absorbed oxygen was removed during sintering (Table 16).

#### 4.7 COMPACTION OF PLATED AND BLENDED POWDERS

Figure 35 shows the relationship between the green compact density and compaction load, obtained in the case of both blended and plated powders. The variation in the range of densities of the blended powder compacts pressed at 250 KN was  $\pm 0.04 \text{ g/cm}^3$ , although a smaller variation was obtained when higher compaction loads were used. Although the plated powders showed a similar behaviour, the mean green densities obtained in plated powder compacts were lower than those obtained in blended powder compacts after compaction at the same load (7.02 and  $6.75 \text{ g/cm}^3$  respectively at a compaction load of 350 KN). A change in the nickel content did not bring about any appreciable change in the compaction characteristics of either the blended or plated materials.

#### 4.8 PROPERTIES AND MICROSTRUCTURE OF Fe-Ni-C ALLOYS

In order to assess the suitability of plated powders for powder metallurgical applications, the modulus of rupture of compacts made from this material was compared to that obtained from compacts prepared from conventional blended powders. A microstructural examination of the

compacts made from the two different materials was also undertaken in order to examine the influence of micro-structure on the properties.

#### 4.8.1 Influence of Porosity On The Modulus of Rupture Of Fe-Ni-C Alloys

(A) Iron - 1.75% Nickel - 0.35% Carbon Alloys:-

Tables 17 and 18 give the values of modulus of rupture of compacts prepared from both blended and plated powders and sintered for periods ranging between 30 and 240 minutes. For every sintering treatment, compacts were pressed under three compacting loads in order to provide a range of sintered densities and so establish a relationship between modulus of rupture and total porosity after any particular sintering treatment. The following two general conclusions can be drawn from the results, irrespective of the type of powder used:-

(i) An increase in the value of modulus of rupture was obtained with increase in the density of compacts sintered for similar periods of time. The increased density resulted from the use of higher compaction pressures. (Viz:- in blended powder compacts 105B and 109B the modulus of rupture increased from 786 to 1027 N/mm<sup>2</sup>).

(ii) An increase in the value of modulus of rupture was also obtained with an increase in the period of sintering of compacts that possessed similar levels of density. (Viz: in compacts 104B and 120B the modulus of rupture increased from 924 to 1062 N/mm<sup>2</sup> when the period of sintering was increased from 30 to 240 minutes).

Figure 36 (line 1) shows the relationship between the modulus of rupture and the total porosity obtained from compacts that had been prepared from blended powders. A linear regression analysis was used to obtain the equation of the line; viz:-

$$R (\underline{+92} \text{ N/mm}^2) = 1553 - 63.4P \quad (\text{EQ 4.1})$$

Where R = modulus of rupture in  $\text{N/mm}^2$

P = total porosity in %

A correlation coefficient of -0.91 was obtained for the above relationship. Although all the results lie close to the line represented by EQ 4.1, Figure 36 shows that compacts that had been sintered for longer periods (viz:- 240 minutes) generally possessed strengths higher than those predicted by EQ 4.1 whereas the strengths of compacts sintered for shorter periods (viz:- 30 minutes) were equal to or lower than those predicted by the above relationship.

Figure 36 (line 2) shows the relationship between modulus of rupture and total porosity for compacts prepared from plated powders. The following relationship was obtained using a simple linear regression analysis;

$$R (\underline{+44} \text{ N/mm}^2) = 1701 - 74.9P \quad (\text{EQ 4.2})$$

Where R = modulus of rupture in  $\text{N/mm}^2$

and P = total porosity in %

the correlation coefficient for the above relationship was -0.99.

According to the above relationship, the modulus of rupture of a porosity-free compact made from plated powders should be  $1701 \text{ N/mm}^2$  as compared to  $1553 \text{ N/mm}^2$  for similar compacts made from blended powders (EQ 4.1). Figure 36 (line 2) also indicates that an increase in the period of sintering produced only a small increase in the value of the modulus of rupture, especially in compacts possessing high levels of porosity. It is also evident that at low porosity levels, compacts prepared from plated powders were slightly superior to those prepared from blended powders. However, at higher porosity levels the two materials exhibited similar values of the modulus of rupture. It is also interesting to note that blended powder compacts that had been sintered for longer periods (viz - 240 minutes) lay closer to the line (EQ 4.2) for plated powder than to that of blended powder compacts (EQ 4.1).

(B) Iron - 3.25% Nickel - 0.35% Carbon Alloys:-

Although the mean nickel content for this series of alloys was intended to be 3.25% nickel, chemical analysis of the sintered compacts showed that the blended and plated powder compacts generally possessed 3.5% and 3.0% nickel respectively.

Tables 19 and 20 show the modulus of rupture of sintered compacts prepared from both blended and plated powders. As in the case of compacts containing 1.75% nickel, the results obtained from 3.25% nickel compacts also show that for any fixed period of sintering, the modulus of rupture increased as the density of the compacts increased. Furthermore,

in the case of compacts possessing similar levels of sintered densities, the highest values of modulus of rupture were obtained from compacts that had been sintered for the longest periods. The range of sintered densities obtained for any given period of sintering was the result of using the different compaction pressures used in the preparation of green compacts. Figure 37 shows the relationship between modulus of rupture and total porosity obtained from compacts prepared from both blended and plated materials. A simple linear regression analysis was used to arrive at the following relationships for the two materials respectively:-

For blended powder compacts sintered for 30 to 240 minutes -

$$R(+72 \text{ N/mm}^2) = 1700 - 73.52P \quad (\text{EQ 4.3})$$

For plated powder compacts sintered for 120 and 240 minutes -

$$R(+53 \text{ N/mm}^2) = 1653 - 62.2P \quad (\text{EQ 4.4})$$

Where  $R$  = modulus of rupture in  $\text{N/mm}^2$

$P$  = total porosity in %

Figure 37 again shows that, in the case of the blended materials, compacts that had been sintered for longer periods (viz - 240 minutes) possessed higher values of modulus of rupture than those predicted by the above relationship (EQ 4.3). The plated materials, on the other hand, showed a very significant improvement as the period of sintering increased. The compacts that had been sintered

for only 30 minutes possessed values of modulus of rupture that were much lower than those obtained with the use of blended powders. A slight improvement was obtained after sintering for 60 minutes and the modulus of rupture levels were now equivalent to those obtained with blended powders.

However, a further increase in the period of sintering to 120 and 240 minutes brought a marked improvement in the value of modulus of rupture of the plated powder compacts.

Thus the plated powder compacts that had been sintered for 120 and 240 minutes were superior to the corresponding compacts made from blended powders.

(C) Iron - 4.25% Nickel - 0.35% Carbon Alloys:-

Table 21 gives the values of modulus of rupture obtained from blended powder compacts sintered for periods ranging between 30 and 240 minutes. The results shown in Table 21, clearly indicate that after any particular sintering treatment the value of the modulus of rupture increased as the density of the compact increased. Furthermore, at any fixed density level an increase in the value of modulus of rupture was obtained by an increase in the period of sintering.

Table 22 gives the values of modulus of rupture of iron - 4% nickel alloy compacts prepared from nickel coated iron powders and sintered for periods between 30 and 240 minutes. Because of the limited quantity of powder available and the practical difficulties involved in the control of the carbon content of the sintered compacts made from plated powders, compacts of the above composition could not be

prepared to a wide range of densities for each sintering treatment, as had been the case with compacts made from blended powders. However, the limited results obtained indicated a gradual improvement in the values of modulus of rupture as the period of sintering was increased.

Figure 38 shows the relationships obtained between modulus of rupture and total porosity for iron - 4.25% nickel compacts prepared from both blended and plated powders and sintered for periods between 30 and 240 minutes. The following relationships between the modulus of rupture and total porosity were obtained for compacts made from blended powders.

(i) for compacts sintered for 30 minutes

$$R(+25 \text{ N/mm}^2) = 1651 - 68.38P \quad (\text{EQ 4.5})$$

(ii) for compacts sintered for 60 minutes

$$R(+32 \text{ N/mm}^2) = 1657 - 65.78P \quad (\text{EQ 4.6})$$

(iii) for compacts sintered for 120 minutes

$$R(+65 \text{ N/mm}^2) = 1793 - 74.7P \quad (\text{EQ 4.7})$$

(iv) for compacts sintered for 240 minutes

$$R(+37 \text{ N/mm}^2) = 1833 - 78.92P \quad (\text{EQ 4.8})$$

The experimental results were subjected to a simple linear regression analysis to obtain the above relationships.

The improvement associated with the use of increased periods of sintering is evident from the above relationships. A similar regression analysis was carried out for all the experimental results obtained from blended powder compacts irrespective of the sintering treatment; the following single relationship, with a correlation coefficient of -0.97, was obtained:-

$$R(\pm 69 \text{ N/mm}^2) = 1830 - 80.9P \quad (\text{EQ 4.9})$$

Where R = Modulus of rupture in  $\text{N/mm}^2$

P = Total porosity in %

Figure 38 clearly shows the influence of longer periods of sintering on modulus of rupture at any given density level, although the effect at lower densities (i.e. high porosity levels) was less pronounced.

The results obtained with the use of plated powders were also subjected to a simple linear regression analysis and the following relationship was obtained between modulus of rupture and total porosity:-

$$R(\pm 42 \text{ N/mm}^2) = 2045 - 97.24P \quad (\text{EQ 4.10})$$

Where R = modulus of rupture in  $\text{N/mm}^2$

P = total porosity in %

The above relationship was valid for all the results obtained from plated powder compacts irrespective of the sintering time employed. It is evident from Figure 38 (line 5) that plated powder compacts that had been sintered

for longer periods (viz - 240 minutes) possessed superior modulus of rupture than those predicted by EQ 4.10. The plated powder compacts that had been sintered for 240 minutes were also superior to those made from blended powders but compacts that had been sintered for 120 minutes or less possessed similar values of modulus of rupture irrespective of the type of powder used.

#### 4.8.2 Microstructure of Iron-Nickel-Carbon Alloy Compacts Made From Both Blended and Plated Powders

##### (A) Iron - 1.75% Nickel - 0.35% Carbon Alloys:-

Figure 39 shows the heterogeneous structure obtained after quenching of a compact previously sintered for 30 minutes at 1150°C. The structure contained large light-etching areas in positions that were probably originally occupied by several nickel particles agglomerated together: these areas did not appear to have undergone any transformation during quenching. The remainder of the structure consists of dark etching transformation products. The structure of a compact also sintered for 30 minutes but tempered for 60 minutes at 600°C subsequent to quenching from the sintering temperature is shown in Figure 40. The tempering treatment did not affect the appearance of the light etching areas but some carbide precipitation was observed in the darker etching regions. In the tempered structure, there was also some evidence of the paths taken during interparticle diffusion. The structures of both quenched and tempered samples showed the presence of both interconnected and coarse isolated pores.

In the microstructure of a compact that had been sintered for 60 minutes prior to quenching, (Figure 41) the smaller of the light-etching areas were no longer present but the larger ones still remained and again did not appear to have undergone any transformation during quenching. Apart from these light etching areas, the structure appeared to be mainly martensitic, as was the case in compacts sintered for 30 minutes. However, at higher magnification (Figure 42) a variation in the morphology of the structure was revealed. Apart from the darker etching martensitic phase, there were some patches of light etching transformation products that appeared similar to bainites. The structure also suggested the presence of some wide plates that were similar to those generally found in Fe-Ni alloys. These plates were observed near to the very light etching areas which did not show any transformation products. A large number of isolated pores could be seen, although some interconnected porosity was also present.

An increase in the period of sintering from 60 to 240 minutes did not bring about any major changes in the microstructure (Figure 43) except that the light etching areas had become very diffuse and the overall structure appeared more uniform than that of compacts sintered for 60 minutes (Figure 41). The structure at a higher magnification (Figure 44) showed a mixture of dark and light etching transformation products which generally appeared martensitic. The lighter etching plates were observed in areas which were probably originally occupied by nickel particle agglomerates. However, there were also some blocky light etching areas

which appeared similar to bainites. The longer period of sintering has also brought about the spherodisation of the pores, the majority of which had round edges and a convex shape.

Figure 45 shows the microstructure of a plated powder compact that had been sintered for 30 minutes at  $1150^{\circ}\text{C}$  and quenched into water. There was some evidence of a light etching network around darker etching areas. Higher magnification (Figure 46) revealed that this light etching network was only partially transformed on quenching. However, sintering for a period of 60 minutes (Figure 47) removed this network and the structure appeared more uniform. Although, the transformation to martensite had occurred to a greater extent after the longer sintering treatment, there appeared to be some small patches of light etching regions (Figure 48). Another important feature revealed by the microphotographs of compacts sintered for periods up to 60 minutes was the presence of elongated and interconnected pores.

Figure 49 shows the homogeneous structure obtained after quenching a compact sintered for 120 minutes. The structure appeared to be predominantly martensitic although microphotographs taken at a higher magnification suggested the presence of some patches of a non-martensitic light etching phase (Figure 50). A further increase in the period of sintering did not bring about any changes in the microstructure, although a greater proportion of rounded pores were observed.

(B) Iron - 3.25% Nickel - 0.35% Carbon Alloys:-

Figure 51 shows the microstructure of a 3.25% nickel steel compact made from blended powders and sintered for 30 minutes at 1150°C prior to quenching into water. The structure is very similar to that produced in the 1.75% nickel alloy compact made from similar materials, (see Figure 39). The light etching areas revealed the original position of agglomerates of nickel particles which was surrounded by a transformation product which appeared to be predominantly martensitic. The shape and position of these light etching areas also revealed the interparticle diffusion paths. The structure as revealed at a higher magnification (Figure 52) supported the view that the nickel particle agglomerates (light etching areas) had not undergone any transformation on quenching although the areas surrounding these agglomerates were predominantly martensitic. It is also interesting to note that, although there were some interconnected pores, there were also a large number of pores with rounded edges, despite the relatively short period of sintering. This probably reflects the relatively high green density possessed by these compacts. In compacts sintered for 60 minutes (Figure 53) the larger light etching austenitic areas were still present although the majority of the smaller ones had disappeared. The extent of homogenisation that has occurred in compacts sintered for 60 minutes was evident in the tempered structure (Figure 54). The structure revealed the presence of large patches of light-etching austenitic regions which did not contain any visible carbide

particles. There were also some diffused light etching regions which showed limited carbide precipitation, suggesting that transformation to martensite had occurred to a limited extent in these areas.

Figure 55 shows the structure of a similar specimen that had been sintered for 240 minutes prior to quenching from the sintering temperature. The structure no longer contained many distinct light etching austenitic regions, although some areas appeared to etch more lightly than others. An examination at a higher magnification (Figure 56) supports the view that the structure was predominantly martensitic. Some transformation product, which appeared non-martensitic was observed within the lighter etching regions. Some isolated coarse pores were seen even after the longest sintering period (viz: 240 minutes) although, in general, the porosity was spherical or near spherical in shape.

The microstructure of a 3.0% nickel alloy compact that had been made from nickel coated iron powder sintered for 30 minutes and then quenched is shown in Figure 57. The nickel that had covered the original iron powder particles had not completely diffused into the powder particles but appeared as a network of nickel rich areas (light etching) around the iron powder particles (dark etching). As a result of the sharp nickel concentration gradient and thus the varying response to the etchant, it was difficult to reveal a clear structure. However, it appears that the iron rich regions had transformed to darker etching martensite and that the light etching nickel rich network

had partially transformed to light etching martensites. This view was confirmed by examination of the structure at a higher magnification (Figure 58) which showed that the light etching network had also undergone transformation during quenching. It is also interesting to note the presence of thin interconnected porosity which separated the powder particles. Figure 59 shows the structure of a similar compact but sintered for 60 minutes prior to quenching. It is clear that diffusion of nickel was still not complete although a distinct light etching network was no longer observed. Examination of the structure at a higher magnification (Figure 60) again revealed that the predominant transformation product was martensitic in nature. Transformation to martensite also appeared to have occurred in the lighter etching areas to a greater extent than that observed in compacts sintered for only 30 minutes. However, small areas of untransformed austenite could still be observed together with some light etching plates which appeared to be bainitic in nature. The pores were still elongated and interconnected although the thin interconnected pores that separated individual powder particles in compacts sintered for only 30 minutes (Figure 57) were no longer clearly visible.

Figures 61 and 62 show the microstructures of plated powder compacts sintered for 120 and 240 minutes prior to quenching and clearly indicate the very uniform microstructure that has resulted from the increased homogeneity. The structures consisted predominantly of martensite, although there were some areas where the plates were wide and lighter

etching which probably suggested the presence of some bainites (Figure 63). The porosity, even after the longest period of sintering (viz: 240 minutes), appeared to be generally interconnected although there were some isolated coarse pores with rounded edges.

(C) Iron - 4.25% Nickel - 0.35% Carbon Alloys

Figure 64 shows the microstructure of a 4.25% nickel alloy compact that had been prepared using blended powders and then sintered for 30 minutes prior to quenching. The structure was similar to that observed in blended powder compacts of 3.25% nickel sintered for 30 minutes with large light etching areas surrounded by dark etching transformation products which appeared to be martensitic in nature. An increase in the period of sintering to 60 minutes (Figure 65) did not bring about any major changes in the structure; the light etching areas had become more diffused and there was some evidence of interparticle diffusion of nickel. An examination at a higher magnification (Figure 66) suggested that the transformation product obtained on quenching was predominantly martensitic. The centres of the light etching areas did not show any transformation product although there was some evidence of light etching martensites towards the edges of these parts of the structure. The pores, even after just 60 minutes of sintering, appeared coarse and isolated with round edges; although a few thin interconnected pores could also be seen.

The structure obtained on quenching a similar compact that had been sintered for 240 minutes is shown in Figure 67.

This long period of sintering brought about considerable homogenisation although some light etching areas, which have not undergone any transformation, were still present. In addition, there were some areas which had transformed to light etching martensites. These were probably the regions where diffusion of nickel had occurred to an appreciable extent and thus retention of the high temperature phase was avoided. These views were confirmed by an examination of the structure at a higher magnification which clearly showed three distinct regions (Figure 68):

- (i) light etching area which showed no transformation product,
- (ii) light etching transformation product which appeared to be martensitic,
- (iii) dark etching martensites.

The pores were generally convex in shape and a large number were almost spherical, which suggests that sintering of the powder particles had reached the stage of pore spherodization.

Figure 69 shows the microstructure of a 4.0% nickel compact that had been prepared from plated powders and sintered for 30 minutes prior to quenching. It is evident that, within the short period of sintering available, the nickel coating had not been able to diffuse completely into the iron powder particles so that a light etching network surrounded the dark etching regions in the structure. Although the network was similar to that observed in a 3% nickel compact sintered for the same period (Figure 57) it was somewhat wider and rather more diffuse than that observed in the

3% nickel compact. It is also interesting to note the presence of long thin interconnected pores within the light-etching network which reflects the poor adhesion between individual particles of the plated powder. The dark-etching regions appeared predominantly martensitic and there was also evidence of transformation within the light-etching network. The structure of a similar compact that had been sintered for 60 minutes prior to quenching is shown in Figure 70. The diffusion of nickel had occurred to a greater extent as a result of the increased period of sintering and the light-etching network was no longer clearly visible. However, patches of light etching regions could still be seen. The structure at a higher magnification (Figure 71) suggested that the lighter etching regions had undergone considerable transformation during quenching. The wide plates in these light etching areas and near pores also indicated the formation of some bainitic products during quenching. The darker etching regions appeared predominantly martensitic. The long thin interconnected pores, similar to that observed in compacts sintered for 30 minutes, were still present.

Figures 72 and 73 show the structures obtained on quenching compacts that had been sintered for 120 and 240 minutes respectively. The diffusion of nickel appeared almost complete and thus has resulted in a very uniform structure that is predominantly martensitic in nature. It is also interesting to note that in the compact that had been sintered for 120 minutes, some long interconnected pores were still

present. In addition, some of these pores were open to the surface of the specimen and were thus filled with the cold setting resin in which they were mounted. Some open pores were also observed in compacts that had been sintered for 240 minutes. Figure 74 shows the structure of the compact that had been sintered for 120 minutes at a higher magnification. Although the structure appears to be predominantly martensitic there were some wide plates that suggested the occurrence of bainitic transformation during quenching.

#### 4.8.3 The Homogeneity of Blended and Plated Powder Compacts Sintered at 1150°C

The homogeneity of compacts, prepared from both blended and plated powders, that were sintered at 1150°C for periods ranging between 30 and 240 minutes, was determined by the method described in Section 3.8. These determinations were only made in the case of 3.25 and 4.25% nickel compacts.

##### (A) Iron - 3.25% Nickel - 0.35% Carbon Alloys:-

Figure 75 shows the relationship between the homogenisation parameter (as defined in Section 3.8) and the period of sintering in the case of 3.25% nickel compacts made from blended powders. A relatively large fall in the value of the homogenisation parameter (H) was observed in the first 120 minutes of sintering which reflects the rapidity at which homogenisation had occurred within this period of sintering. However, only a small fall in the value of the

homogenisation parameter was obtained when the period of sintering was increased from 120 to 240 minutes. The value of H after 240 minutes of sintering was 0.68. However, it should be emphasised that only one measurement of the homogenisation parameter was made for each period of sintering and that previous work<sup>(90)</sup> has shown a considerable scatter in similar measurements of this property.

Figure 76 shows the relationship between the homogenisation parameter (H) and the period of sintering for 3.0% nickel compacts made from plated powders. In comparison to the corresponding curve for blended powder compacts, the plated powder compacts possessed greater homogeneity (i.e. lower values of homogenisation parameter) even after the shortest period of sintering. (Viz:- 1.12 for plated powder compacts as compared to 5.8 for blended powder compacts). However, the shape of the two curves (Figures 75 and 76) were very similar. The plated powder compacts exhibit rapid homogenisation in the first 60 minutes of sintering as indicated by the sharp decline in the value of the homogenisation parameter, but any increase in the period of sintering beyond 60 minutes resulted in a relatively small fall in the value of this property, which reached a value of 0.27 after 240 minutes of sintering. The corresponding value for a blended powder compact was 0.68.

(B) Iron - 4.25% Nickel - 0.35% Carbon Alloys:-

Figure 77 shows the relationship between the homogenisation parameter (H) and period of sintering obtained

from specimens that contained 4.25% nickel and had been prepared from blended powders. The curve is very similar to that obtained for 3.25% nickel compacts also prepared from blended powders, and shows that a rapid increase in the degree of homogeneity occurred during the first 120 minutes of sintering: this was followed by a relatively slow decline during the next 120 minutes. The homogenisation parameter (H) after the longest period of sintering (i.e. 240 minutes) was 0.85 as compared to 0.68 in the case of the 3.25% nickel compact sintered for the same period. It should again be emphasised that only one measurement of the homogenisation parameter was made at each sintering time.

Figure 78 shows the relationship between the homogenisation parameter and sintering time for 4.0% nickel compacts prepared from plated powders. Compared to the corresponding curve obtained from blended materials, the plated powder compacts exhibited a greater degree of homogeneity (i.e. possessed lower value of homogenisation parameter) even after the shortest period of sintering (viz:- 2.3 for the plated powder compacts as compared to 6.5 for the corresponding blended powder compact). However, a comparison with the 3.0% nickel compacts also prepared from plated powders shows that the higher nickel content of the 4.0% nickel compacts has resulted in a higher value of the homogenisation parameter. (Viz:- 2.3 for the 4.0% nickel compact sintered for 30 minutes as compared to 1.12 for the corresponding 3.0% nickel compact). Although the difference in the homogenisation parameter between the two

plated powders (i.e. 3.0 and 4.0% nickel) decreased as the period of sintering was increased, the former were always more homogeneous than the latter after identical sintering treatments. The shape of the homogenisation curve was similar to those obtained from the examination of the other powders and showed rapid homogenisation in the first 60 minutes of sintering followed by a gradual decline in the rate of homogenisation as the period of sintering was increased. The value of the homogenisation parameter after the longest period of sintering (viz:- 240 minutes) was 0.54 as compared to 0.85 for the corresponding compact made from blended powders.

CHAPTER FIVE  
DISCUSSION OF RESULTS

## 5. DISCUSSION OF RESULTS

### 5.1 MECHANISMS OF CHARGE CONDUCTION IN A FLUIDISED BED ELECTRODE

In a conventional electroplating cell which does not contain any conducting particles suspended in the plating solution, ion conduction within the electrolyte occurs as a result of the migration of ions under the influence of an electric field. An increase in the cell current and consequently the current density leads to depletion of metal ions in the vicinity of the electrode and thus produces concentration polarization<sup>(3)</sup>. Consequently, under conventional electroplating conditions electro-winning of lean solutions cannot be carried out at sufficiently high current densities. However, several workers<sup>(49-52,55,56)</sup> have shown that the use of fluidised bed electrodes results in increased overall cell current without changing the current per unit surface area of the electrode. Conversely, the use of fluidised bed electrodes reduces the current per unit surface area of electrode (current density) for a fixed overall cell current and thus avoid concentration polarization. In addition, the vigorous agitation in the fluidised bed also helps to reduce concentration polarization.

Although the fluidised bed used in the present investigation was not as dense as those used by other workers<sup>(49-52, 55, 56)</sup>, the presence of iron powder particles within the bed resulted in an increase in the overall cell current for a fixed potential across the cell, the effect being reflected in the appreciable decrease

in the average resistance of the cell (see Table 9 Ex NXIII and NII). Several workers<sup>(49-52, 55, 56)</sup> have reported effective reductions in the resistances of the plating cells that contain fluidised bed electrodes and that such reductions are believed to be associated with charge conduction mechanisms that involve the powder particles. The mechanisms that contribute to the decrease in the resistance of the cell are<sup>(49)</sup>:-

- (i) migration of ions under the influence of the applied potential difference coupled with the short circuiting of the conduction paths by the solid powder particles.(Fig. 2a)
- (ii) charge conduction through chains of powder particles. (Fig. 2b)
- (iii) a conductive mechanism by which the electric double layer of the particle becomes charged by contact with the current feeder or another charged particle and then moves to another part of the bed where it is discharged by charge sharing with another particle or by electrochemical reaction.(Fig. 2c)

An overall effect of the above mechanisms would be to increase the electrode surface area, the limiting current density and decrease the ohmic resistance of the cell. However, because of the practical difficulties involved, a detailed examination of the charge conduction mechanisms operating within a fluidised bed electrode was considered beyond the scope of the present investigation. Nevertheless, some observations made during the present work suggested an

appreciable increase in the cathodic surface area.

Figure 79 shows branch like growth on the cathode rods after the plating operations. Chemical analysis showed that these branch like structures were composed of nickel coated iron powder particles. It appears that during the process of plating, the iron powder particles had formed a chain, one end of which was in contact with the cathode current feeder. Subsequent plating on these chains had welded the particles together and attachment of additional powder particles to the chain already formed resulted in the extension of the branch like structures observed. However, the formation of a large number of long chains requires a high density of particles in the bed. Therefore, it seems improbable that the formation of chains of powder particles occurred to any great extent in the fluidised beds used in the present work, which contained only 1,000 grams of iron powder in 1600cm<sup>3</sup> of plating solution

Flett<sup>(51)</sup> and other workers<sup>(50,54)</sup> reported that as the expanded bed height increased the cell current increased to a maximum point beyond which any further increase in the bed height resulted in a decrease in the cell current. They believed that the initial increase in the cell current was a result of increased surface area as compared to a static bed. However, further increase in the bed height caused a loss of electronic contact which outweighed any advantages gained by the increase in surface area. The above authors found a 33% bed expansion to be the optimum. Since the density of the bed used in the present work was less

than the optimum level, it seems reasonable to assume that charge conduction via the formation of particle chains was not the dominant mechanism. Nevertheless, since in the 'anode - bag cells' a decrease in the resistance was observed as a result of the addition of iron powder particles, it is likely that a convective mechanism was in operation: thus the electric double layer of the particle was charged by contact with the current feeder or another charged particle. The particle so charged then moved to another part of the bed where it lost its charge either to another particle or by electrochemical reaction.

However, in comparison to the 'anode - bag cell', that using a porous refractory membrane, possessed a relatively high resistance (Table 7 and Table 9 Ex NII). The results obtained showed that there was a build up of nickel ions within the anode chamber indicating that either the process of dissolution was more efficient than that of nickel deposition or that the nickel ions were not being transported easily from the anode to the cathode compartment. Several workers<sup>(17, 22)</sup> have found that the use of electrolytic nickel anode, in the presence of chloride ions, produces anode efficiency that approaches 100%. However, since in the refractory membrane cell, the anode efficiencies achieved were only of the order of 94%, it suggests that the porous membrane was a barrier to the free passage of nickel ions which consequently resulted in a build up of nickel ions in the anode chamber. Furthermore, it should be pointed out that in the refractory membrane cell, the iron powder

particles were confined within the walls of the porous refractory tube (cathode chamber) and thus the charge conduction mechanism within the anode chamber was the migration of ions under the influence of an electric field. Since it has already been shown that the presence of powder particles enhanced charge conduction, it appears that the high resistance of this cell was caused by the porous membrane which restricted the free passage of ions into the cathode chamber.

A further increase in the resistance of the refractory membrane cell was observed when the quantity of iron powder in a fixed volume of the plating solution was increased. A fixed volume of fluid can support a fixed mass of powder in suspension at a constant flowrate of the fluidising gas and any further addition of powder will lead to a stagnant layer of powder on the fluidising membrane. Although increasing the flow rate of the fluidising gas removed the stagnant layer, it also led to aggravated fluidisation and spurting of the bed. It appears that in the aggravated stage of fluidisation, the iron powder particles were enveloped by gas bubbles which broke near the surface and caused spurting of the bed. The presence of the envelope of gas would inhibit electronic contact between powder particles and consequently result in higher cell resistance. However, further work is required to fully understand the mechanisms operating during electroplating of powder particles in a three-phase fluidised bed and such a research programme is currently being carried out (206).

## 5.2 INFLUENCE OF MEMBRANE MATERIAL ON THE PLATING PROCESS

(A) Refractory Membrane:- Figure 13 to 15 show the relationship between both cell current and plating time and cell potential and plating time, which were recorded during experiments carried out in the refractory membrane cell. Apart from the initial rise in the cell current which was controlled by regulating the cell potential, the cell current remained almost constant throughout the experiment which suggested the absence of any significant polarisation. An examination of the theoretical and experimental values of the mass of nickel deposited showed a difference of approximately 3.0 grams between the two values. The corresponding values of deposition efficiencies were of the order of 82.0% for experiments MI and MIII (Table 7) and 72.0% for experiment MII, which had a higher density of the fluidised bed coupled with a higher cell resistance. However, the mass of nickel deposited on the cathode rods was not included in the calculation of these cathode efficiencies and it would, therefore, appear that the process of plating nickel onto iron powder particles was reasonably efficient. Nevertheless, electroplating of nickel onto iron powder particles, in a cell of this type would still not be an economical proposition because of the low plating rates obtained - a maximum of 1.92% nickel on 750 grams of iron powder in 60 minutes of plating. Such a plating rate would require long times for producing alloy powders of commercial compositions and would thus render the process uneconomical. The rate of plating is controlled by the

current density which in turn is dependent on the nickel ion concentration and the cell resistance. In the plating cell utilising a porous refractory membrane, the cell resistances were relatively high and thus restricted the use of very high current densities. Furthermore, since the sulphamate solution used in present investigations, has been shown to be suitable for operation at very high current densities<sup>(26, 27)</sup>, it appears that the major drawback of the refractory membrane was its high cell resistance.

(B) Fabric Anode Bags:- Table 8, gives the results of the experiments carried out with anode bags made from different types of fabric. The lowest cell resistance was obtained in cells that employed anode bags made of 100% triacetate fabric. However, in these cells, a fall in the cell current was observed after approximately 45 minutes of plating (Figure 16). This behaviour was in contrast to that observed in the cell employing a porous refractory membrane in which the cell current remained constant after the initial stabilising period (Figures 13-15). It was observed that iron powder had entered the triacetate bags where it partially covered the surface of the nickel shot (Figure 21). This powder was probably responsible for the increase in cell resistance after 45 minutes, since it prevented contact between anode and solution.

The use of an outer anode bag made of 65% polyester - 35% cotton material greatly reduced the quantity of iron powder entering the anode bag but this was achieved at the cost of a small increase in the initial resistance of the

cell. The use of polyester-cotton fabric bags was also associated with substantial increase in the anode efficiency which increased to approximately 90%. Such a high level of anode efficiency clearly indicated the absence of any significant interference in the dissolution process by any iron powder that may have passed through the membrane between anolyte and catholyte. However, despite the high anode efficiency, the apparent deposition efficiency achieved was only 103% which is considerably lower than the levels obtained with the use of 100% triacetate fabric anode bags.

An examination of the polyester cotton bag provided a possible explanation of the poor apparent deposition efficiency obtained. The shiny globules seen in Figure 24 are rigidly attached to the fabric and a chemical analysis of the particles showed that they contained a very high percentage of nickel. The small quantity of powder trapped within the bag was also found to be very rich in nickel. If, in the calculation of the apparent deposition efficiency, the mass of nickel deposited onto the powder trapped within the bag was included the efficiency would be very similar to that obtained with the use of 100% triacetate bags. However, no apparent reason could be found for deposition on the fabric bag. It is possible that powder particles were entrapped in the weave of the fabric and subsequent electroless deposition had led to the formation of the globules seen in Figure 24. However, since deposition on the bag was only observed when an outer bag made of polyester-cotton fabric was used with the inner bag made of

100% triacetate fabric, it seems unlikely that the entrapment of powder particles could have caused the observed deposition. It has been reported that electrostatic charge can be developed in polymeric materials and that the nature of charge depends on the two materials in contact and the direction in which they move with respect to each other<sup>(207)</sup>. However, since the bags were held in an aqueous media, the development of electrostatic charge which could lead to nickel deposition on the bag and on the particles in contact with it, appears unlikely. In order to avoid such a deposition, it was decided to use both bags made of the polyester-cotton fabric. Although no deposition was observed on the bag, the resistance of the cell had risen to 0.72 ohms which is even higher than that obtained in the cell employing a porous refractory membrane. However, despite the high resistance, the apparent deposition efficiency was well above 100%. Nevertheless, because of the relatively low current density achieved ( $8.1 \text{ A/dm}^2$ ), only 26.5 grams of nickel was deposited as compared to 80.0 grams in the case of cells employing triacetate fabric bags. It would, therefore, appear that the performance of the cells should not be judged only on the basis of the apparent deposition efficiency. If the above mentioned process was to be used for electro-winning of metals from lean solutions, it would be necessary to obtain a high rate of plating in order to recover the metal in the shortest period of time. The cells utilising polyester fabric bags could only be operated at a relatively slow rate of plating and were therefore considered unsuitable for this purpose.

From the above considerations, it is clear that the membrane material employed to separate the anode from the cathode should be impervious to iron powder particles and yet allow free passage of nickel ions. Furthermore, the material should also be resistant to acidic attack of the plating solution.

### 5.3 RELATIONSHIPS BETWEEN PERIOD OF PLATING, TOTAL ELECTRIC CHARGE PASSED, AVERAGE CURRENT DENSITY AND MASS OF NICKEL DEPOSITED

Figure 28 shows the relationship between the total quantity of electric charge passed and the mass of nickel deposited. According to Faraday's law, the passage of one ampere-hour of electric charge deposits 1.095 grams of nickel in an electroplating cell operating at 100% efficiency<sup>(8)</sup>. A straight line that conforms to Faraday's law is also shown in Figure 28. It is evident that the process of electrodeposition of nickel onto iron powder particles involved efficiencies above that which could be expected from any electroplating process: this clearly suggests the simultaneous occurrence of a second process which also contributed to the deposition of nickel.

Since there is no a priori reason why the charge passed should affect the electroless component of the process, the quantity of electroless deposition should be independent of the quantity of electric charge passed. Therefore, the relationship between the total electric charge passed and the quantity of nickel deposited for the two processes occurring simultaneously should be a straight line parallel

to the line that represents Faraday's law (i.e. 100% efficiency), provided the efficiency of the electrolytic process is independent of the quantity of charge passed. Although it was possible to represent the results obtained by a single straight line when the current density lay below  $17 \text{ A/dm}^2$ , the use of higher current densities was associated with an increased contribution from the electroless process. The contribution of the electroless component was also found to increase as the quantity of charge passed was increased (Figure 28).

The rate of deposition was found to increase as the current density was increased (Figure 29) as would be expected in any process that involved electrodeposition<sup>(3-7)</sup>. However, the rate of deposition was found to be greatest in the first 30 minutes of plating after which a gradual decline in this property was observed. Such behaviour would be expected if the second process was based on chemical replacement of iron by nickel ions in solution (cementation) because such a process would slow down as the iron powder particles were covered with nickel and less iron substrate was directly available for the replacement reaction. Although, cementation reactions generally result in porous coating and thus do not inhibit contact between the plating solution and the powder substrate, the simultaneous occurrence of electrodeposition produced a denser coating which consequently decreased the contribution of the electroless component of the process. The effect of current density on the rate of deposition of nickel onto iron powder

is clearly shown in Figure 30. The two important features of the relationship are:-

- (i) a positive intercept on the ordinate axis,
- and (ii) a sharp increase in the rate of deposition obtained at a current density of  $\sim 17 \text{ A/dm}^2$ .

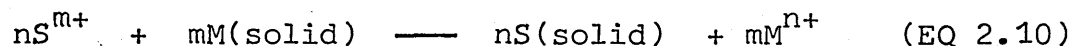
The positive intercept on the ordinate axis again indicates the presence of an electroless process, since if only electroplating was involved the relationship would be represented by a straight line through the origin. The reason for the sharp increase in the rate of deposition at current densities in the vicinity of  $17 \text{ A/dm}^2$  is not very clear but may result from increased bath temperature.

Although no significant increase in the bath temperature was detected, this could have been masked by the adiabatic expansion of the fluidising gas. However, it seems probable that at these high current densities local increases in the temperature of the solution occurred which enhanced the contributions of the electroless component of the deposition process. The dependence of the electroless process on temperature will be discussed in greater detail in the next section.

#### 5.4 ELECTROLESS NICKEL COATING

Electroless nickel plating has been practiced for several years and is well documented<sup>(68-75)</sup>. The process normally requires the presence of a reducing agent within the plating solution, which in the case of nickel deposition is usually sodium hypophosphite. However, the term

'electroless deposition' as used in the present context, also includes processes that do not involve the use of a reducing agent. It would, therefore, appear that under the circumstances of the present investigation, the coating of iron powder particles with nickel resulted from a cementation reaction as represented by the following equation:-



Cementation of metal is known to occur when the electrode (reduction) potential of a metal M in a solution of  $M^{n+}$  ions is more negative than that of a metal S in a solution of its ions<sup>(84)</sup>. Since the above condition is fulfilled in the iron-nickel system, it is theoretically possible to cement nickel from its solution onto an iron substrate, although the rate at which this reaction occurs is usually very slow. It has been shown that both a sheet of well cleaned steel<sup>(87)</sup> and iron powder particles<sup>(208)</sup> can be coated with nickel using the cementation reaction. The sheet obtained a very thin coating of nickel but it was claimed that composite nickel coated iron powder containing up to 50% nickel could be prepared in this manner. However, in the present investigation it was found that small solid objects of steel placed in a heated solution of nickel sulphamate did not receive any coating of nickel (Table 11) but substantial nickel deposition was obtained when the solid objects were replaced by iron powder particles. The substantial deposition obtained by the use of iron powder would appear to be associated with the very large surface area of such small particulate materials. In electroless plating from nickel solutions that contained sodium hypophosphite, it

has been observed that the efficiency and the rate of deposition increased when the mass of powder within a fixed volume of solution was increased<sup>(75)</sup>. The advantages gained were attributed to the increased surface area available for the reaction.

It is evident from Figure 31 that the initial rate of deposition was high but after 15 minutes of plating the rate fell to a lower value which appeared to remain constant throughout the experiment (60 minutes). However, an extension of the period of plating to 120 minutes showed that the rate of deposition gradually fell as the period of plating increased (Figure 32). Furthermore, addition of fresh solution after 105 minutes of plating resulted in a substantial increase in the rate of deposition. Nevertheless, the rate at this stage was still not as high as that obtained during the first 15 minutes of the experiment.

However, the temperature of the solution had now decreased to 58°C from an initial value of 70°C which would also cause a reduction in the rate of deposition (see Figure 31).

Similar observations have also been reported in the cementation of copper<sup>(86)</sup> on iron and also of nickel on iron powder from nickel chloride solutions<sup>(208)</sup>. Figures 31 and 32 clearly indicate that the factors which influence the rate of deposition are:-

- (i) the nickel ion concentration of the solution; the rate decreases with decreasing concentrations of nickel ions in solution.

(ii) the temperature of the solution; the rate also decreases with decrease in solution temperature.

Several workers<sup>(86, 209)</sup> have shown that, in the case of cementation of copper on iron substrate, the rate constant initially increased with increasing cupric ion concentration, reached a maximum and then decreased with any further increase in cupric ion concentration. The variation in the value of the rate constant was explained in terms of the morphology of the deposit. This view was substantiated with scanning electron microphotographs of the deposits which showed that above an optimum level of cupric ion concentration the deposits became more dense and thus decreased the effective deposition surface area<sup>(209)</sup>. Schaleh et al<sup>(86)</sup> also found that addition of thiouria, which is known to produce a denser deposit in the case of electrodeposition of copper, reduced the rate constant for the cementation reaction. An examination of the cementation reaction using nickel chloride and nickel sulphamate solution showed that the quantity of nickel deposited on iron powder with the use of the latter was considerably smaller than that with the former<sup>(208)</sup>. However, scanning electron microscopy revealed that in the case of the former the deposits were composed of tiny globules as compared to the more even deposit of the latter. From the above considerations, it appears that the decrease in the rate of electroless deposition observed with prolonged plating time was also dependent on the nature of the coating and consequently the amount of iron substrate directly available for the cementation

reaction. The importance of the iron substrate available for reaction was further emphasised when the addition of a silicone based antifoam agent resulted in a substantially reduced rate of deposition (Figure 33). During frothing of the bed, the powder particles were entrapped within the gas bubbles and thus direct contact between the substrate and the nickel ions in solution was inhibited. The anti-foam agent forms a monoatomic layer on the powder particles and render them wettable and thus avoid the formation of a stable froth<sup>(210)</sup>. However, the presence of the anti-foam agent on the surface of the particle apparently inhibits the cementation reaction.

Lines 'A' and 'B' (Figure 80) show the combined effect of electroless and electroplating at 63°C and 48°C respectively when the electrolytic component is 100% efficient. The displacement between the two lines A and B shows the marked effect of a small increase in temperature, on the electroless component. Most of the experimental results fall within the band formed by the two lines. The points lying just outside the band are those where a high current density was used which favours higher solution temperatures and thus higher contributions from the electroless component of the plating process.

#### 5.5 INFLUENCE OF S-NICKEL\* ON THE ELECTRODEPOSITION OF NICKEL ONTO IRON POWDER

Several authors have reported that the use of S-Nickel anodes in the electrolytic deposition of nickel results in

---

\* Trade name for nickel shot containing 0.05% sulphur.

better anode corrosion and therefore higher anode efficiencies<sup>(18-21)</sup>. However, during the course of the present investigations, a considerable scatter in the levels of anode efficiency was observed, particularly when anode bags made of triacetate fabric were employed. It was observed that iron powder entered the anode bags and covered the nickel shot, which adversely affected the anode dissolution efficiency (Figure 21). The quantity of iron powder entering the bag was found to be dependent on the type of fabric used; thus the triacetate fabric admitted more powder than the tightly woven polyester cotton material. Consequently, cells that used triacetate fabric bags exhibited poorer anode efficiencies than those using polyester cotton anode bags (viz - Ex NII and NVII, Table 8). Studies carried out at International Nickel Co.<sup>(21)</sup> on the suitability of various types of fabrics for anode bags indicated that both cotton and terylene\* materials with a close weave were satisfactory for the purpose. However, it should be remembered that these studies were carried out to determine whether sulphur sludge was being incorporated in the deposit in any appreciable quantity so as to cause poor surface finish. Although, the results did not give any conclusive evidence to establish whether all the sludge produced from the anodes was being withheld within the bag, the use of twin bags was recommended for better surface finish.

---

\* Trade name for triacetate fabrics.

A comparison of the experiments carried out with pure nickel and S-Nickel shot revealed that slightly better anode efficiencies were obtained with the latter when triacetate fabric bags were employed (viz: Ex NIV and NXI, Table 8). However, when polyester cotton bags were employed no significant difference between the two types of anode material was observed (viz: Ex VII and NXII, Table 8).

Although slightly better anode efficiencies were obtained with S-Nickel shot (with triacetate fabric bag), the deposition efficiency was dramatically reduced (viz: Ex NIX - XI, Table 8). Since the conditions of plating were similar to those used with pure nickel anode material, it appears that the fall in the deposition efficiency was caused by the sulphur alloyed in the S-Nickel shot. Parkinson<sup>(22)</sup> who advocated the use of pure electrolytic nickel anodes in preference to S-Nickel because of the high impurity level of the latter, also reported that the sludge produced from S-Nickel anodes was in excess of 0.18% of the amount of anode dissolved. The sludge was found to contain a large fraction of non-metallic sulphides most of which was finer than 44 microns. Since the anode bags used in the present work allowed the entry of iron powder particles most of which were bigger than 44 microns, it would be reasonable to conclude that a large part of the sludge produced found its way into the fluidised bed. Although, the reasons for the relatively poor efficiencies obtained with the use of S-Nickel shot are not clear, it is possible that the fine sludge particles found their way onto the surface of iron powders and thus restricted contact

between the solution and the iron substrate. It is also possible that some of the sludge was dissolved in the solution and consequently the higher impurity level of the latter may have adversely affected the deposition efficiency. However, the above views could not be experimentally confirmed since it was not possible to detect the low levels of sulphur involved. Further work, involving intentional additions of very fine sulphide particles to the fluidised bed, is recommended in order to establish the effect of sulphur on the deposition efficiency.

#### 5.6 RELATIONSHIPS BETWEEN POROSITY, MODULUS OF RUPTURE AND HOMOGENISATION PARAMETER OF SINTERED COMPACTS

It is evident from the measurements of the density of sintered compacts that those made from plated powder possessed greater levels of porosity than those prepared from blended powders after identical treatments (Tables 17-22). Such a difference would be expected since the former exhibited lower compressibility than the latter (Figure 35). It is well established that compressibility of powder particles is governed by the particle size distribution within the powder mass and also by the surface condition (Viz:- oxide layers etc.) of the individual particles. The plated powders used in the present investigation contained larger fractions of coarse particles than the sponge iron powder used for the preparation of blended powder compacts (Table 13). Furthermore, the fine particle size of the nickel powder used in these compacts also increased their compressibility. In addition, to the

larger quantities of coarser fractions, the plated powders also contained greater amounts of oxygen, (Table 15). It is believed that oxygen was absorbed onto the surface of the powder particles during the drying operation.

#### 5.6.1 Iron - 1.75% Nickel Compacts:-

The relationship between porosity and modulus of rupture for 1.75% nickel compacts prepared from both blended and plated powders is shown in Figure 36. The relationship, in the case of the former, can be represented by the following equation:

$$R(+92 \text{ N/mm}^2) = 1553 - 63.4P \quad (\text{EQ 4.1})$$

and in the case of the latter by:

$$R(+44 \text{ N/mm}^2) = 1701 - 74.9P \quad (\text{EQ 4.2})$$

The high degree of correlation coefficients obtained for the two equations (-0.91 and -0.99 respectively) suggested that the only factor governing the modulus of rupture of these compacts was porosity and that at any given density an increase in the period of sintering did not make any significant contribution.

Linear equations of this type have also been used to relate porosity to the tensile strength of sintered compacts (98,190,195). Some theoretical relationships of this type include stress concentration factors that relate to the shape of the pores in the material (190, 195). Dixon et al (190) found that agreement between the experimental and theoretical tensile strengths in the case of

Haynes's<sup>(195)</sup> equation could only be obtained with the use of variable values of 'b', which decreased as the time of sintering increased. The stress concentration factor, F, in Pohl's<sup>(200)</sup> equation (EQ 2.22) was also found to decrease from 3.75 to 2.75 when the period of sintering of pre-alloyed powder compacts was increased from 0.25 hour to 8 hours. These values of the stress concentration factor were similar to those quoted by other workers<sup>(197,199)</sup> However, Dixon et al reported that tensile strengths of compacts possessing low degree of homogeneity ( $H > 0.45$ ) could not be predicted with the use of Pohl's equation incorporating 'F' values in the above range. The authors concluded that tensile strength of sintered material was dependent on both porosity and the degree of homogenisation.

Although no measurements of the degree of homogeneity were made for 1.75% nickel compacts in the present investigation, it appears reasonable to assume that compacts sintered for 240 minutes were more homogeneous than those sintered for only 30 minutes. In the case of blended powder compacts the expected increase in homogeneity that resulted from increasing periods of sintering did not affect the modulus of rupture to any significant extent (Viz:- S. Nos. 101B and 118B, Table 17). Similarly, in the case of plated powder compacts, no significant improvement in the value of modulus of rupture was obtained with increasing periods of sintering (Viz:- S. Nos. 103P and 114P, Table 18). Thus the present work on the modulus

of rupture of iron alloys that contain 1.75% nickel does not agree with the relationships between tensile strength, homogeneity and pore shape observed in similar materials<sup>(190)</sup>.

Dixon et al also reported that plated powder compacts were more homogeneous than those made from blended powders after any given sintering treatment and possessed higher tensile strengths at a given density level. A comparison of the values of modulus of rupture obtained from the two powders used in the present investigation, shows that at porosity levels of less than 10%, the plated powder compacts were slightly better than those made from blended powders when each material had been sintered for up to 120 minutes. However, no difference in the modulus of rupture of the two materials was observed when they were sintered for 240 minutes. When the porosity of the compacts was greater than 10%, the value of modulus of rupture was found to be independent of the type of powder used.

Thus, it would appear that in the case of the modulus of rupture, the degree of porosity in the material has a much greater effect than the degree of homogeneity. This may be due to the stronger influence of the stress concentrations associated with the pores on the modulus of rupture. There is some evidence that the porosity in the plated material is very angular with many pores interconnected (Figure 47).

### 5.6.2 Iron - 3.25% Nickel Compacts

Figure 37 shows the relationship between modulus of rupture and porosity of 3.25% nickel compacts prepared from both blended and plated powders, which had been sintered for periods of between 30 and 240 minutes. In the case of blended powder compacts, the relationship between modulus of rupture and porosity was found to conform to the following equation:

$$R(+72 \text{ N/mm}^2) = 1700 - 73.52P \quad (\text{EQ 4.3})$$

irrespective of the period of sintering.

In contrast, the modulus of rupture of compacts prepared from plated powders showed a marked increase as the period of sintering was increased and analysis of covariance (parallel regression analysis) showed that the relationship between modulus of rupture and porosity for the above compacts could be represented by four parallel lines conforming to the following equations:-

$$(i) \quad R_{(30)*} = 1487 - 63.54P \quad (\text{EQ 5.1})$$

$$(ii) \quad R_{(60)*} = 1580 - 63.54P \quad (\text{EQ 5.2})$$

$$(iii) \quad R_{(120)*} = 1682 - 63.54P \quad (\text{EQ 5.3})$$

$$(iv) \quad R_{(240)*} = 1654 - 63.54P \quad (\text{EQ 5.4})$$

The degree of homogeneity of both blended and plated powder compacts was determined using the method

---

\* Figures in parentheses refer to the period of sintering in minutes.

developed by Dixon et al,<sup>(190)</sup>. The results show that the degree of homogeneity increased with increasing periods of sintering irrespective of the type of powder used (Figures 75 and 76). However, under identical sintering conditions, the plated powder compacts were found to be significantly more homogeneous than those made from blended powders. Dixon et al, who also investigated 3% nickel compacts prepared from both blended and plated powders, found that the highest tensile strengths were obtained when the homogenisation parameter was less than or equal to a critical value of 0.45. Furthermore, compacts made from blended powders did not achieve this value even after 8 hours of sintering at 1150°C. In comparison, the plated powder compacts attained this value after sintering for periods in excess of one hour. Although the values of the homogenisation parameter obtained in the present investigation from blended powder compacts were generally lower than those reported by Dixon et al, the critical value was not reached even after four hours of sintering. The plated powder compacts, on the other hand, approached this level of homogeneity after sintering for two hours. In view of the considerable scatter associated with the measurement of the homogenisation parameter, the results of the present work appear to be in reasonable agreement with those of Dixon et al.

Figure 81 shows the influence of the degree of homogeneity on the modulus of rupture of compacts made from both blended and plated powders. In the case of the former an increase of approximately 150 N/mm<sup>2</sup> was associated

with a decrease in the value of the homogenisation parameter (H) from 5.81 to 0.68. However, there was a difference of 1.9% in the densities of the two compacts. According to the relationship between the modulus of rupture and porosity of these compacts (EQ 4.3), such a difference would account for a difference of 139 N/mm<sup>2</sup> in the value of modulus of rupture. Therefore, it appears that the modulus of rupture of blended powder compacts was relatively independent of the degree of homogeneity.

In the case of plated powders, a marked increase in the modulus of rupture ( $\sim 224$  N/mm<sup>2</sup>) was obtained as the homogenisation parameter (H) decreased from 1.11 to 0.49 but no further improvement was obtained when the value of 'H' decreased to 0.29 (Figure 8<sup>Curve 3</sup>). A similar sharp increase in tensile strengths of 3.25% nickel plated powder compacts was reported by Dixon et al<sup>(190)</sup>, who found that the tensile strength increased sharply until a value of homogenisation parameter equal to 0.45 was reached after which a further decrease in the value of homogenisation parameter did not result in any significant improvement in tensile strength.

The modulus of rupture values obtained from 3.25% nickel plated powder compacts obtained during the present work were subjected to a multiple regression analysis to incorporate the effect of homogeneity on the relationship between modulus of rupture and porosity (EQ 5.1 to 5.4). The following equation, with a correlation coefficient of -0.95 was obtained:

$$R(+77 \text{ N/mm}^2) = 1640 - 238.5(H) - 54.9(P) \quad (\text{EQ 5.5})$$

However, the above equation does not apply to compacts made from blended powders which possessed a much lower degree of homogeneity. Dixon et al reported that 3% nickel compacts made from blended powders did not achieve values of homogenisation parameter(H) lower than 1.5 and generally possessed significantly lower tensile strengths than plated powder compacts at a given density level. This was not observed in the case of modulus of rupture measurements made during the present work.

For the purpose of comparison, values of modulus of rupture of blended powder compacts at similar density levels to those prepared from plated powders have also been plotted in Figure 81 (lines 2 and 3). It is evident that blended powder compacts possessed slightly lower values of modulus of rupture than those made from plated powders when each of them had been sintered for 120 minutes or more. However, when the period of sintering was limited to 30 minutes, the blended powder compacts were superior to those made from plated powders. Since these blended powder compacts possessed high values of modulus of rupture despite the possession of low homogeneity, it appears that the modulus of rupture of plated powder compacts may have been adversely affected by other factors; viz: microstructure and pore shape.

### 5.6.3 Iron - 4.25% Nickel Compacts

Unlike the blended powder compacts that contained 3.25% nickel, those containing 4.25% nickel showed that at a fixed

level of porosity higher values of modulus of rupture were obtained when longer periods of sintering were employed (Figure 38). A parallel regression analysis of the results showed that the relationship between modulus of rupture and porosity after various periods of sintering could be represented by the following set of parallel lines:-

$$R_{(30)*} = 1678 - 70.9P \quad (\text{EQ 5.6})$$

$$R_{(60)*} = 1709 - 70.9P \quad (\text{EQ 5.7})$$

$$R_{(120)*} = 1751 - 70.9P \quad (\text{EQ 5.8})$$

$$R_{(240)*} = 1758 - 70.9P \quad (\text{EQ 5.9})$$

Since these compacts became increasingly more homogeneous with increasing periods of sintering (Figure 77), it appears that the increase in the value of the constants of the above equations produced by the increase in the period of sintering was associated with increased homogeneity. A multiple regression analysis was carried out to determine the combined effect of porosity (P) and homogenisation parameter (H) on the modulus of rupture of these compacts. The following relationship, with a correlation coefficient of -0.99, was obtained:-

$$R_{(+40 \text{ N/mm}^2)} = 1774 - 13.51(H) - 71.13(P) \quad (\text{EQ 5.10})$$

---

\* Figures in parentheses refer to the period of sintering in minutes.

Similar analysis could not be undertaken in the case of compacts prepared from plated material on account of insufficient data at each sintering time. This was due to the difficulties involved in the maintenance of a constant level of carbon in sintered compacts made from this material. However, it is evident from the results obtained that the modulus of rupture of these compacts increased with reduced porosity and increased sintering times (Figure 38 - line 5). The following relationship was obtained:-

$$R(+42 \text{ N/mm}^2) = 2045 - 97.24P \quad (\text{EQ 4.10})$$

The homogenisation parameter of these compacts was also determined (Figure 78) and was found to be lower than that obtained with the use of blended material sintered for identical times (Figure 77).

The modulus of rupture of compacts made from plated powders was also calculated using the relationship obtained for blended powder compacts of the same composition (EQ 5.10) and a comparison of calculated and experimental values is given in Table 23. It is evident that there is close agreement between the calculated and experimental values in the case of compacts that had been sintered for 60 minutes or more. However, the relationship fails to predict the modulus of rupture of plated powder compacts sintered for 30 minutes. This may be explained by reference to variations in the microstructure and the shape of the pores.

## 5.7 RELATIONSHIP BETWEEN MICROSTRUCTURE, HOMOGENEITY AND MODULUS OF RUPTURE OF SINTERED COMPACTS

### 5.7.1 Iron - 1.75% Nickel Compacts

(A) Blended Powders:- It is evident from the previous discussion (Section 5.6.1.) that at a given level of density, an increase in the period of sintering did not result in any significant increase in the value of modulus of rupture of the compacts prepared from blended powders. However, microstructural examination revealed one distinct difference between compacts sintered for 30 and 240 minutes. While the former contained many small patches of austenite with a sharp interface at the periphery (Figure 39), these had become much reduced in number in the latter. Furthermore, the austenite areas in the latter had become much more diffuse with no clear boundary between them and the other phases in the structure (Figure 43). Dixon et al<sup>(190)</sup> reported the presence of such areas in 3% nickel compacts even after 480 minutes of sintering and that these areas significantly lowered the tensile strength of the compacts. However, the results of the present work using 1.75% nickel compacts prepared from blended powders do not show a similar relationship between such austenitic areas and the modulus of rupture.

(B) Plated Powders:- The plated powder compacts, like those made from blended material, possessed moduli of rupture values that were unaffected by sintering time when allowance was made for change in density. However,

the structure of these compacts was generally more uniform than those of blended powders, although compacts sintered for 30 minutes indicated the presence of a light etching network (Figure 46) which disappeared when the period of sintering was increased to 60 minutes. Although the presence of a similar light etching network in 3% nickel compacts has been reported to adversely affect the tensile strength of the compacts<sup>(190)</sup>, the modulus of rupture of the 1.75% nickel compacts was unaffected by this type of microstructure. Thus compacts sintered for longer periods did not possess any higher values of modulus of rupture than those sintered for 30 minutes when compared at equal densities (Figure 36).

It is also evident from Figure 36 that only those blended powder compacts that had been sintered for 240 minutes possessed values of modulus of rupture that were similar to those obtained with the use of plated powders. The longer period of sintering of the blended powder compacts had promoted the diffusion of nickel and therefore produced a more uniform structure (Figure 43). However, the benefits of uniform structures, obtained either by prolonged sintering or by the use of plated powders, were only evident at low levels of porosity. At higher porosity levels all compacts, irrespective of the period of sintering and the type of powder used, possessed similar values of modulus of rupture. Therefore, it is probable that at higher levels of porosity, the stress concentration effects of the pores outweigh the advantages of a more uniform structure.

### 5.7.2 Iron - 3.25% Nickel Compacts

(A) Blended Powders:- It has already been shown that although the homogenisation parameter decreased with increasing periods of sintering, it was not accompanied by any significant increase in the modulus of rupture of the sintered compacts. This decrease in the value of homogenisation parameter was reflected in the microstructure of the compacts. The structures corresponding to compacts sintered for 30 minutes showed large patches of light etching areas which had not undergone any transformation during quenching (Figure 51). Although such areas were also observed in compacts sintered for 240 minutes, they were less pronounced (Figure 55) and thus suggested a greater degree of homogeneity. The structures, which appeared to consist largely of lath and acicular martensite were similar to those reported by Dixon et al<sup>(190)</sup>. These authors concluded that the tensile strengths of compacts made from blended material were always inferior to those made from plated powders when comparisons were made at equal levels of porosity. This was due to the presence of patches of light-etching austenitic areas in the microstructure of blended powder compacts. However, the results of the present investigation indicate that the modulus of rupture was not affected by the presence of such areas.

(B) Plated Powders:- Unlike the compacts made from blended powders those made from plated material showed that at a fixed level of porosity, the modulus of rupture increased

with an increase in the time of sintering (Figure 37). The reduction in the value of the homogenisation parameter that resulted from this increase in sintering time led to a more uniform microstructure. Thus the light-etching network observed in compacts sintered for 30 minutes (Figure 57) was greatly reduced in compacts sintered for 60 minutes (Figure 59) and totally removed from those that had been sintered for 120 minutes. The last named specimen contained a uniform microstructure consisting mainly of lath and accicular martensite. Hence, the improvement in modulus of rupture produced by increased time of sintering appears to be associated with a more uniform structure.

A sharp increase in the value of modulus of rupture was also obtained as the value of the homogenisation parameter decreased from 1.11 after 30 minutes of sintering to 0.29 after 240 minutes of sintering (Figure 81). Dixon et al, who also obtained a similar increase in the tensile strength of 3% nickel compacts prepared from plated powders, believed that the very poor tensile strengths of compacts sintered for shorter periods were due to the presence of the light-etching network.

However, it is possible that the comparatively low values of modulus of rupture of compacts sintered for periods up to 60 minutes may also be due to the shape of the pores. A close examination of the structure of the plated material revealed the presence of long interconnected pores within the network which suggests poor sinterability of the

powder particles and lower values of modulus of rupture. Therefore, it seems that a significant proportion of the improvement obtained by an increase in the period of sintering from 30 to 120 minutes may be due to the change in the shape of the pores rather than just the removal of the light etching network.

Dixon et al (90, 190) observed a marked difference ( $\approx 110 \text{ N/mm}^2$  at 10% porosity) between the tensile strengths of plated and blended powder compacts sintered for 240 minutes. These authors attributed the superior properties of plated powder compacts to the more uniform structures obtained in these compacts. However, in the present work, the difference in the modulus of rupture of the two compacts was only  $\approx 50 \text{ N/mm}^2$ . Consequently, it appears that modulus of rupture was less sensitive than tensile strength to changes in the microstructure.

### 5.7.3 Iron - 4.25% Nickel Compacts

(A) Blended Powders:- Unlike the other blended powder compacts examined, those containing 4.25% nickel showed a statistically significant increase in the modulus of rupture as the period of sintering was increased (EQ 5.6 - 5.9, Section 5.6.3). Furthermore, a significant relationship was also obtained between modulus of rupture, homogenisation parameter and porosity,

$$R(+40 \text{ N/mm}^2) = 1774 - 13.51(H) - 71.13P \quad (\text{EQ 5.10})$$

It is evident from this relationship that the modulus of rupture of the compacts was more strongly influenced by

porosity than by the homogenisation parameter. According to the above relationship the difference in the modulus of rupture of compacts sintered for 30 and 240 minutes would be approximately  $76 \text{ N/mm}^2$  at a given level of porosity. Since this increase is believed to be due to the increased homogeneity of the latter, differences in the microstructures of the two compacts may provide an explanation for the observed difference in the level of modulus of rupture. The structure of the two compacts consisted of the following two major phases:- (Figure 64 and 67),

- (i) light etching areas showing no transformation,
- (ii) dark etching transformation products.

In the case of shorter period of sintering, relatively little diffusion of nickel was possible and consequently large light etching areas were observed (Figure 64). The high alloy content of these areas suppressed the transformation during quenching into water. However, the longer period of sintering allowed diffusion of nickel to a considerable extent and thus produced a structure (Figure 67) which did not contain as much light etching constituents as in the case of the specimen sintered for the shorter time. Apart from these light etching areas, the structures of the two compacts were predominantly martensitic. Therefore, it would appear that the presence of large quantities of the light etching phase is detrimental to the modulus of rupture. Similar views were expressed by Dixon et al who found that tensile strengths of blended powder compacts sintered for short periods were lower than those obtained by the use of compacts that possessed a higher degree of homogeneity.

(B) Plated Powders:- It has been shown that the relationship showing the influence of homogenisation parameter (H) and porosity (P) on the modulus of rupture of 4.25% nickel compacts made from blended powders, can explain all the results obtained from plated powder compacts except those that had been sintered for 30 minutes (EQ 5.10). The micro-structure of this compact (Figure 69) was similar to that of 3% nickel compact sintered for the same period (Figure 57). The light etching network suggested that the diffusion of nickel was not complete after the short sintering treatment and consequently the surface of the powder particles still possessed a coating rich in nickel, which because of its high hardenability, had not fully transformed during quenching. The variable structure thus produced could account for its relatively low value of modulus of rupture. However, <sup>Case of</sup> as in the 3% nickel compacts, long interconnected pores were seen within the network which indicated the poor bonding between the powder particles. Therefore it is probable that the relatively low value of modulus of rupture was caused by the combined effect of the two factors mentioned above.

An increase in the period of sintering removed the light etching network and produced a uniform structure that was predominantly martensitic (Figure 72). However, despite their greater homogeneity and more uniform structure which contained no light etching austenitic areas, the plated powder compacts that had been sintered for 120 minutes did not possess higher values of modulus of rupture than

those made from blended powders. The microstructure revealed the presence of some open pores. However, compacts sintered for 240 minutes, do not show such pores and consequently possess higher modulus of rupture than those made from blended powders. The superiority of these compacts could be attributed to the more uniform structures of these compacts which were predominantly martensitic (Figure 73). Nevertheless, the improvement obtained was very small, as was the case in the compacts containing 3% nickel, and therefore suggests that modulus of rupture was relatively insensitive to changes in the microstructure.

#### 5.8 INFLUENCE OF NICKEL CONTENT ON THE MODULUS OF RUPTURE OF SINTERED COMPACTS

Figure 82 (a) shows the effect of increasing nickel content on the modulus of rupture of blended powder compacts that possessed a range of porosity levels. The relationships between modulus of rupture and porosity at three nickel contents may be represented by the following equations:-

(i) 1.75% Nickel

$$R(\pm 92 \text{ N/mm}^2) = 1553 - 63.4P \quad (\text{EQ 4.1})$$

(ii) 3.25% Nickel

$$R(\pm 72 \text{ N/mm}^2) = 1700 - 73.52P \quad (\text{EQ 4.3})$$

(iii) 4.25% Nickel

$$R(\pm 69 \text{ N/mm}^2) = 1830 - 80.9P \quad (\text{EQ 4.9})$$

As would be expected, an increase in the nickel content resulted in higher values of modulus of rupture. However,

this increase was only obtained in compacts of high density. The magnitude of the increase in the modulus of rupture decreased as the level of the porosity in the compacts increased and at porosities in excess of  $\sim 14\%$  all compacts possessed similar values of modulus of rupture, irrespective of nickel contents.

The plated powder compacts also showed similar behaviour (Figure 82(b)). The relationships between the modulus of rupture and porosity, irrespective of the period of sintering, at the three nickel contents may be represented by the following equations:-

$$(i) \quad 1.75\% \text{ Nickel} \\ R(+44 \text{ N/mm}^2) = 1701 - 74.9P \quad (\text{EQ 4.2})$$

$$(ii) \quad 3.25\% \text{ Nickel} \\ R(+164 \text{ N/mm}^2) = 1647 - 66.99P \quad (\text{EQ 5.11})$$

$$(iii) \quad 4.25\% \text{ Nickel} \\ R(+42 \text{ N/mm}^2) = 2045 - 97.24P \quad (\text{EQ 4.10})$$

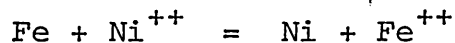
Throughout the range of compositions examined, the compacts prepared from plated powders possessed higher values of modulus of rupture than blended material of similar porosity. However, the superiority of the plated material was found to decrease with increasing porosity and at porosity levels approaching 14%, the values of modulus of rupture were independent of both the nickel content and the type of powder used. It is therefore evident that modulus of rupture was most strongly influenced by porosity and that the beneficial effects of other factors

such as compositional changes and homogeneity could only be realized in compacts possessing low levels of porosity.

CHAPTER SIX  
CONCLUSIONS

## 6. CONCLUSIONS

1. A plating cell that employs a three-phase fluidised bed has been developed for the purpose of coating nickel onto iron powders.
2. The apparent deposition efficiency of the electro-deposition process frequently exceeded 100%, which indicated that some process other than electro-deposition was also involved.
3. The use of S-nickel shot as anode material lowered the apparent deposition efficiency.
4. The deposition of nickel in the absence of an applied electric potential has been shown to be due to a cementation reaction.



5. Provided that the nickel concentration and the temperature of the solution were maintained at constant levels, the rate of the cementation reaction was independent of time.
6. In the case where electro-deposition occurred simultaneously with electroless plating, the latter was affected by the current density used. This was probably associated with the effect of current density on the quantity of heat generated in the fluidised bed.

7. Irrespective of the type of powder used, the modulus of rupture of sintered compacts was found to be more strongly dependent on porosity than on the variations in microstructure viz quantity and distribution of retained austenite.
8. At a constant level of porosity, the modulus of rupture of compacts was not affected by either the period of sintering or the consequent homogeneity provided that the nickel content of the blended and plated powders was limited to 3.25% and 1.75% respectively.
9. The following relationship between homogenisation parameter (H), modulus of rupture (R) and porosity (P) was obtained for plated powder compacts containing 3.25% nickel.

$$R = 1640 - 238.5 H - 54.9 P$$

However, it was also pointed out that the low values of modulus of rupture of compacts sintered for short periods was not entirely due to the relatively high value of the homogenisation parameter but also due to the shape of the pores.

In the case of blended powder compacts containing 4.25% nickel the following relationship was obtained:

$$R = 1894 - 35.0 H - 80.5 P$$

The above relationship also explained the results obtained by the use of plated material of similar

composition provided that the period of sintering employed was not less than 60 minutes at 1150°C.

10. In the case of both blended and plated powder compacts, the modulus of rupture increased as the nickel content was increased, the increase being greatest at low levels of porosity. However, at high porosity levels all compacts possessed similar values of modulus of rupture regardless of nickel content.
11. Compacts prepared from plated powders possessed higher values of modulus of rupture than those obtained by the use of blended material. This effect was again more pronounced at low levels of porosity and at porosities approaching 14% all compacts possessed similar values of modulus of rupture regardless of the type of powder used.

REFERENCES

1. Delahay, P. (Ed.) : Advances in Electrochemistry and Electrochemical Engineering, Vol. 1, Interscience Publishers, 1961.
2. Crow, D.R. : Principles and Applications of Electrochemistry, London Chapman and Hall, 1973.
3. Dennis, J.K. and Such, T.E. : Nickel and Chromium Plating, Newnes-Butterworth, 1972.
4. Glasstone, S. : An Introduction to Electrochemistry, D.Van Nostrand Co. Inc., 1964.
5. Kortum, G. : Treatise on Electrochemistry, Elsevier Publishing Co., 1965.
6. Vagramyan, A.T. and Solov'eva, Z.A. : Technology of Electrodeposition, Robert Draper, 1961.
7. Lyons, E.H. Jr. : Modern Electroplating, (Ed) Lowenheim, F.A., J. Wiley & Sons, 1973, P.1.
8. Brown, H. and Knapp, B.B. : ibid, P.287.
9. Gabe, D.R. : Metal Finishing J. 1971, Vol. 17, No. 21, P. 276.
10. West, J.M. : Electrodeposition and Corrosion Processes, Van Nostrand Reinhold Co., 1965.
11. Bloor, D.W. : Electroplating, 1971, Vol.24, No.6, P.7.
12. Kortum, G. and Bockris, J.O'm : Textbook of Electrochemistry Vol.II& Elsevier Pub. Co., 1951.
13. Hart, A.C. : Trans. I.M.F., 1973, Vol.51, P.69.
14. Hoar, T.P. : Trans. I.M.F., 1962, Vol.39, P.166.
15. Hoar, T.P., Mears, D.C. and Rothwell, G.P. : Corr. Sci., 1965, Vol.5, P.27.
16. Hoar, T.P. : ibid 1967, Vol.7, P.341.
17. Saubestre, E.B. : Plating, 1958, Vol.45, P.927.
18. Di Bari, G.A. and Petrocelli, J.V. : J. Electro. Chem. Society, 1965, Vol.112, P.99.
19. Fischer, G.L. and Morris, P.E. : Trans. I.M.F., 1975, Vol.53, P.145.

20. Watson, S.A. : Metal Finishing J., 1972, Vol.18, No.1, P.18.
21. Watson, S.A. : ibid, 1972, Vol.18, No.2, P.36.
22. Parkinson, R. : Electroplating, 1974, Vol.27, No. 2, P.8.
23. Roehl, E.J., and Wesley, W.A. : Plating, 1950, Vol.37, P.142.
24. Struyk, E. and Carlson, C. : ibid, P.1242 .
25. Barrett, R.C. : Proc. Am. Electroplaters Soc. 1954, Vol.41, P.169.
26. Hammond, R.A.F. : Pt. I-IV, Metal Finishing J., 1972, Vol.18, Nos. 6-9.
27. Kendrick, R.J. : Trans. I.M.F., 1964, Vol.42, P.235.
28. Wesley, W.A. and Roehl, E.J. : Trans. Electro Chem. Soc., 1944, Vol.86, P.419.
29. Graham Kenneth, A. (Ed.) : Electroplating Engineering Handbook. Van Nostrand Reinhold Co. 1971, P.2 .
30. Wesley, W.A., Sellers, W.W., and Roehl, E.J. : Proc. Am. Electroplaters Soc., 1949, Vol.36, P.79
31. Blum, W. and Kasper, C. : Trans. Faraday Society, 1935, Vol.31, P.1203.
32. Watson, S.A. : Trans. I.M.F., Vol.37, P.39.
33. Sathyanarayana, S., and Ramachar, T.L. : J.Sci.Ind.Res. India, 1957, Vol.16A, P.78.
34. Watson, S.A. : Plating 1950, Vol.37, P.1045.
35. Wesley, W.A. and Carey, J.W. : Trans. Electro. Chem. Soc., 1939, Vol.75, P.209.
36. Kendrick, R.J. : Trans. I.M.F., 1966, Vol.44, P.78.
37. Cupery, M.E. : U.S. Patent No. 2318592
38. Faruq Marikar, Y.M. and Varu, K.I. : Metal Finishing, 1969, Aug. P.59.
39. Venkatachalam, S. : J. Sci.Ind.Res., 1962, May, Vol.21D, P.145.
40. Venkatachalam, S., and Ramachar, T.L. : Electroplating and Metal Finishing, 1961, Vol.14, P.3.
41. Shenoi, B.A., Subramaniam, R. and Indira, K.S. : ibid, 1968, Vol.21 (10), P.336.

42. Ericson, H. : as cited in Ref. 26 Pt. 1.
43. Fanner, D.A. and Hammond, R.A.F. : Trans. I.M.F., 1959, Vol.36, P.32.
44. Marti, J.L., and Lanza, G.P. : Proc. Symp. on Sulphamic Acid and its Electro. Met. Applicn., 1966, P.215.
45. Diggin, M.B. : Trans. I.M.F., 1954, Vol.31, P.243.
46. Diggin, M.B. : Metal Progress 1954, Vol.66, Oct., P.132.
47. Marti, J.L. : Plating, 1966, Vol.53, No.1, P.61.
48. Backhurst, J.R. et.al. : British Patent No. 1,194,181.
49. Sabacky, B.J., and Evans, J.W. : Met. Trans. 1977, Vol.8B, Mar., P.5.
50. Backhurst, J.R. et al : J. Electrochem. Society, 1969, Vol.116, P.1600.
51. Flett, D.S. : Chem. Ind., 1975, 16th Dec., P.983.
52. Flett, D.S. : ibid, 1971, 13th March, P.300.
53. Wragg, A.A. : ibid, 1975, 19th April, P.333.
54. Kreysa, G. and Heitz, E.A. : ibid, P.332.
55. Fleischmann, M. and Kelsall, G.H. : ibid, P.329.
56. Gabe, D.R. and Carbin, D.C. : ibid, P.335.
57. Handley, D. and Eardley, D.C. : ibid, P.330.
58. Ibl. Norbert. : ibid, P.326.
59. Wilkinson, J.A. and Haines, K.P. : Trans. Inst. Mining & Met. 1972, Vol.81, P.157.
60. Foster, J. and Kariapper, A.M.J. : Trans. I.M.F., 1973, Vol.51, P.27.
61. Meredith, R.E. and Tobias, C.W. : J. Electro Chem. Society, 1961, Vol.108, P.286.
62. Salt, F.W. : Symp. on Chem. Engrg. in Iron & Steel Industry, March 1968, Swansea, P.169.
63. Meddings, B, Huffman, H.R. and Mackiw, V.N. : New Types of Metal Powders, H.H. Hausner (Ed) Gordon & Breach, Sc. Pub. 1963, P.29.

64. Owen, L.W. : Metallurgia, 1959, Vol.59, P.165.
65. Clements, P.J. and Sale, F.R. : Met. Trans. Sept. 1976, Vol.7B, P.435.
66. Cline, J. and Wulff, J. : J. Electrochem. Soc., 1951, Vol.98, P.385.
67. Holbrook, K.A. and Twish, P.J. : Plating, 1969, Vol.56, P.523.
68. Mijner, C.H. : Electro Deposition & Surface Treatment, 1975, Vol.3, No.4, P.261.
69. Badet, Pierre : Galvano, 1968, Oct., Vol.37(381), P.661.
70. Donahue, F.M. and Yu, C.U. : Electrochem. Acta, 1971, Jan., Vol.15, P.237.
71. Gouda, V.K., Shawki, S., and El-Tawil, H. : Metal Finishing 1972, May, P.77.
72. Walker, R. Dr., and Campbell, F. : Electroplating and Metal Finishing, 1976, Vol.29, P.10.
73. Murski, K. : Metal Finishing 1970, Vol.68, No.12, P.36.
74. Greenwood, J.D. : Electroplating, 1970, Vol.23, No.4, 21, and No.5, P.35.
75. Rao, B.V., et. al. : Trans Indian Inst. of Metals, 1973, Vol.26, No.1, P.1.
76. Lamb, V.A. : Techniques of Metal Research, Ed. Bunshah, R.F., 1968, Vol.1, Part 3, P.1311.
77. Robins, H.C. : Electroplating, 1969, Vol.22(12), P.29-32.
78. Lunyatskas, : Protection of Metals, 1968, Vol.4, (3), P.314.
79. Feldstein, N. and Amodio, P.R. : Plating, 1969, Vol.56(11), P.1246.
80. Wesley, W.A. : ibid, 1950, Vol.37, P.732.
81. Lund, J.A.H., Mackiw, V.A. and Warner, J.P. : Canadian Patent 1964, No.685,697.
82. Kunda, W. : High Temp. - High Pressure, 1971, Vol.3, P.593.
83. Burkin, A.R. : Met. Reviews 111, 1967, Vol.12, P.1.

84. Conaway, B.E. and Bockris, J.O'm (Ed) : Modern Aspects of Electrochem. Chap.5, Vol.11, Plenum Press 1975.
85. Prema, R, and Rao, P.V.V. : Trans. Soc. for Advancement Electro Chem. Sci. & Tech., July-Sept. 1973, P.93.
86. Schaleh, E. and Nicol, M.J. : Inst. of Min. & Met., March, 1978, Vol.87, P.C16.
87. Wesley, W.A. and Copson, H.R. : J. Electrochem. Soc., 1948, Vol.94, P.20.
88. Rigg, T. : Unpublished report.
89. Lund, J.A., Irvine, W.R., and Mackiw, V.A. : Powder Met. 1962, No.10, P.219.
90. Dixon, H. : Ph.D. Thesis, Sheffield City Polytechnic, 1977,
91. Zapf, G. : Powder Met. 1961, No.7, P.218.
92. Zapf, G. : ibid, 1970, Vol.13, No.26, P.130.
93. Krishnamoorthy, G.M. : ibid, 1971, Vol.14, No.27, P.164.
94. Squire, A. : Trans. A.I.M.E. 1947, Vol. 171, P.473.
95. Squire, A. : ibid, P.484.
96. Cundill, R.T., Marsh, E. and Ridal, K.A. : Powder Met. 1970, Vol.13, No.26, P.165.
97. Hulthen, S.I. : ibid, P.235.
98. Esper, F.J., Exner, H.E., and Metzler, H. : ibid, 1975, Vol.18, No.35, P.107.
99. Poster, A.R. and Hausner, H.H. : Modern Dev. in Powder Met. Vol.2, H.H. Hausner (Ed), 1966, P.26.
100. Lenel, F.V., Ansell, G.S., and Strife, J.R. : Mod. Dev. in Powder Met., 1974, p.275, Plenum Press.
101. Tracey, V.A. : Powder Met., 1966, Vol.9, No.17, P.54.
102. Dixon, R.H.T. and Clayton. : P.M. for Engineers, 1971, Machinery Pub.
103. Walker, E.V., Worn, D.K., and Walters, R.E.S. : Symp. on Powder Met., 1954, I.S.I. Spl. Rep.58.
104. Marshall, P.R. : Metals and Materials, Met. Reviews -123, 1968, Vol.13, P.53.
105. Hausner, H.H. : 7th Plansee Seminar, 1971, Paper No. 5.

106. Goetzl, G.G. : Treatise on Powder Met., Vol.1, Interscience Pub., 1949.
107. Marshall, P .R. : Powder Met. 1966, Vol.9, No.18, P.163.
108. Kunin, N.F. and Yurchenko, B.D. : Sov. P.M. Metal Cerm., 1968, Vol.2(62), P.91.
109. Kunin, N.F., and Yurchenko, B.D. : ibid, Vol.8(68), 1968, P.604.
110. Donachie, M.J. and Burr, M.F. : J. of Metals, 1963, Vol.15, No.11, P.849.
111. Hausner, H.H. and Sheinhartz, I. : Proc. of Metal Powder Assoc., 1954, P.6.
112. Hoganas Iron Powder Handbook. : Hoganas Co., Sweden, 1959.
113. Yarnton, D. and Davies, T.J. : Powder Met. 1963, No.11, P.1.
114. Afanasév, L.N., Perel'man, V.E., and Roman, O.V. : Sov. P.M. and Metal Cerm., 1969, June, Vol.6(78), P.456.
115. Reid, A. : Powder Met. 1965, Vol.8, No.16, P.215.
116. Geiger, E. and Jamison, R.S. : Powder Met. (Ed) Leszynski, W. Interscience 1961, P.585.
117. Leopold, P.M. and Nelson, R.C. : Int. J. of Powder Met. Vol.1(3), P.37, and ibid Vol.1(4), P.37-40.
118. James, P.J. : Powder Met. Inst. 1972, Vol.4(2), P.82, and ibid 1972, Vol.4(4), P.193.
119. Unckel, H. : Ref. 106, P.280.
120. Morgan, W.R. and Sands, R.L. : Metals and Materials, Met. Review 134, 1969, Vol.14, P.85.
121. Van Buren, C.E. and Hirsch, H.H. : Persp. in Powder Met. 1967, Vol.1, Chap.3, P.27, Plenum Press.
122. Sellors, R.G.R. : Powder Met. 1970, Vol.13, No.26, P.85.
123. Jackson, H.C. : Persp. in Powder Met. 1967, Vol.1, Chap.2, P.13.
124. Cull, G.W. : Powder Met. 1970, Vol.13, No.26, P.156.
125. Brown, G.T. : Proc. P.M. Group Meeting, Eastbourn, 11-13 Oct. 1976, Paper No.19.

126. Corso, S. and Giardano, V. : ibid, Paper No.15.
127. Davies, R. and Negm, M. : ibid, Paper No.18.
128. Huppmann, W.J. and Petzow, G. : ibid, Paper No.14.
129. Jones, P.K. : Powder Met. 1970, Vol.13, No.26, P.115.
130. Thummler, F. and Thomma, W. : Metals and Materials, Met. Review 115, June 1967, Vol.12, P.69.
131. Kuczynski, G.C. : Acta. Met. 1956, Vol.4, No.1, P.58.
132. Kuczynski, G.C. : Powder Met. 1963, No.12, P.1.
133. Kuczynski, G.C. : P.M. for High Performance Application, Burke, John J. & Weiss, Volker (Ed), P.101.
134. Kuczynski, G.C. : Trans. A.I.M.E. 1949, Vol.185, P.169.
135. Rhines, F.N. : Proc. Metal Powder Assoc. 1958, P.91.
136. DeHoff, R.T., Rummel, R.A., Rhines, F.T. and Long, A.H. : Powder Met. Leszynski W. (Ed) P.31, Interscience Pub.
137. Eremenko, V.N. and Nizhenko, V.I. : Sov. Powder Met. 1963, Vol.3, P.270.
138. DeHoff, R.T. and Aigeltinger, E.H. : Persp. in Powder Met., Roll, K.H. & Hausner, H.H. (Ed), 1970, Vol.5, P.81.
139. Rockford, J.G.R. : Scripta Met. 1969, Vol.3, P.333.
140. Coble, R.L. : Sintering and Related Phenomena, Metals Science Research, Vol.6, Kuczynski, G.C. (Ed) P.177, Plenum Press.
141. Moon, J.R. : Powder Met. Int. 1971, Vol.3(3), P.147 and Vol.3(4), P.194.
142. Stone, H.E.N. : Metallurgia, 1966, Vol.66, P.151.
143. Lenel, F.V. : Powder Met. for High Performance Applications, Burke, John J. and Weiss Volker. (Ed) P.119.
144. Tikkanen, M.H., Lindroos, V.K. and Ylasaari, S. : Int. J. of Powder Met. 1970, Vol.6, No.3, P.43.

145. Ichinnose, H. and Kuczynski, G.C. : Acta. Met. March, 1962, Vol.10, P.209.
146. Alexander, B.H. and Balluffi, R.W. : ibid, Nov. 1957, Vol.5, P.666.
147. Raja Rao, W., Jatkar, A.D., and Tendolkar, G.S. : Int. J. of Powder Met., 1970, Vol.6, No.3, P.65.
148. Gifkins, R.C. : J. Australian Inst. of Metals, 1969, Vol.14(2), P.92.
149. Mikijelj, V., Samsonov, G.V., and Ristic, M.M. : Science of Sintering, 1977, Vol.9, No.2, P.197.
150. Stabelin, P.F., and Kuczynski, G.C. : Acta. Met. 1963, Vol.11, P.1327.
151. Kuczynski, G.C., Matsumara, G. and Cullity, B.D. : Acta. Met. 1960, Vol.8, No.3, P.209.
152. Margerand, R, and Eudier, M. : Powder Met. 1963, No.12, P.17.
153. Fisher, B. and Rudman, P.S. : Acta. Met. 1962, Vol.10, P.37.
154. Jones, W.D. : Fund. Prin. of Powder Met., 1960, W. Clowes & Sons.
155. Huseby, R. : Manuf. Engr. & Management, 1970, Vol.64(5), P.27.
156. Hulthen, S.I. and Gustavsson, G. : Int. J. of Powder Met., 1968, Vol.4(3), P.27.
157. Kravic, A.F. and Gloor, A.B. : Powder Met., 1966, Vol.9, No.18, P.185.
158. Burr, D.J. and Krishnamoorthy, G.M. : Powder Met. 1973, Vol.16, No.31, P.33.
159. Burr, M.F. and Donachie, M.J. : Trans. A.S.M., 1963, Vol.56, P.863.
160. Eggleston, J.H. and Spangler, F.L. : SME Tech. Paper, CM72-812.
161. Bobo, L.L. : Ind. Heating 1968, Vol.35(12), P.2322
162. Lindskog, P. : Powder Met. 1970, Vol.13, No.26, P.280.
163. Chadwick, R. and Broadfield, E.R. : I.S.I. Spl. Rep. 38, 1947.
164. Munro, P.M. : Powder Met. Int. 1972, Vol.4, No.1, P.20.
165. Fischer, J.J. : Modern Dev. in Powder Met. Hausner, H.H. (Ed) 1974, Vol.8, P.75.

165. Fedorov, N.I.,  
Tsyarkin, A.T.,  
Samoilov, V.A.,  
Nosenko, A.S. : Soviet Powder Met. and Metal  
Cerm., 1972, Vol.11,(8), P.651.
167. Arbstedt, P.G. : Metals Technology, Vol.3, May-June  
1976, P.214.
168. Napara-Velgina, S.G.  
and Radomyselskii, I.D.,  
and Gorb, M.L. : Sov. Powder Met. and Metal Cerm.  
1973, Vol.12(12), P.960.
169. Harrison, L. and  
Dixon, R.H.T. : Powder Met., 1962, No.9, P.247.
170. Greetham, G. and  
Reid, A. : ibid, 1969, Vol.12, No.23, P.79.
171. Zapf, G. and Dalal, K. : Proc. 1976, Int. Powder Met. Conf.  
Chicago.
172. Durdaller, C. : Progress in Powder Met. Vol.25,  
1969, Proc. 25th Annual P.M. Conf.  
(M.P.I.F.), N.Y. May, 1969.
173. Crooks, S.R. : Metal Progress, 1958, Vol.54, No.6,  
P.68.
174. Adler, A. : Materials Engr. 1968, March, P.32.
175. Delisle, L. and  
Finger, A. : A.I.M.M.E. Tech. Paper 2046, 1946.
176. Benesovsky, P. : Metal Progress, 1954, Vol.50, No.4,  
P.200.
177. Delisle, L. and  
Knopp, W.V. : Trans. Am. Inst. Min. Met. Engrs.  
Tech. Pub. 2340, 1948.
178. Holcomb, R.T. : Metal Progress 1973, Vol.103, No.5,  
P.65.
179. Holcomb, R.T., and  
Lovenduski, J. : Modern Developments in Powder Met.  
Vol.8, Hausner, H.H. (Ed), P.85.
180. Williams, N.J. and  
Burr, D.J. : Metallurgia & Metal Forming, March,  
1973, Vol.40, No.3, P.84.
181. Zapf, G., Hoffman, G.,  
and Dalal, K. : Powder Met. 1975, Vol.18, No.35,  
P.214.
182. Rhines, F.N. and Colton : Powder Met. Wulff, J.J. (Ed), 1942,  
ASM, Chap.6, P.67.
183. Rhines, F.N. and  
Meussner, R.A. : Symp. on Powder Met., 1943, ASTM,  
P.25.
184. Lindskog, P. and  
Skoglund, G. : 3rd Eur. Powder Met. Symp., Nov.  
1971, Conf. Suppl. Pt.1, P.375.
185. Eloff, P.C. and  
Kaufman, S.M. : Powder Met. Int. 1971, Vol.3(2), P.71

186. Heck, F.W. : Proc. Int. Powder Met. Conf., 1970
187. Fischer, J.J., Tundermann, J.H. and Heck, F.W. : The Int. J. of Powder Met. & P.Tech. 1974, Vol.10, No.4, P.267.
188. Fischer, J.J. and Heck, F.W. : Mod. Dev. in P. Met., Hausner, H.H. (Ed), 1971, Vol.5, P.478.
189. Svensson, L.E. : Powder Met. 1974, Vol.17, No.34, P.271.
190. Dixon, H., Fletcher, A.J.F. and Cundill, R.T. : Powder Met. 1978, Vol.21, No.3, P.131.
191. Young, J.W. : Iron Age, Feb. 1955, Vol.175, P.119.
192. Kravic, A.F. : J. Soc. Automotive Engrs. 1961, Vol.77(7), P.45.
193. McAdam, G.D. : J.I.S.I., Aug. 1951, Vol.168, P.346.
194. Eudier, M. : Powder Met. 1962, No. 9, P.278.
195. Haynes, R. : ibid, 1971, Vol.14, No.27, P.64.
196. Haynes, R. : ibid, P.71.
197. Nazare, S. and Ondracek, G. : Powder Met. Int. 1974, Vol.6(1), P.8.
198. Gallina, V. and Mannone, G. : Powder Met. 1968, Vol.11, No.21, P.73.
199. Mackenzie, J.K. : Proc. Phys. Soc., 1950, B, 1, 63, P.2.
200. Pohl, D. : Europ. Symp. Uber. Pulvermetallurgie, Stuttgart 1968, Band 11 Bericht Nr.6, 7, Und. Arch. Eisenhuttw, demnachst.
201. Jenkins, I. : Powder Met. 1964, Vol.7, No.13, P.68.
202. Kaufman, M. and Mocarski, S. : Int. J. of P. Met., 1971, Vol.7, No.3, P.19.
203. Dudrova, E. and Kubelik, J. : Powder Met. Int. 1971, Vol.3(4), P.183.
204. Salak, A., Miskovic, V., Dudrova, E. and Rudnayova, E. : Powder Met. Int. 1974, Vol.6(3), P.128.
205. Landgraf, C.L. : Metal Progress 1974, Vol.105, No.6, P.95.
206. Luis, C. and Fletcher, A.J. : to be published.
207. Shashoua, V.E. : J. of Polymer Science, 1958, Vol.XXXIII, P.65.

208. Singleton, H.F. : "The Electroless Plating of  
Nickel Onto Iron Powder" Project  
Report, Sheffield City Polytechnic,  
April, 1979.
209. Annamalai, V. and : Hydro Metallurgy, 1979, Vol.4,  
Murr, L.E. P.57-82.
210. Stephenson, R.M. : Intro. to Chem. Process  
Industries. Reinhold Pub. Corp.,  
1966, P.408.

APPENDIX  
INDUSTRIAL CASE STUDY

INDUSTRIAL CASE STUDY

Preparation of Coated Powders in a Fluidised Bed

You are required to suggest a design for a plating cell that is capable of the production of 10 tonnes of iron powder coated with 3% nickel in a single week of 40 hours. Your design should be costed and an estimate made of the running cost involved. This information should be used to compare the cost of this new material with that<sup>of</sup> both blended and atomised material of the same composition.

Where appropriate you should make your own estimates of the costs of particular operations but you may assume the following:

1. Cost of blended powders - £ 356.15/tonne
2. Cost of atomised powder - £ 450.00/tonne
3. Wages of operatives @ - £ 60/week of 5 days
4. Overheads - 15% of running costs
5. Working year/week - 48 wks with 40 hrs/wk
6. Discount rate @ - 25%
7. Corporation tax @ - 52%
8. Tax is charged in the year after the tax liability is incurred.
9. Project is to be written off in eight years.
10. Capital allowances charged against a tax-free policy.
11. The unit is financially self-contained.
12. Suitable buildings, power and water facilities are available.

## COATING OF IRON POWDER WITH NICKEL USING ELECTRO-PLATING TECHNIQUES

### (i) INTRODUCTION

The process of producing nickel coated iron powder is a relatively new process. A patent was granted to Sheritt Gordon Mines, Canada, in the year 1964 for the process of manufacturing nickel coated iron powders. The process consisted of the reduction of an ammonical solution of a nickel salt by hydrogen under relatively high pressures. However, the use of electroplating techniques for the purpose of producing coated powders has not been reported in any detail. Salt<sup>(62)</sup> has, however, shown that electroplating techniques can be used for coating stainless steel powders with iron or nickel. The work recorded here has shown very promising results for the above mentioned process. The process is carried out in a specially designed cell utilising a novel three phase fluidised bed system, consisting of solid iron powder, the electroplating solution and the fluidising gas. A number of stainless steel rods act as cathode current distributors and the anode consists of 100% triacetate fabric bags filled with pure-nickel shot .

### (ii) THE PLATING CELL - LABORATORY AND INDUSTRIAL SCALE

Fig.7(a) shows the design of the laboratory scale plating cell and Table 24 gives the experimental details. The proposed data corresponding to the industrial scale plating cell is also given in Table 24.

Dimensions and Capacity:- The laboratory scale plating cell was constructed from a 15.25 cm diameter perspex tube. The height of the plating cell was 40.65 cm and that of the fluidised bed was 10.79 cm which gave a working volume of 1970.84 cm<sup>3</sup>. This cell was capable of producing 1 kg of plated powder, containing up to 8% nickel per hour.

The proposed industrial scale plant for producing 3% Ni coating on iron powder is to have a capacity of 10 tonnes per week of 40 hours. Thus the plating cell should be capable of producing 250 kg of 3% Ni plated powders per hour.

Although fluidised beds of such capacity are relatively common in the chemical industry, there are certain restrictions to their use in the present system. If the capacity of the cell is increased, the cathodic surface area (i.e. the area for contact between powder particles and cathode) will also have to be increased accordingly with the consequent requirement of a greater output from the rectifier. Assuming a constant value for the cell resistance, a higher d.c. voltage will be required for the current necessary in order to achieve the appropriate current density. It should also be remembered that high values of voltages and amperage will result in excessive heat generation and any consequent effect on the plating solution.

Keeping these restrictions in view, the required output may be achieved by the use of five plating cells arranged in parallel. Thus the capacity of each cell will be 50 kg/hour. However, the laboratory scale data shows that at the appropriate current density, 3% nickel coated can be produced in approximately 23 minutes. Assuming that it takes

seven minutes to empty and refill the plating cells, the size of a single batch must be 25 kg per cell. Therefore, the working volume that is required to maintain this capacity is:

$$\begin{aligned}
 &= \text{Laboratory scale working volume X25} \\
 &= 1970.84 \times 25 \text{ cm}^3 \\
 &= 49271 \text{ cm}^3
 \end{aligned}$$

In order to maintain similar fluidisation conditions in the industrial scale plating cell, the height of the cell has been kept constant and the increase in the working volume has been achieved by increasing the diameter of the plating cell. Therefore, the diameter of the industrial scale plating cell will be:

$$\begin{aligned}
 &= 2 \left[ \sqrt{\frac{\text{Working volume}}{\pi \times \text{Height of bed}}} \right] \\
 &= 2 \left[ \sqrt{\frac{49271}{\pi \times 10.79}} \right]
 \end{aligned}$$

Diameter = 76.25 cm

The design and the dimensions of the industrial scale plating cell is shown in Fig.83.

Cathodic Surface Area:- The cathodic surface area should be increased in the same proportion as the working volume of the cell so that the density of the cathode current distributor rods per unit volume of the bed remains the same in both the laboratory scale and industrial scale plating cells. Working on this basis, the cathodic surface area required would be 58.53 dm<sup>2</sup> and thus for a current density of 17.65 A/dm<sup>2</sup> the total current required would be 1033.05 amperes. If the resistance of the cell is 0.23 ohms, the

voltage necessary to attain the required current will be 237.60 volts. Rectifiers of such output range are not generally available. Moreover, the heat generated would also lead to difficulties in controlling the temperature of the solution. However, preliminary investigation on the effect of reducing the number of cathode rods showed that the plating rate was not affected until the cathodic surface area was reduced to a very small value. Furthermore, since the mechanisms of charge conduction within fluidised bed electrodes is believed to be predominantly electronic<sup>(49)</sup>, it has been assumed that a five-fold increase in the cathodic surface area of the industrial plating cell will be sufficient. Thus the cathodic surface area is

$$= 11.71 \text{ dm}^2$$

Anodic Surface Area:- The laboratory-scale plating cell utilised a single anode unit having a surface area of  $1.34 \text{ dm}^2$ . The anode bag comprised of twin terylene bags, the inner bags being filled with nickel shot. Fig.9 shows the anode bag. In the industrial scale plating cell, the anodic surface area has been increased five fold to  $6.70 \text{ dm}^2$  with the use of four different anode units. The arrangement of the anodes is shown in Fig.83. It should, however, be noted that the use of too many anode units may adversely affect fluidisation.

Cell Resistance, Current Density, Voltage and Amperage:-

Although the average cell resistance and current density are the same in both laboratory and industrial scale plating cells, the voltage and amperage have to be adjusted so as to attain the appropriate current density over the increased electrode surface area.

(i) Cell resistance =  $0.23\Omega$

(ii) Current density necessary =  $17.65 \text{ A/dm}^2$

Thus amperes required = Current density x C surface area  
=  $17.65 \times 11.71$   
= 206.68 amperes

Voltage required = Amperes x cell resistance  
=  $206.68 \times 0.23$   
= 47.53 volts

In order to work out the output that is needed from the rectifier, the overall resistance of the five plating cells arranged in parallel and the total current passing through these cells has to be considered.

Thus  $R = 4.599 \times 10^{-2}$  ohms

Total current through the five cells =  $206.68 \times 5$  amperes  
= 1033.4 amperes

Thus voltage =  $1033.4 \times 4.599 \times 10^{-2}$   
= 47.53 volts

Thus the output required from the rectifier is at least 47.53 volts and 1033.4 amperes.

### Fluidising Gas Rate:-

In the process of electro-coating of powders, fluidisation plays a very critical role. It is important that the gas flow rate is maintained so as to suspend all powder particles and thus expose the entire surface area of the particles. At low flow rates of gas, powder particles tend to settle on the membrane and are, therefore, not plated. On the other hand at high flow rates, the bed reaches a state of aggravated fluidisation and the powder particles become enveloped by a film of gas which increases the resistance of the cell.

The laboratory scale cell has a membrane surface area of  $182.1 \text{ cm}^2$  and the flow rate required for incipient fluidisation was 30 litres/min, (or  $0.1648 \text{ litres/minute/cm}^2$  of membrane area). The membrane surface area of the industrial scale cell is  $4561.5 \text{ cm}^2$  and therefore, the gas flow rate required =  $4561.5 \times 0.1648 \text{ litres per minute}$   
= 751.9 litres per minute.

The compressor should be capable of supplying this flow rate.

### Rate of Plating:-

If the plating rate for the industrial scale plating cell is to remain the same as that of laboratory scale cell, then the total period of cathodic contact, for each powder particle, in both the cells should be the same. This suggests that the cathodic surface area per unit volume of the bed should be kept the same in both plating cells (i.e. the cathodic surface area should be increased in the same ratio

as the working volume.) However, this would only be true if each powder particle only made direct contact with the cathode current distributor. In practice, powder particles can become cathodic through a chain of particles or by contact with another charged particles<sup>(49)</sup>.

With a plating rate of 0.1312 wt % Ni per minute, 3% Ni coated iron powder can be produced in approximately 23 minutes.

### THE COMPLETE PLANT

The plant can be divided into three distinct sections:-

1. The plating section.
2. The purification section.
3. The drying section

Fig.84 shows the complete lay-out of the plant.

The plating section consists of five plating cells arranged in parallel. Two bus bars running on either side of the cells supply the current. An overhead hopper, which can be slid into position over each plating cell, feeds the powder. Each cell has separate piping connections to the storage tank for the supply of the plating solution. The cells are also connected to the settling tank through separate pipe lines for pumping the slurry into the settling tank. This section is provided with one operator to supervise all the five cells.

The purification section consists of a settling tank, two filter units, a reaction tank, a check tank and a storage tank and a tank for storing powder and water slurry.

No. of Units.	Unit	Capacity	Cost £
1	Settling tank	100 gallons	250
2	Filters	500 gallons/hr	2000
1	Reaction tank	400 gallons	2000
1	Check tank	400 gallons	1000
1	Storage tank	1000 gallons	2000
1	Tank for powder-water slurry to be fed to centrifuge	200 gallons	250
<u>Total Costs</u>			7,500

The purification cycle for the purpose of recycling used plating solution consists of:-

1. Filtering the clear solution from the settling tank into the reaction tanks.
2. A slurry of nickel carbonate is added, with constant stirring, to the solution maintained at 60°C till the pH reaches 5.5.
3. 0.5 litres of 30 volume hydrogen peroxide is added for each 450 litres of solution. Stirring is continued and temperature maintained for 4 hours.

4. Activated carbon in the proportion of 0.2-0.9 kg per 450 litres is then added and temperature and agitation are maintained overnight.
5. The solution is allowed to settle and then filtered into the check tank.
6. The strength of the solution is checked and diluted to the working strength. The pH is adjusted to its working value by means of 10 per cent sulphamic acid solution. The solution is then pumped into the storage tank for re-use.

The powder from the settling tank is received in a tank and clean water is added to it. This slurry is then fed into a continuous type centrifuge. The washed powder from the centrifuge is then fed into the drying chamber. The drying plant consists of a number of circular discs, which are electrically heated, and arranged on top of one another. A rotating rake is provided to avoid agglomeration of powders. Hot air is passed up the column and the dried powder is collected at the bottom. The dried powders are then stored for delivery.

## I CAPITAL COSTS

(i) Adjustments on existing site	:	£2000
(ii) Cost of compressor unit	:	£1150
(iii) Cost of rectifier unit	:	£5000
(iv) Cost of purification plant	:	£7500
(v) Cost of centrifuge and drying plant	:	£1100
(vi) Cost of chemicals at start	:	£6870
(vii) Cost of 5 plating cells @ £120/cell	:	£600
		<hr/>
		£34,120
		<hr/>
		TOTAL OUTLAY

The cost of chemicals at start, has been included in the capital costs because this solution is to be recycled into the system after it has passed through a purification cycle and the lost nickel ions have been replenished. The cost incurred during the purification cycle is thus the processing cost involved with regards to the solution itself.

## II PROCESSING COSTS

Assume anode efficiency to be 85%. The relatively poor anode efficiency is because some of the iron powder enters the anode bags and passivates the anode.

$$\begin{aligned} \text{Total bath of 25 kg of plated powder} &= 206.68 \times \frac{23}{60} \\ &= 79.22 \text{ amp-hrs} \end{aligned}$$

$$\begin{aligned} \therefore \text{Nickel dissolved from anode} &= 79.22 \times 1.095 \\ &= 86.75 \text{ gms} \end{aligned}$$

$$\begin{aligned} \text{Weight of nickel deposited on powder} &= 25 \times \frac{3}{100} \\ &= 0.75 \text{ kg or 750 gms} \end{aligned}$$

$$\begin{aligned} \therefore \text{Weight of nickel being despatched from solution} & \\ &= 750 - 86.75 \\ &= 663.25 \text{ gms} \end{aligned}$$

$$\begin{aligned} \therefore 663.25 \text{ gms of nickel will have to be replaced} & \\ \text{during the purification cycle by the addition of} & \\ \text{NiCo}_3 \quad \text{i.e.} \quad \frac{663.25 \times 118.7}{58.7} &= 1341.19 \text{ gms} \end{aligned}$$

$\text{NiCO}_3$  per batch

$$\begin{aligned} \text{or NiCo}_3 \text{ required per tonne powder} &= 1341.19 \times \frac{1000}{25} \\ &= 53.65 \text{ kg.} \end{aligned}$$

$$\begin{aligned} \text{Cost of addition} &= 53.65 \times \text{£}1.62 \\ &= \text{£}87/\text{tonne of powder} \end{aligned}$$

(i) Anode Requirements

$$\begin{aligned}\text{Ni shot required} &= 86.75 \times \frac{1000}{25} \\ &= 3.47 \text{ kg/tonne of powder}\end{aligned}$$

$$\text{Cost} = \frac{3.47}{100} \times 2673 = \text{£}9.28/\text{tonne}$$

$$\begin{aligned}\text{Anode bags required @ £}5.72/\text{tonne powder} \\ &= \text{£}5.72 \text{ per tonne of powder}\end{aligned}$$

(NOTE - 320 bags are required per tonne of powder, an approximate price of 0.018 pence per bag has been assumed.)

Total Anode Costs:-

$$= 9.28 + 5.72 = \text{£}15/\text{tonne}$$

Power Consumption:-

$$\begin{aligned}&= \text{voltage} \times \text{amperes} \times \text{time (hrs)} \\ &= \frac{47.53 \times (206.68 \times 5) \times 8}{1000} \\ &= 392.73 \text{ kW-hr/day or per two tonne} \\ &\quad \text{powder}\end{aligned}$$

$$\text{Thus} = 196.37 \text{ kW-hr/tonne of powder}$$

$$\begin{aligned}\therefore \text{Power costs @ 1.25 pence per kW-hr} \\ &= \text{£}2.45/\text{tonne}\end{aligned}$$

Drying Costs:-

It has been assumed that 200 kW-hr will be required to dry every tonne of powder.

$$\begin{aligned}\therefore \text{costs} &= 200 \times 1.25 \\ &= \text{£}2.50/\text{tonne}\end{aligned}$$

Compressor Running Costs:-

The compressor uses 7.5 kW-hr power is required per tonne. An extra amount is being charged also, to take care of any additional requirements for the compressor. The compressor running costs are = £0.5/tonne

Processing Costs:- Per annum (480 tonnes/annum)

1. Iron Powder @ £278/tonne	£133440
2. Chemicals for Purification @ £87/tonne	£41760
3. Anode Requirements @ £15/tonne	£7200
4. Power Consumption @ £2.45/tonne	£1176
5. Drying Costs @ £2.5/tonne	£1200
6. Compressor Running Costs @ £0.5/tonne	£240
7. Wages of Three Operatives @ £60/week per operator	£8640

Total Processing Costs £193656

Maintenance Costs:- @ 10% of Capital Costs = £3412

Overheads:- @ 15% of Processing Costs = £29048.4

Costs prior to taxation discounted @ 25%

= Overheads + Processing Costs + Maintenance

= 29048.4 + 193656 + 3412

= £226116.4

= 226116.4 (0.8 + 0.64 + 0.512 + 0.4096 + 0.32768 +  
0.262144 + 0.209715 + 0.167772)

= 226116 x 3.328911

= £752721.37

### III COSTS AFTER TAXATION

Corporation Tax - @ 52%

Discount Rate - 25%

CAPITAL ALLOWANCES:- These are to be charged against a tax - free policy. This suggests that it is most advantageous to charge the maximum capital allowances in the early years of the project. However, the total capital allowance cannot be charged in the first tax-year unless the tax to be paid is greater than the capital sum. Thus the most profitable capital allowance has been worked out as follows:

1st year - 48% of capital sum

2nd year - 48% of capital sum

3rd year - 4% of capital sum

Year

$$\begin{array}{rcl} 2 & = & 0.52 \left[ (480x - 226116.4) - (0.48 \times 34120) \right] 0.64 \\ 3 & = & 0.52 \left[ (480x - 226116.4) - (0.48 \times 34120) \right] 0.512 \\ 4 & = & 0.52 \left[ (480x - 226116.4) - (0.04 \times 34120) \right] 0.4096 \\ 5 & = & 0.52 \left[ (480x - 226116.4) \right] 0.32768 \\ 6 & = & 0.52 \left[ (480x - 226116.4) \right] 0.262144 \\ 7 & = & 0.52 \left[ (480x - 226116.4) \right] 0.209715 \\ 8 & = & 0.52 \left[ (480x - 226116.4) \right] 0.167772 \\ 9 & = & 0.52 \left[ (480x - 226116.4) \right] 0.134218 \end{array}$$

$$\sum_2^9 = 664.717x - 323233.65$$

TOTAL COSTS AFTER TAXATION

$$= 664.717x - 323233.65 + 752721.37$$

$$= 664.717x + 429487.72$$

INCOME

$$\sum_1^8 = [(480x) (0.8 + 0.64 + 0.512 + 0.4096 + 0.32768 + 0.262144 + 0.209715 + 0.167772)]$$

$$= (480x) 3.328911$$

$$= 1597.8773x$$

PROFIT = INCOME - TOTAL COSTS

$$= 1597.8773x - 664.717x - 429487.72$$

$$= 933.1603x - 429487.72$$

. . At apparent break even point, the selling price (x)

Will be =  $\frac{429487.72}{933.1603}$

$$933.1603$$

$$= \text{£}460.25/\text{tonne of powder}$$

At a 125% (including Capital) Return on Investment, the

Selling Price will be

$$= \frac{0.25 \times 34120 + 34120 + 429487.72}{933.1603}$$

$$933.1603$$

$$= \text{£}505.96/\text{tonne of powder}$$

## CONCLUSIONS

Price of 3% nickel blended powder = £356.15/tonne

(Nickel powder @ £2673/tonne; Iron powder @ £278/tonne)

Price of atomised 3% nickel powder = £450/tonne

Price of nickel-coated iron powder (3% Ni) = £505.96/tonne

The plated powders are the most expensive and the blended the least. However, in the case of the latter, additional costs are incurred during blending. Moreover, the compacts made from blended powders have the inherent disadvantage of a greater degree of inhomogeneity and thus require longer periods of sintering. The lack of sufficient homogeneity could also lead to the need of higher percentages of nickel in order to achieve required levels of strength. Thus with the use of plated powders, which result in more homogeneous structures, similar strengths could be obtained in leaner alloys. The atomised powders generally show poor compressibility and thus possess inferior properties after a specific compacting and sintering treatment.

The relatively high cost of plated powders could have resulted from the use of nickel sulphamate solution which is five times as expensive as the commonly used nickel chloride plating solution. Although sulphamate solutions have the advantage of high rates of plating, further work involving the appraisal of other plating solutions for the purpose, is necessary to justify its choice.

TABLE 1 COMPOSITIONS OF BATHS USED FOR NICKEL DEPOSITION

CONSTITUENTS OF SOLUTIONS (typical concentrations) g/l.	TYPE OF BATH					
	WATTS TYPE	HARD WATTS	100% CHLORIDE AND HIGH CHLORIDE*	FLUOBORATE	CONVENTIONAL SULPHAMATE	CONCENTRATED SULPHAMATE
Nickel Sulphate (NiSO <sub>4</sub> 6H <sub>2</sub> O)	150 - 400	180 - 230	0 - 200			
Nickel Chloride (NiCl <sub>2</sub> 6H <sub>2</sub> O)	20 - 80		150 - 300		0 - 15	5 - 15
Nickel Fluoborate (Ni(BF <sub>4</sub> ) <sub>2</sub> )				200 - 450		
Nickel Sulphamate (Ni(SO <sub>3</sub> NH <sub>2</sub> ) <sub>2</sub> 4H <sub>2</sub> O)					300 - 450	550 - 650
Boric Acid (H <sub>3</sub> BO <sub>3</sub> )	15 - 50	30	20 - 50	22 - 37	30 - 45	30 - 40
Others		Ammonium Chloride-25				

\* Total Concentration of Nickel Salts does not exceed 300 g/l

**TABLE 2 CHARACTERISTICS OF SOME COMMERCIAL NICKEL PLATING SOLUTIONS**

	TYPE OF SOLUTION				
	WATTS	CHLORIDE	FLUOBORATE	CONVENTIONAL SULPHAMATE	CONCENTRATED SULPHAMATE
Nickel Concentration (g/l)	34 - 90	62 - 74	50 - 114	54 - 82	100 - 140
pH (electrometric)	1.5 - 4.5	2.0	2.0 - 3.5	3.0 - 4.5	3.0 - 4.5
Operating temperature (°C)	45 - 65	50 - 70	40 - 80	40 - 60	40 - 60
Current density (A/dm <sup>2</sup> )	2.5 - 10	2.5 - 10	4 - 10	2 - 30	maximum 43
Cathodic Efficiency (%)	97 - 99	98 - 99	97 - 99	97 - 99	98 - 100
Anodic Efficiency (%)	98 - 100	~ 100	98 - 100	~ 100	~ 100
Throwing Power	Low	Very High	Very High	Moderate	High
Hardness of deposit (DPH)	140 - 160	230 - 260	159 - 183	180 - 220	220 - 400
Residual Stress (N/mm <sup>2</sup> )	124 - 241	264 - 340	110 - 193	0 - 110	~ 110 - 804
Rate of Plating	Slow	Moderate to High	High	Moderate to High	Very High
Resistivity (ohm-cm) (at Ni Concentration of 75 g/l)	10.2	5.6	5.6	-	-
Tolerance of Fe as impurity	Moderate	Moderate	Relatively High	200 ppm	200 ppm

TABLE 3      OPERATING CONDITIONS\* OF A LABORATORY  
SCALE PLANT FOR COATING STAINLESS STEEL  
POWDER WITH IRON

Weight of stainless steel powder used (-100 mesh)	60 g
Composition of iron plating solution	2.3M FeCl <sub>2</sub>
pH	1.0
Temperature	70°C
Rate of flow of solution	18 ml/min
Cell current	3 amperes
Cell potential	18 volts
Fluidised bed height	37 cm

\* obtained from Reference No. 62

TABLE 4 - MECHANICAL PROPERTIES OF SINTERED AND HEAT TREATED LOW ALLOY STEELS

Type of Powder	Composition %			Sintering Temperature (°C)	Period of Sintering (min)	Austenitising Temperature (°C)	Tempering Temperature	Density (g/cc)	Tensile Strength (N/mm <sup>2</sup> )	Elongation (%)	Modulus of Rupture (N/mm <sup>2</sup> )	Ref.
	C	Ni	Mo									
Blended	0.40	1.75	-	1120	30	-	-	6.40*	-	-	600**	172
Blended	0.40	1.75	0.50	1120	30	843	427	7.00*	-	-	1122	179
Pre-Alloyed	0.40	1.75	0.47	1120	30	843	427	7.00*	-	-	1250	179
Blended	0.50	2.00	-	1120	20	871	204	7.20	-	-	1379	205
Pre-Alloyed	0.50	1.90	0.50	1120	20	871	204	7.20	-	-	1896	205
Blended	0.75	2.00	-	1120	30	843	260	6.50*	676	N.G.	1051	174
Blended	0.75	4.00	-	1120	30	843	260	6.50*	703	N.G.	1082	174
Blended	0.40	3.00	-	1120	30	-	-	6.40*	-	-	655**	172
Blended	0.50	2.00	-	1320	60	875	200	7.22	934	2.0	-	157
Blended	0.50	5.00	-	1320	60	875	200	7.27	1560	1.0	-	157
Blended	0.40	3.00	-	1300	60	870	600	6.90	442	2.6	-	164
Blended	0.40	5.00	-	1300	60	870	600	6.90	503	5.6	-	164
Blended	0.34	3.50	-	1100	180	825	400	7.20	524	6.1	-	177
Blended	0.51	5.00	0.50	1300	60	870	600	7.12	1000	2.2	-	180
Blended	0.49	5.00	0.50	1300	60	870	650	7.10	740	3.6	-	158
Blended	0.33	3.00	-	1150	120	QST	600	6.98	390	2.0	-	190
Pre-Alloyed	0.33	3.00	-	1150	120	QST	600	6.52	399	2.2	-	190
Plated	0.33	3.00	-	1150	120	QST	600	6.75	446	1.9	-	190

\* - Green Density

\*\* - As sintered strength

N.G. - Not given

QST:- Quenched from Sintering Temperature.

TABLE 5    COMPOSITIONS AND OPERATING CONDITIONS OF  
SULPHAMATE SOLUTIONS USED

Type of Solution	Composition (g/l)			Operating Conditions		
	Nickel Sulphamate $\text{Ni}(\text{SO}_3\text{NH}_2)_2 \cdot 4\text{H}_2\text{O}$	Nickel Chloride $\text{NiCl}_2 \cdot 6\text{H}_2\text{O}$	Boric Acid $\text{H}_3\text{BO}_3$	pH (electrometric)	Temperature (°C)	Average Current Density (A/dm <sup>2</sup> )
Conventional Sulphamate	370 (86.7)*	5.0	40.0	3.0	60	7.0
Concentrated Sulphamate	525 - 600 (125 - 144)*	5.0	40.0	3.0	60	8.0 - 20.0

\* Nickel content of solution (g Ni/l)

TABLE 6      FABRICS USED TO MAKE ANODE BAGS AND THE  
COMBINATION IN WHICH THEY WERE USED

	FABRIC USED FOR MAKING	
	INNER ANODE BAG	OUTER ANODE BAG
1	100% Triacetate	100% Triacetate
2	Canvas	-
3	100% Triacetate	65% Polyester - 35% Cotton
4	65% Polyester - 35% Cotton	65% Polyester - 35% Cotton

TABLE 7 - PERFORMANCE OF THE REFRACTORY MEMBRANE PLATING CELL

EXPT NO	VOLUME OF SOLUTION (l)	STRENGTH OF SOLUTION (g-Ni/l)		MASS OF POWDER (g)	QUANTITY OF ELECTRIC CHARGE PASSED (AMP-HR)	AVERAGE CELL RESISTANCE (Ohms)	AVERAGE CURRENT DENSITY (A/dm <sup>2</sup> )	NICKEL CONTENT OF PLATED POWDER (%)	TOTAL MASS OF NICKEL DEPOSITED (g)		DEPOSITION EFFICIENCY (%)
		START	FINISH*						THEORETICAL AT 100% EFFICIENCY	ACTUAL	
MI	1.2	87.8	98.1	750	15.13	0.58	7.1	1.83	16.57	13.73	82.9
MII	1.1	84.3	89.5	800	11.00	0.64	6.8	1.08	12.04	8.64	71.8
MIII	1.2	87.8	107.2***	750	15.10	0.58	7.0	1.92	16.53	13.44	81.3
			88.8***								

\* - Not corrected for evaporation losses

\*\* - Solution from anode chamber

\*\*\* - Solution from cathode chamber

TABLE 8 EFFECT OF VARIOUS OPERATING CONDITIONS ON THE ELECTROPLATING OF NICKEL ONTO IRON POWDERS USING THE 'ANODE BAG CELL.'

EXPT. NO.	Nickel content of Solution (g Ni/l)		Volume of Solution (l)	Mass of Iron Powder (g)	Anode Bag Fabric		Anode Material	Total Electric Charge Passed (Amp-Hrs)	Average Cell Resistance (Ohms)	Average Current Density (A/dm <sup>2</sup> )	Deposition Efficiency (%)	Dissolution Efficiency (%)	Total mass of nickel Deposited (g)	Mass %Of Nickel deposited (%)
	At Start	At Finish*			Inner	Outer								
NI	122.7	98.7	1.6	1 000	TRIACETATE	TRIACETATE	Pure-Ni	52.39	0.26	17.4	142.9	53.8	82.0	8.20
NII	122.5	103.9	1.6	1 000	"	"	"	38.00	0.23	17.7	157.7	51.5	65.6	6.56
NIII	130.8	101.8	1.6	1 000	"	"	"	36.33	0.31	20.2	229.8	27.7	91.4	9.14
NIV	140.4	135.9	1.6	1 000	"	"	"	27.33	0.36	16.9	148.7	67.4	44.5	4.45
NV	142.0	134.0	1.6	1 000	"	"	"	32.27	0.37	17.9	209.4	42.5	73.6	7.36
NVI	142.23	143.0	1.5	900	CANVAS	-	"	18.95	0.73	8.0	-	46.3	-	-
NVII	140.0	154.0	1.5	900	TRIACETATE	65% POLYESTER 35% COTTON	"	25.10	0.35	13.0	103.5	89.1	28.44	3.16
NVIII	140.9	148.5	1.5	900	65% POLYESTER 35% COTTON	65% POLYESTER 35% COTTON	"	13.90	0.72	8.1	173.9	94.0	26.5	2.94
NIX	118.1	90.5	1.5	900	TRIACETATE	TRIACETATE	S-Ni	30.29	0.33	11.7	85.2	64.8	28.3	3.14
NX	118.1	113.8	1.5	900	"	"	S-Ni	30.62	0.33	11.9	79.5	26.3	26.6	2.96
NXI	120.0	110.3	1.5	900	"	"	S-Ni	27.75	0.35	11.7	78.5	85.4	23.9	2.65
NXII	120.0	108.5	1.5	900	"	65% POLYESTER 35% COTTON	S-Ni	29.37	0.42	11.4	91.2	83.3	29.3	3.26

\* - Not Corrected for Evaporation Losses

TABLE 9      EFFECT OF IRON POWDER AND ANODE BAG

TYPE ON CELL RESISTANCE

EXPT. NO.	ANODE BAG FABRIC		ANODE MATERIAL	CELL RESISTANCE (Ohms)	REMARKS
	INNER	OUTER			
NXIII	TRIACETATE	TRIACETATE	PURE-NI	0.41	Plating Without Powder  Only Single Bag Used
NI	"	"	"	0.26	
NVII	"	POLYESTER	"	0.35	
NVIII	POLYESTER	"	"	0.72	
NVI	CANVAS	-	"	0.73	
NIX	TRIACETATE	TRIACETATE	S-NICKEL	0.33	
NXII	"	POLYESTER	"	0.42	

TABLE 10      'ELECTROLESS' PLATING WITH AND WITHOUT  
ANODE ASSEMBLY IN POSITION

1. Weight of iron Powder used = 1 000 g
2. Volume of plating used = 1.6 l

EXPT. NO.	NICKEL CONTENT OF SOLUTION		WEIGHT OF ANODE ASSEMBLY		SOLUTION TEMPERATURE (°C) AFTER				MASS % Ni DEPOSITED AFTER				
	AT START	AT FINISH**	AT START (g)	AT FINISH (g)	0 (min)	15 (min)	30 (min)	45 (min)	60 (min)	15 (min)	30 (min)	45 (min)	60 (min)
NXXIII	138.1	136.9	494.0	493.3	62	54	51	49	48	1.10	1.37	1.52	1.84
NXXVIII*	134.8	135.8	-	-	62	51	48	46	46	1.11	1.26	1.47	1.70

\* Anode Bags Not in Position

\*\* Not Corrected For Evaporation Losses

TABLE 11 'ELECTROLESS PLATING' OF NICKEL ON SOLID OBJECTS

NATURE OF SOLID OBJECT	WEIGHT OF OBJECT gms		NICKEL CONTENT OF OBJECT AFTER PLATING	COMPOSITION OF SOLUTION				SOLUTION TEMPERATURE (°C) AFTER					
	START	FINISH		AT START		AT FINISH*		0 min	15 min	30 min	45 min	60 min	
				NICKEL g/l	IRON g/l	NICKEL g/l	IRON g/l						
1. BOLT (MILD STEEL)	31.2991	31.2933	TRACE										
2. WASHER (MILD STEEL)	3.9834	3.9814	NIL	142.7	0.13	150.3	0.15						
3. PIECE (ELECTROLYTIC IRON)	55.2455	55.2426	NIL										

\* Not Corrected for Evaporation Losses

TABLE 12      OXYGEN CONTENT OF COATED POWDER

PERIOD OF PLATING (minutes)	Oxygen in PLATED POWDER (mass %)
00 start	0.68*
15	1.525
30	0.873
45	3.128
50	1.225

\* Sponge iron powder - basic oxygen content

TABLE 13    SIEVE ANALYSES OF SPONGE IRON AND NICKEL COATED SPONGE IRON POWDERS

SIEVE SIZE (microns)	% MASS RETAINED BEFORE PLATING	% MASS RETAINED AFTER PLATING			NICKEL CONTENT OF VARIOUS SIEVE FRACTIONS (Mass %)		
		MEAN NICKEL CONTENT OF UNSIEVED POWDER					
		4.06%	5.36%	9.14%			
-53	23.46	18.40	15.82	15.05	5.11	7.71	11.97
+53	12.07	10.90	10.92	10.40	4.20	5.80	9.78
+63	13.74	12.10	13.10	13.34	3.73	5.24	9.27
+75	22.07	25.18	23.48	23.44	3.57	4.74	8.43
+90	12.45	15.22	12.87	12.78	3.42	4.49	8.34
+106	14.95	14.87	18.21	18.69	3.42	4.65	8.17
+125	1.22	2.43	3.20	3.36	3.47	4.77	8.60
+150	0.045	0.90	2.40	2.86	3.86	5.48	9.52

TABLE 14

PLATING NICKEL ONTO -106 + 90  $\mu\text{m}$  SIZE IRON  
 POWDER IN A CELL EMPLOYING 100% TRIACETATE FABRIC  
 ANODE BAGS AND PURE NICKEL SHOT

	EXPERIMENTAL CONDITIONS	
1	Nickel content of solution at start	134.2 g Ni/l
2	Nickel content of solution at finish	105.3 g Ni/l*
3	Volume of solution at start	1.6 l
4	Volume of solution at finish	1.2 l**
5	Mass of iron powder used	1000 g
6	Size of powder used	-106 + 90 $\mu\text{m}$
7	Period of plating	45 min
8	Average cell resistance	0.39 ohms
9	Average current density	16.82 A/dm <sup>2</sup>
10	Quantity of electric charge passed	27.25 amp-hr
11	Total mass of nickel deposited	93.7 g
12	Apparent deposition efficiency	314%
13	Anode dissolution efficiency	59.2%
14	Mean nickel content of plated powder	9.37%

Sieve Size ( $\mu\text{m}$ )	Nickel Content (mass %)
-106 + 90	10.38
+106	9.34
+125	9.35
+150	10.84

\* Not corrected for evaporation losses

\*\* Does not include losses due to evaporation and solution trapped within powder particles

TABLE 15  
MEAN PARTICLE SIZES AND CHEMICAL ANALYSIS

Material	Particle Size (µm)	Chemical Composition (%)									
		C	Si	Mn	Ni	Cr	S	P	O <sub>2</sub>	Fe	
Sponge Iron Powder	-	0.024	0.065	0.34	0.064	0.04	0.04	0.05	0.68	Bal	
Carbony Nickel	3.7	-	-	-	98.30	-	-	-	-	-	
Natural Graphite (Analytical Grade)	3.8	95.5	-	-	-	-	-	-	-	-	
Plated Powder I	-	0.024	0.065	0.34	1.75	0.04	0.04	0.05	0.95	Bal	
Plated Powder II	-	0.024	0.065	0.34	3.17	0.04	0.04	0.05	1.30	Bal	
Plated Powder III	-	0.024	0.065	0.34	4.06	0.04	0.04	0.05	2.40	Bal	

TABLE 16  
OXYGEN CONTENT OF SINTERED COMPACTS

Material	Period of Sintering (min)	Nickel %	Oxygen Before Sintering %	Oxygen After Sintering %
Sponge Iron Powder	-	-	0.68	-
Plated Powder I	240	1.75	0.95	0.26
Blended Powder	240	1.75	-	0.086
Plated Powder	240	3.17	1.30	0.35
Blended Powder	240	3.50	-	0.084
Plated Powder	240	4.06	2.40	0.37
Blended Powder	240	4.25	-	0.068

TABLE 17

## PROPERTIES OF Fe-1.75% Ni ALLOY COMPACTS

## MADE FROM BLENDED POWDERS

COMPOSITION:- Fe - 1.75  $\pm$ 0.05% Ni - 0.35  $\pm$ 0.05% C

S. No.	Period of Sintering (min)	Sintered Density (%)	Modulus of Rupture (N/mm <sup>2</sup> )
101B	30	89.7	889
102B	"	90.8	958
103B	"	91.4	924
104B	"	91.7	924
105B	60	87.7	786
106B	"	88.0	807
107B	"	90.0	917
108B	"	90.2	938
109B	"	92.2	1027
110B	"	92.0	1007
111B	120	87.6	758
112B	"	89.3	821
113B	"	90.6	945
114B	"	90.6	979
115B	"	92.2	1041
116B	"	92.2	1083
117B	240	89.1	883
118B	"	89.3	917
119B	"	91.1	1062
120B	"	91.6	1062
121B	"	92.5	1151
122B	"	92.8	1145

TABLE 18

PROPERTIES OF Fe-1.75% Ni ALLOY COMPACTSMADE FROM PLATED POWDERSCOMPOSITION:- Fe - 1.75  $\pm$ 0.03% Ni - 0.35  $\pm$ 0.05% C

S. No.	Period of Sintering (min)	Sintered Density (%)	Modulus of Rupture (N/mm <sup>2</sup> )
101P	30	85.0	586
102P	"	86.1	648
103P	"	86.5	676
104P	60	87.0	696
105P	"	87.3	772
106P	"	89.7	896
107P	120	86.2	676
108P	"	87.0	765
109P	"	87.5	752
110P	"	87.7	772
111P	"	88.4	807
112P	"	88.9	869
113P	240	85.5	634
114P	"	86.7	696
115P	"	90.0	979
116P	"	90.9	1041

TABLE 19

PROPERTIES OF Fe-3.5% Ni ALLOY COMPACTSMADE FROM BLENDED POWDERSCOMPOSITION:- Fe - 3.5  $\pm$ 0.05% Ni - 0.35  $\pm$ 0.05% C

S. No.	Period of Sintering (min)	Sintered Density (%)	Modulus of Rupture (N/mm <sup>2</sup> )
301B	30	86.5	703
302B	"	86.6	690
303B	"	89.0	866
304B	"	89.4	910
305B	"	90.0	1020
306B	"	90.8	1041
307B	60	88.0	752
308B	"	88.3	862
309B	"	88.8	869
310B	"	92.2	1062
311B	120	89.4	896
312B	"	89.0	917
313B	"	92.6	1145
314B	"	92.5	1103
315B	"	91.0	1055
316B	"	92.7	1165
317B	240	89.7	979
318B	"	89.5	965
319B	"	91.2	1083
320B	"	91.7	1062
321B	"	92.7	1186
322B	"	92.5	1151

TABLE 20

## PROPERTIES OF 3.00% Ni ALLOY COMPACTS

## MADE FROM PLATED POWDERS

COMPOSITION:- Fe - 3.00  $\pm$ 0.15% Ni - 0.35  $\pm$ 0.05% C

S. No.	Period of Sintering (min)	Sintered Density (%)	Modulus of Rupture (N/mm <sup>2</sup> )
301P	30	85.0	552
302P	"	86.5	655
303P	"	87.0	655
304P	"	87.3	641
305P	"	88.0	724
306P	60	86.2	696
307P	"	87.1	730
308P	"	88.0	800
309P	"	89.0	862
310P	"	88.1	896
311P	120	85.6	779
312P	"	86.0	752
313P	"	86.5	841
314P	"	86.9	883
315P	"	87.6	889
316P	"	88.7	948
317P	240	85.6	730
318P	"	86.9	800
319P	"	87.6	869
320P	"	87.8	896
321P	"	88.8	952
322P	"	89.0	958

TABLE 21      PROPERTIES OF Fe-4.25% Ni ALLOY COMPACTS

MADE FROM BLENDED POWDERS

COMPOSITION:- Fe - 4.25  $\pm$ 0.05% Ni - 0.38  $\pm$ 0.05% C

S. No.	Period of Sintering (min)	Sintered Density (%)	Modulus of Rupture (N/mm <sup>2</sup> )
401 B	30	86.9	758
402 B	"	86.9	758
403 B	"	89.7	938
404 B	"	90.0	958
405 B	"	91.4	1055
406 B	"	91.3	1076
407 B	60	87.9	876
408 B	"	88.1	862
409 B	"	89.9	993
410 B	"	90.5	1014
411 B	"	91.0	1083
412 B	"	91.8	1117
413 B	120	89.2	1007
414 B	"	90.6	1110
415 B	"	90.7	1069
416 B	"	91.5	1186
417 B	"	92.0	1165
418 B	240	88.7	958
419 B	"	89.0	952
420 B	"	91.0	1131
421 B	"	91.1	1103
422 B	"	92.0	1207
423 B	"	92.4	1241

TABLE 22      PROPERTIES OF Fe-4.0% Ni ALLOY COMPACTS  
MADE FROM PLATED POWDERS

COMPOSITIONS:- Fe - 4.0  $\pm$  0.1% Ni - 0.35 + 0.05% C

S. No.	Period of Sintering (min)	Sintered Density (%)	Modulus of Rupture (N/mm <sup>2</sup> )
401P	30	85.3	634
402P	"	86.5	710
403P	"	87.5	821
404P	60	88.0	883
405P	120	89.0	965
406P	"	89.4	993
407P	240	89.0	1007
408P	"	90.0	1083

TABLE 23 OBSERVED AND CALCULATED VALUES OF MODULUS OF RUPTURE OF 4.25% NICKEL

COMPACTS MADE FROM PLATED POWDERS

S.No	Period of Sintering (min)	Sintered Density %	Modulus of Rupture N/mm <sup>2</sup>		Δ Modulus of Rupture Obs. - Calc.
			Observed	Calculated	
401P	30	85.3	634	697	-63
402P	30	86.5	710	783	-73
403P	30	87.5	821	854	-33
404P	60	88.0	883	899	-16
405P	120	89.0	965	980	-15
406P	120	89.4	993	1 009	-16
407P	240	89.0	1 007	985	+22
408P	240	90.0	1 083	1 057	+26

TABLE 24 - PLATING CELL DATA

	LABORATORY SCALE	INDUSTRIAL SCALE
1. Cell diameter (cm)	15.25	76.25
2. Cell height (cm)	40.54	40.54
3. Fluidised bed height (cm)	10.79	10.79
4. Working volume (cm <sup>3</sup> )	1910.84	49271.0
5. Weight of powder (kg)	1.0	25.0
6. Volume of solution (litres)	1.6	40.0
7. Cathodic surface area (dm <sup>2</sup> )	2.34	11.71
8. Anode surface area (dm <sup>2</sup> )	1.34	6.70
9. Current density (A/dm <sup>2</sup> )	17.65	17.65
10. Cell resistance (ohms)	0.23	0.23
11. Amperes required (amps)	41.33	203.68
12. Voltage required (volts)	9.5	47.53
13. Rectifier output	12 V-250 A	60 V-2000A
14. Rate of plating (wt%Ni/min)	0.1312	0.1312
15. Time required for 3% Ni (min)	23.0	23.0
16. Membrane surface area (cm <sup>2</sup> )	182.1	4561.5
17. Gas flow rate (litres/min)	30.0	751.9

FIGURES AND DIAGRAMS

**Fig. 1** Relationship Between Anodic Current and Potential for Metals which Exhibit the Passivity Phenomenon(11).

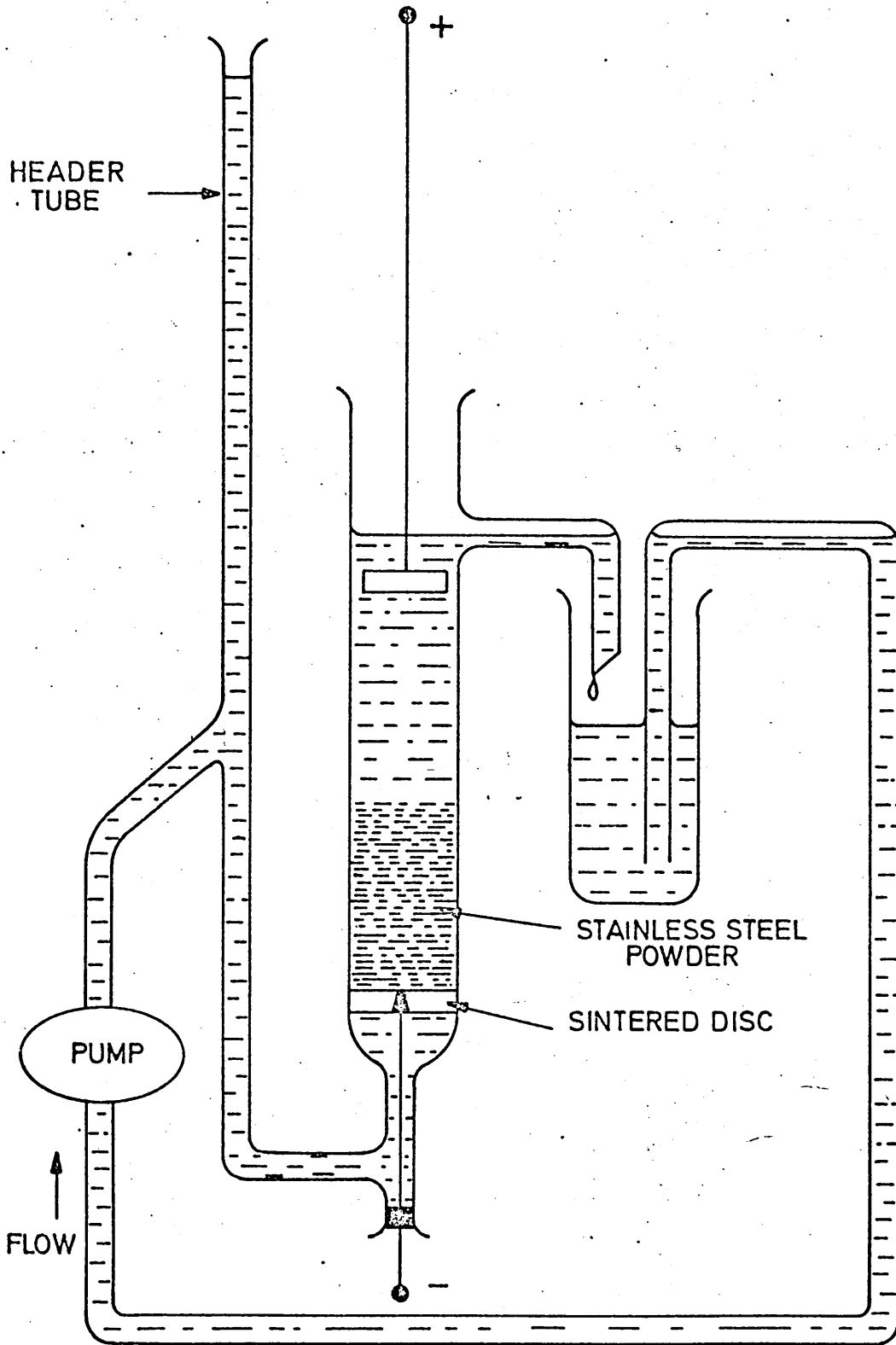
**Fig. 2a** Ionic Conduction together with Short Circuiting of Conduction Paths through the Particles(49).

**Fig. 2b** Electronic Charge Conduction through Particles in Contact.

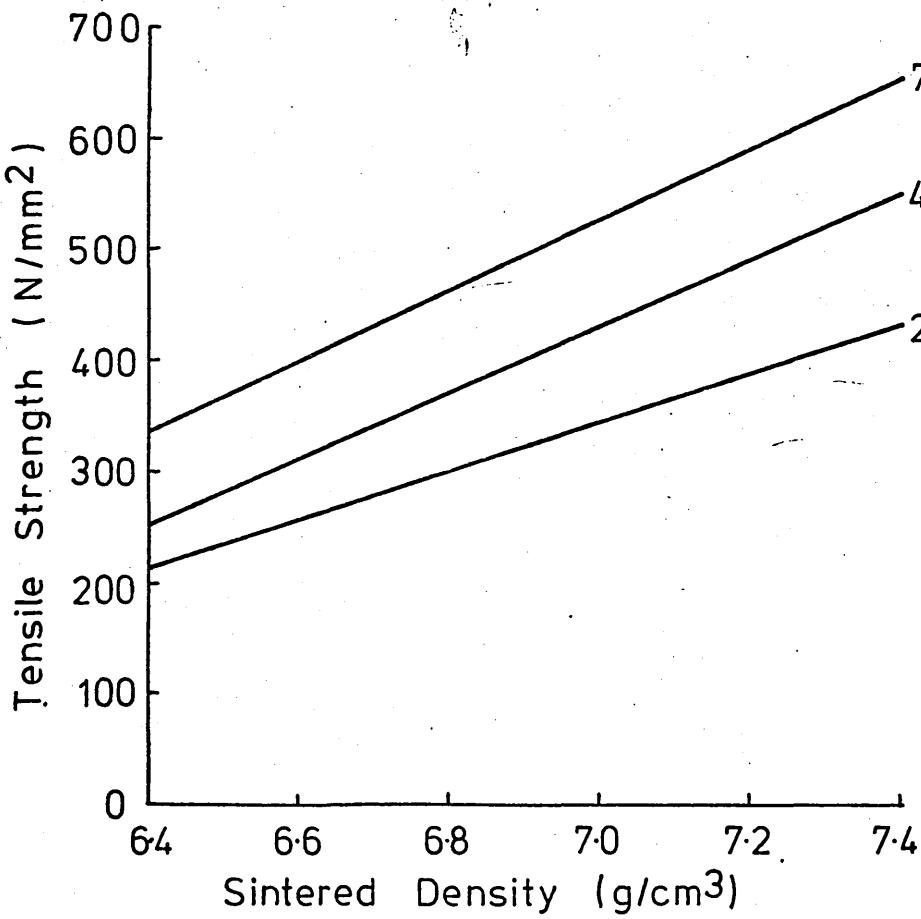
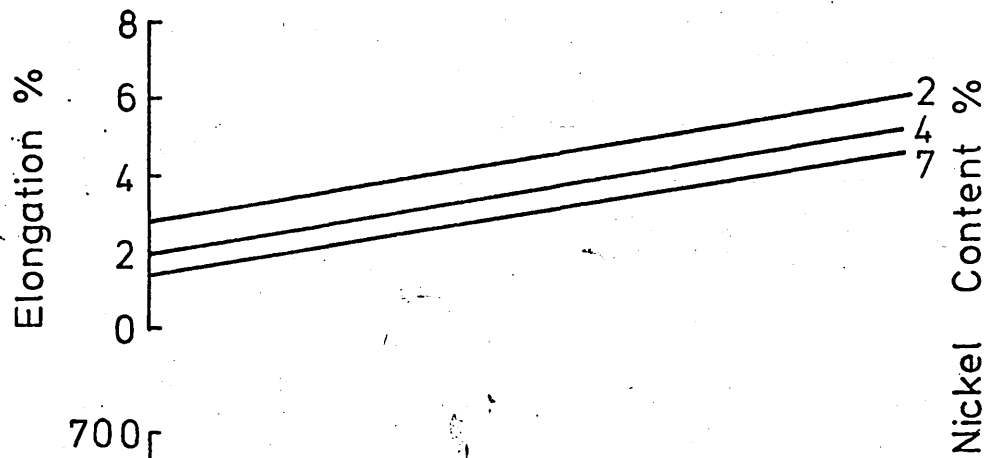
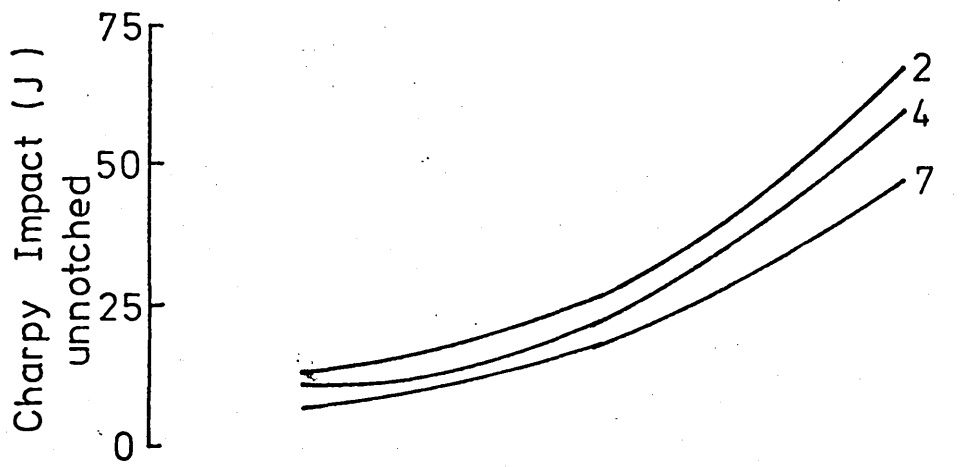
**Fig. 2c** 'Conductive' Charge Conduction Mechanism.



Fig. 3      Apparatus for Plating a Fluidized Bed  
              of Powder (62).



**Fig. 4** Relationship Between Density and Mechanical Properties of Sintered Iron-Nickel Steels Containing 0.3 - 0.6% Carbon (192).



**Fig. 5**      **Tensile Strength as a Function of Total  
Porosity for Sintered Compacts Pressed at  
Different Pressures (203).**

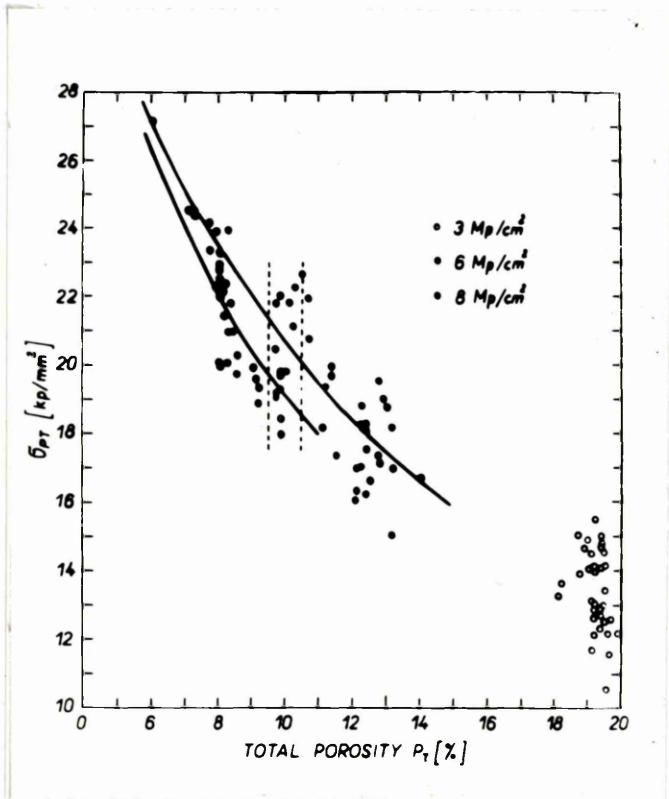


**Fig. 6a** Design of Plating Cell Utilising a Porous Refractory Membrane.

**Key to Fig. 6a**

1. Perspex Tube (15.25 cm  $\Phi$ ).
2. Electrolytic Nickel Sheet Anode Shaped in a Tubular Form.
3. Porous Refractory Tube (6.35 cm  $\Phi$ ).
4. Stainless Steel Cathode Rods.
5. Plastic Fasteners.
6. Copper Flange Welded to a Copper Tube (7).
7. Copper Tube.
8. Gas Inlet Tube.
9. Fluidising Membrane, Vyon - D.
10. Silicone Rubber.
11. Perspex Flange attached to the Perspex Tube (1).
12. Stainless Steel Fasteners.
13. Copper Plate attached to Cathode Rods (4).

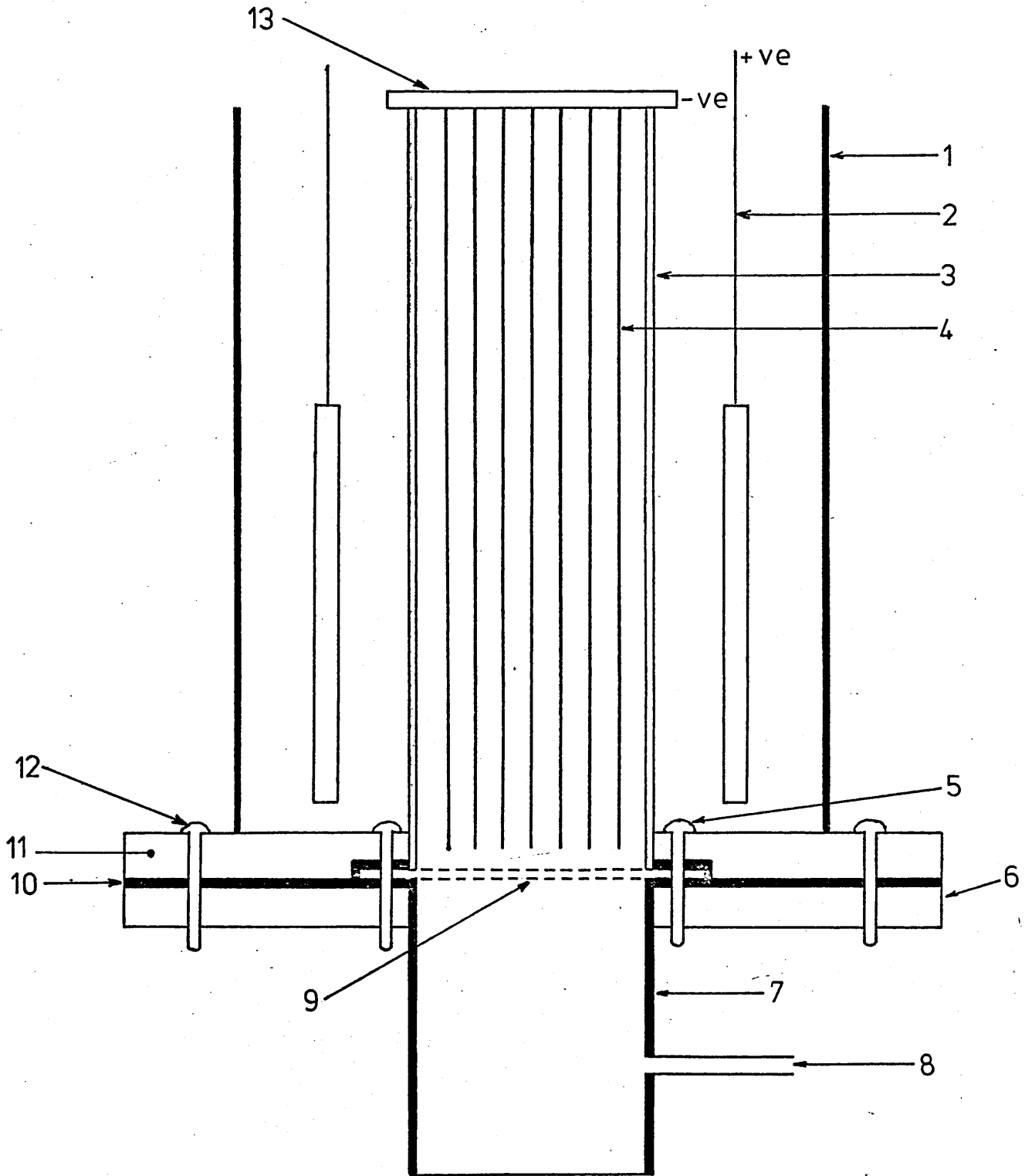
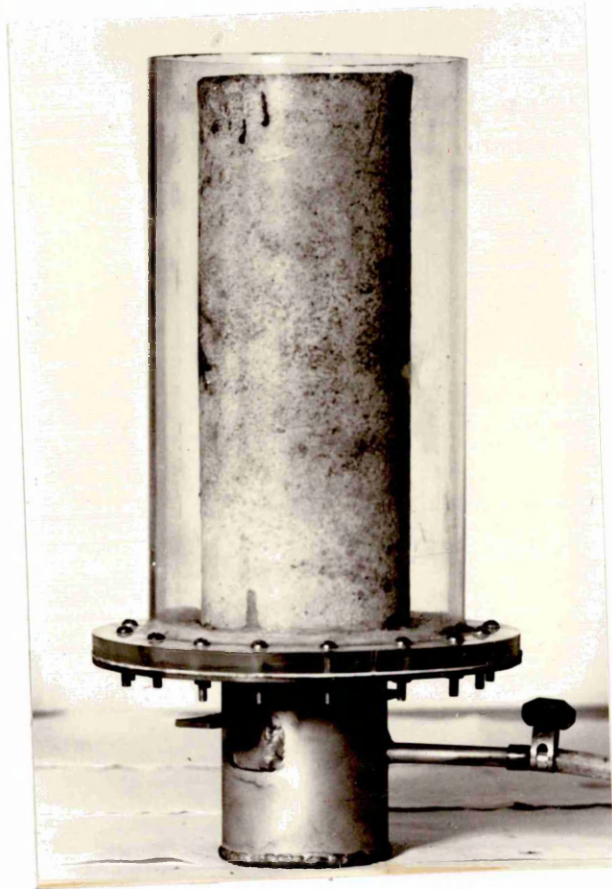


Fig. 6b Stage I Plating Cell Utilising a Porous Refractory Membrane.



**Fig. 7a**      **Design of Plating Cell Employing Fabric Anode Bags.**

**Key to Fig. 7a.**

1.    Perspex Tube (15.25 cm  $\Phi$  ).
2.    Perspex Flanges.
3.    O-ring.
4.    Fluidising Membrane Vyon - D.
5.    Gas Inlet Tube.
6.    Stainless Steel Fasteners.
7.    Silicone Rubber.
8.    Stainless Steel Cathode Rods.
9.    Fabric Anode Bags Containing Nickel Shots.
10.   Pure Nickel Conducting Rod.
11.   Copper Plate Attached to Cathode Rods (8).
12.   Perspex Holder for Anode Assembly.

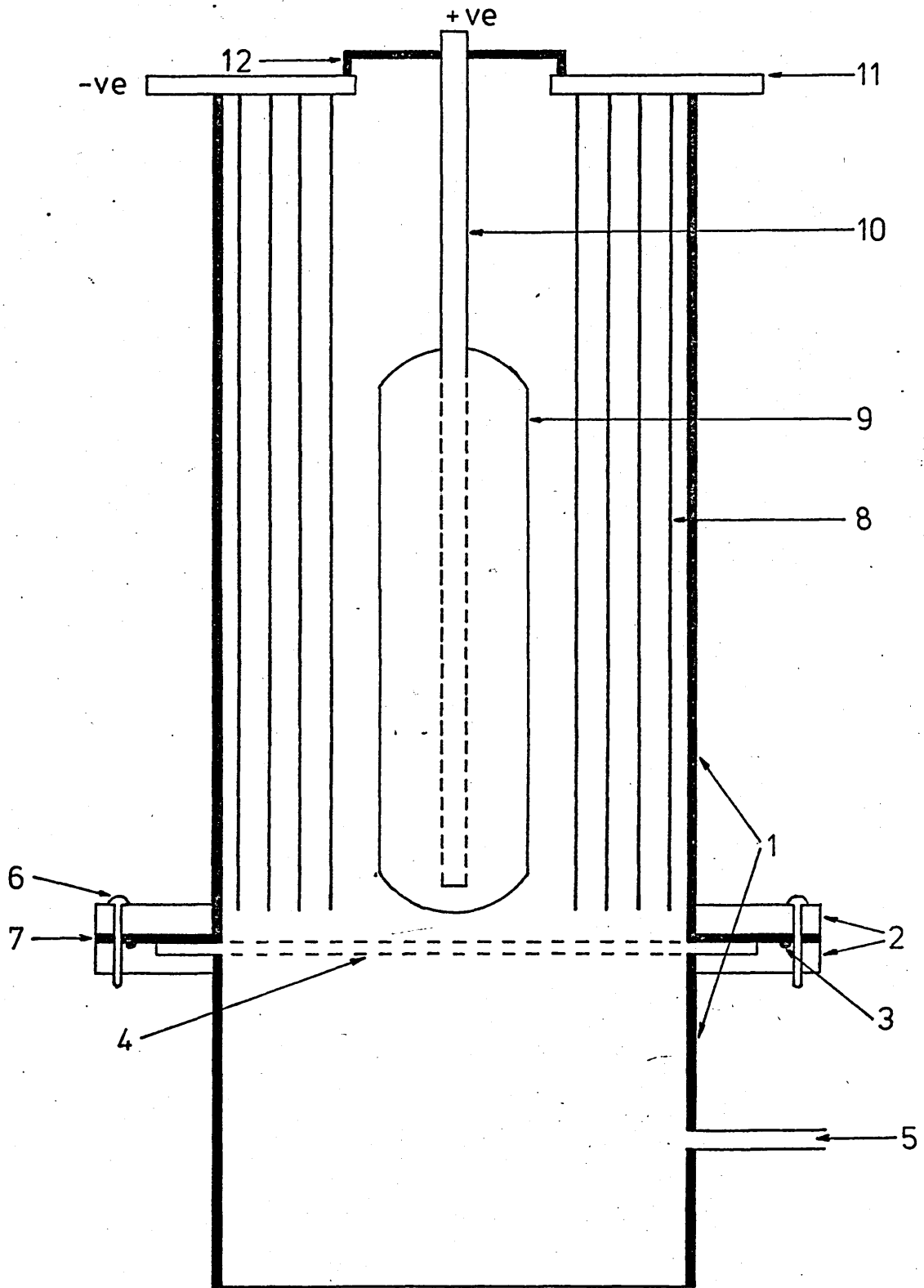


**Fig. 7b** Stage II Plating Cell Employing Fabric Anode Bags.

1. Plating Cell.
2. Water Bath.
3. Gas Flowmeter.
4. Power Service.

**Fig. 8** Stage II Plating Cell made from QVF Glass Columns.

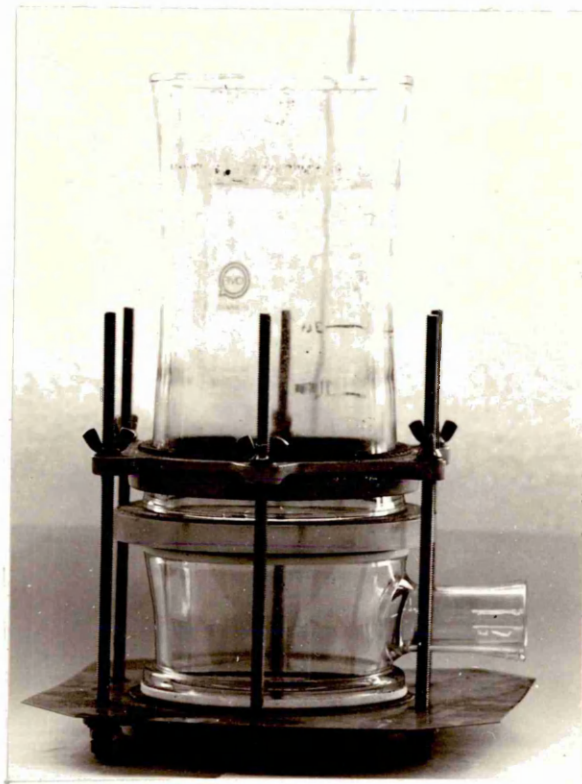
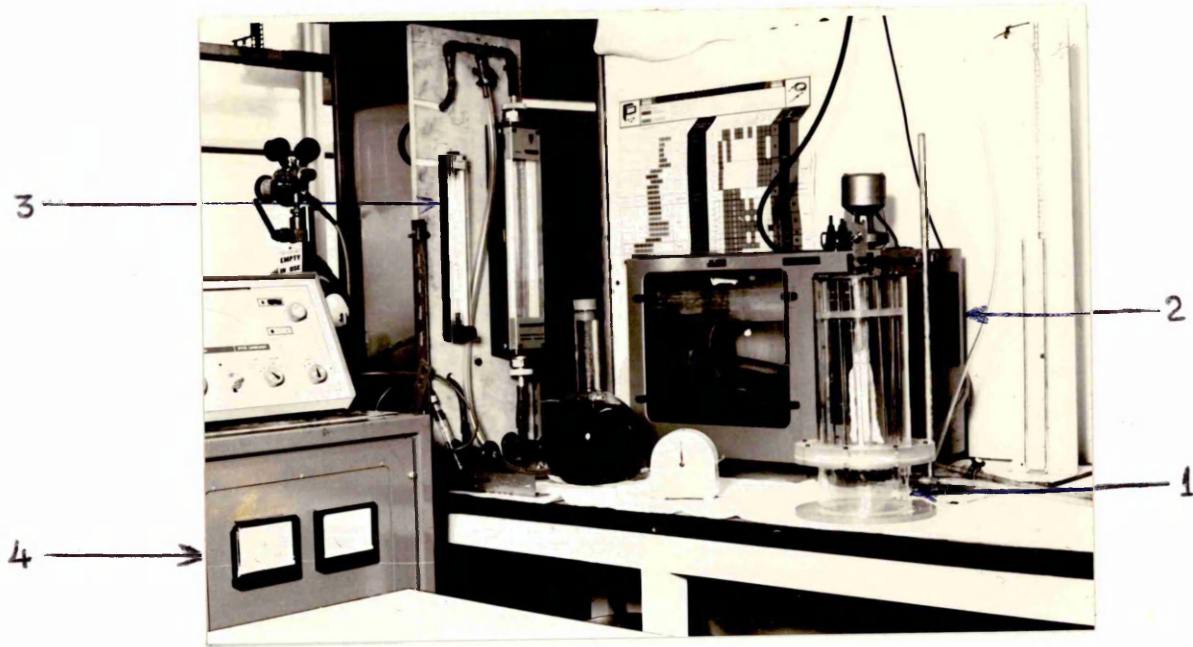


**Fig. 9** Anode Assembly Consisting of Nickel Shots  
Contained in 100% Triacetate Fabric Bag.

**Fig. 10** Cathode Assembly Consisting of Stainless  
Steel Rods attached to a Copper Plate.

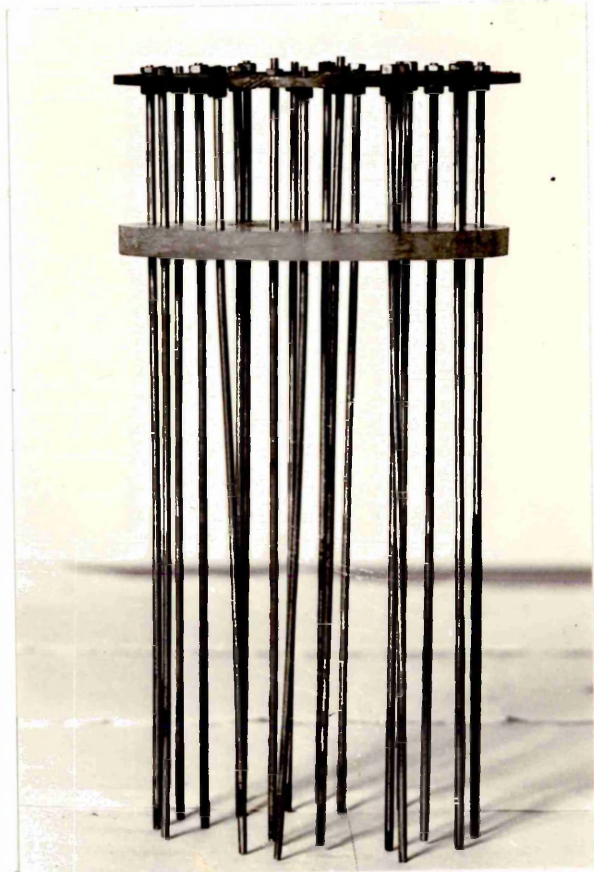
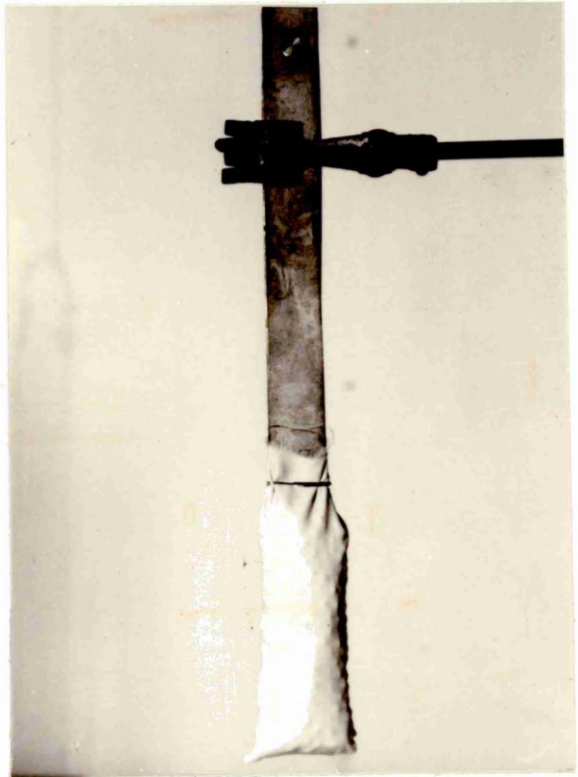
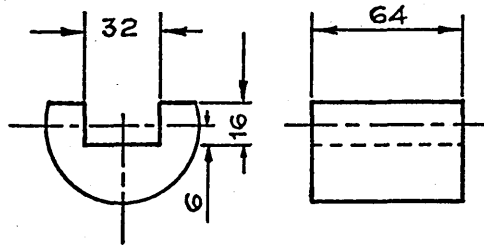
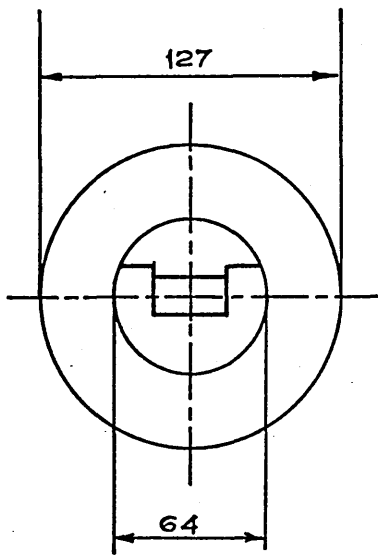
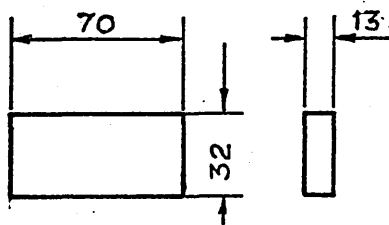
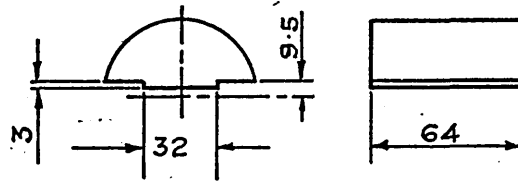


**Fig. 11** Details of Die and Punches for making  
Modulus of Rupture Test Specimens  
(MPIF - 13-62).

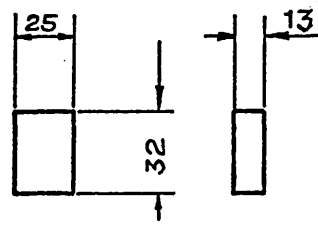
All dimensions are in mm.



DIE INSERTS



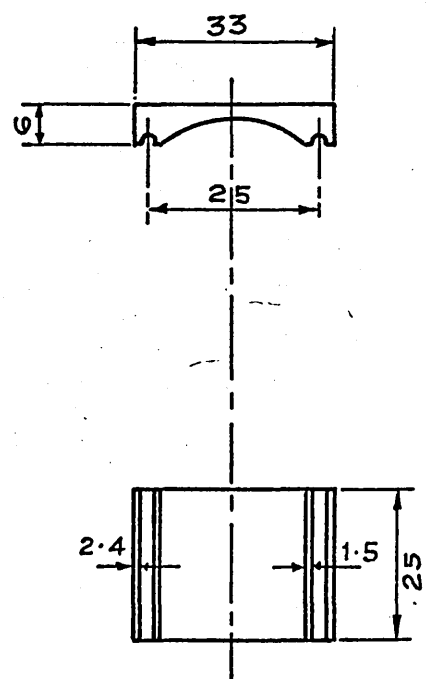
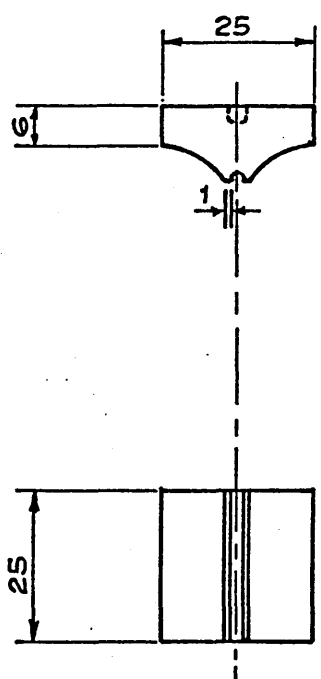
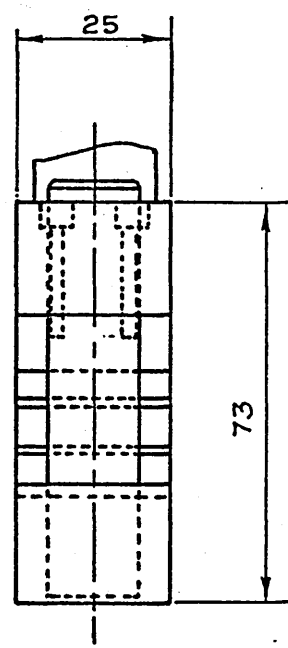
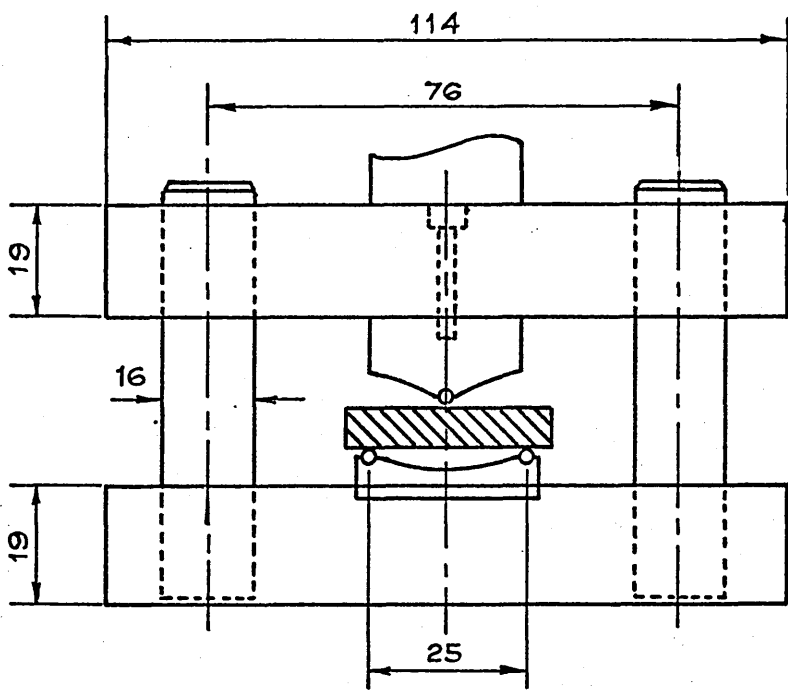
UPPER PUNCH



LOWER PUNCH

Fig. 12 Details of Testing Equipment for the  
Determination of Modulus of Rupture.  
(MPIF - 13-62).

All dimensions are in mm.



  
 3 mm  
 DRILL ROD

Figs 13 to 15 Relationship Between (i) Cell Current and Plating Time and (ii) Cell Potential and Plating Time for Experiments Carried Out in the Refractory Membrane Cell.

----- Cell potential  
———— Cell current

Fig. 13 Experiment M<sub>I</sub> (Table 7)

Fig. 14 Experiment M<sub>II</sub> (Table 7)

Fig. 15 Experiment M<sub>III</sub> (Table 7)

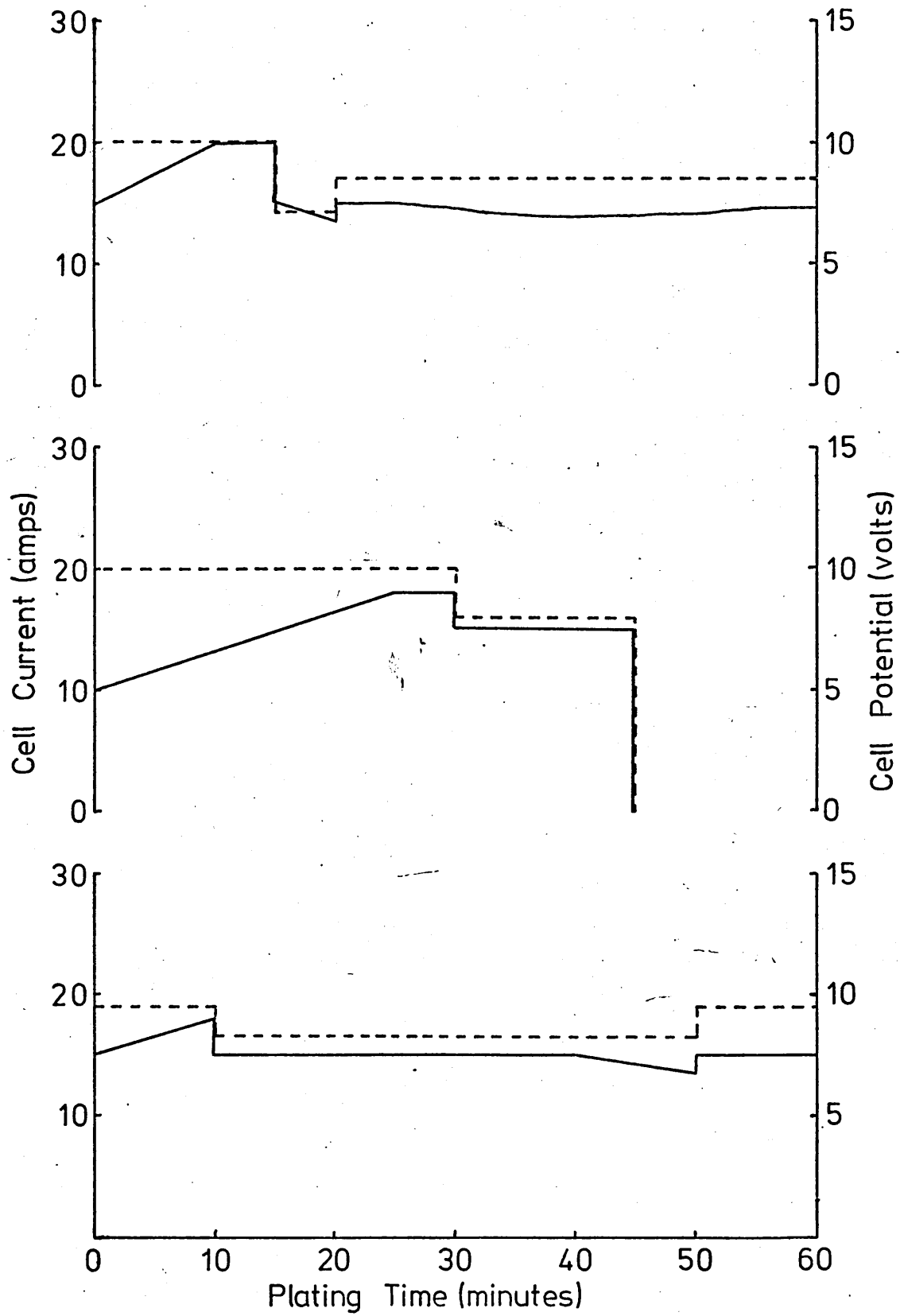
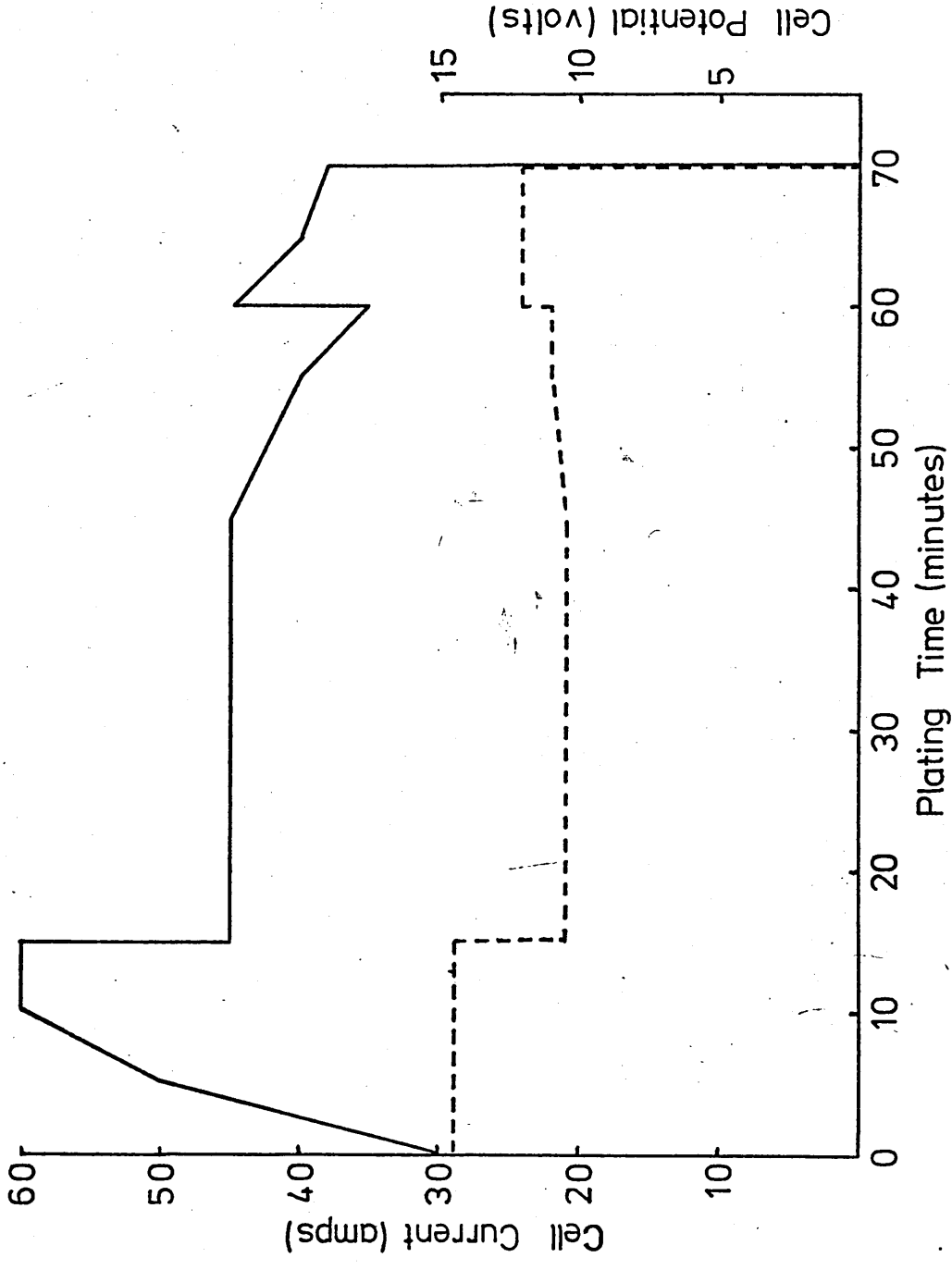


Fig. 16 Relationship Between (i) Cell Current and Plating Time and (ii) Cell Potential and Plating Time for Experiment Carried out in a Cell Employing 100% Triacetate Anode Bags (Experiment No. N<sub>I</sub>, Table 8).

----- Cell Potential

———— Cell Current

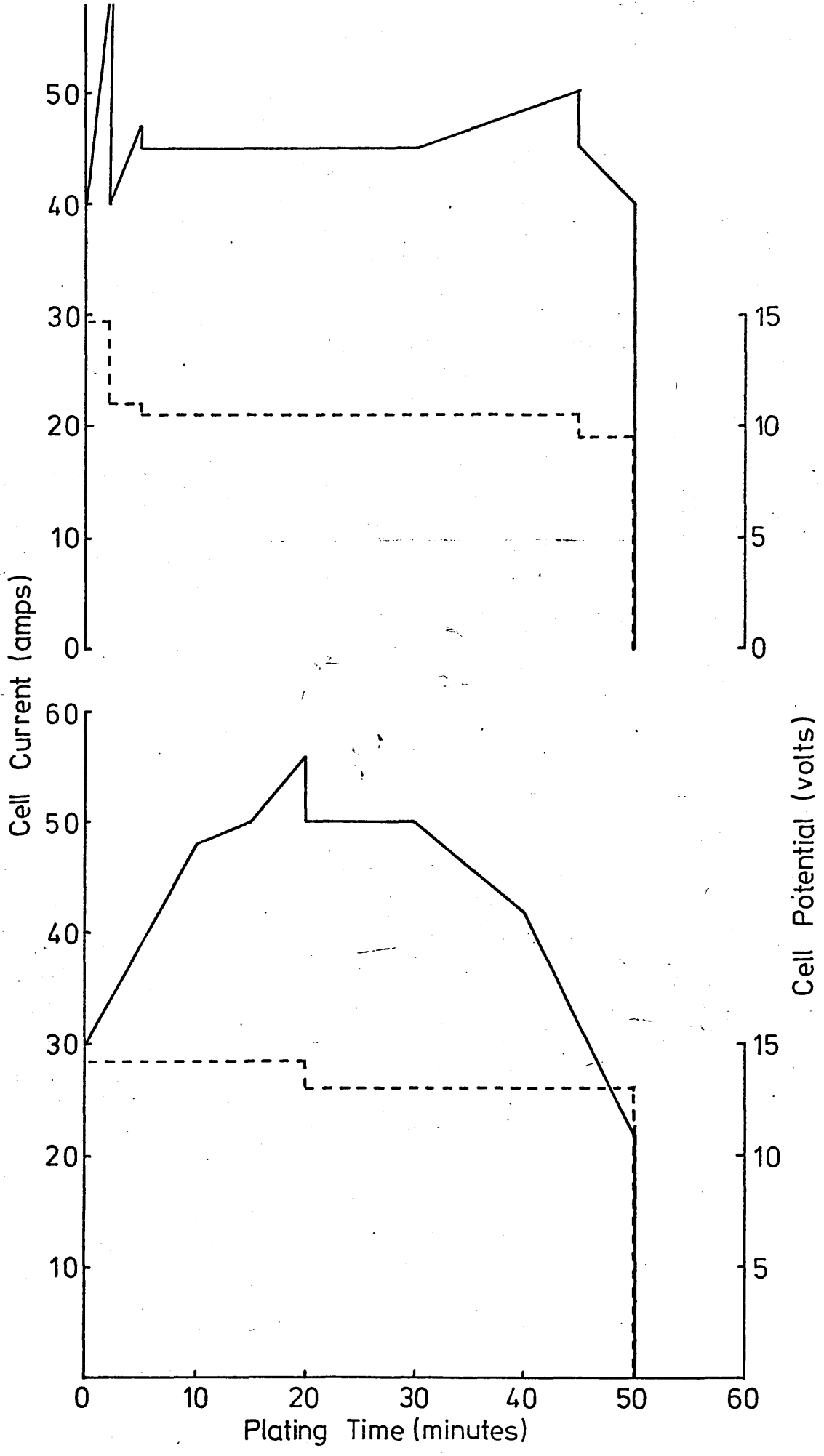


Figs. 17 & 18 Relationship Between (i) Cell Current and Plating Time and (ii) Cell Potential and Plating Time for Experiments Carried Out in a Cell Employing 100% Triacetate Anode Bags.

----- Cell Potential  
——— Cell Current

Fig. 17 Experiment No. N<sub>II</sub> (Table 8)

Fig. 18 Experiment No. N<sub>III</sub> (Table 8)



Figs. 19 & 20 Relationship Between (i) Cell Current and Plating Time and (ii) Cell Potential and Plating Time for Experiments Carried Out in a Cell Employing 100% Triacetate Fabric Anode Bags.

----- Cell Potential  
——— Cell Current

Fig. 19 Experiment No. N<sub>IV</sub> (Table 8)

Fig. 20 Experiment No. N<sub>V</sub> (Table 8)

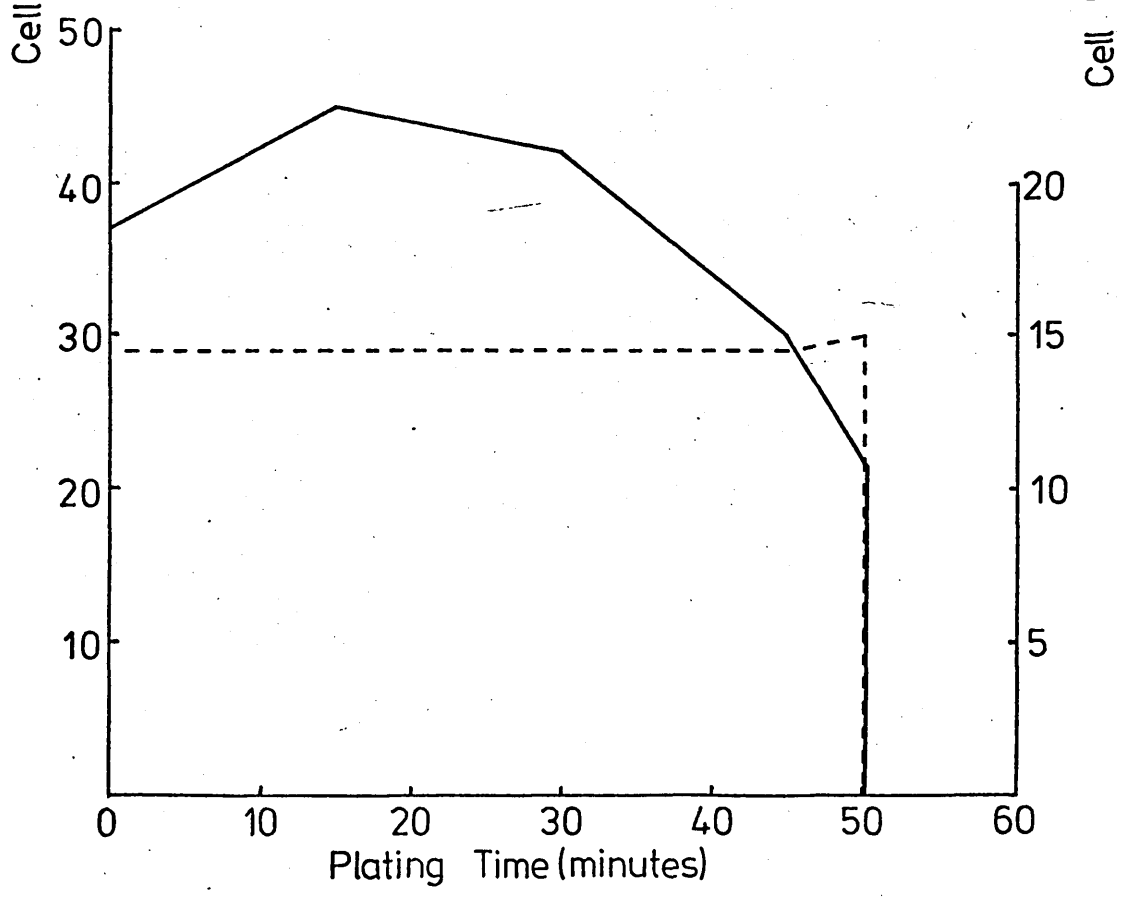
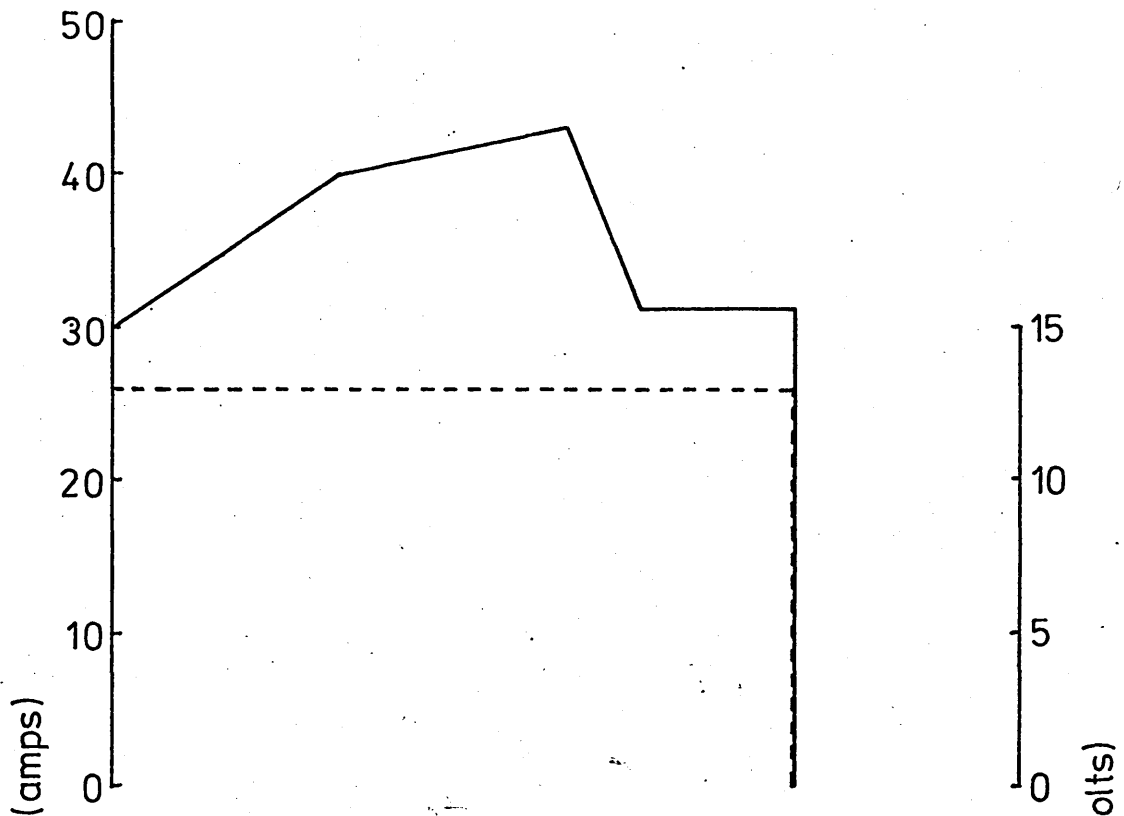


Fig. 21      Portion of 100% Triacetate Fabric Anode Bag  
Showing Dark Rings Formed by Iron Powder  
Particles that Covered the Nickel Shot.

Fig. 22      Relationship Between (i) Cell Current and  
Plating Time and (ii) Cell Potential and  
Plating Time for a Cell Utilising a Single  
Anode Bag made of Canvas Type Material.  
(Experiment No. N<sub>VI</sub>, Table 8).

----- Cell Potential  
———— Cell Current

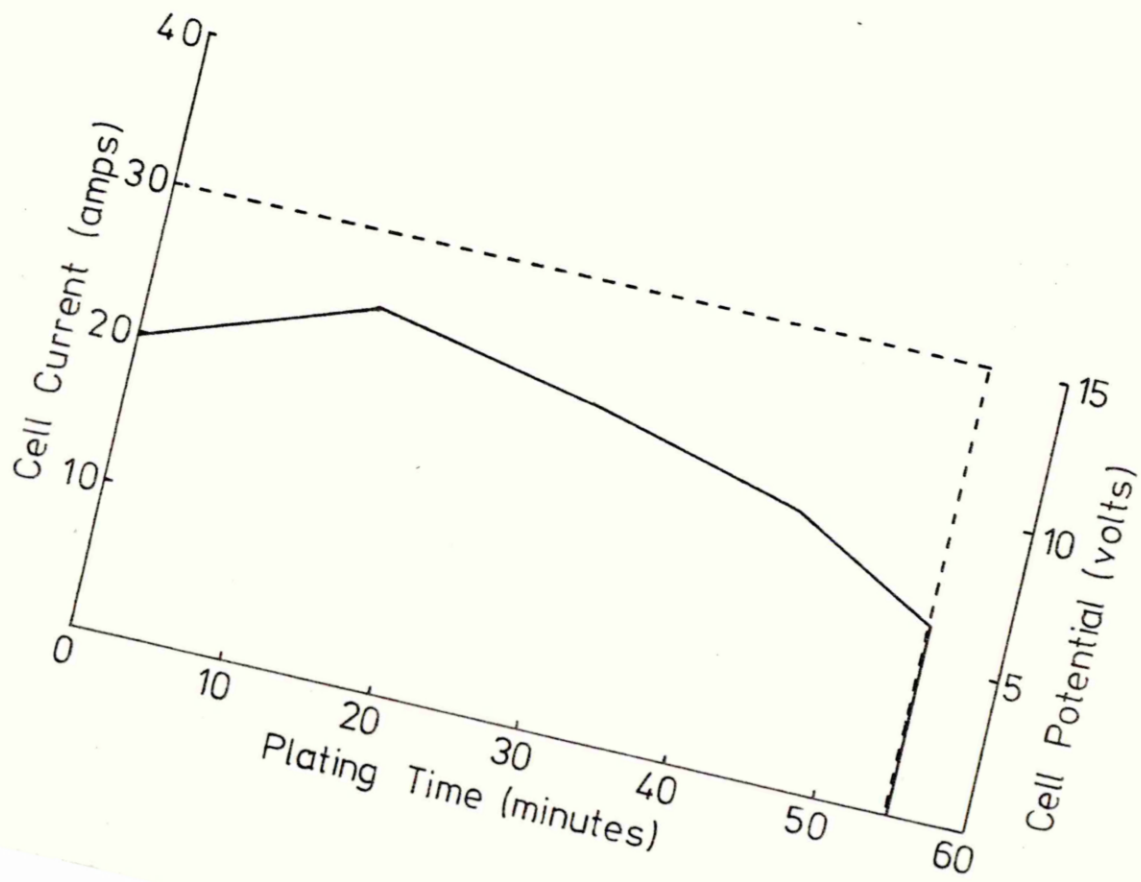
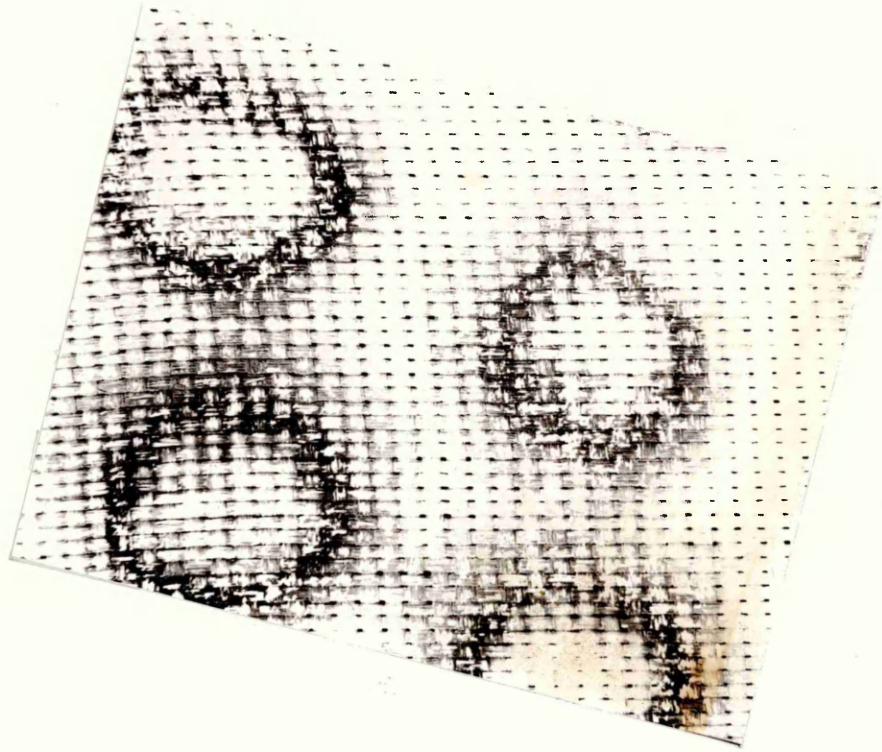


Fig. 23 Relationship Between (i) Cell Current and Plating Time and (ii) Cell Potential and Plating Time for a Cell Employing an Outer Anode Bag made of 65% Polyester 35% Cotton Fabric (Experiment No. N<sub>VII</sub>).

----- Cell Potential  
——— Cell Current

Fig. 24 Portion of 65% Polyester 35% Cotton Anode Bag Showing Nickel Deposition.

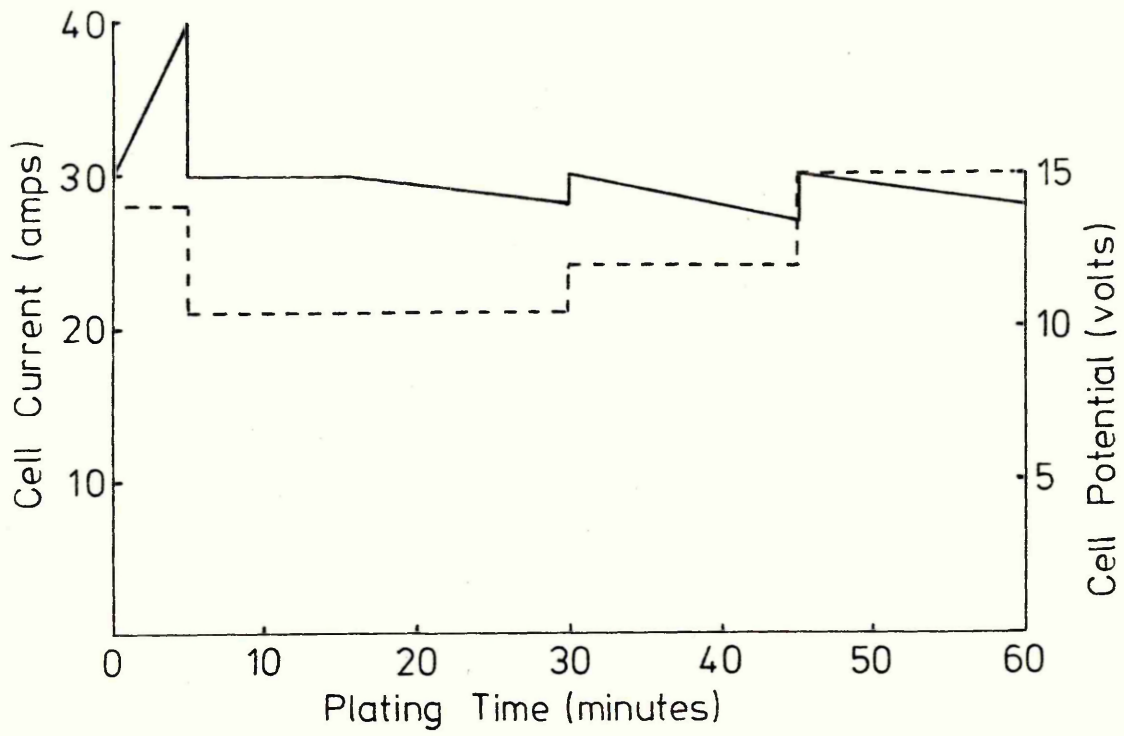


Fig. 25 Relationship Between (i) Cell Current and Plating Time and (ii) Cell Potential and Plating Time for a Cell Employing Both Anode Bags made of 65% Polyester 35% Cotton Fabric (Experiment No. N<sub>VIII</sub>, Table 8)

----- Cell Potential  
——— Cell Current

Fig. 26 Relationship Between (i) Cell Current and Plating Time and (ii) Cell Potential and Plating Time for Experiments Using S-Nickel Shot. (Experiment N<sub>IX</sub> Table 8).

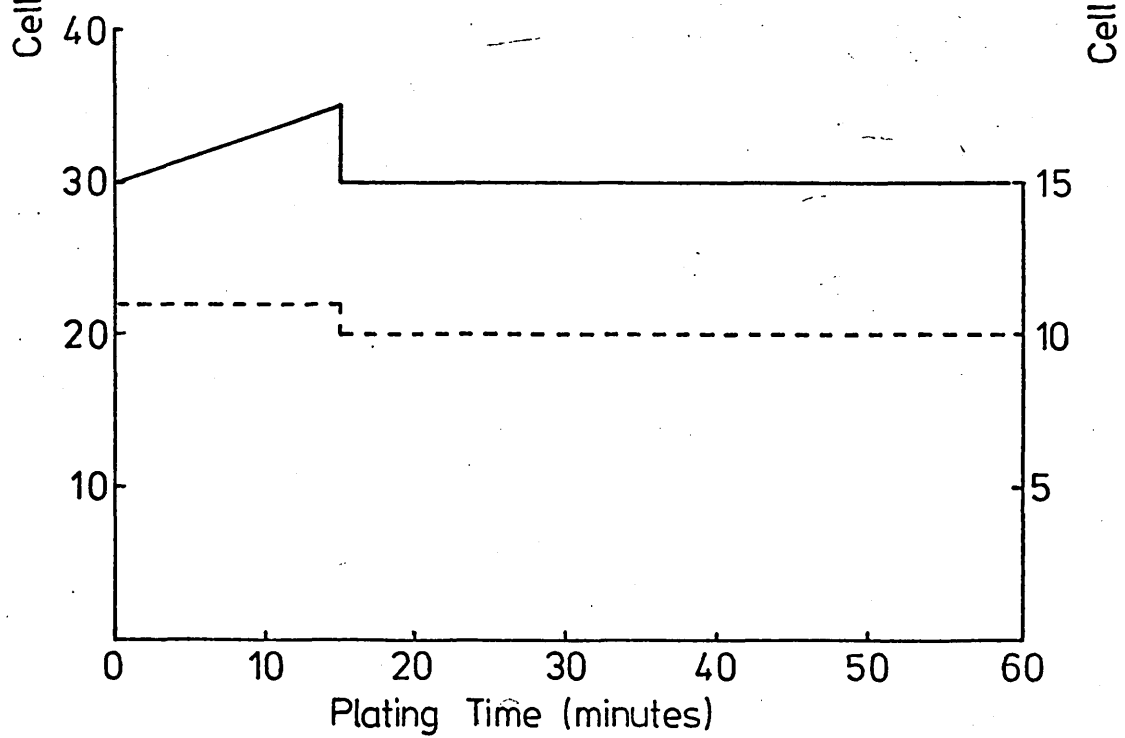
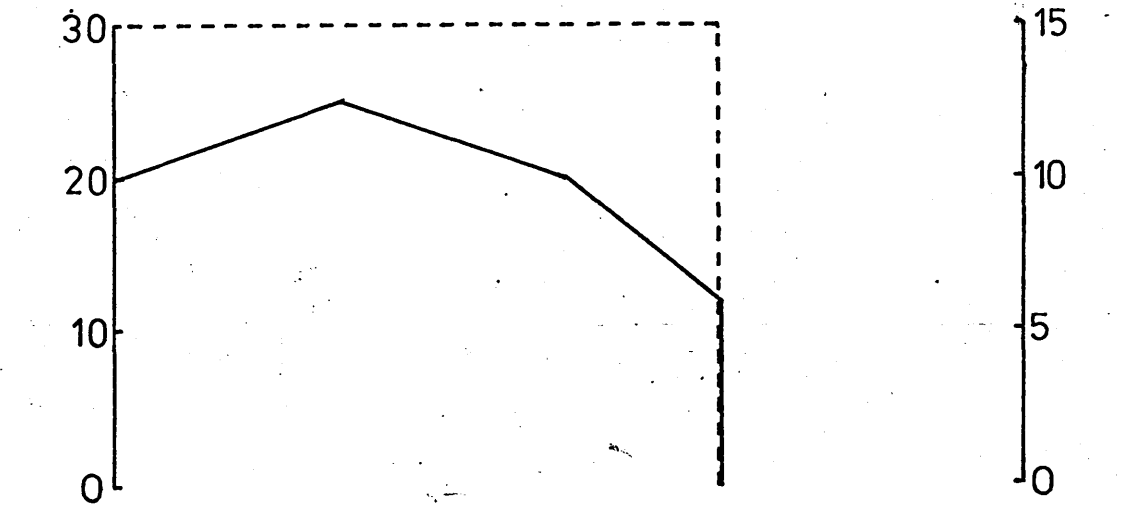


Fig. 27 Relationship Between (i) Cell Current and Plating Time and (ii) Cell Potential and Plating Time for the Cell that Contained no Iron Powder.  
(Experiment No. N<sub>XIII</sub>, Table 9).

----- Cell Potential  
——— Cell Current

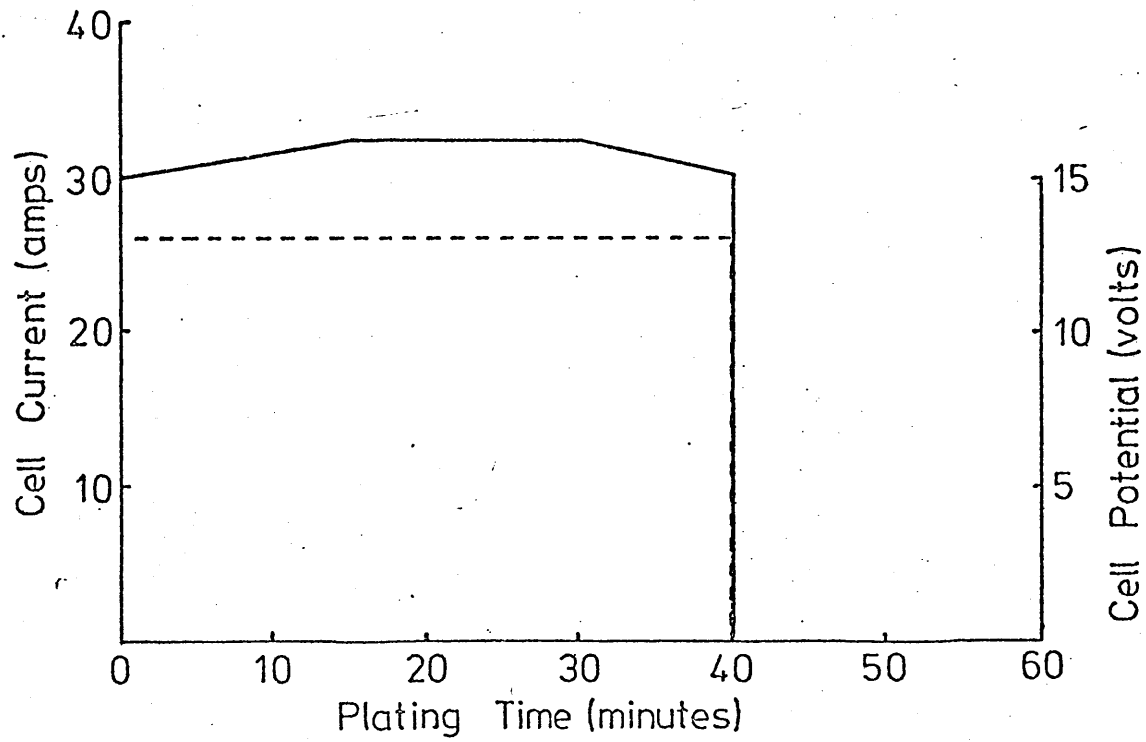
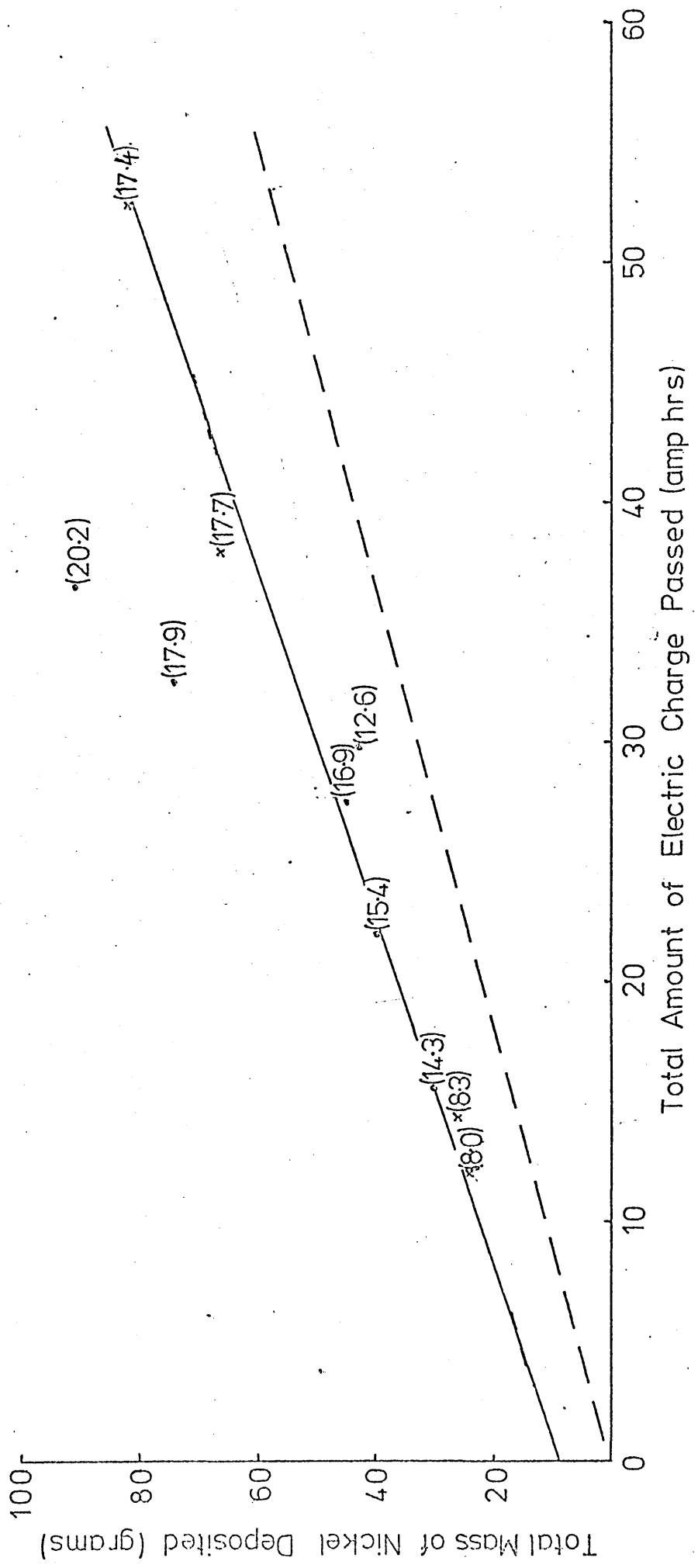


Fig. 28 Relationship Between Mass of Nickel Deposited and Total Amount of Electric Charge Passed.

Key

- x :- Cathode assembly comprising of 24 rods.
- :- " " " " 20 " .
- :- Maximum electrodepositon at 100% efficiency  
Figures in parentheses refer to current density (A/dm<sup>2</sup>).



**Fig. 29** Relationship Between Mass % Nickel Deposited  
and Plating Time at a Range of Current  
Densities.

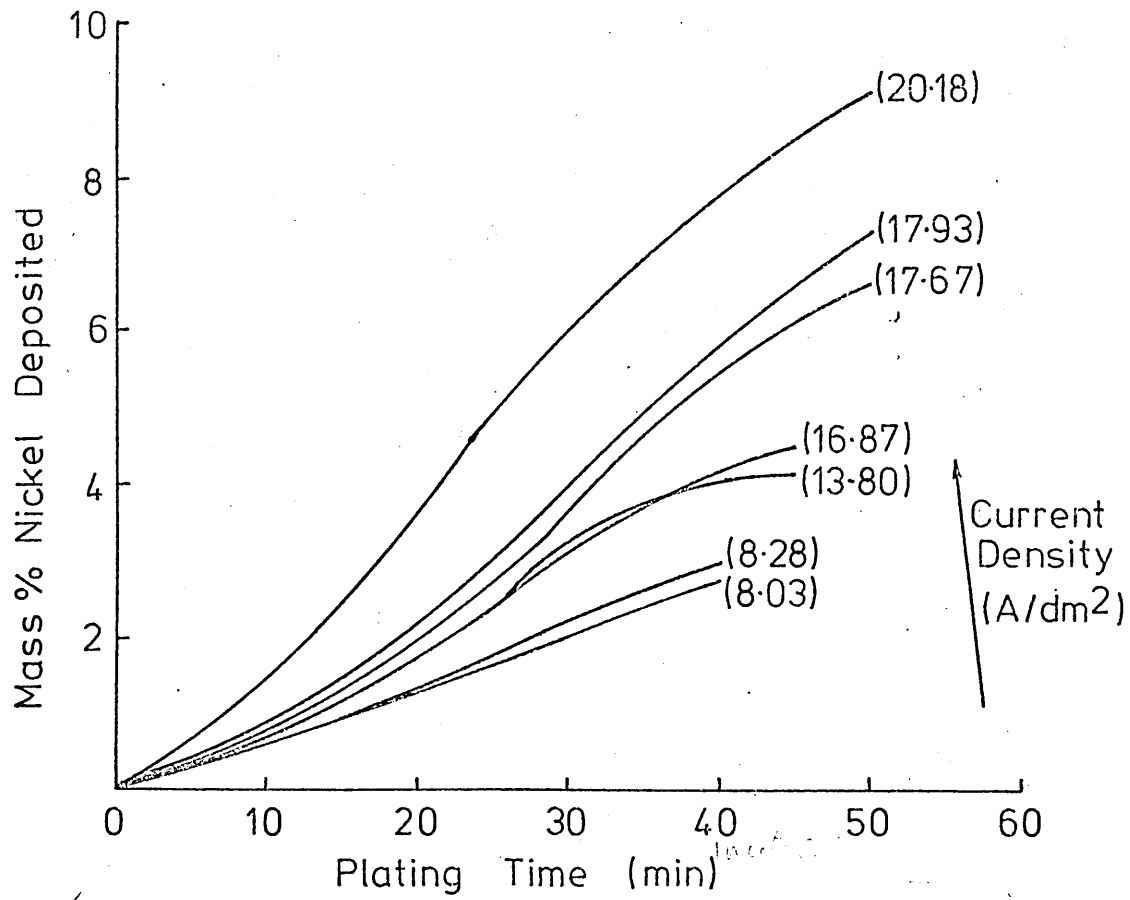


Fig. 30 Relationship Between Rate of Deposition of  
Nickel and Average Current Density Used.

x :- Cathode assembly comprising of 24 rods.

• :- " " " " 20 " .

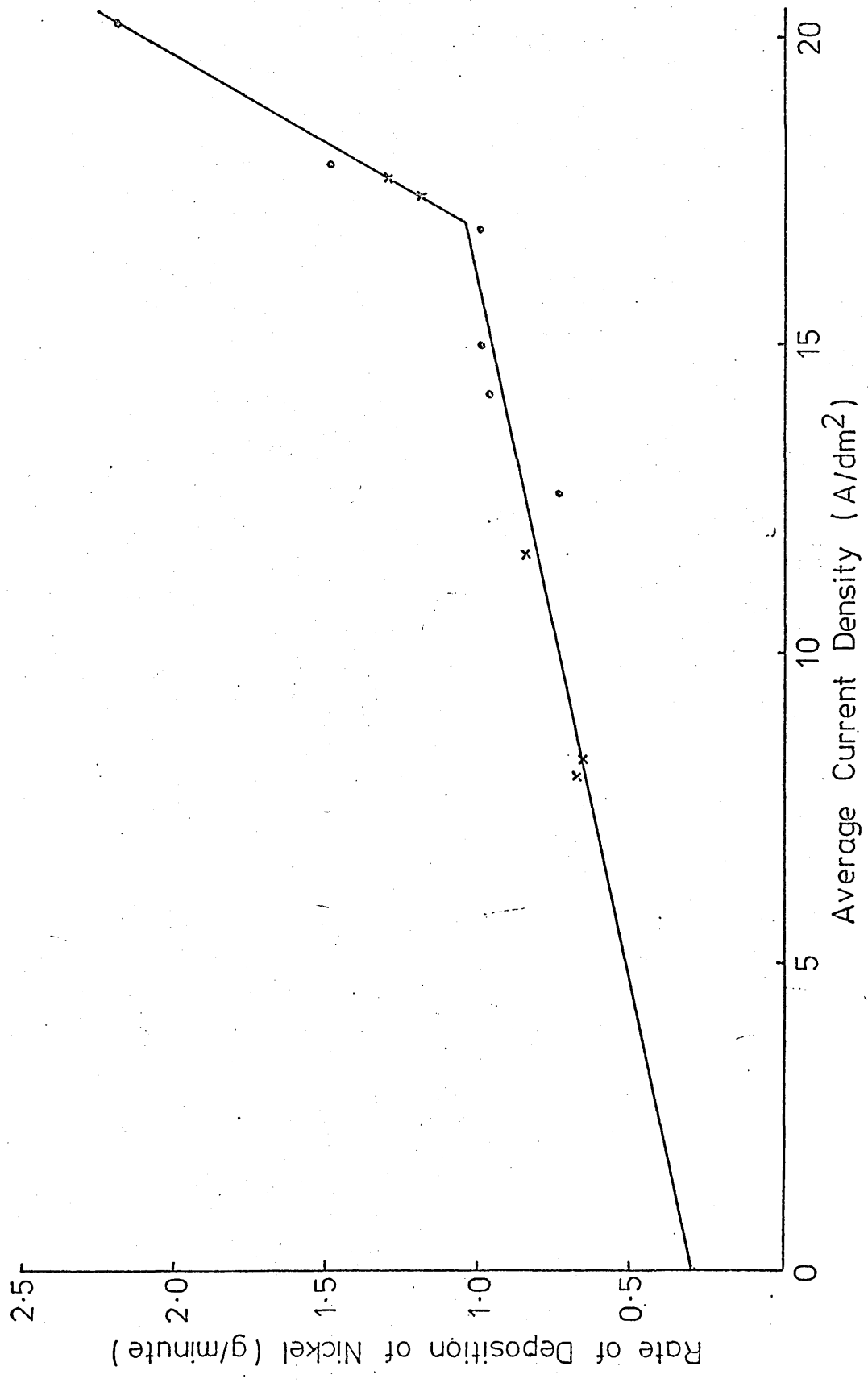


Fig. 31 Relationship Between Mass % Nickel Deposited and Plating Time at a Range of Solution Temperatures for Experiments Carried Out in the Absence of an Applied Potential.

	Average Temperatures ( $^{\circ}\text{C}$ )
1.	53
2.	48
3.	51
4.	50
5.	58
6.	63

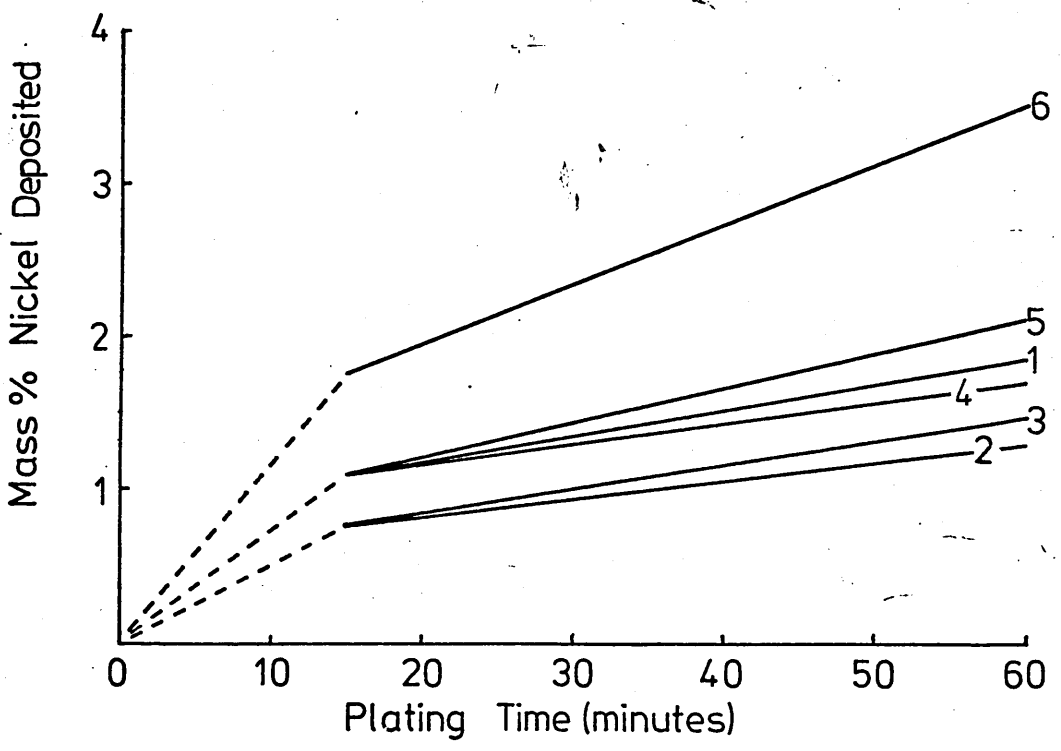
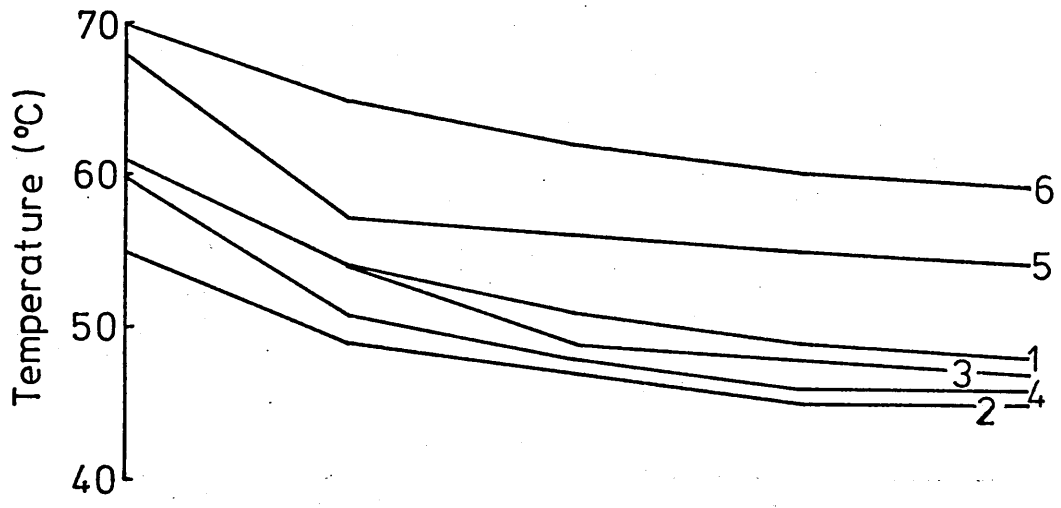
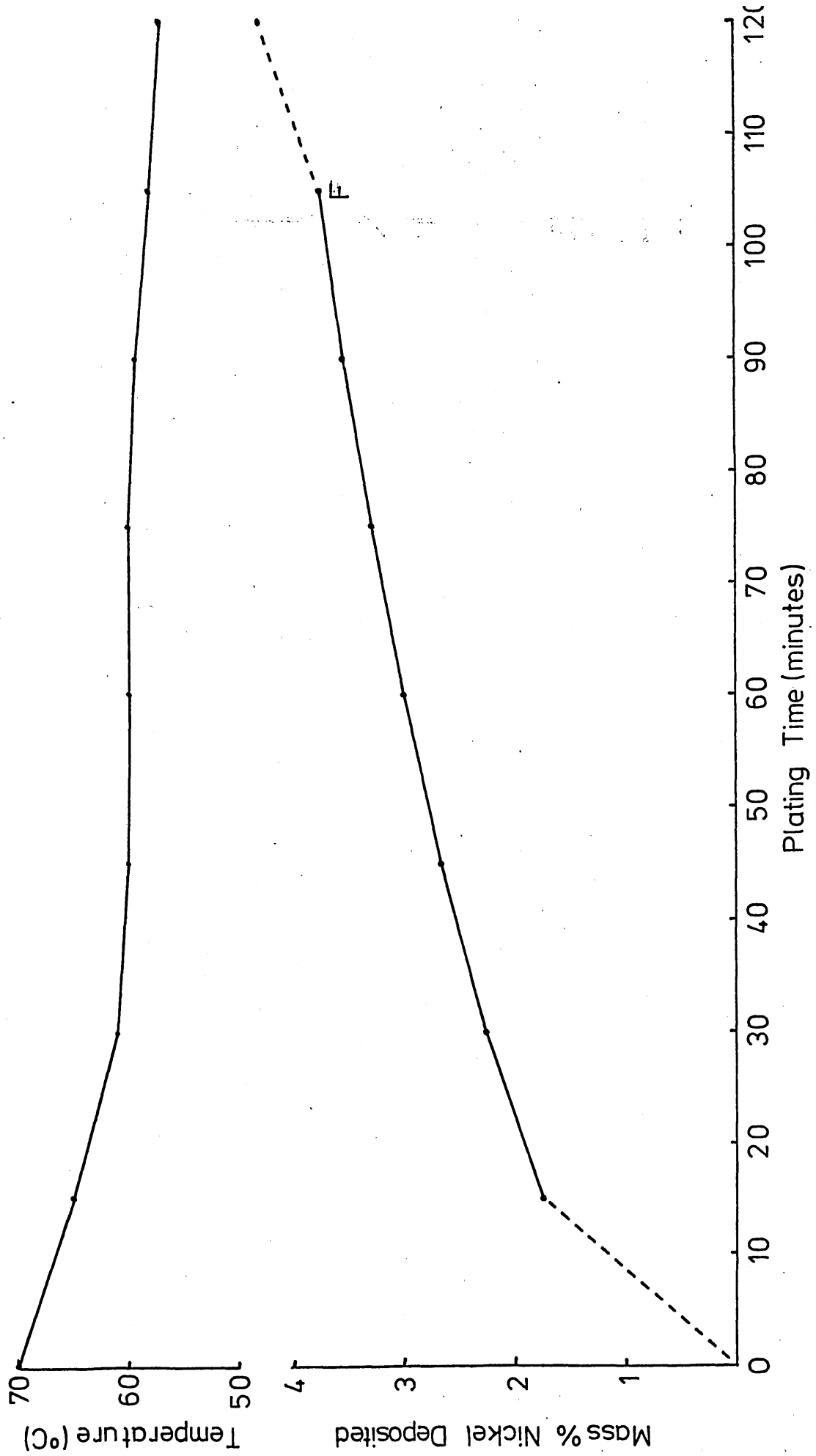


Fig. 32 Influence of Prolonged Period of Plating on  
the Deposition of Nickel on Iron Powders in  
the Absence of an Applied Potential.

F -0.25 litre of fresh solution added.



**Fig. 33**

**Influence of the Addition of Anti-Foam Agent  
on the Amount of Nickel Deposited on Iron  
Powders in the Absence of an Applied Potential.**

- 1. Experiment without the addition of anti-foam agent.**
- 2. Experiment with the addition of anti-foam agent.**

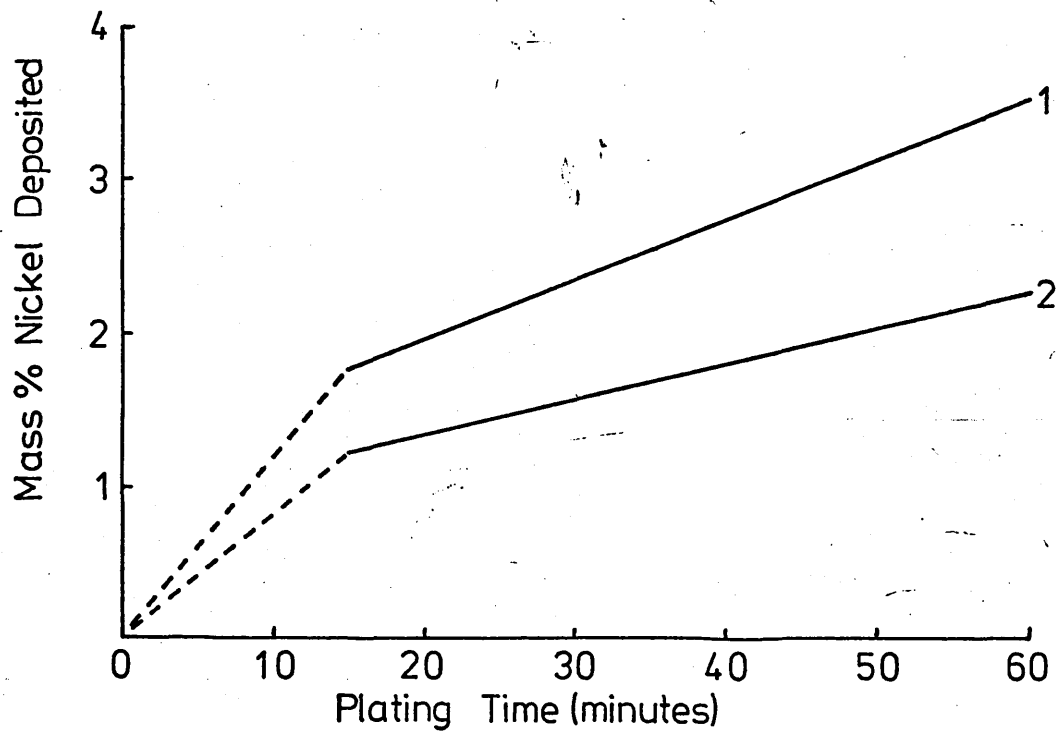
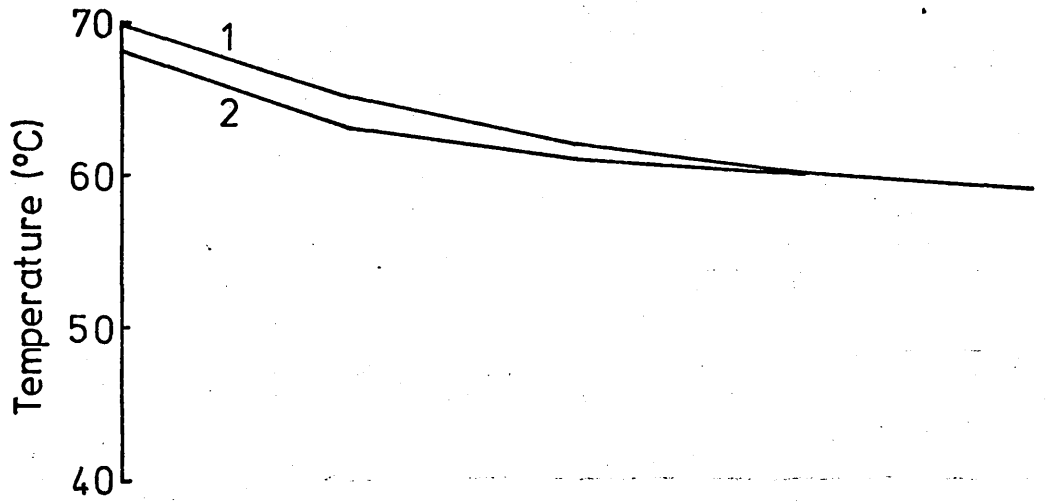
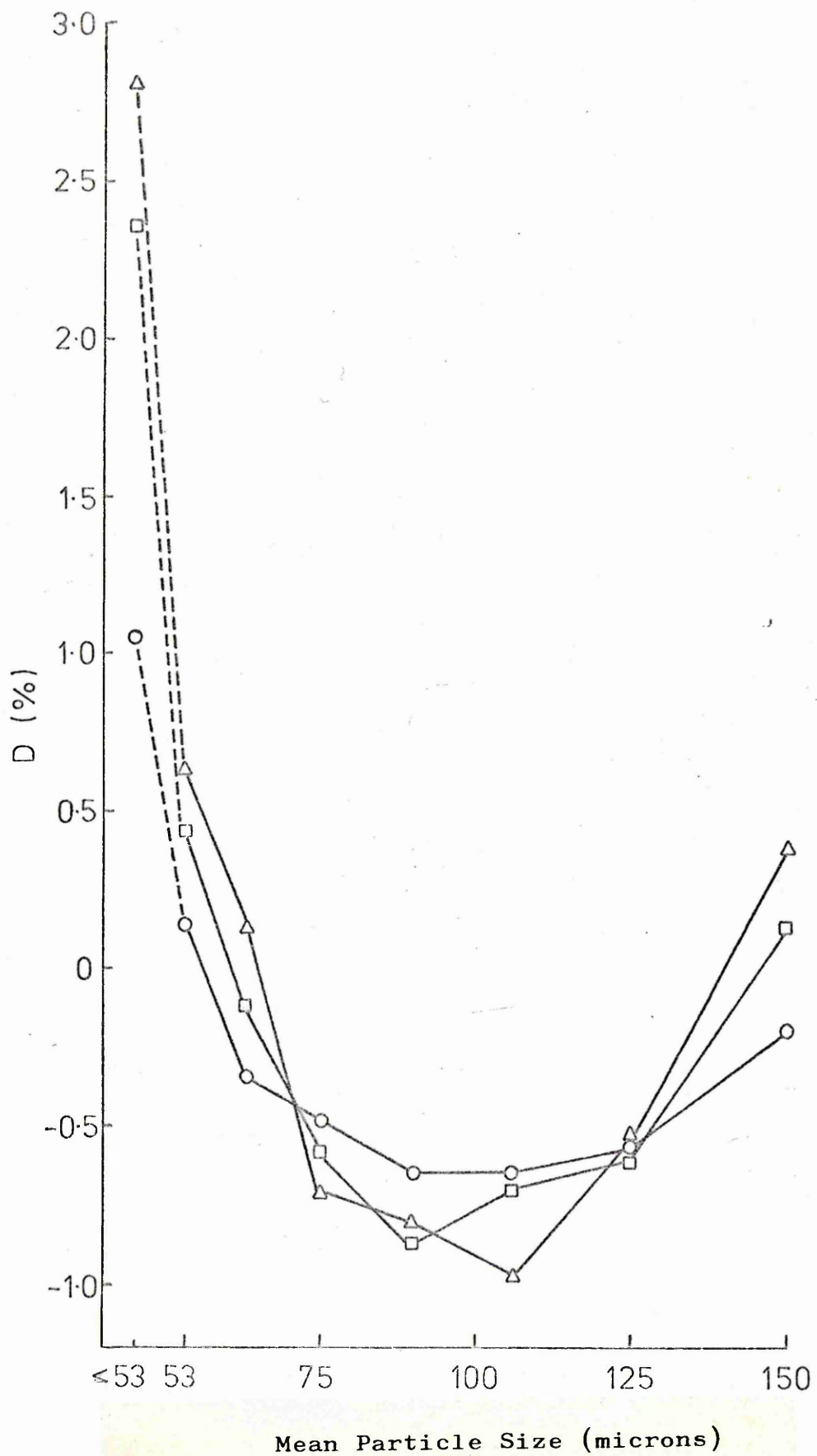


Fig. 34 Relationship Between Sieve Size and Nickel Content of Plated Powders.

$D$  (%) = Nickel content of unsieved powder (%) - Nickel content of sieved fraction (%).

Nickel Content of Unsieved Powder

$\Delta$	9.14%
$\square$	5.36%
0	4.06%



**Fig. 35** Influence of Compaction Load on the Green Density of Compacts made from Blended and Plated Powders.

1. Blended Powder Compacts.
2. Plated Powder Compacts.

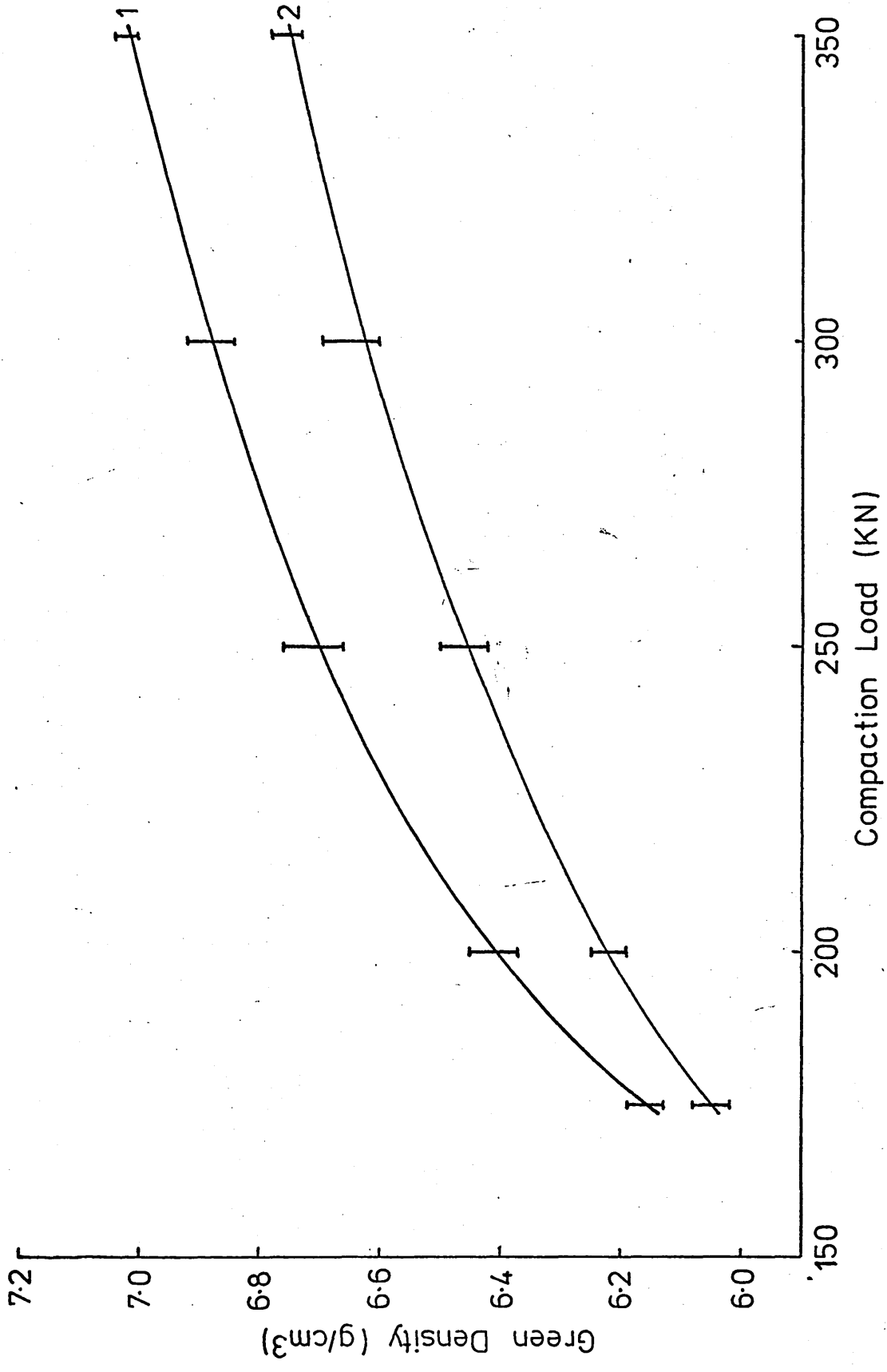
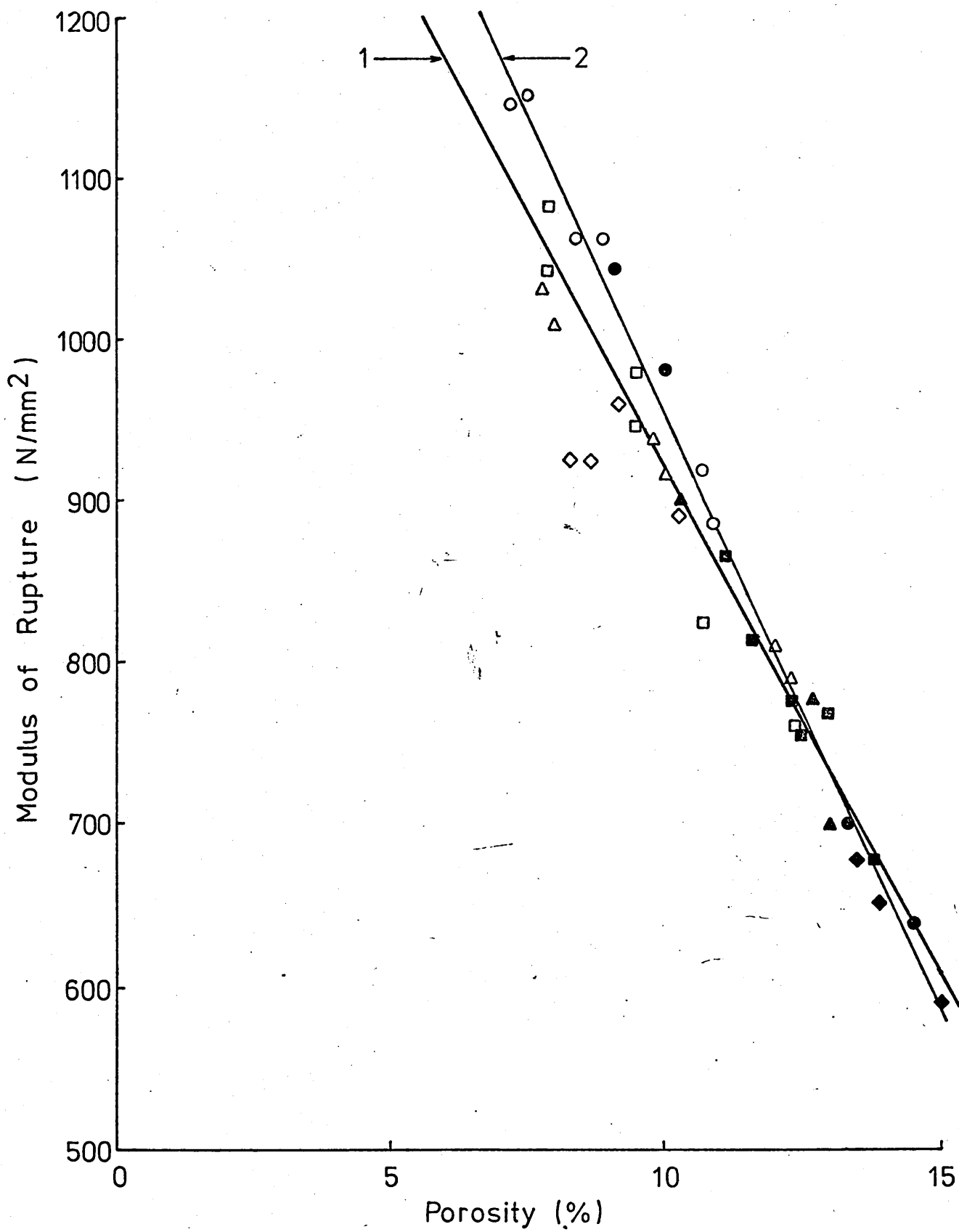


Fig. 36 Relationship between Modulus of Rupture and Porosity of Sintered Compacts Containing 1.75% Nickel.

1. Blended Powder Compacts
2. Plated Powder Compacts

◇	-	Blended Powder Compact Sintered for 30 minutes				
△	-	"	"	"	"	60
□	-	"	"	"	"	120
○	-	"	"	"	"	240
◇	-	Plated	"	"	"	30
△	-	"	"	"	"	60
■	-	"	"	"	"	120
○	-	"	"	"	"	240



**Fig. 37** Relationship between Modulus of Rupture and Porosity of Sintered Compacts Containing 3.25% Nickel.

- 1. Blended Powder Compacts**
- 2. Plated Powder Compacts sintered for 120 or 240 minutes**

**For key to Symbols see Fig. 36**

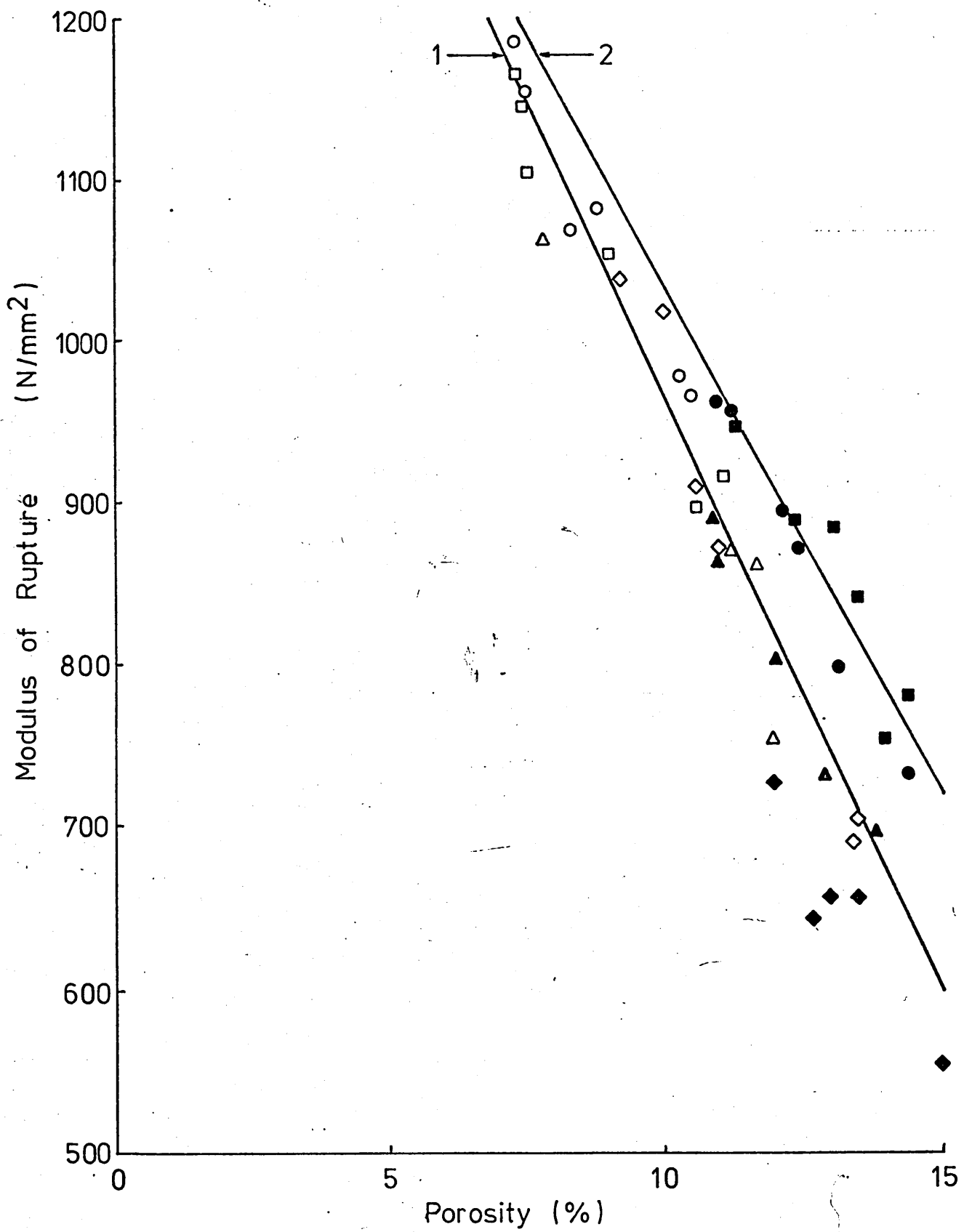


**Fig. 38** Relationship between Modulus of Rupture and Porosity of Sintered Compacts Containing 4.25% Nickel.

1. Blended Powder Compacts Sintered for 30 minutes
2. " " " " " 60 "
3. " " " " " 120 "
4. " " " " " 240 "
5. Plated " " " " 30 to 240 minutes.

For key to Symbols used see Fig. 36

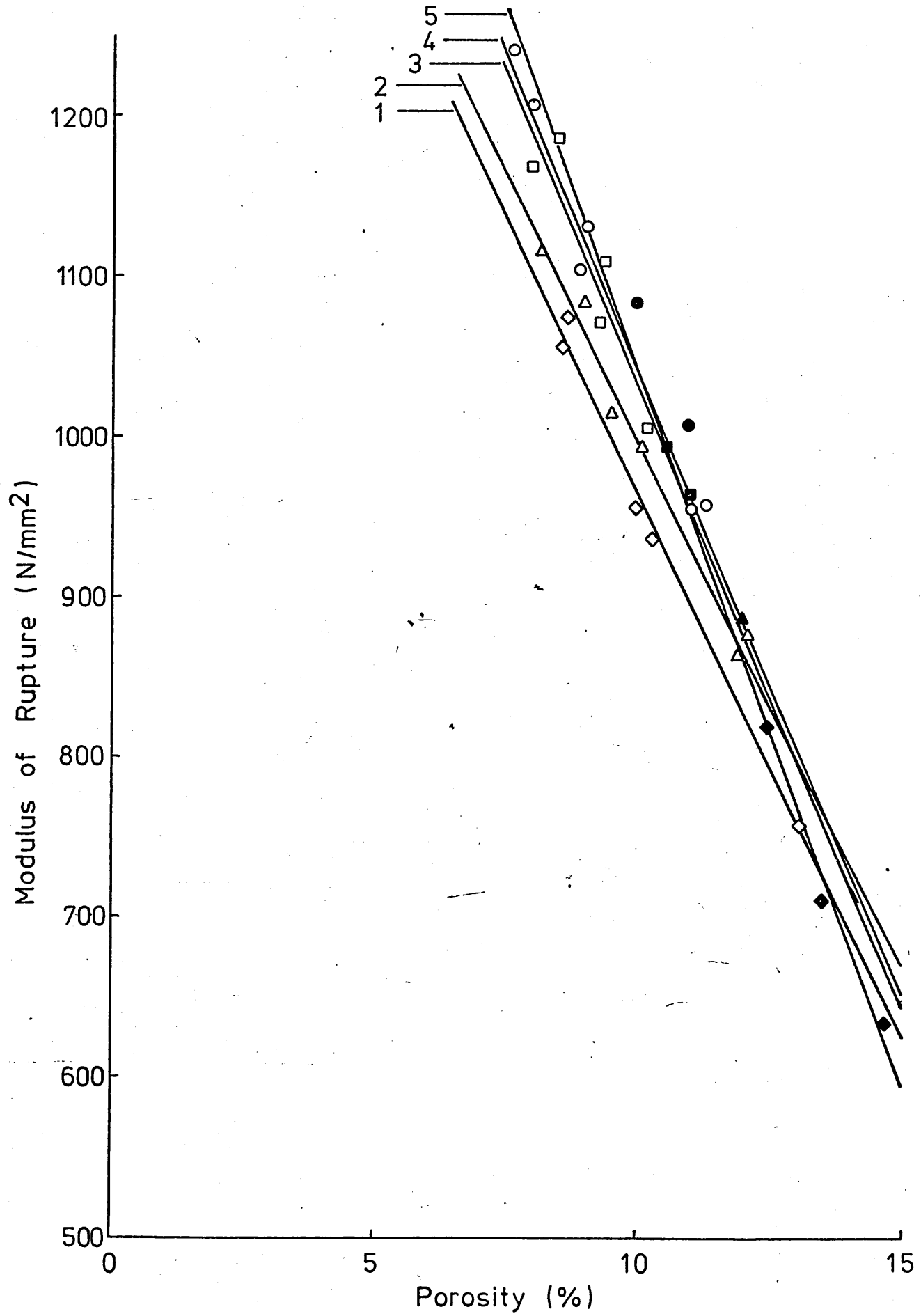


Fig. 39 1.75% Ni Blended Powder Compact Sintered  
for 30 Minutes at 1150°C.

Mag. 256X

Fig. 40 1.75% Ni Blended Powder Compact Sintered for  
30 Minutes at 1150°C and tempered at 600°C  
for 60 Minutes.

Mag. 256X

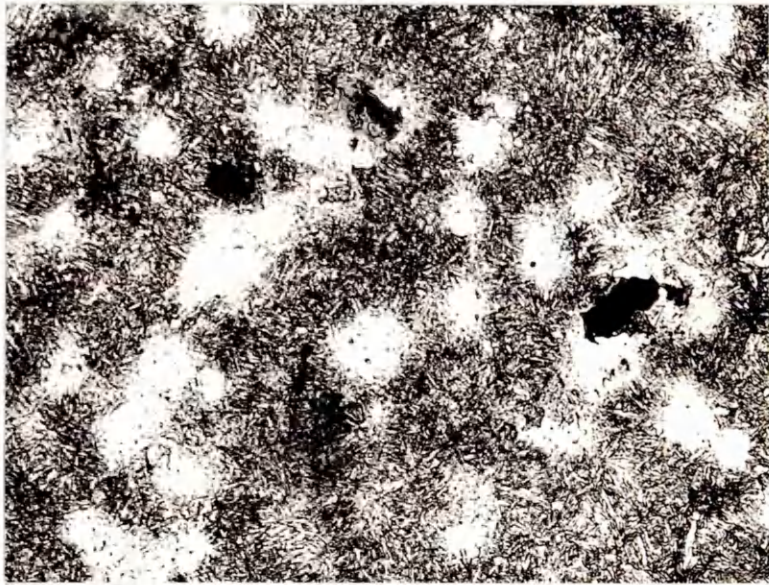


Fig. 41 1.75% Ni Blended Powder Compact Sintered for  
60 Minutes at 1150°C.

Mag. 256X

Fig. 42 1.75% Ni Blended Powder Compact Sintered for  
60 Minutes at 1150°C.

Mag. 1000X

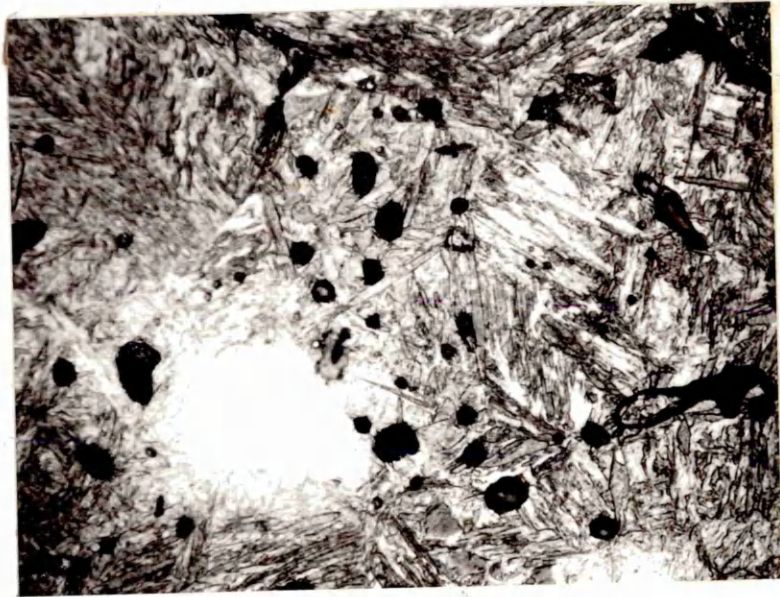
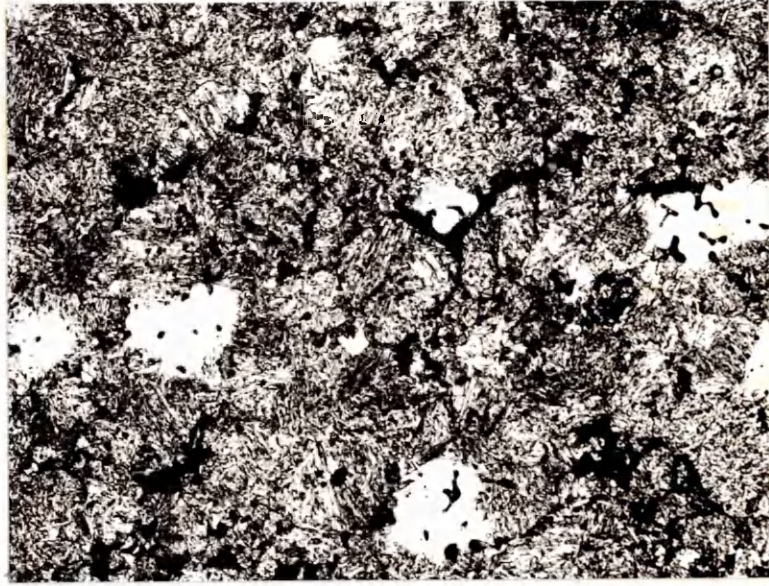


Fig. 43 1.75% Ni Blended Powder Compact Sintered for  
240 Minutes at 1150°C.  
Mag. 256X

Fig. 44 1.75% Ni Blended Powder Compact Sintered for  
240 Minutes at 1150°C.  
Mag. 1000X

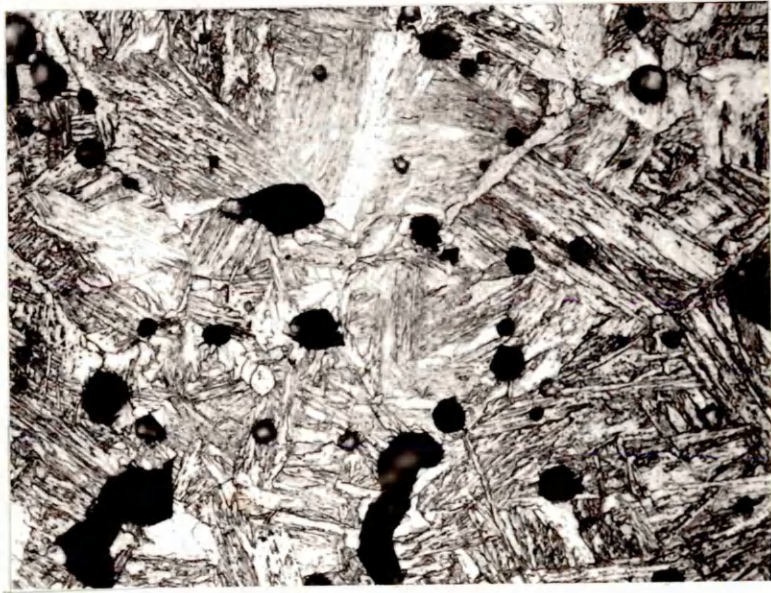


Fig. 45 1.75% Ni Plated Powder Compact Sintered for  
30 Minutes at 1150°C.

Mag. 256X

Fig. 46 1.75% Ni Plated Powder Compact Sintered for  
30 Minutes at 1150°C.

Mag. 1000X

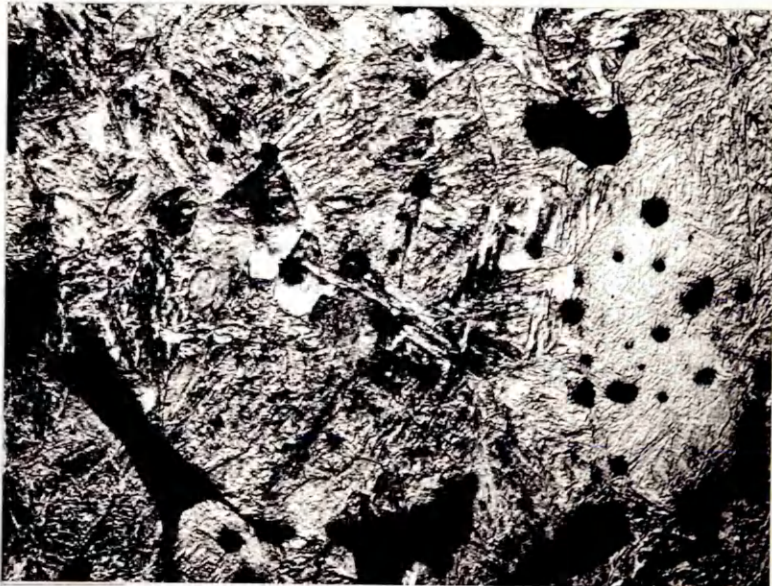
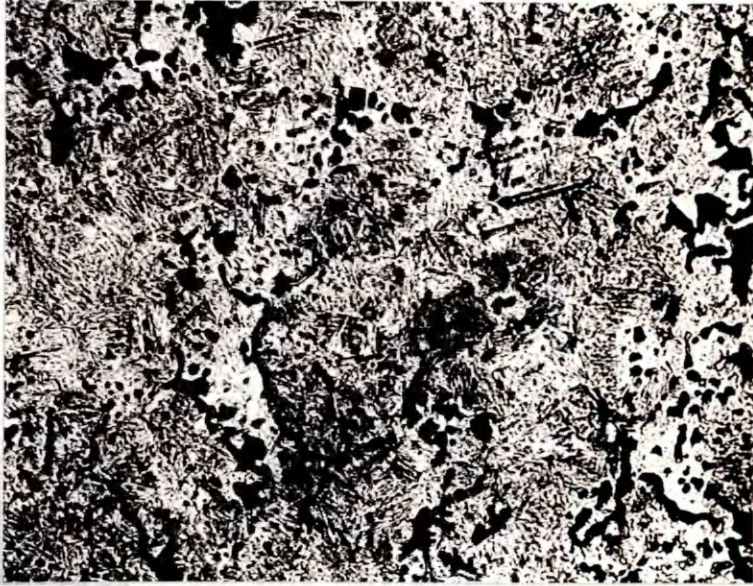


Fig. 47 1.75% Ni Plated Powder Compact Sintered for  
60 Minutes at 1150°C.

Mag. 256X

Fig. 48 1.75% Ni Plated Powder Compact Sintered for  
60 Minutes at 1150°C.

Mag. 1000X

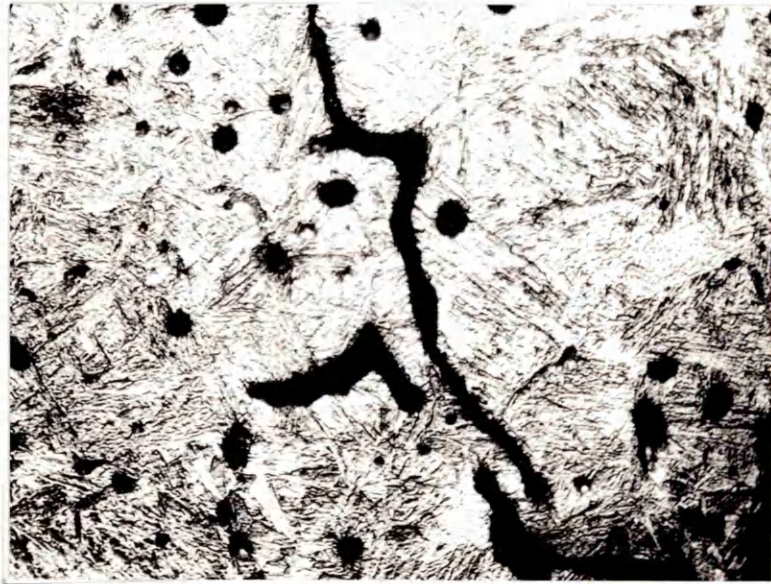
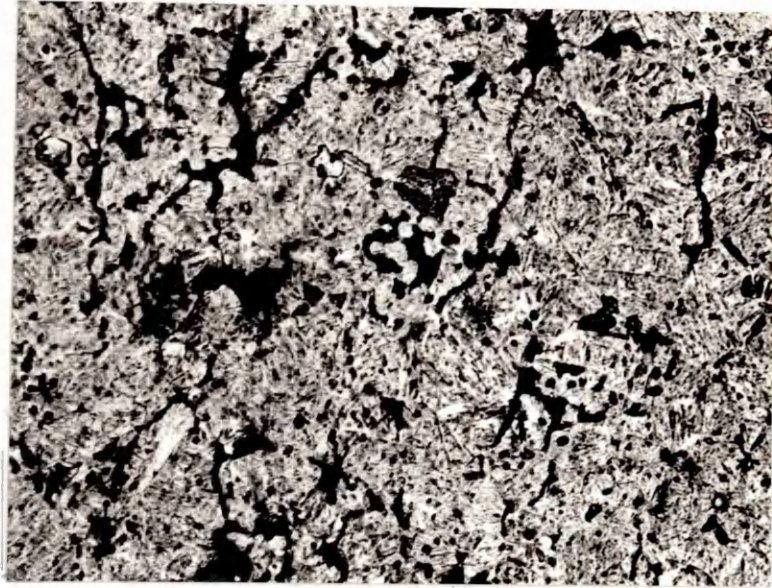


Fig. 49 1.75% Ni Plated Powder Compact Sintered for  
120 Minutes at 1150°C.

Mag. 256X

Fig. 50 1.75% Ni Plated Powder Compact Sintered for  
120 Minutes at 1150°C.

Mag. 1000X

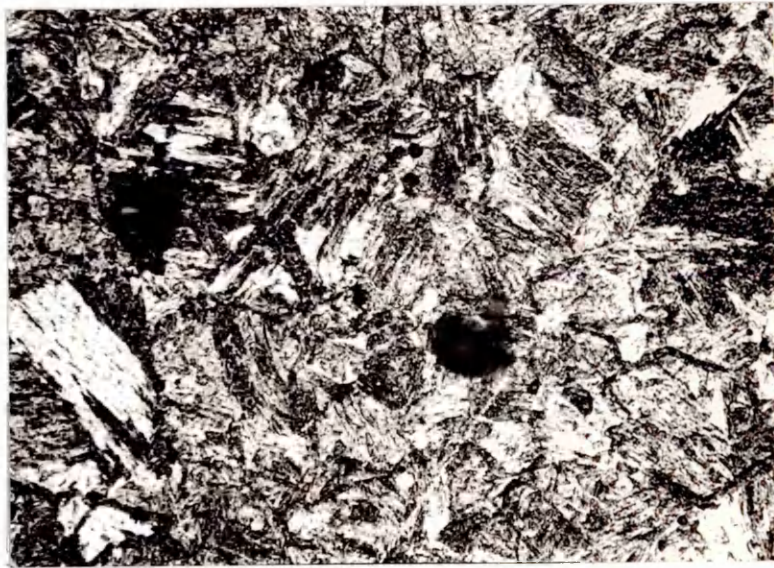


Fig. 51 3.25% Ni Blended Powder Compact Sintered for  
30 Minutes at 1150°C.

Mag. 256X

Fig. 52 3.25% Ni Blended Powder Compact Sintered for  
30 Minutes at 1150°C.

Mag. 1000X



**Fig. 53** 3.25% Ni Blended Powder Compact Sintered for  
60 Minutes at 1150°C.

Mag. 256X

**Fig. 54** 3.25% Ni Blended Powder Compact Sintered for  
60 Minutes at 1150°C and tempered at 600°C  
for 60 Minutes.

Mag. 256X

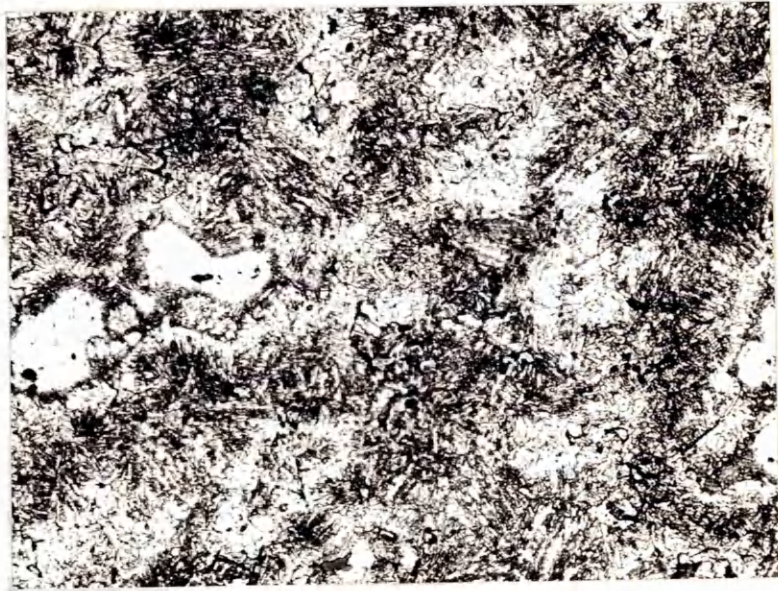
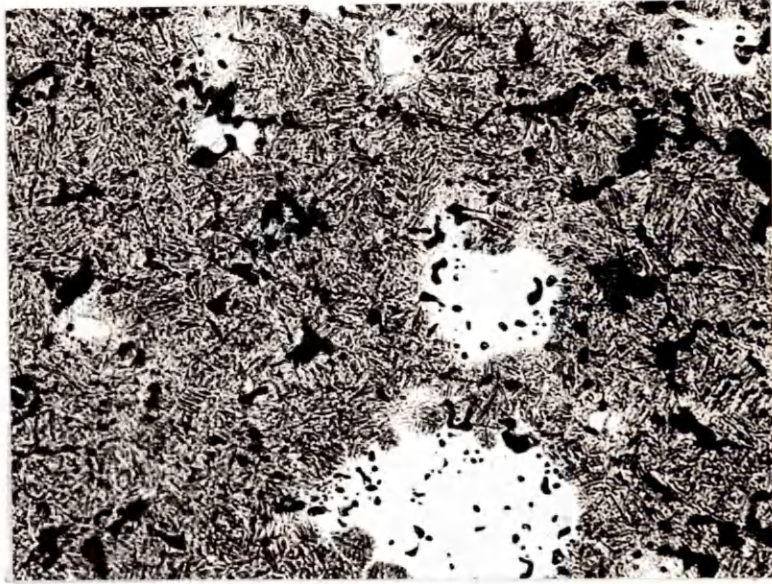


Fig. 55 3.25% Ni Blended Powder Compact Sintered for  
240 Minutes at 1150°C.

Mag. 256X

Fig. 56 3.25% Ni Blended Powder Compact Sintered for  
240 Minutes at 1150°C.

Mag. 1000X

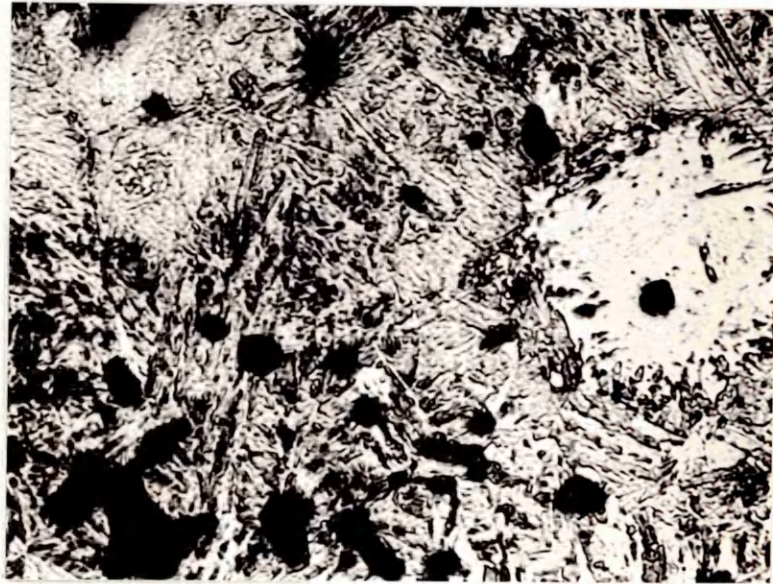
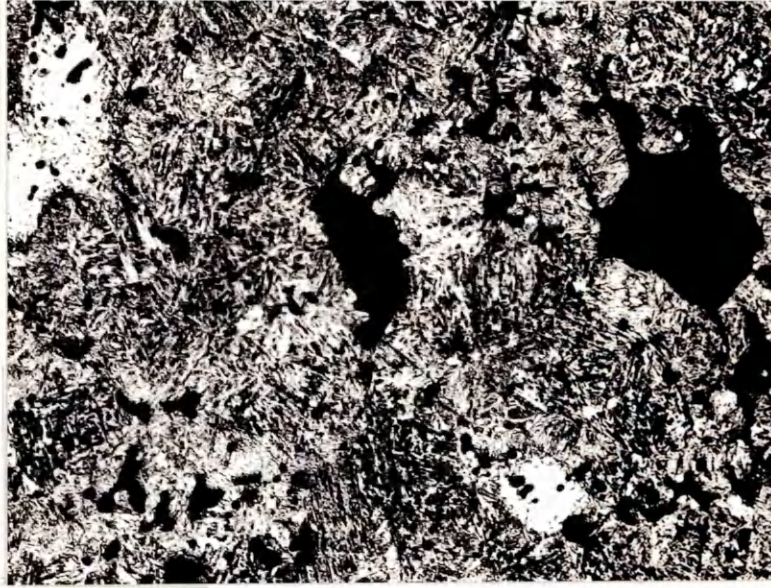


Fig. 57 3.0% Ni Plated Powder Compact Sintered for 30  
Minutes at 1150°C.

Mag. 256X

Fig. 58 3.0% Ni Plated Powder Compact Sintered for  
30 Minutes at 1150°C.

Mag. 1000X

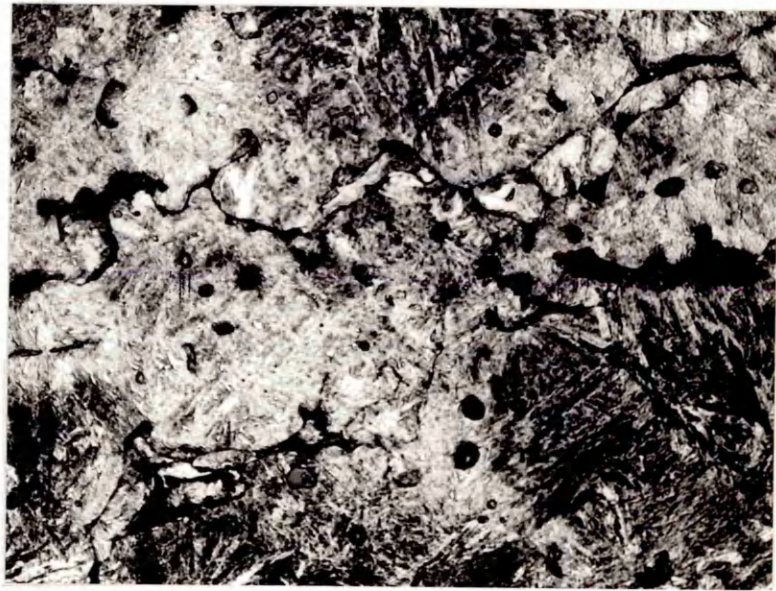
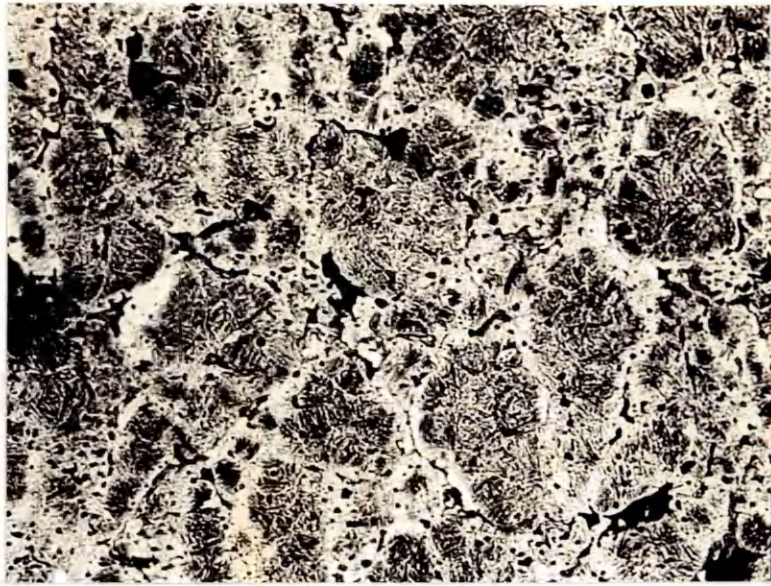


Fig. 59 3.0% Ni Plated Powder Compact Sintered for  
60 Minutes at 1150°C.

Mag. 256X

Fig. 60 3.0% Ni Plated Powder Compact Sintered for  
60 Minutes at 1150°C.

Mag. 1000X

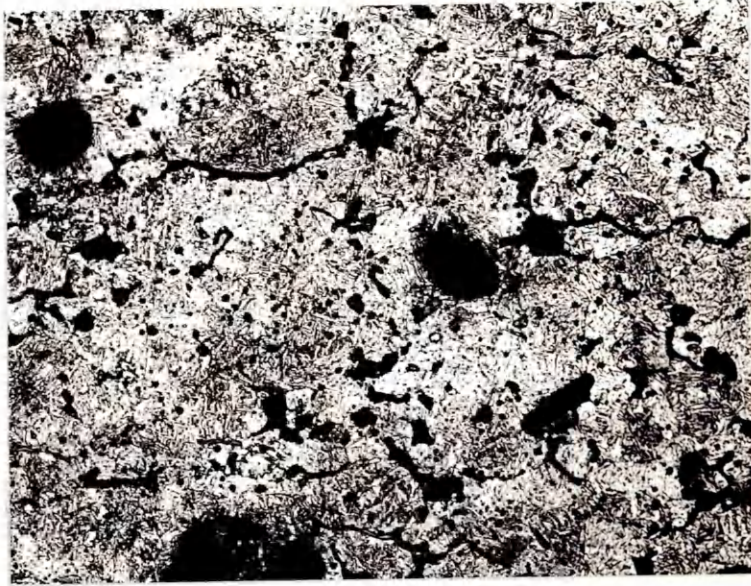


Fig. 61 3.0% Ni Plated Powder Compact Sintered for  
120 Minutes at 1150°C.

Mag. 256X

Fig. 62 3.0% Ni Plated Powder Compact Sintered for  
240 Minutes at 1150°C.

Mag. 256X

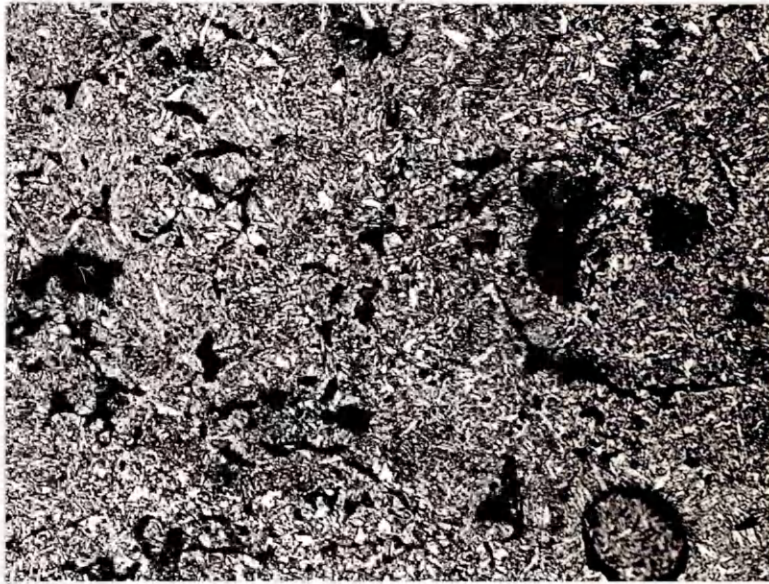
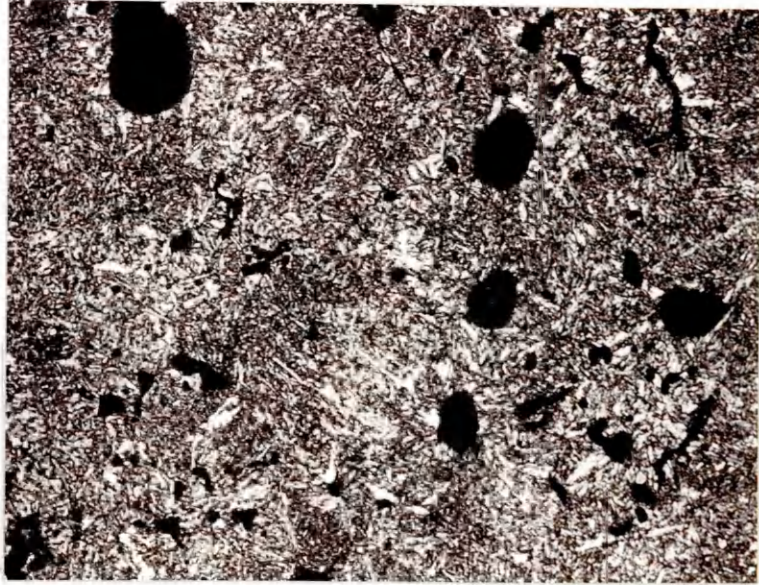


Fig. 63 3.0% Ni Plated Powder Compact Sintered for  
240 Minutes at 1150°C.  
Mag. 1000X

Fig. 64 4.25% Ni Blended Powder Compacts Sintered for  
30 Minutes at 1150°C.  
Mag. 256X

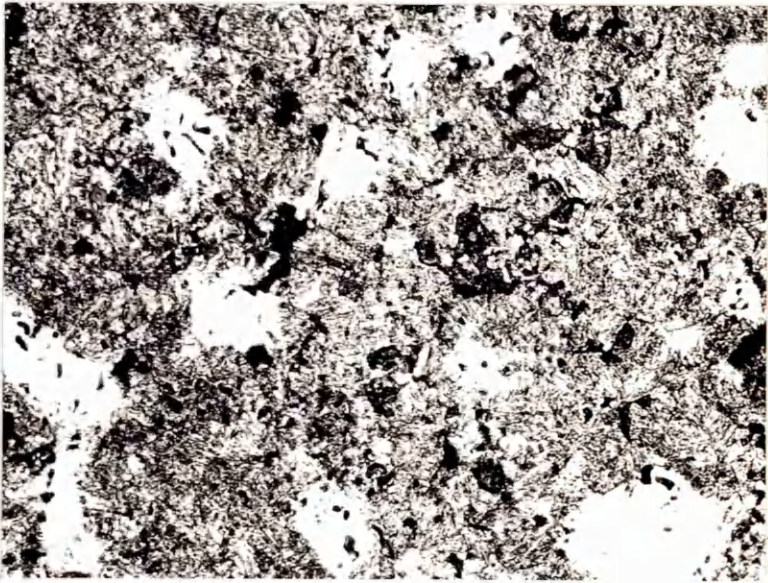
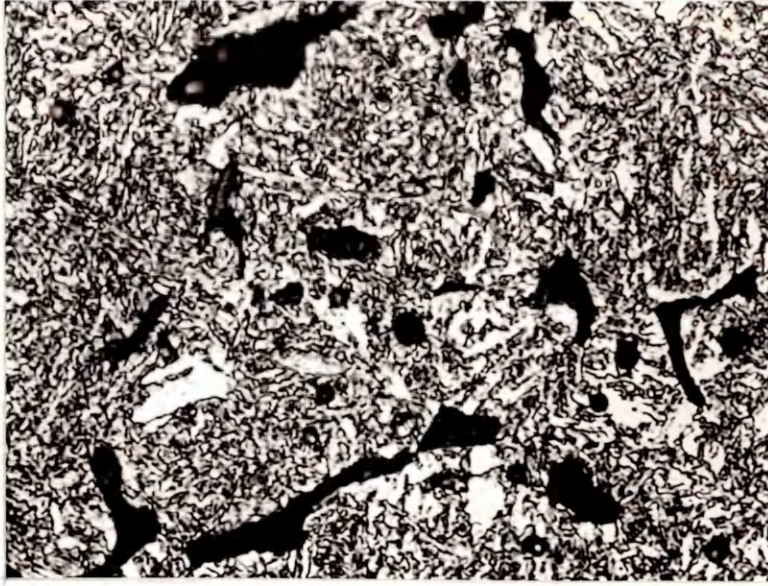


Fig. 65 4.25% Ni Blended Powder Compact Sintered for  
60 Minutes at 1150°C.

Mag. 256X

Fig. 66 4.25% Ni Blended Powder Compact Sintered for  
60 Minutes at 1150°C.

Mag. 1000X

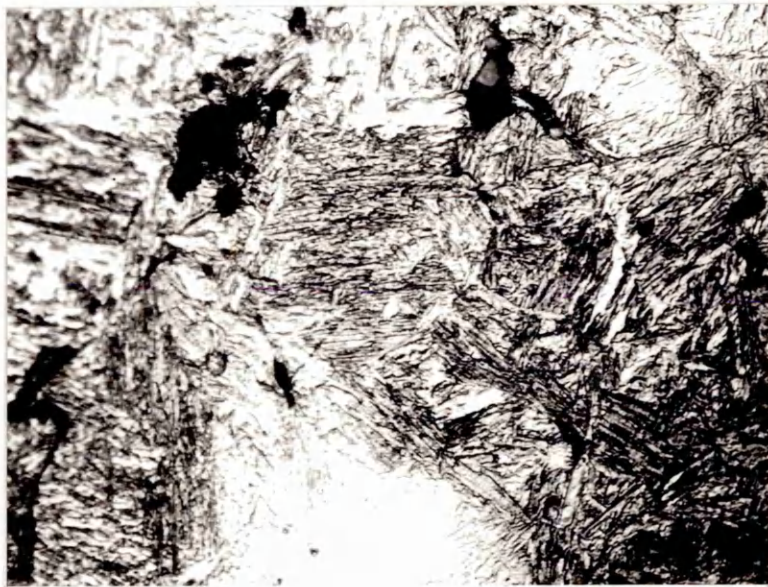
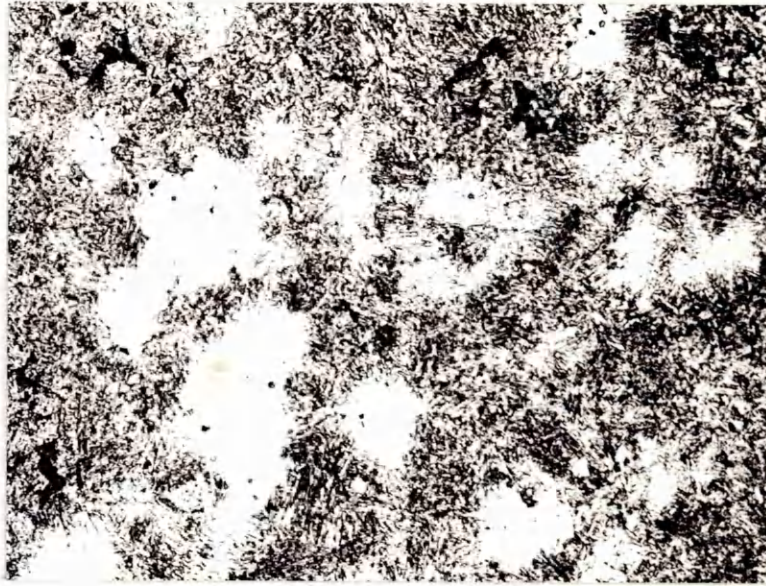


Fig. 67 4.25% Ni Blended Powder Compact Sintered for  
240 Minutes at 1150°C.

Mag. 256X

Fig. 68 4.25% Ni Blended Powder Sintered for 240  
Minutes at 1150°C.

Mag. 1000X

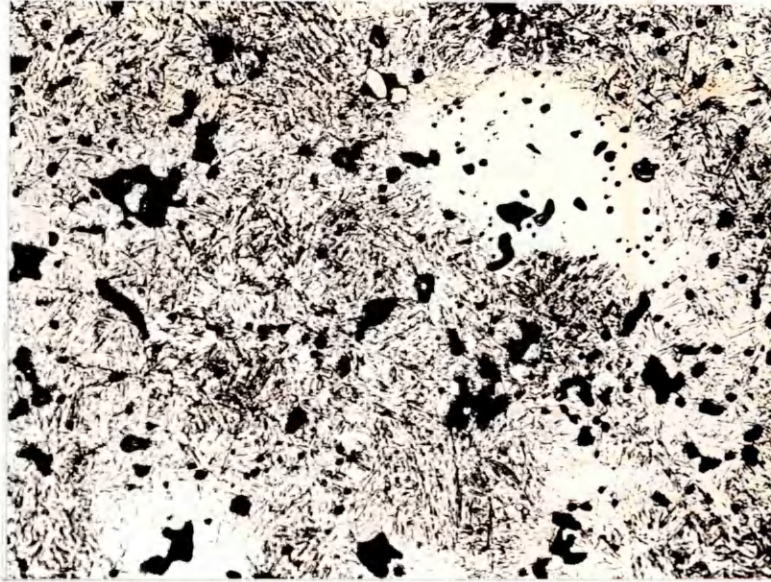


Fig. 69 4.0% Ni Plated Powder Compact Sintered  
for 30 Minutes at 1150°C.  
Mag. 256X

Fig. 70 4.0% Ni Plated Powder Compact Sintered for  
60 Minutes at 1150°C.  
Mag. 256X

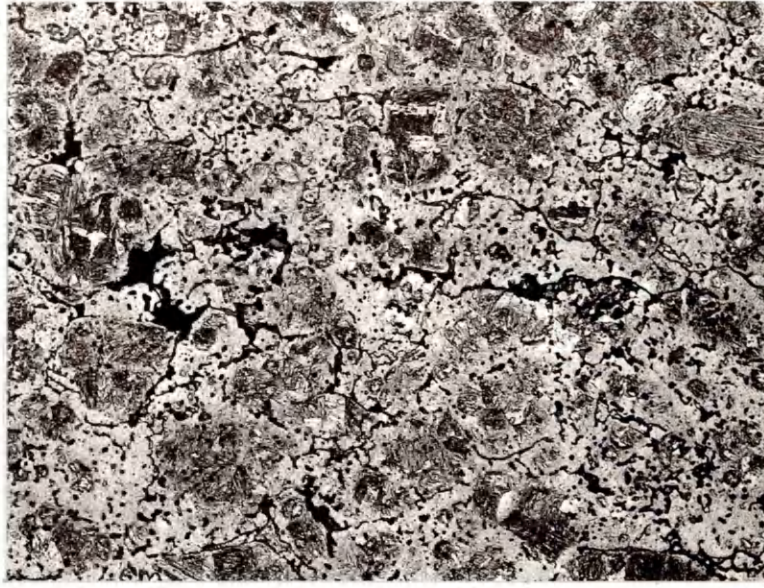


Fig. 71 4.0% Ni Plated Powder Compact Sintered for  
60 Minutes at 1150°C.

Mag. 1000X

Fig. 72 4.0% Ni Plated Powder Compact Sintered for  
120 Minutes at 1150°C.

Mag. 256X

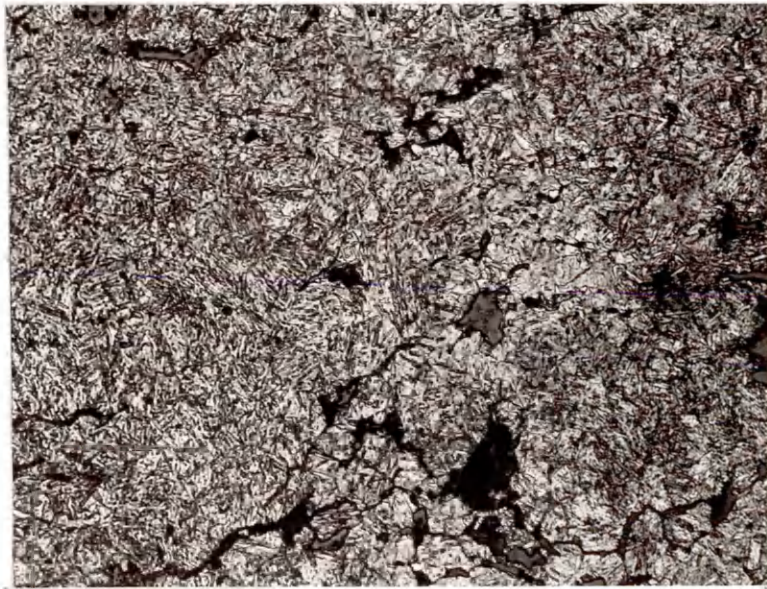
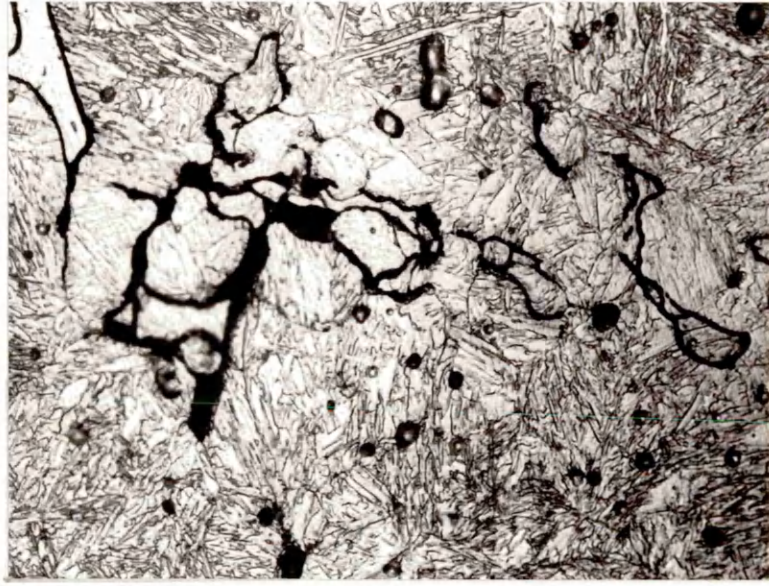


Fig. 73 4.0% Ni Plated Powder Compact Sintered for  
240 Minutes at 1150°C.

Mag. 256X

Fig. 74 4.0% Ni Plated Powder Compact Sintered for  
120 Minutes at 1150°C.

Mag. 1000X

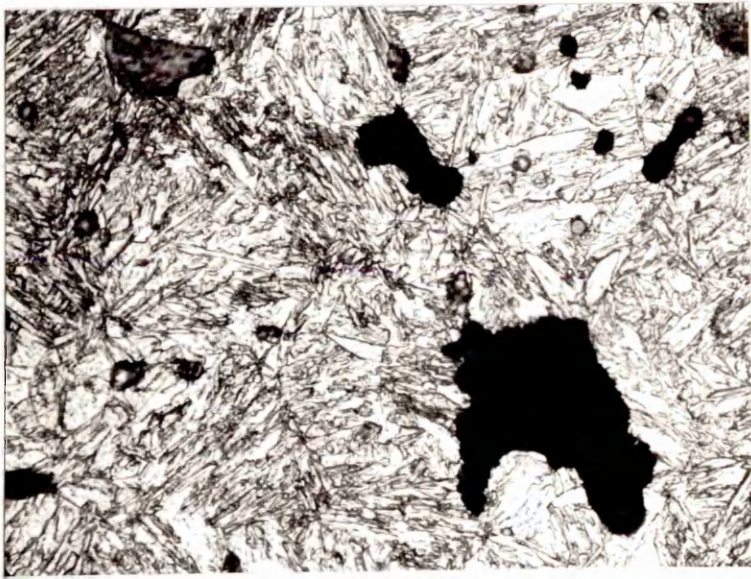
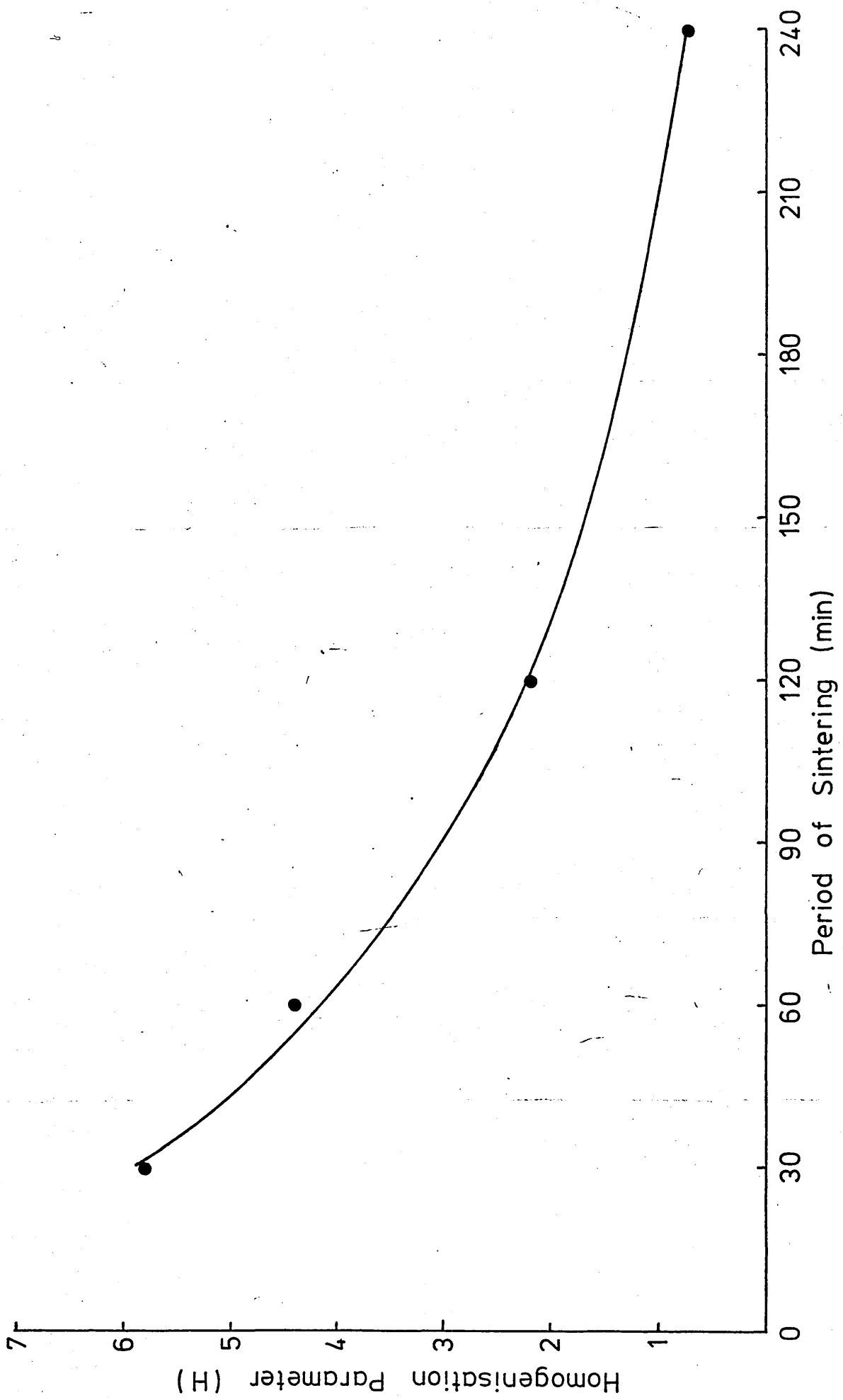
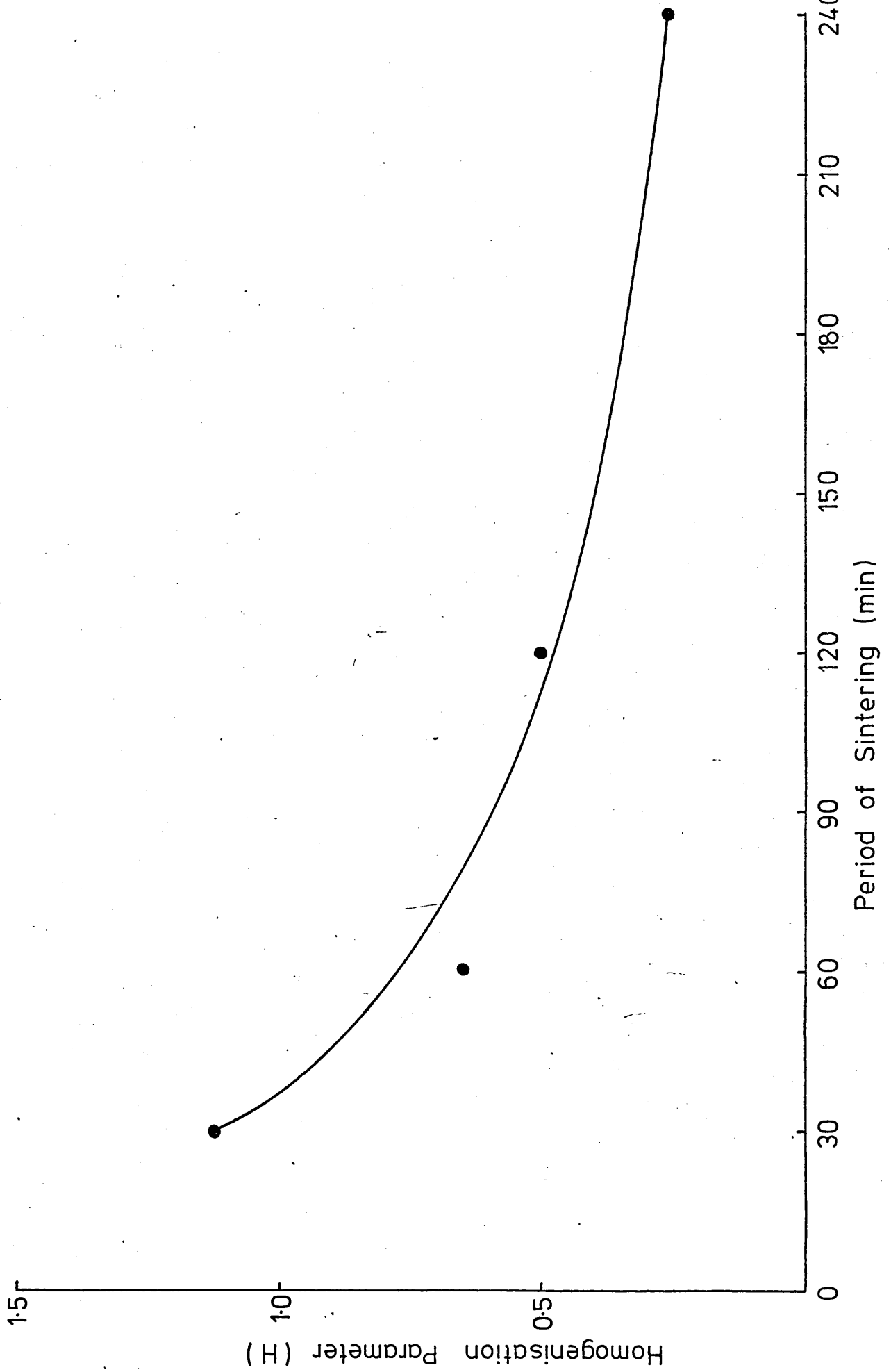


Fig. 75 Relationship between the Homogenisation  
Parameter and Period of Sintering of 3.25%  
Ni Blended Powder Compacts.



**Fig. 76** Relationship Between the Homogenisation  
Parameter and Period of Sintering of 3.0%  
Ni Plated Powder Compacts.



**Fig. 77** Relationship between the Homogenisation  
Parameter and Period of Sintering of 4.25%  
Ni Blended Powder Compacts.

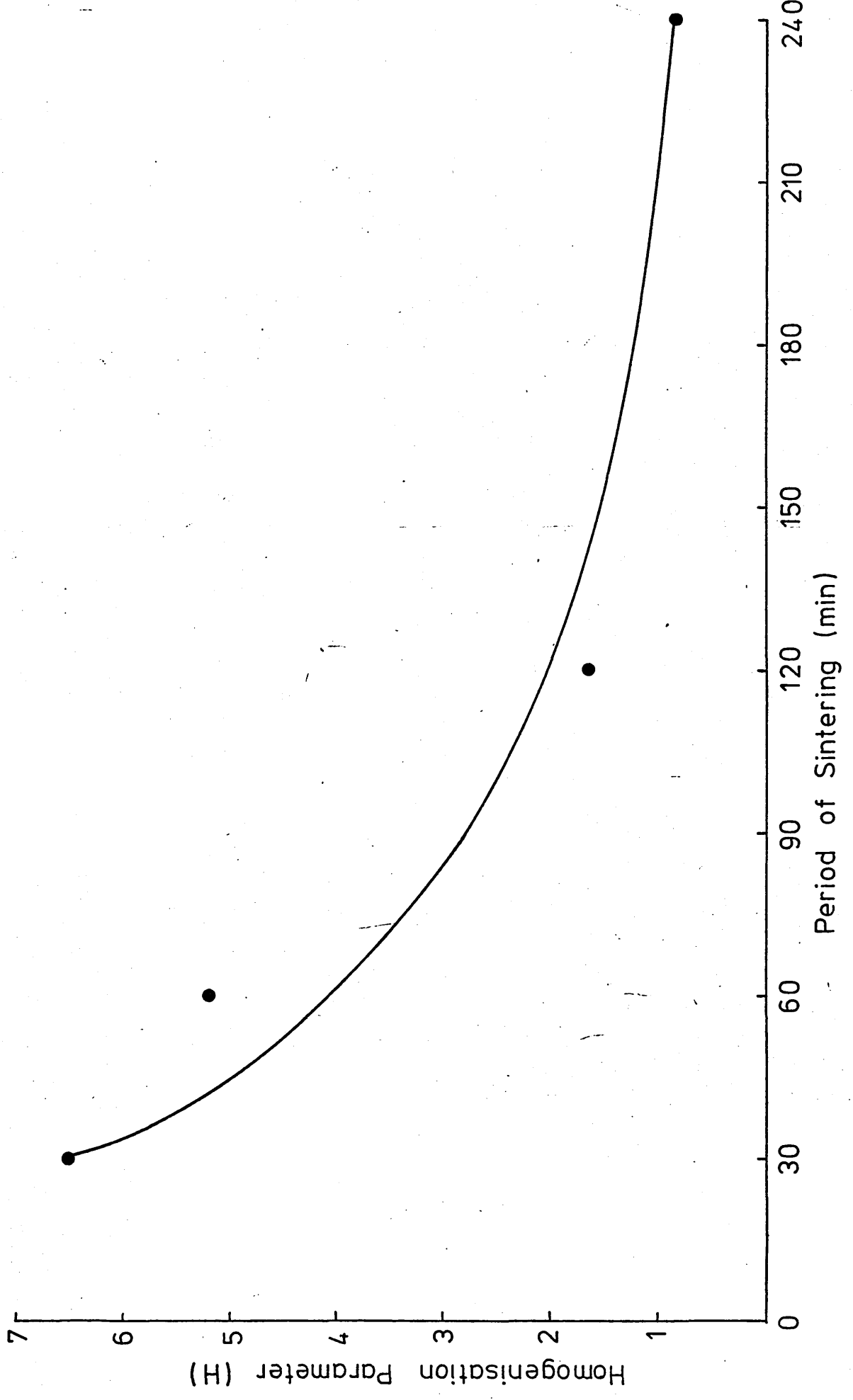


Fig. 78 Relationship between the Homogenisation  
Parameter and Period of Sintering of 4.0%  
Ni Plated Powder Compact.

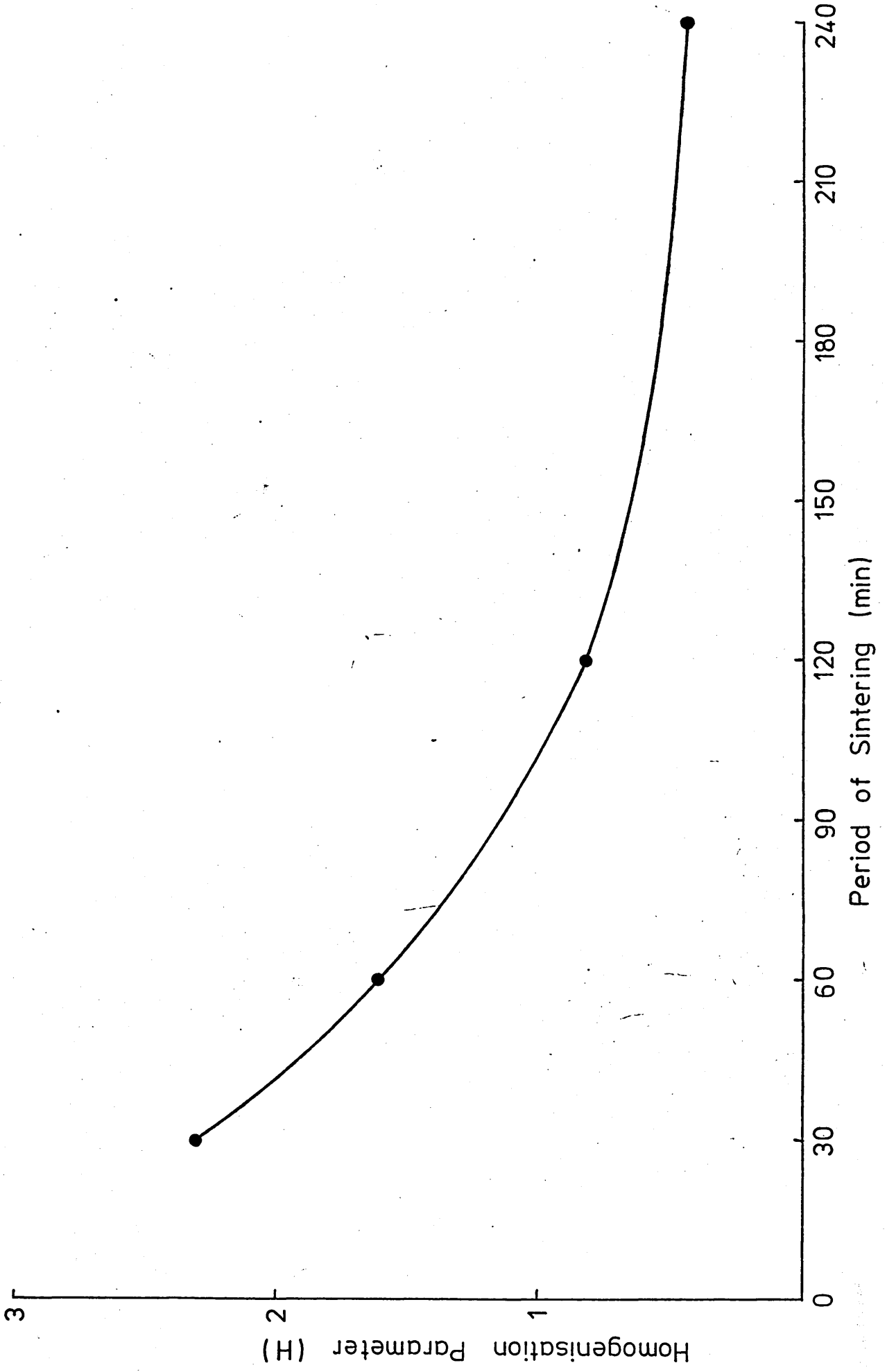


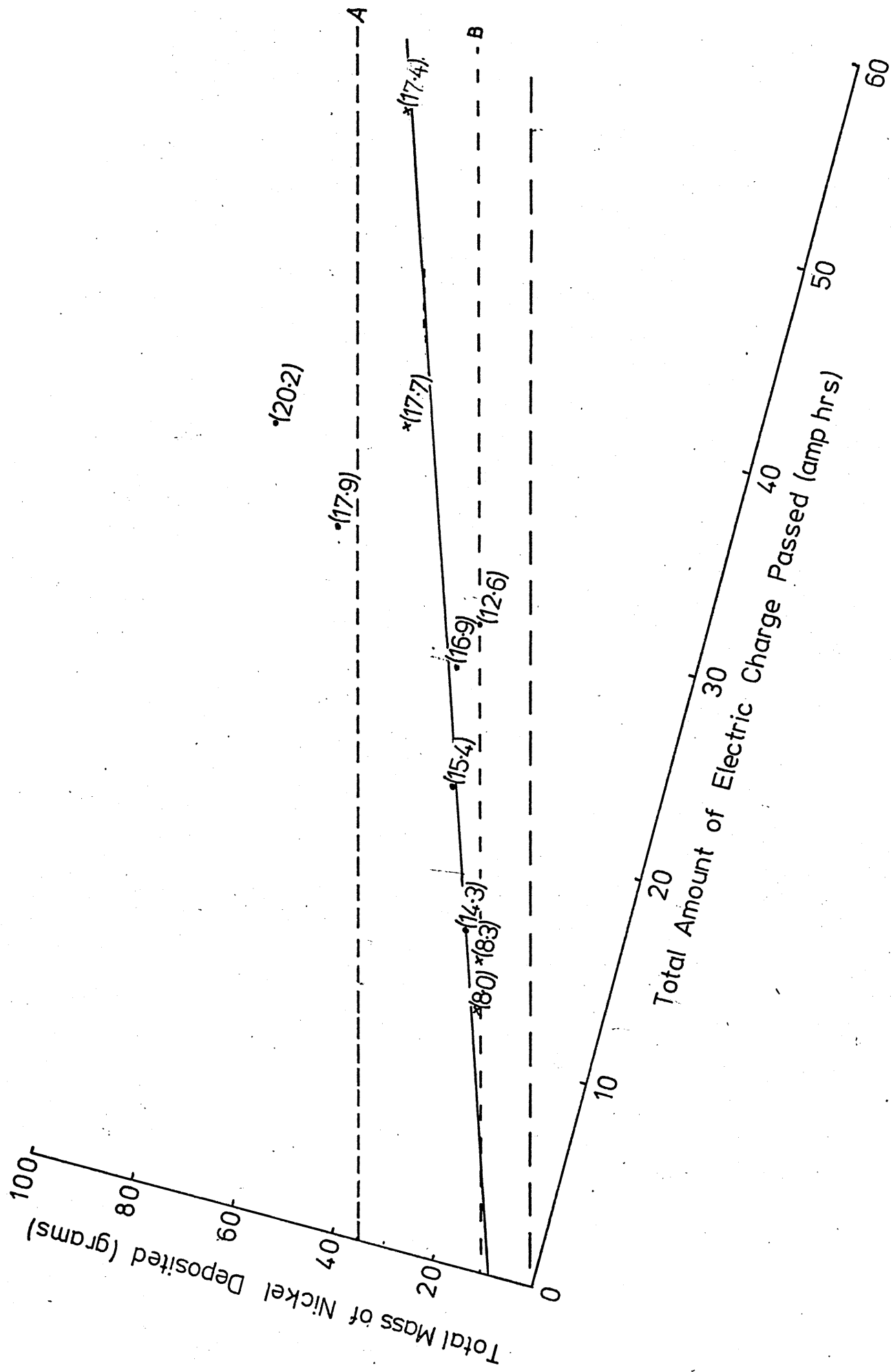
Fig. 79 Portion of Stainless Steel Cathode rods  
showing the Formation of Chains of Powder  
Particles.



Fig. 80 Relationship between Total Mass of Nickel Deposited and Total amount of Electric Charge Passed.

- A. Contribution of the electroless process at 63°C.
- B. Contribution of the electroless process at 48°C.
- - - Relationship obeying Faraday's Law.

Figures in parentheses refer to current density ( $\text{A}/\text{dm}^2$ )



**Fig. 81** Relationship between the Homogenisation Parameter and Modulus of Rupture of 3.25% Ni Compacts prepared from both Blended and Plated Powders.

**For Key to Symbols see Fig. 36.**

Figures in parentheses refer to sintered density as a percentage of the theoretical density

1. Blended Powder Compacts
2. Blended Powder Compacts
3. Plated Powder Compacts

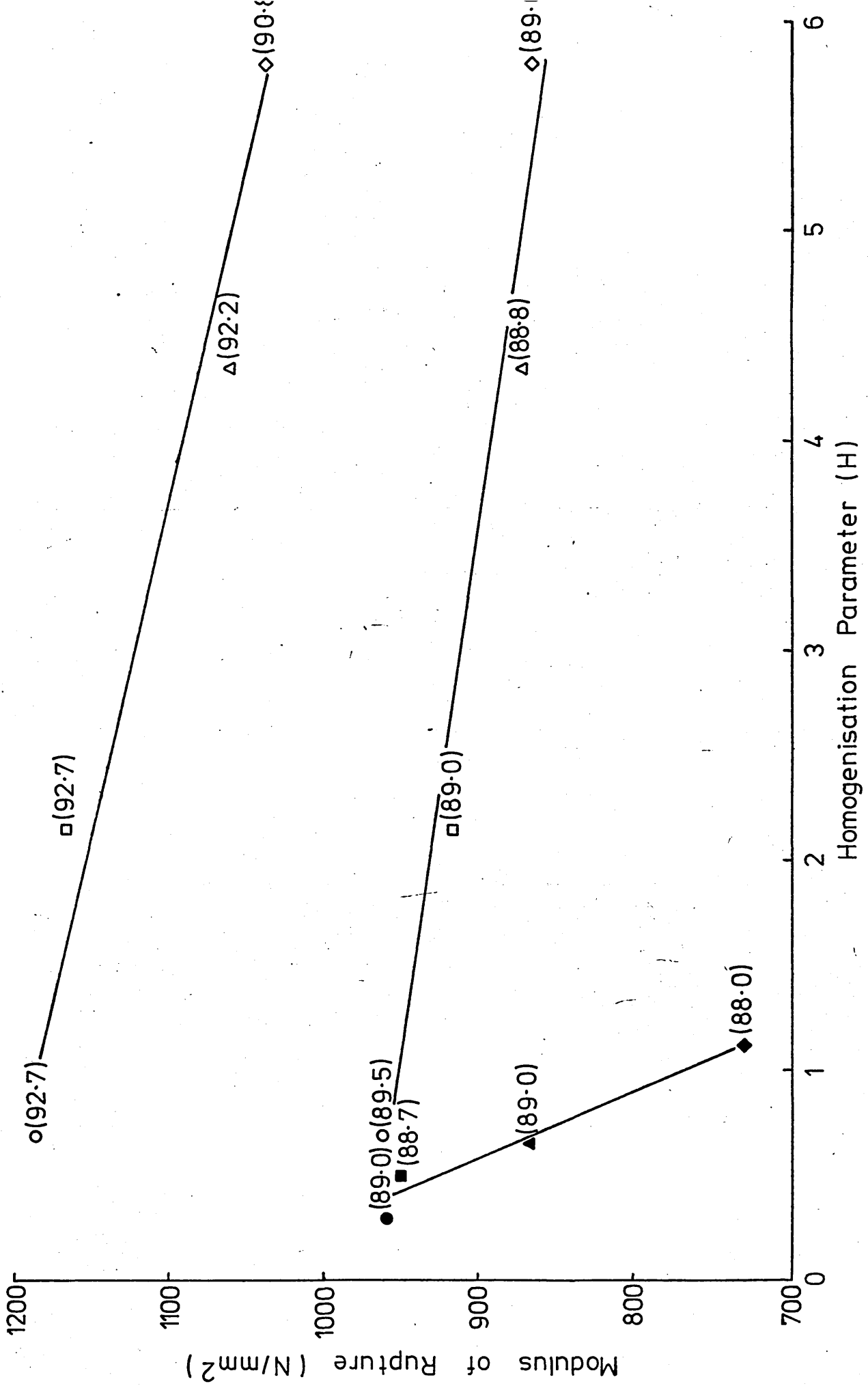


Fig. 82 Influence of Nickel Content on Modulus of Rupture of Sintered Compacts made from both Blended and Plated Powders.

B—— Blended Powder Compacts

P—— Plated Powder Compacts

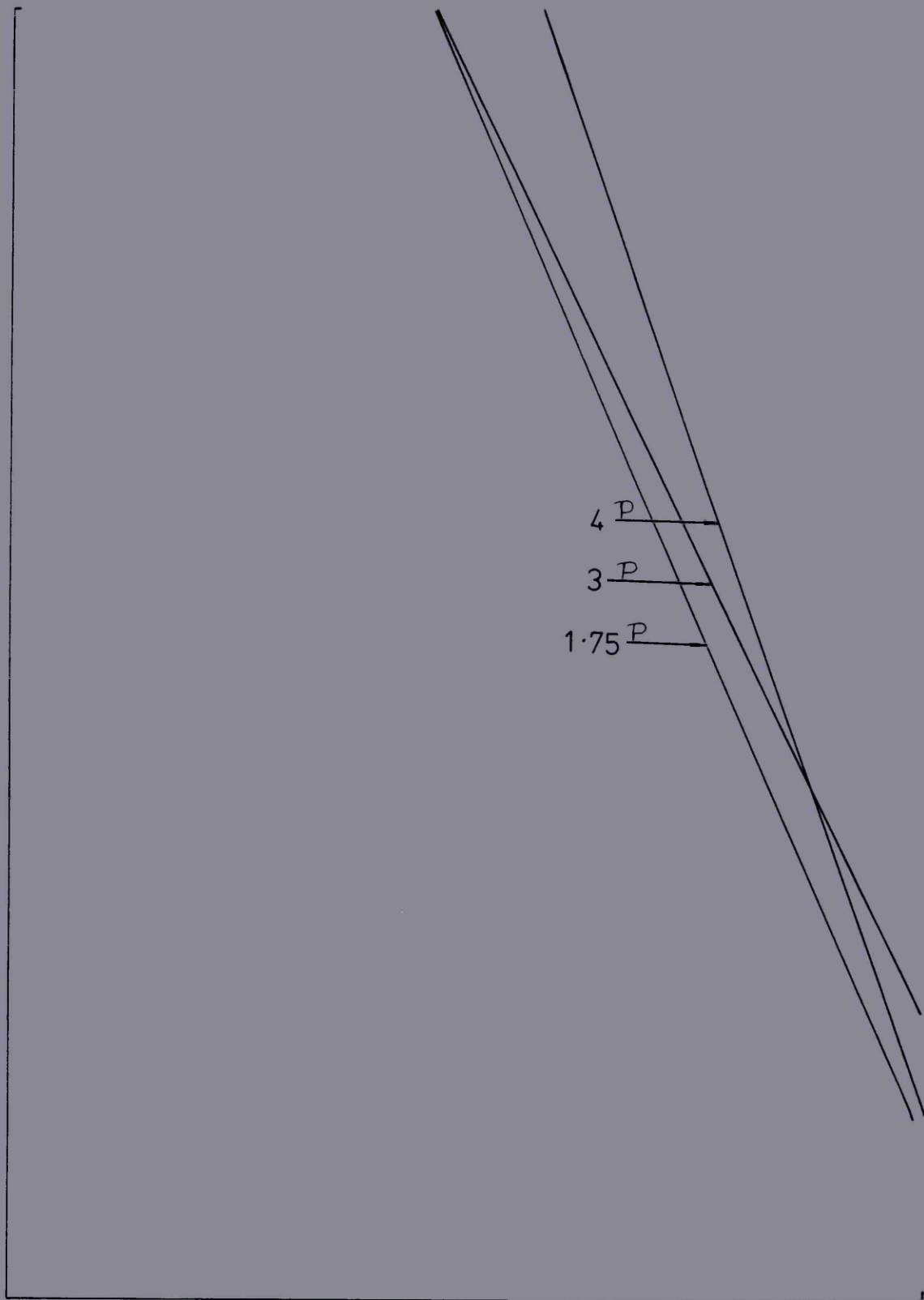


Fig-82(a)

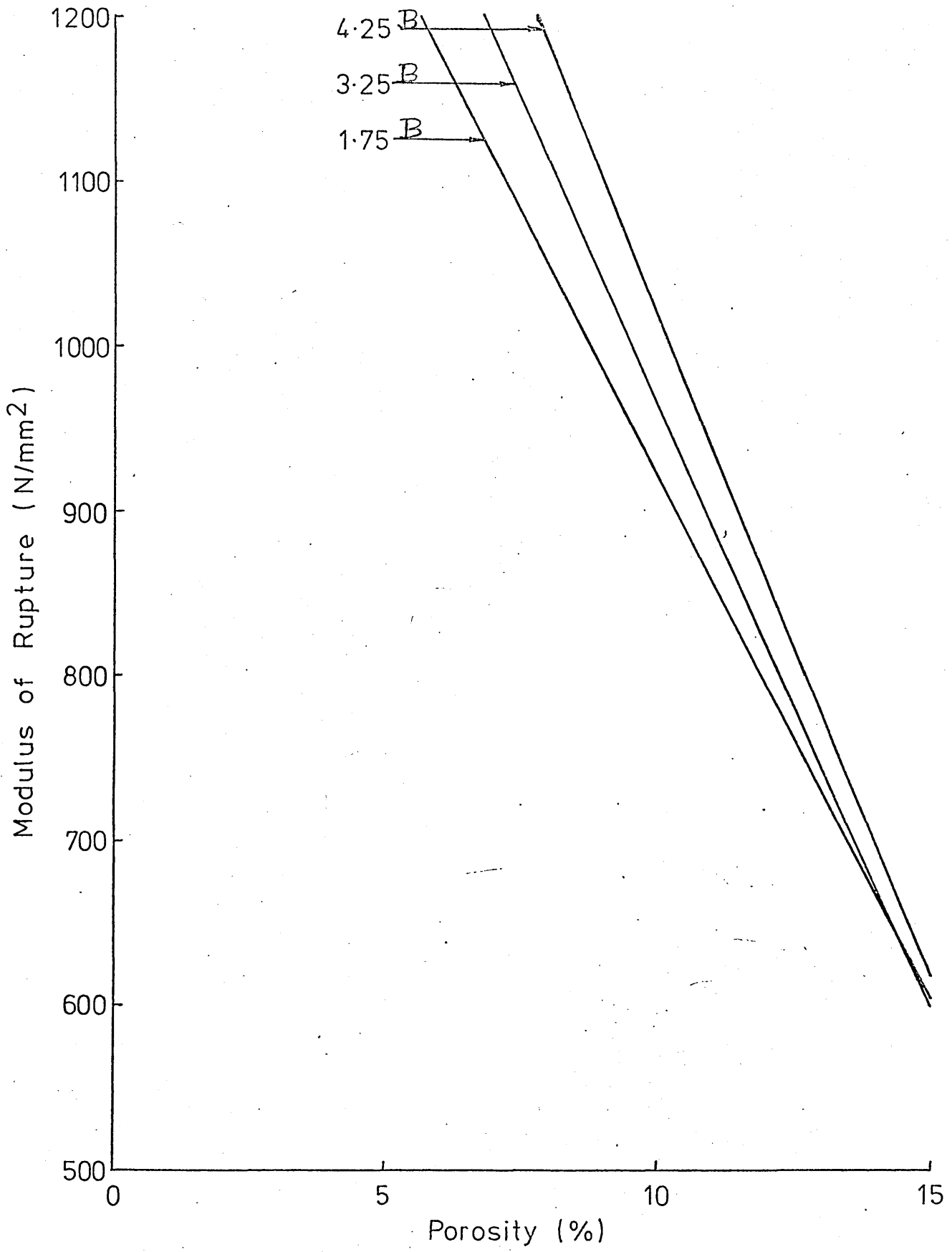
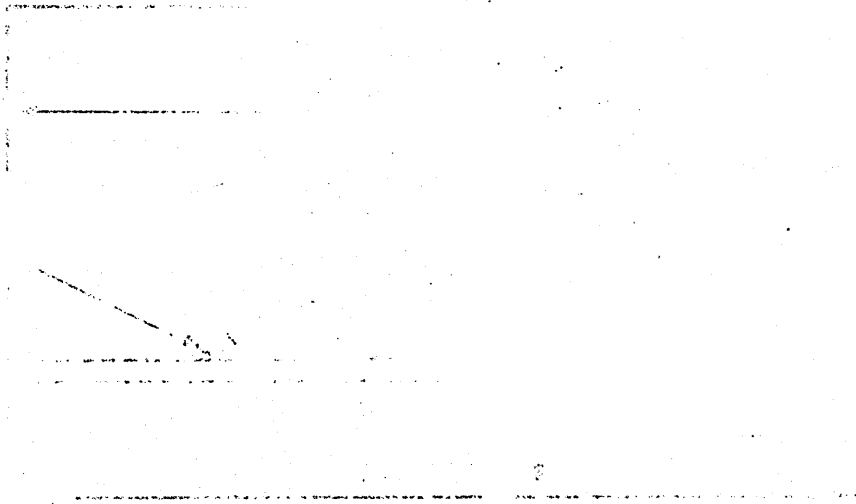
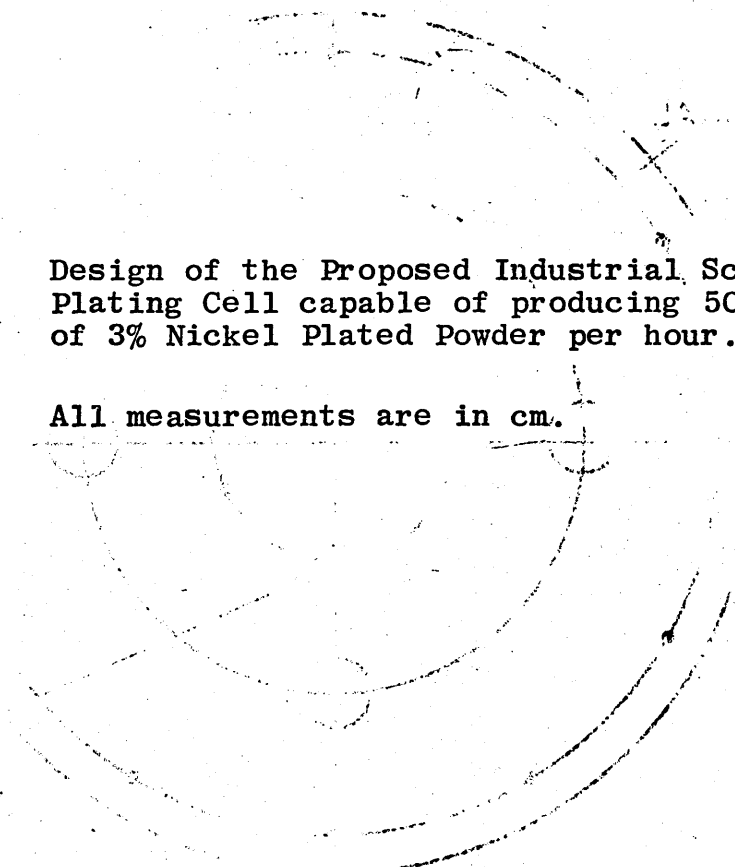


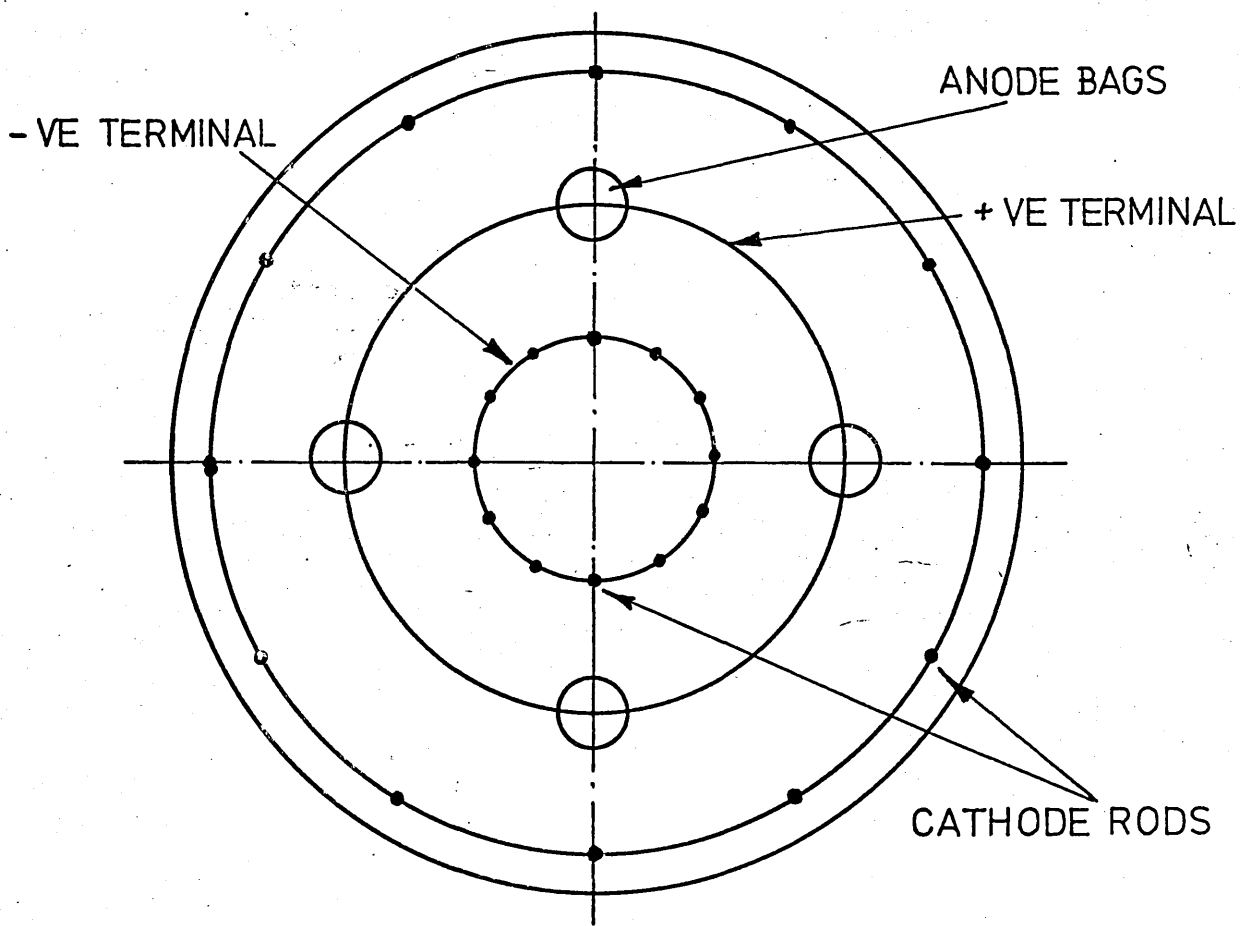
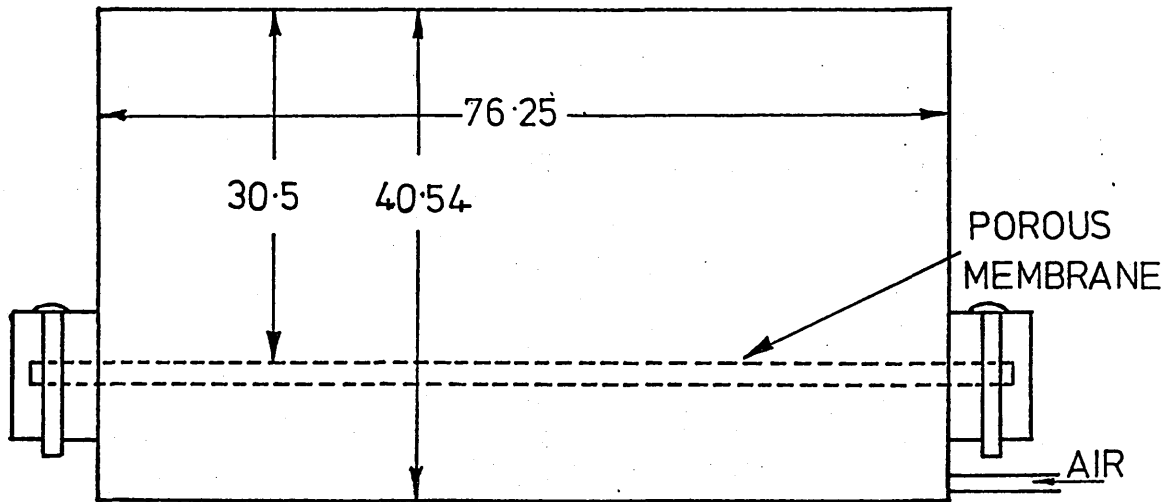
Fig-82(b)



**Fig. 83** Design of the Proposed Industrial Scale Plating Cell capable of producing 50 kg of 3% Nickel Plated Powder per hour.

All measurements are in cm.





THE PLATING CELL

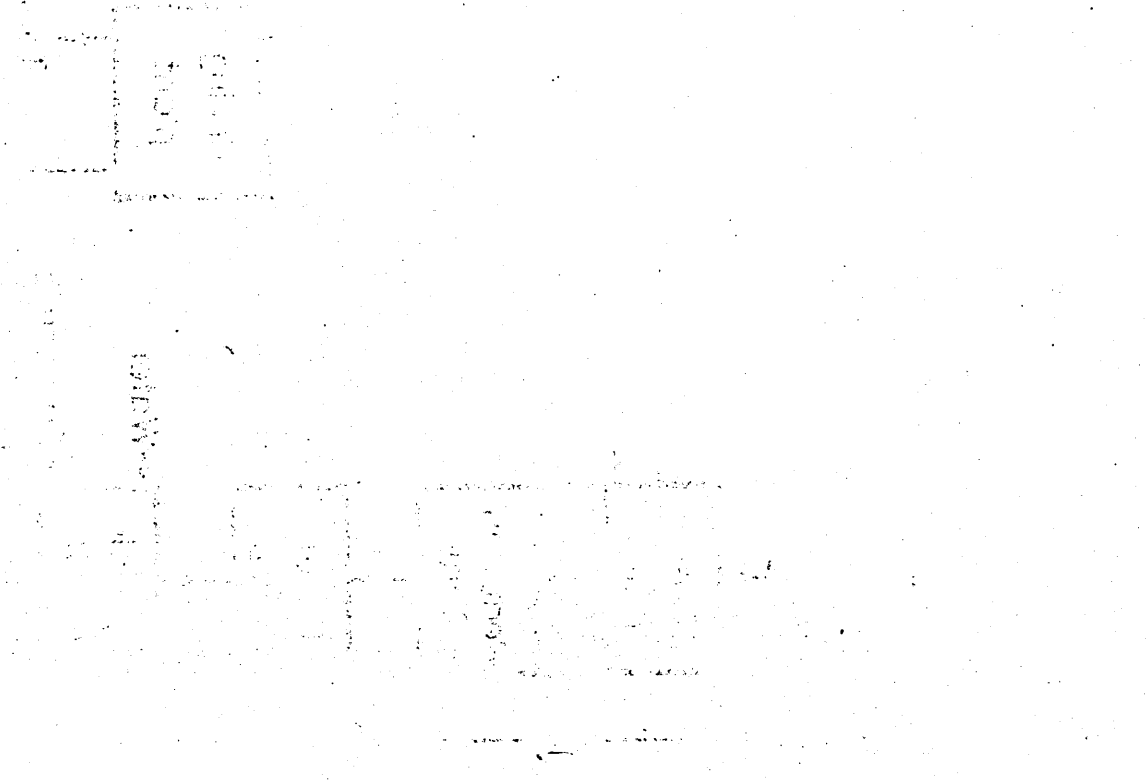


**Fig. 84** Proposed General Layout of the Plant  
Capable of Producing 10 tonnes of 3%  
Nickel Plated Powder per 40 hr week.

GENERAL LAYOUT OF THE PLANT

